Discovery of Antifungal Compounds Produced by *Pelargonium sidoides*-associated Microorganisms

Lauren Anita du Toit

Thesis presented in partial fulfilment of the requirements for the degree of Master of Science in the Faculty of Science at Stellenbosch University

Date: March 2020

Promoter: Dr. Heinrich Volschenk

Co-Promoters: Dr. Kim Trollope and Prof. Marina Rautenbach

DECLARATION

By submitting this thesis electronically, I declare that the entirety of the work contained therein is my own, original work, that I am the sole author thereof (save to the extent explicitly otherwise stated), that reproduction and publication thereof by Stellenbosch University will not infringe any third party rights and that I have not previously in its entirety or in part submitted it for obtaining any qualification.

March 2020

Lauren Anita du Toit

SUMMARY

Pathogenic fungi cause pervasive diseases with a global impact on human health, agricultural crop yields, food security and natural biodiversity. The incidence of fungal infections continues to rise with increasing rates of drug resistance as a result of the wide-spread use of antifungals in the medical and agricultural sectors. New drug-tolerant pathogenic fungal species also emerge in the wake of global warming. Precariously, only a few new antifungal drugs are in development as these compounds must target fungal cells exclusively, to negate any toxic effects on co-treated mammalian and plant cells. In search of new antifungal drugs, antimicrobial peptides such as lipopeptides (LPs) have received particular attention. In plants, microbial LP producers improve the plant's overall health by inducing systemic resistance and direct antagonism towards invading pathogens. In this study, tubers of the traditional South African medical plant, *Pelargonium sidoides* were selected as a potential source of LP-producing microbiota. It has previously been shown that *P. sidoides* has potent antimicrobial properties. However, the microbial species associated with *P. sidoides*, and the bioactive compounds they produce, remain mostly unknown. Therefore, this study aimed to characterise these *P. sidoides*-associated microbes and some of their bioactive compounds, in terms of their structure, haemolytic activity and antifungal activity against a panel of human and plant fungal pathogens. The panel included *Candida albicans*, *Cryptococcus neoformans*, *Botrytis cinerea and Fusarium oxysporum* f. sp. *cubense* as they are closely related to antibiotic resistant strains which continue to threaten human health, most severely in sub-Saharan Africa, and agriculture, globally. A total of 68 microbial isolates were characterised from wild *P. sidoides* tubers. Four of these isolates had antifungal activity against the entire panel of fungal pathogens. Using molecular techniques, the isolates were identified as two *Penicillium* and two *Bacillus* species. Optimisation of culture conditions for antifungal LP production led to the characterisation of two LPs, fengycin A and iturin $A_{Q,}$ produced by *Bacillus* sp. YC2. These LPs were characterised using ultra-performance liquid chromatography-tandem mass spectroscopy (UPLC-MS/MS). Iturin A_Q may be a structural variant of iturin A, a well-known antifungal LP produced by many *Bacillus* species. Extracts containing fengycin A and iturin A_Q showed antifungal activity against the yeast cells of *C. neoformans* and *C. albicans* and the spore and mycelial cell morphologies of *B. cinerea* and *F. oxysporum*. These findings suggest that LP extracts produced by isolate YC2 could be applied to treating these pervasive fungal pathogens in future studies.

OPSOMMING

Middel weerstandige patogeniese swamme veroorsaak steeds deurdringende siektes wat die wêreld se sterftesyfers, die opbrengste van landbougewasse, voedselsekerheid, natuurlike biodiversiteit en verskeie vervaardigingsprosesse beïnvloed. Hierdie infeksies duur voort soos antifungale weerstandigheid voortgaan om te ontwikkel na aanleiding van die wydverspreide toediening van dieselfde antifungale geneesmiddelklasse op dieselfde mediese en landboupatogene. Hierdie patogene is nou goed aangepas om effektiewe behandeling te ontduik. Biomediese navorsing het begin om antimikrobiese peptiede, insluitend antifungale lipopeptiede (LPs) te karakteriseer in die soeke na lukrake antifungale medisinale oplossings. Hierdie amfipatiese verbindings word hoofsaaklik as verdedigende verbindings vervaardig om spesifieke omgewingsantagoniste af te weer. Antagoniste sluit swamspesies in wat meeding om oorlewing op die medisinale plante se oppervlaktes. Dit word voorgestel dat hierdie LP-mikrobiese produsente die plant se gesondheid verbeter deur sistemiese weerstandigheid (ISR) te veroorsaak of deur ‘n bydrae te lewer tot die plant se antimikrobiese eienskappe. In hierdie studie was die Suid-Afrikaanse geranium (*Pelargonium sidoides*) geselekteer as 'n monster bron vir LP-produserende mikrobes. Hierdie medisinale plant het kragtige antimikrobiese eienskappe. Die mikrobiese spesies wat met *P. sidoides* geassosieer word, en die bioaktiewe verbindings wat hulle produseer, bly egter ongeïdentifiseer en nie gekenmerk nie. In hierdie studie was 68 suiwer kolonies geïsoleer en gekenmerk deur wilde knolle van *P. sidoides*. Vier van hierdie mikrobiese isolate het antifungale werking teen *Botrytis cinerea*, *Candida albicans*, *Cryptococcus neoformans* en *Fusarium oxysporum* f. sp. *cubense*. Hierdie mikrobes was geselekteer vir molekulêre identifikasie en geïdentifiseer as *Penicillium* en *Bacillus* sp. Hulle is ook gekweek vir antimikrobiese LP-produksie en twee LP's, fengycin A en iturin A_Q, gekenmerk deur UPLC-MS/MS. Een gekarakteriseerde LP kan 'n strukturele variant van iturien A. wees. Uittreksels wat die twee LP's bevat, het antifungale aktiwiteit teen die geselekteerde patogeniese swamme as gisselle, spore en swam hifes gehad. As dieselfde LP's in toekomstige studies in *P. sidoides*-uittreksels (EPs 7630) opgespoor word, kan dit bydra tot die antifungale werking van EP's 7630. Hierdie bevindings sal die ekologiese belang van mikrobiese LP's vir plante en hul gepaardgaande mikrobes bevestig, en die potensiaal om meer van hierdie verbindings te gebruik uitlig om deurdringende swamsiektes in toekomstige medisinale en landboukundige toepassings te behandel.

BIOGRAPHICAL SKETCH

Lauren du Toit was born in Bellville, South Africa (April 2, 1993). She was home-schooled through Cambridge correspondence course and matriculated from Paarl Girls' High School with two distinctions in 2011. She enrolled at Stellenbosch University in 2013 and obtained a BSc (Molecular Biology and Biotechnology) degree in 2015 and a Hons (Microbiology) degree in 2016.

ACKNOWLEDGEMENTS

I wish to express my sincere gratitude and appreciation to the following persons and institutions for their invaluable contributions to the successful completion of this study:

Dr. Heinrich Volschenk, Department of Microbiology, Stellenbosch University, who acted as my promoter, for his guidance, moral support, and the immense opportunity to work in his laboratory as a postgraduate student.

Dr. Kim Trollope, Department of Microbiology, Stellenbosch University, who acted as my co-promoter, for her guidance, sincere advice, moral support, essential encouragement and hours spent working with me in the laboratory to finish this project on time.

Prof. Marina Rautenbach, Department of Biochemistry, Stellenbosch University, who acted as my co-promoter, for her guidance, moral support and a wealth of knowledge and expertise regarding antimicrobial peptides and LC-MS (and MS/MS) technology.

Dr. Diane Mostert, Department of Plant Pathology, Stellenbosch University, who acted as a collaborator concerning the construction of several phylogenetic trees used in the characterisation of unknown bacterial and fungal species isolated from *Pelargonium sidoides* tuber.

Colleagues and the staff, Department of Microbiology, Stellenbosch University, for their support, kind words and assistance over the years.

My friends and family, for their encouragement and support; especially regarding the long hours spent in the lab. A very special thank you to my sisters (Nicole Catharine and Megan Ceris du Toit), my brother (William Thomas Franklin du Toit), my parents (Angela and Hank du Toit), my cousins (Jarryd Kyle Barnes and Reece Christian Barnes) and my boyfriend (Robin Thomas Sättele).

Uncle Eugene and Aunty Cornell Coetzee, for their encouragement, prayers and financial support directed towards my studies and growth as a person.

The National Research Foundation (NRF) and Stellenbosch University for their financial support and many opportunities given so that I may grow and learn more about science.

DECLARATION BY THE CANDIDATE

This dissertation is presented as a compilation of fi chapters. Each chapter is introduced separately and is written according to the style of the Journal Applied Microbiology and Biotechnology. The contributions of all authors are tabulated below. The overall contributions of the promoters to the study are not quantifiable.

Chapter 1	**General Introduction and Project Aims**		
Authors	Lauren Anita du Toit		
Nature of contribution	**Name**	**email address**	**Extent of contribution**
Drafting	Lauren Anita du Toit	17585139@sun.ac.za	100%
Editing	Dr. Heinrich Volschenk	volschenkh@sun.ac.za	33%
	Dr. Kim Trollope	kim@sun.ac.za	33%
	Prof. Marina Rautenbach	mra@sun.ac.za	33%

Chapter 2	**Literature review**		
Title	Antimicrobial lipopeptides as an emerging class of antifungal drugs		
Authors	Lauren Anita du Toit		
Nature of contribution	**Name**	**email address**	**Extent of contribution**
Drafting	Lauren Anita du Toit	17585139@sun.ac.za	100%
Editing	Dr. Heinrich Volschenk	volschenkh@sun.ac.za	33%
	Dr. Kim Trollope	kim@sun.ac.za	33%
	Prof. Marina Rautenbach	mra@sun.ac.za	33%

Chapter 3	**Research results I**		
Title	Isolation and identification of *Pelargonium sidoides*-associated microorganisms with antifungal activity		
Authors	Lauren Anita du Toit		
Nature of contribution	**Name**	**email address**	**Extent of contribution**
Designed & performed experiments, data analysis, manuscript drafting	Lauren Anita du Toit	17585139@sun.ac.za	95%
	Dr. Diane Mostert	diane@sun.ac.za	5%
Editing	Dr. Heinrich Volschenk	volschenkh@sun.ac.za	33%
	Dr. Kim Trollope	kim@sun.ac.za	33%
	Dr. Diane Mostert	diane@sun.ac.za	33%

Chapter 4	**Research results II**
Title	Identification and characterisation of antifungal compounds from *Pelargonium sidoides*-associated microorganisms
Authors	Lauren Anita du Toit

Nature of contribution	**Name**	**email address**	**Extent of contribution**
Designed & performed experiments, data analysis, manuscript drafting	Lauren Anita du Toit	17585139@sun.ac.za	70%
	Prof. Marina Rautenbach	mra@sun.ac.za	30%
Editing	Dr. Heinrich Volschenk	volschenkh@sun.ac.za	25%
	Dr. Kim Trollope	kim@sun.ac.za	25%
	Prof. Marina Rautenbach	mra@sun.ac.za	50%

Chapter 5	**General discussion and final conclusions**
Authors	Lauren Anita du Toit

Nature of contribution	**Name**	**email address**	**Extent of contribution**
Drafting	Lauren Anita du Toit	17585139@sun.ac.za	100%
Editing	Dr. Heinrich Volschenk	volschenkh@sun.ac.za	33%
	Dr. Kim Trollope	kim@sun.ac.za	33%
	Prof. Marina Rautenbach	mra@sun.ac.za	33%

DECLARATION BY CO-AUTHORS

The undersigned hereby confirm that:

1. the declaration above accurately reflects the nature and extent of the contributions of the candidate and the co-authors to Chapters 1 to 5,
2. no other authors contributed to Chapters 1 to 5, besides those specified above, and
3. potential conflicts of interest have been revealed to all interested parties and that the necessary arrangements have been made to use the material in Chapters 1 to 5 of this dissertation.

Signature	Institutional affiliation	Date
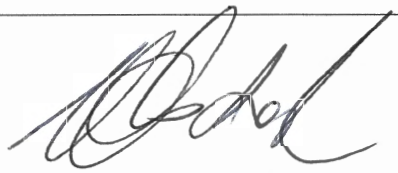 **Dr Heinrich Volschenk**	Stellenbosch University	**25-02-2020**
 **Dr Kim Trollope**	Stellenbosch University	**25-02-2020**
 **Prof Marina Rautenbach**	Stellenbosch University	**25-02-2020**

CONTENTS

CHAPTER 1

General Introduction and Aims

Chapter 1

General Introduction and Aims

1.1 Introduction

A need for novel antifungal compounds has emerged in response to failing drug efficacy of existing drug classes (Azevedo *et al.*, 2015; Pianalto and Alspaugh, 2016). The current antifungal drugs have been extensively used since their discovery in the mid to late 1900s in a broad range of clinical, agricultural and food-related settings, and as a result, fungal species have acquired resistance (Fisher *et al*., 2018). Even if treated with high doses of antifungal drugs that were effective in the past, drug resistant pathogenic fungi can survive and spread infection (Casadevall, 2019). Climate change is also selecting for thermal tolerance in environmental fungi and more species are adapting to grow at mammalian temperatures. This increases their potential to infect human and animal hosts (Casadevall, 2019). Currently, the impact of these phenomena are substantial losses in human life, especially for immune-compromised individuals living in Sub-Saharan Africa, (Guinea, 2014; Mpoza *et al.,* 2018; Pianalto and Alspaugh, 2016) and agriculture, around the globe (Godfray *et al*., 2016; Lucas, 2017).

Drug resistant fungal pathogens affecting human health include those responsible for life-threatening systemic infections such as candidiasis, cryptococcosis, aspergillosis, pneumocystis pneumonia and mucormycosis (Chen *et al*., 2016; Guinea, 2014; Mpoza *et al.*, 2018). These diseases primarily affect individuals with weakened immune systems, for example, individuals undergoing chemotherapy, taking immune suppressants following organ transplantation or diagnosed with HIV or AIDS (Almeida *et al.,* 2019). An estimated 1.5-1.6 million human lives are lost per annum due to these invasive fungal infections (Almeida *et al.,* 2019; Pianalto and Alspaugh, 2016), although the majority of these cases are reported in Sub-Saharan Africa where there is a high incidence of HIV/AIDs (Africa and Abrantes, 2017). Human mortality data presented by Brown *et al.* (2012) and the World Health Organization (WHO) in 2015 and 2017 (Almeida *et al.,* 2019), suggest that some of these fungal diseases are now less treatable than other major infectious diseases like HIV/AIDS, tuberculosis and malaria.

Fungal pathogens which affect various crop species, many of which are staple foods, include *Magnaporthe oryzae*, *Puccinia graminis*, *Ustilago maydis*, *Phakopsora pachyrhizi,*

Fusarium oxysporum and *Botrytis cinerea* (Breeze, 2019; Khan *et al*., 2017; Lewis *et al*., 2018). Respectively, these pathogens decimate rice, wheat, maize, soybean, bananas, plantain and berry crops. Collectively, fungal crop pathogens result in 70% of all major crop losses worldwide (Lucas, 2017). It is suggested that many of these crops are at particular risk to infection as they are farmed using grafts or genetically identical seeds and therefore, all susceptible to the same plant diseases (Lucas, 2017). Furthermore, despite billions of dollars spent on fungicidal products, many fungal pathogens are becoming increasingly resistant to treatment with outdated antifungal treatments used in crop protection (Hahn, 2014; Peterson and Kaur, 2018).

In the search for new antifungal drug classes, biotechnology and modern medicine are revisiting traditional medicinal plants as potential sources of novel antifungal compounds (Aboobaker *et al.,* 2019; Nath *et al*., 2015). Case in point is the South African geranium, *Pelargonium sidoides* DC tuber extracts used traditionally to treat upper respiratory tract infections, wound treatment and stomach disorders (Aboobaker *et al.,* 2019; Street and Prinsloo, 2013). Extracts prepared from *P. sidoides* tubers contain a wide range of antimicrobial compounds with potent antimicrobial properties including several fungal pathogens (Mativandlela *et al*., 2006; Samie *et al*., 2019; Street and Prinsloo, 2013). However, the microbiota associated with *P. sidoides* tubers and the antimicrobial compounds they produce have not been identified or characterised extensively. There are only two studies which describe bioactive compounds produced by fungal endophytes isolated from *P. sidoides* (Aboobaker *et al.,* 2019; Mangany*i et al.,* 2019). This despite research indicating that many medicinal plant-associated microbes produce a wide range of potent antimicrobial compounds, some of which may contribute to the medicinal properties of the host flora (Huang *et al.,* 2008; Nath *et al*., 2015; Schafhauser *et al.,* 2019).

Microbiota associated with both medicinal and ornamental plants are known to produce a range of antimicrobial compounds that either improve plant health or stimulate the plant's immune system (Albert, 2013; Rebotiloe *et al*., 2018). These metabolites include several steroids, alkaloids, flavonoids as well as peptides. Antifungal peptides, which include antifungal lipopeptides, are among the most recently discovered classes of antifungal drugs. These amphipathic compounds have several advantageous properties as antimicrobial agents, including rapid antifungal action, multiple cellular targets, vast structural diversity as well as biodegradability. These properties of antifungal peptides make them ideal candidates for future drug development and application in clinical environments or as more

environmentally friendly crop protectants (Raaijmakers *et al*., 2010; Rautenbach *et al.*, 2016; Troskie *et al*., 2014). If these bioactive compounds are produced more efficiently by the microbiota than by an associated plant host, they will also side-step the need for harvesting compounds from plant parts in the future. Using microbes to produce bioactive compounds is usually far more time and cost-effective than growing plants for this purpose, as plants require more time and space to grow to maturity.

To address the gaps in knowledge concerning the *P. sidoides* microbiota and the antimicrobial compounds they produce, this thesis provides a comprehensive literature review on lipopeptides as a promising antifungal drug class in Chapter 2. Chapter 3 presents the isolation and identification of *P. sidoides*-associated microbes with antifungal activity. Work performed to optimise the production and characterise some antifungal compounds produced by the isolated microbes are detailed in Chapter 4. Final conclusions are drawn in Chapter 5.

1.2 Aims and Objectives

This study aimed to explore the production of antifungal LPs by *P. sidoides* tuber-associated microbiota.

To achieve these aims, the following objectives were set:

- To isolate and screen fungal and bacterial microbiota associated with *P. sidoides* tubers for broad-spectrum and high relative antifungal activity against a panel of fungal pathogens (Chapter 3).
- To identify antifungal producing microbiota using multi-locus sequence phylogeny and phenotypic data (Chapter 3).
- To optimise the culturing conditions of producer organisms for increased antifungal compound production (Chapter 3).
- To characterise the inhibition phenotype of antifungal extracts against different fungal cell morphologies (Chapter 4).
- To identify antifungal LPs in biologically active microbial extracts using UPLC-MS analysis and MSe analysis (Chapter 4).

1.3 Outcomes

The work presented in this dissertation demonstrates the potential for exploring microbiota associated with *P. sidoides* tubers as a resource for new antifungal compounds. Optimising the culturing conditions of selected isolates afforded the production of detectable amounts of antifungal compounds, specifically LPs, with antifungal activity against specific human (*C. neoformans* and *C. albicans*) and agricultural (*B. cinerea* and *F. oxysporum*) pathogenic fungi. The specific outcomes of this study include:

- The genus-level identification of four microbial isolates from *P. sidoides* tubers with broad-spectrum (isolates YC2, SC6, A1 and C5) and the highest relative (isolates A1 and C5) antifungal activity against human (*C. neoformans* and *C. albicans*) and agricultural (*B. cinerea* and *F. oxysporum*) pathogenic fungi.
- Methods for enhanced antifungal compound and LP production applied to both bacterial and fungal isolates from wild *P. sidoides* tubers.
- Methods to extract, purify, store and characterise LPs using UPLC-MS/MS from previously uncharacterised samples.
- The discovery of a potentially novel iturin A analogue, denominated iturin A_Q.

Principles developed in this study can be readily applied to other isolates from *P. sidoides* tubers, or plant-associated microbes in general, for their characterisation or the characterisation of some of the bioactive compounds they produce. The four bioactive microbial extracts screened for antifungal activity could also be screened against a broader range of fungal pathogens or analysed for additional LPs or other sought-after bioactive compounds.

1.4 References

Aboobaker Z, Viljoen A, Chen W, Crous PW, Maharaj VJ, van Vuuren S. 2019. Endophytic fungi isolated from *Pelargonium sidoides* DC: Antimicrobial interaction and isolation of a bioactive compound. South African Journal of Botany **122**: 535-542

Africa C, Abrantes P. 2017. *Candida* antifungal drug resistance in sub-Saharan African populations: A systematic review. F1000 Research **5**: 1-9

Albert M. 2013. Peptides as triggers of plant defence. Journal of Experimental Botany **64**: 5269-5279

Almeida F, Rodrigues ML, Coelho C. 2019. The still underestimated problem of fungal diseases worldwide. Frontiers in Microbiology **10**: 1-5

Azevedo MM, Teixeira-Santos R, Silva AP, Cruz L, Ricardo E, Pina-Vaz C, Rodrigues AG. 2015. The effect of antibacterial and non-antibacterial compounds alone or associated with antifungals upon fungi. Frontiers in Microbiology **6**: 1-7

Breeze E. 2019. 97 Shades of gray: genetic interactions of the gray mold, *Botrytis cinerea,* with wild and domesticated tomato. The Plant Cell **31**: 280-281

Brown GD, Denning DW, Gow NAR, Levitz SM, Netea MG, White TC. 2012. Hidden killers: Human fungal infections. Science Translational Medicine **4**: 165

Casadevall A. 2019. Global catastrophic threats from the fungal kingdom: Fungal catastrophic threats. Current Topics in Microbiology and Immunology **1**: 1-12

Chen AJ, Frisvad JC, Sun BD, Varga J, Kocsubé S, Dijksterhuis J, Kim D, Hong S, Houbraken J, Samson R. 2016. *Aspergillus* section *Nidulantes* (formerly *Emericella*): Polyphasic taxonomy, chemistry and biology. Studies in Mycology **84**: 1-118

Fisher MC, Hawkins NJ, Sanglard D, Gurr SJ. 2018. Worldwide emergence of resistance to antifungal drugs challenges human health and food security. Science **360**: 739-742

Godfray HC, Mason-D'Croz D, Robinson S. 2016. Food system consequences of a fungal disease epidemic in a major crop. Philosophical Transactions of the Royal Society B: Biological Sciences **371**: 20150467

Guinea J. 2014. Global trends in the distribution of *Candida* species causing candidemia. Clinical Microbiology and Infection **20**: 5-10

Hahn M. 2014. The rising threat of fungicide resistance in plant pathogenic fungi: *Botrytis* as a case study. Journal of chemical Biology **7**: 133-141

Huang W, Cai Y, Hyde K. Corke H, Sun M. 2008. Biodiversity of endophytic fungi associated with 29 traditional Chinese medicinal plants. Fungal Diversity **33**: 61-75

Khan N, Maymon M, Hirsch AM. 2017. Combating *Fusarium* infection using *Bacillus*-based antimicrobials. Microorganisms **5**: 75

Lewis CM, Persoons A, Bebber DP, Kigathi RN, Maintz J, Findlay K, Bueno-Sancho V, Corredor-Moreno P, Harrington SA, Kangara N, Berlin A, García R, Germán SE, Hanzalová A, Hodson DP, Hovmøller MS, Huerta-Espino J, Imtiaz M, Mirza JI, Justesen AF, Niks RE, Omrani A, Patpour M, Pretorius ZA, Roohparvar R, Sela H, Singh RP, Steffenson B, Visser

B, Fenwick PM, Thomas J, Wulff BBH, Saunders DGO. 2018. Potential for re-emergence of wheat stem rust in the United Kingdom. Communications Biology **1**: 1-9

Lucas J. 2017. Fungi, food crops, and biosecurity: Advances and challenges. Advances in Food Security and Sustainability **1**: 1-40

Manganyi MC, Tchatchouang C-DK, Regnier T, Bezuidenhout CC, Ateba CN. 2019. Bioactive compound produced by endophytic fungi isolated from *Pelargonium sidoides* against selected bacteria of clinical importance. Mycobiology **47**: 335-339

Mativandlela SPN, Lall N, Meyer JJM. 2006. Antibacterial, antifungal and antitubercular activity of (the roots of) *Pelargonium reniforme* (CURT) and *Pelargonium sidoides* (DC) (*Geraniaceae*) root extracts. South African Journal of Botany **72**: 232-237

Mpoza E, Rhein J, Abassi M. 2018. Emerging fluconazole resistance: Implications for the management of cryptococcal meningitis. Medical Mycology Case Reports **19**: 30-32

Nath A, Chattopadhyay A, Joshi SR. 2015. Biological activity of endophytic fungi of *Rauwolfia serpentina* Benth: An ethnomedicinal plant used in folk medicines in northeast India. Proceedings of the National Academy of Sciences, India Section B: Biological Sciences **85**: 233-240

Peterson E, Kaur P. 2018. Antibiotic resistance mechanisms in bacteria: Relationships between resistance determinants of antibiotic producers, environmental bacteria, and clinical pathogens. Frontiers in Microbiology **9**: 2928

Pianalto KM, Alspaugh JA. 2016. New horizons in antifungal therapy. Journal of Fungi **2**: 26

Raaijmakers JM, De Brujin I, Nybroe O and Ongena M. 2010. Natural functions of lipopeptides from *Bacillus* and *Pseudomonas*: More than surfactants and antibiotics. Federation of European Microbiological Societies Microbiology Reviews **34**: 1037-1062

Rautenbach M, Troskie A, Vosloo JA. 2016. Antifungal peptides: To be or not to be membrane active. Biochimie **130**:132-145

Rebotiloe F, Eunice U, Mahloro H. 2018. Isolation and identification of bacterial endophytes from *Crinum macowanii* Baker. African Journal of Biotechnology **17**: 1040-1047

Samie S, Trollope KM, Joubert LM, Makunga NP, Volschenk H. 2019. The antifungal and *Cryptococcus neoformans* virulence attenuating activity of *Pelargonium sidoides* extracts. Journal of ethnopharmacology **235**: 122-132

Street R, Prinsloo G. 2013. Commercially important medicinal plants of South Africa: A review. Journal of Chemistry **2013**:1-16

Troskie AM, de Beer A, Vosloo JA, Jacobs K, Rautenbach M. 2014. Inhibition of agronomically relevant fungal phytopathogens by tyrocidines, cyclic antimicrobial peptides isolated from *Bacillus aneurinolyticus*. Microbiology SGM **160**: 2089-20101

World Health Organization. 2015. World Health Statistics 2015. [online] Available at: https://www.who.int/gho/publications/world_health_statistics/2015/en/ [Accessed 18 Sep. 2019]

CHAPTER 2

Literature Review:

Antimicrobial Lipopeptides as an Emerging Class of Antifungal Compounds

Chapter 2

Antimicrobial Lipopeptides as an Emerging Class of Antifungal Compounds

2.1 Global impact of pathogenic fungi

Members of the fungal kingdom play a pervasive global role in human and animal health, agriculture, and manufacturing as well as earth's ecosystem health and natural biodiversity. While some fungal species are key to the production of food and fermented beverages, phytopathogenic fungi jeopardise agricultural crop yields or contaminate, as part of their secondary metabolism, food supplies with mycotoxins. All of which pose a risk to food security, i.e., the need to feed a growing world population. Similarly, several fungi are associated with human health, either as commensal members of our microbiome or the production of antibiotics, while a few dozen fungi regularly cause human disease, ranging from mucosal infections to deadly systemic and invasive mycoses.

2.1.1 Pathogenic fungi and human disease

It is estimated that 1.5-1.6 million human deaths are caused by invasive fungal infections every year (Kupferschmidt, 2019; Almeida *et al.,* 2019). The top three fungal diseases affecting human health worldwide are cryptococcosis, candidiasis and aspergillosis. Most of these fungal diseases are caused by opportunistic fungal pathogens, which infect individuals with compromised or weakened immune systems (e.g. people infected with HIV/AIDS, having chemotherapy or taking immune system suppressants to avoid the rejection of a donor organ). Healthy individuals can, however, also be at risk from a few emerging pathogens such as blastomycosis, coccidioidomycosis and histoplasmosis.

It is suggested that the fungal species causing human disease developed a capacity for virulence by first adapting to survive predation from a third-party agent, amoeboid predators (Casadevall, 2019). Virulence factors, like melanin synthesis, capsule formation and producing phospholipases, protect pathogenic fungi from both amoeboid predators and macrophages (Steenbergen *et al.,* 2001; Casadevall, 2017). These interactions have been observed in *Cryptococcus*, *Aspergillus, Histoplasma,* and *Sporothrix* species (Steenbergen *et al.,* 2004). In addition to this, fungi with pathogenic

potential have had to overcome endothermy which restricts most environmental fungi from causing mycotic disease in warm-blooded organisms (Garcia-Solache and Casadevall, 2010). Most environmental fungi are restricted to grow at 12°C-30°C and are more likely to infect cold-blooded animals (e.g. amphibious species) or plants (Robert and Casadevall, 2009). However, as a result of global warming, some environmental fungi are now adapting to grow at higher ambient temperatures and may present a more significant threat to mammalian species than ever before (Garcia-Solache and Casadevall, 2010). This has been observed for several basidiomycetes which were analysed for increased temperature tolerance and demonstrates the rapid adaptive capabilities of certain fungal species if provided with sufficient selection pressure (Almeida *et al.,* 2019; de Crecy *et al.,* 2009; Robert *et al.,* 2015).

Currently, only four classes of antifungal drugs are available to treat life-threatening fungal infections, with only a few new drugs in the pharmaceutical drug development pipeline. Combined with the emergence of drug resistance, some fungal infections, for example, cryptococcal meningitis (180 000 global annual deaths), are now comparable with particularly aggressive infectious diseases such as HIV/AIDS, malaria (429 000 global annual deaths) and tuberculosis (1.6 million global annual deaths) in terms of global annual mortality rates (Rajasingham *et al.,* 2017). However, it should be noted that these statistics collected by Brown *et al.* (2012) and the World Health Organization (WHO) (2015) do not take into account underlying illnesses or immune dysfunctions.

Drug resistant yeast species which cause candidiasis and cryptococcosis are most alarming as rates of resistance to all four known antifungal drug classes (i.e. multi-drug resistance) are on the increase in these human pathogens. Over 20 *Candida* species can infect individuals with both impaired and intact immune systems. However, just five species (*C. albicans*, *C. glabrata*, *C. parapsilosis*, *C. tropicalis*, and *C. krusei*) are responsible for 95% of all *Candida* infections, and one species cause an estimated 62% of these cases, *C. albicans* (Azie *et al*., 2012; Perea *et al*., 2001; Sanguinetti *et al*., 2005). *Candida* infections can be mucosal or invasive and manifest as blood (candidemia), skin, mouth or vaginal infections. These infections can result from open wounds, surgeries, immune dysfunction or antibiotic treatment which eliminates bacterial species which would naturally compete with *Candida* populations on the human body (Kullberg and Arendrup, 2015). Invasive *Candida* infections associated with hospital settings are particularly worrying as the causative agents must be resistant to many antibiotics to

survive within this environment. The emerging pathogen *C. auris*, is a prime example of this as more cases of infection are reported each year with multi-drug resistant strains being isolated from the hospital environment after patients are diagnosed with candidemia (Jeffery-Smith *et al*., 2018). The significance of this is a global mortality rate of 30% for candidemia, despite the availability of frontline antifungal drugs to treat this disease in many areas of the world (Jeffery-Smith *et al*., 2018). In developing countries, where there is high precedence of HIV/AIDS and limited access to frontline antifungal drugs, the mortality rate for candidemia is even higher, 38-44% (Africa and Abrantes, 2017).

The global mortality rate of cryptococcal meningitis is estimated at around 180,000 people a year and accounts for 10-15% of all AIDS-related mortalities (Brown *et al.*, 2012; Mpoza *et al.,* 2018). Infections are associated with tropical environments and interactions with soil, trees or bird droppings harbouring *Cryptococcus* spores. Both *Cryptococcus gatti* and *Cryptococcus neoformans* can infect immune-compromised individuals, but *C. gatti* has been reported in otherwise healthy individuals (Datta, 2009). Most clinical infections are caused by *C. neoformans* which, after inhalation of spores, the infection spreads from the lungs to the central nervous system and the brain where neurological complications result in death (Brown *et al.,* 2012; Köhler *et al.*, 2014). In sub-Saharan Africa, where a large percentage of the population has HIV/AIDs, *C. neoformans* is the leading cause of meningitis in adults (Datta., 2009).

2.1.2 Pathogenic fungi and agriculture

Although most plant-fungal interactions are beneficial with positive effects on overall plant growth and health (Almeida *et al.,* 2019), some fungi are agricultural crop pathogens responsible for 70% of major crop losses (Almeida *et al.,* 2019; Godfray *et al*., 2016). Many of these food crops are staple foods, such as maize, wheat, soybean, plantain, potatoes and rice, and some are used in secondary industries such as the production of animal feed for meat and dairy farming. In this way, fungal diseases directly impact economic losses in agriculture, global food availability and poverty. The most devastating fungal pathogens which have threatened global food security in recent years include, *Puccinia graminis* (Singh *et al*., 2011; Lucas, 2017; Lewis *et al*., 2018), *Magnaporthe oryzae* (Onega and Asea, 2016)*, Phakospora pachyrhizi* (Campbell *et al.*, 2013)*, Botrytis cinerea* and *Fusarium oxysporum* (Campbell *et al.*, 2013).

Botrytis cinerea and *F. oxysporum* are highly polyphagous, i.e., infecting a broad spectrum of plant hosts and result in the most significant losses in both pre- and post-harvest crops (de Senna and Lathrop, 2017). *B. cinerea* can infect over 1400 known plant hosts (in 586 plant genera and 152 botanical families), including high-value crops such as grapevine and tomato (Breeze, 2019; Hua *et al*., 2018; Mercier *et al.*, 2019). As a necrotrophic pathogen, *B. cinerea* costs the global agricultural sector $10-$100 billion due to failed crops and spoiled produce annually (Hahn, 2014; Watkinson *et al.*, 2015). Concerning just the strawberry industry, *B. cinerea* is responsible for up to 50% of pre-harvest crop losses and nearly half the total expenditure spent on the development and application of new fungicidal sprays (Adnan *et al.*, 2019).

Fusarium oxysporum can infect 150 different plant species, some of which are cereal crops, vegetables, fruits or ornamental plants (Al-Hatmi *et al.*, 2016). Susceptible plant species include varieties of maize, potatoes, tomatoes, cabbage, peas, flax, watermelon, tulip, onion, cotton, peas, basil, peppers, gladiolus, bananas and beans (Khan *et al.,* 2017). Wilt caused by *F. oxysporum* (*Fusarium* wilt) also affects plantain and East African highland bananas which are essential food sources in many African and Asian countries (Price, 1995). *Fusarium* wilt is responsible for the global shift from the Gros Michel banana cultivar to Cavendish bananas as the primary export banana (Thangavelu and Mustaffa, 2012). In recent years, however, a renewed wave of pathogenicity is being led by a different strain of *F. oxysporum,* which originated in South East Asia (Perfect *et al*., 2015). This strain of *Fusarium* wilt has been reported in several hectares of Cavendish banana in India (Damodaran *et al*., 2019). Even with fungicidal treatment, this new wave of *Fusarium* wilt continues to spread throughout South East Asia.

2.2 Failing drug efficacy of current antifungal treatment regimes

Antifungal compounds have been used since their discovery in the mid-late 1900s (1950-1974) to protect humans from disease and starvation (Robbins *et al.,* 2017). The current antifungal armamentarium consists of four classes of antifungal drugs (Table 2.1) to treat human disease and prevent food spoilage or crop damage, namely polyenes, azoles, anti-metabolites and echinocandins (Pianalto and Alspaugh, 2016; Robbins *et al.,* 2017). Fungi, however, continue to adapt and evade these compounds and new solutions are required if older drug solutions cannot be altered or combined with increasing treatment efficacy.

Table 2.1 Antifungal drug classes and examples of antifungal drugs used in medical and agriculture applications (Azevedo *et al.,* 2015; Pianalto and Alspaugh, 2016; Robbins *et al.,* 2017).

Drug class	Medical application	Agri/Food application
Polyenes (1950s)	Amphotericin B	Natamycin
Azoles (1950s)	Fluconazole	Prothioconazole
Anti-metabolites (1950s)	Flucytosine	Dichloropropionic acid
Echinocandins (1970s)	Caspofungin	Not Applicable

Fungal drug discovery and drug development pipelines take far longer and are more expensive, as opposed to antibacterial drugs. The reason for the slow progress in antifungal drug development is attributed to the greater difficulty to formulate antifungal drugs with selective toxicity. Selective toxicity refers to the ability of a drug dose to inhibit or kill a pathogen without harming the host organism (Willey *et al*., 2014). This is especially important for medical and food-related applications. However, selective toxicity is rarely achieved for antifungal compounds as both the fungal and mammalian host cells are eukaryotic and share the same cell components and conserved biological processes. A failure to select for drug targets specific in fungal cells result in toxic side effects. This is especially true for treating patients with weakened immune systems as high doses or prolonged treatment with antifungal agents can result in severe toxicity in patients (Reid *et al*., 2012). Antifungal drugs with some selective toxicity target unique fungal cell envelope components such as chitin, sphingolipids, glycerophospholipids, ergosterol and mannoproteins.

2.2.1 Polyenes

Polyenes target sterols in the phospholipid cell membrane of all eukaryotic cells. As a result, polyenes have limited selective toxicity and at high doses will have adverse side effects. For example, Amphotericin B (AmB), the frontline drug to treat several different life-threatening mycoses, has a high affinity for the fungal sterol, ergosterol, but also human sterol, cholesterol (Malayeri *et al*., 2018). With the global increase in the immunocompromised patient population and the rise in invasive fungal diseases in the 1980s and 1990s, AmB use led to an increased observation of nephrotoxicity. AmB has also become ineffective against some resistant strains of *C. albicans* and *C. neoformans* (Perfect *et al*., 2010; Pianalto and Alspaugh, 2016). Another polyene drug, natamycin, also binds to ergosterol and is effective against both *Fusarium* and *Aspergillus* species

but has the same nephrotoxicity as AmB (Malayeri *et al*., 2018). The mode-of-action for polyene drugs is to bind to sterols in the cell membrane and form aqueous pores or channels in the cell membrane and leak out critical nutrients and ions to the cell exterior (Malayeri *et al*., 2018). To regulate osmotic pressure, hydrogen ion influx and potassium ion efflux pumps are activated. The influx of hydrogen ions results in internal acidification of the fungal cell and a loss in enzymatic function. Eventually, sugars and amino acids also leak out from the arrested cell (Malayeri *et al*., 2018).

2.2.2 Azoles

Azole antifungal agents either contain two (imidazoles) or three nitrogen (triazoles) atoms in their characteristic azole ring structure. The triazoles are less toxic than the imidazoles and far less toxic than polyenes such as AmB (Mazu *et al*., 2016). For this reason, triazoles are used extensively as first-line therapy in clinical applications. The mode-of-action for azoles is to arrest fungal growth by inhibiting the biosynthetic pathway of ergosterol. Lanosterol 14α-demethylase, a cytochrome enzyme, is blocked, preventing the demethylation of lanosterol to ergosterol, and this leads to several membrane abnormalities (Mazu *et al*., 2016). Physical membrane alterations may also affect membrane-bound enzymes which maintain chitin synthesis, nutrient transport and cell proliferation (Mazu *et al*., 2016). Triazoles, fluconazole and itraconazole, are used to treat several yeasts and filamentous fungi which cause mycosis. Azole sprays are also used to protect a wide range of crops (including cereals and fruits) from a myriad of fungal pathogens. However, azole antifungals are characterised by several major shortcomings, including (but not limited to) potentially hazardous drug-drug interactions via interactions with the cytochrome P_{450} enzyme system, erratic absorption leading to unpredictable exposure, nonlinear and saturable pharmacokinetics that requires therapeutic drug monitoring, toxicities associated with their prolonged use, and the emergence of azole resistance (Van Daele *et al.,* 2019). Broad application of azoles in both agricultural and clinical settings has contributed significantly to high levels of resistance (Berger *et al.,* 2017; Price *et al*., 2015). Resistance to azoles exists in *Aspergillus fumigatus*, *C. neoformans* and various *Candida* species (Berger *et al.,* 2017; Chen *et al*., 2016; Gray *et al*., 2012; Guinea, 2014; Howard *et al*., 2009; Mpoza *et al.,* 2018; Price *et al*., 2015; Sionov *et al*., 2009). Resistant strains of both *B. cinerea* and *F. oxysporum* exhibit target-site resistance to azoles and polyenes (Adnan *et al.,* 2019; Hahn, 2014). Many *Fusarium* species are intrinsically resistant to azole antifungals due to a highly effective efflux

mechanism which excretes the antifungal compound from within the cell cytosol (Al-Hatmi *et al.,* 2016).

2.2.3 Anti-metabolites

Flucytosine (5-flourocytosine), an anti-metabolite, inhibit DNA and RNA synthesis by entering the cell through a permease and then converted into 5-fluorouracil (5-FU) by cytosine deaminase. When 5-FU is incorporated into DNA, it is converted into 5-fluorodeoxyuridylic acid monophosphate which interferes with DNA synthesis. 5-Flourocytosine can also be converted into 5-fluorouridine monophosphate, 5-fluorouridine diphosphate and 5-fluorouridine triphosphate. The last of these unnatural nucleotides are incorporated into fungal RNA and prevents protein synthesis (Malayeri *et al*., 2018; Vermes *et al.,* 2000). Flucytosine is prone to drug resistance development, for example, 11.7% of *Cryptococcus* isolates collected in North America, Europe, Asia, Africa and Latin America in 2009 were resistant to flucytosine (Azie *et al*., 2012).

2.2.4 Echinocandins

The echinocandin LPs are cyclic hexapeptides and include caspofungin, micafungin, anidulafungin, pneumocandin, aculeacin and mulundocandin. The mulundocandins have fungicidal activity against *Candida* and *Aspergillus* species and weak fungistatic activity against *Cryptococcus*, *Fusarium, Scedosporium* and *Pneumonocystis* species *(*Pianalto and Alspaugh, 2016). Echinocandins target the β-(1, 3)–glucan synthetase in the cell wall and inhibit glucan synthesis, which is important for maintaining cell wall integrity and protecting the cell from osmotic stress. The loss of functional glucans makes the cell wall rigid and allows ions to leak out from the compromised cell wall. Through the same pores, water enters the cell uncontrollably and the increase in osmotic pressure eventually results in cell lysis (Mazu *et al*., 2016). Echinocandins have very few clinically significant drug-drug interactions and display very favourable tolerability and toxicity profiles (Van Daele *et al.,* 2019). However, some *Candida* species have developed resistance to echinocandins (Africa and Abrantes, 2017). It is hypothesised that this immunity develops as a result of chitin redistribution and uninterrupted β-(1, 3)-glucan synthesis. A random mutation in the FKS1 subunit of β- (1, 3)-glucan synthetase makes it difficult for echinocandins to bind to β-(1, 3)-glucan synthase and inhibit its activity (Walker *et al*., 2010). The same mutation also results in a re-distribution of chitin, which further protects synthesised β-(1, 3)-glucans in β-(1, 3)-glucan-chitin scaffolds. These adaptations

prevent echinocandins from disrupting the cell walls of mutated *Candida* species (Walker *et al*., 2010).

The acquisition of wide-spread drug resistance in pathogenic fungi is attributed to the presence of sub-lethal concentrations of antifungals in the natural environment (Fisher *et al*., 2018; Heimlich *et al.,* 2014; Peterson and Kaur, 2018). This includes environments fed by agricultural run-off or human wastewater systems (Fisher *et al*., 2018). In these environments, commensal fungi express resistance genes and grow uninhibited before exchanging their resistance genes with other pathogenic strains of the same fungal species. Cross-resistance can occur in *Candida, Cryptococcus and Aspergillus* species during sexual reproduction (Heimlich *et al.,* 2014). It allows the pathogenic strains to infect a host and resist the antifungal drug without previous exposure. This highlights the need for more biodegradable antifungal drugs and wastewater treatment plants which eliminate antibiotics and their derivatives (Fisher *et al*., 2018). Drug-resistant commensal strains can also become pathogenic if they accumulate, by horizontal gene transfer or mutation, a sufficient number of resistance genes and other virulence factors to survive within a human, animal or plant host. Virulence factors which increase the likelihood of a pathogen's survival within a mammalian host include biofilm formation and the secretion of haemolysin and phospholipase hydrolases (El-Houssaini *et al.,* 2019). Consequently, there is an urgent need for the development of new antifungal drugs, preferably with novel modes-of-action to avoid cross-resistance and/or cross-toxicities and with increased biodegradability to avoid resistance developing against them as a result of bioaccumulation. This should improve both human health and agricultural production by making antifungal treatments more reliable and sustainable for use by future generations.

2.3 Antimicrobial lipopeptides as alternative antifungal treatment

In the quest for new antifungal compounds, antimicrobial peptides (AMPs) have received particular attention due to their ubiquity, structural diversity and rapid action. The discovery of AMPs dates back to 1939 when gramicidin was first extracted from a soil *Bacillus* strain as an antimicrobial agent against a pneumococci infection (Dubos, 1939). It is argued that antimicrobial peptides display low levels of acquired resistance as they act quickly (within seconds after the initial contact with cell membrane) on multiple cell targets and degrade in the presence of environmental proteases (Raaijmakers *et al*., 2010). This is proposed to reduce the likelihood of cross-resistance development between commensal and pathogenic fungi in the natural environment.

Structurally, AMPs are composed of short chains of amino acids (varying from five to >100) with functional side groups which confer antimicrobial activity (Fig. 2.1). They are produced by both unicellular and multicellular organisms, while LPs are produced only in bacteria and fungi (Baindara and Korpole, 2016). Antimicrobial peptides are classified into six main categories, including linear peptides (e.g. α-helical peptides produced by many multicellular organisms), β-sheet peptides (produced predominantly by unicellular organisms and including the cyclic LPs), peptides with unique amino acids, cyclic peptides with thioether groups, peptaibols and macrocyclic peptides (Epand and Vogel, 1999). Antimicrobial peptides produced by multicellular organisms are generally larger (> 3 kDa) than those produced by unicellular organisms (<1.5 kDa) (Nguyen *et al*., 2011).

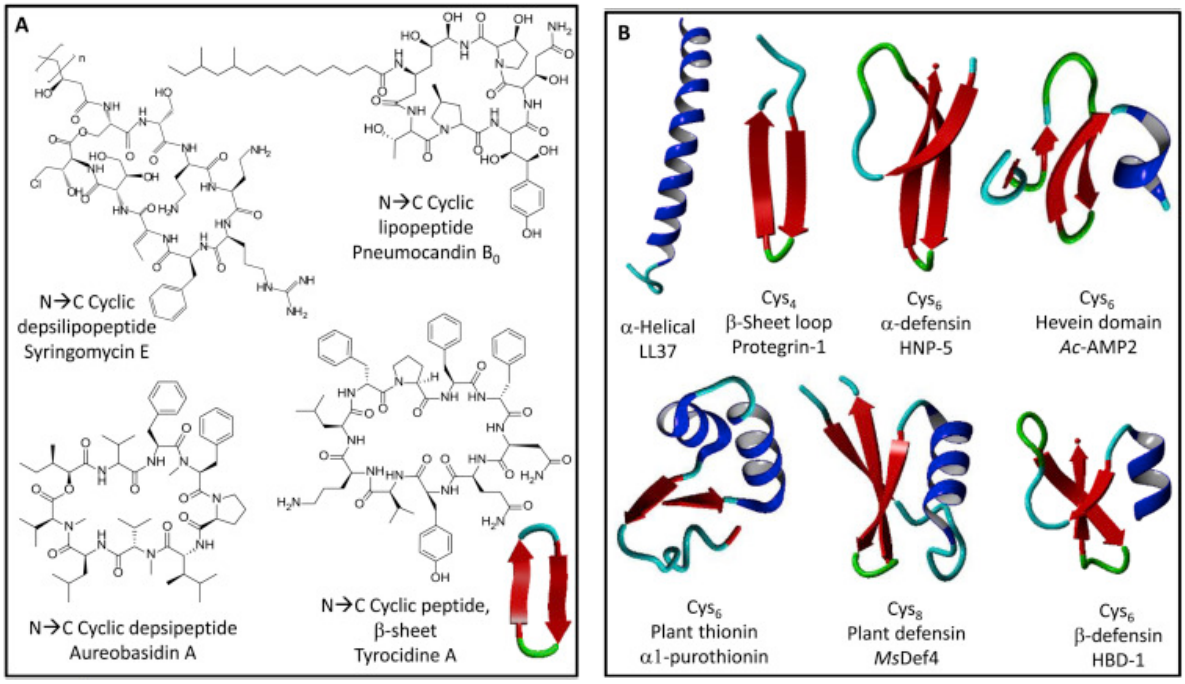

Figure 2.1. Structural diversity of AMPs and AFPs produced by both unicellular (Panel A) and multicellular organisms (Panel B) (Rautenbach *et al*., 2016).

Antimicrobial peptides with antifungal activity, antifungal peptides (AFPs), were first discovered in 1974 (Balkovec *et al*., 1994). The first AFP, echinocandin B, a LP, is produced by *Aspergillus nidulans* and *Aspergillus rugulosus* (Balkovec *et al*., 1994). Other echinocandins were later synthesised following media optimisation and chemical alteration to produce pneumocandin (produced by *Glarea lozoyensis)*, cilofungin (synthesised from echinocandin B), caspofungin (modified from pneumocandin), micafungin (produced by *Coleophoma empetri*) and anidulafungin (modified from echinocandin B). Echinocandins and daptomycin (another commercially available LP)

are used to treat human patients for life-threatening *Candida* and Gram-positive bacterial infections caused by methicillin-resistant *Staphylococcus aureus* (Balkovec *et al*., 1994).

The application of AFPs to food products and agriculture is still in early development, but some studies have confirmed antifungal activity against relevant agricultural pathogens and food contaminants (Keymanesh *et al.,* 2009; Troskie *et al*., 2014). Other studies highlight the use of AFP producers as biocontrol agents as they have inherent environmental fitness and consistently produce AFPs in a natural setting. For example, tyrocidines are a group of cyclic decapeptides produced by *Bacillus brevis* and have been shown to reduce fungal infections of dipped grapevine (Troskie *et al*., 2014). As stated previously, many AFPs also break down to harmless amino acids, rather than accumulating as micro-pollutants, which makes them ideal candidates for use in the outdoor environment and crop protection (Spathelf and Rautenbach, 2009).

Antifungal peptides have multiple modes-of-action and can target sterols, mannoproteins and glycerophospholipids in the cell wall and cell membrane of a susceptible fungal pathogen (Fig. 2.2). From a drug development perspective, having multiple drug targets in the cell is advantageous as the rate of resistance development may be limited by the ability of the cell to alter these different target sites (Raaijmakers *et al*., 2010). Furthermore, the cell membranes of both bacteria and fungi are relatively complex and may require multiple adaptions to alter even a single target site so that it is less susceptible to drug activity (Rautenbach *et al.*, 2016). AFPs with intracellular drug targets can inhibit protein synthesis, nucleic acid synthesis, enzymatic activity and contribute to oxidative stress (Brogden 2005; Nguyen *et al.*, 2011; Nicolas, 2009; Jenssen *et al*., 2006).

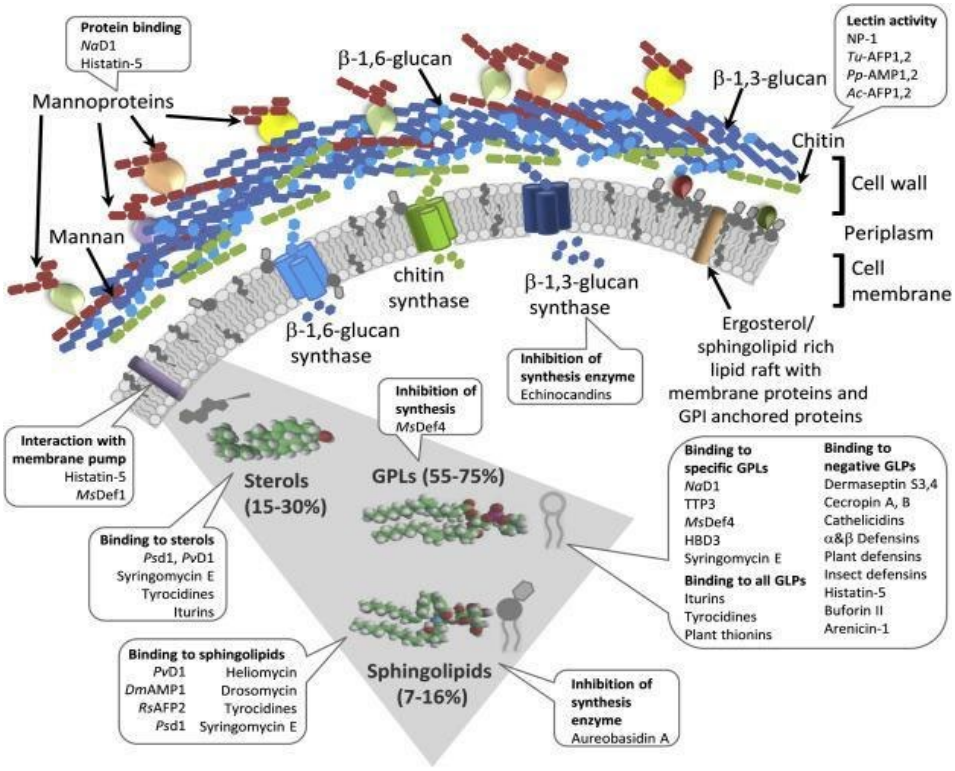

Figure 2.2. Fungal cell wall, cell membrane and cell interior with multiple targets for interaction with several different AFPs (Rautenbach *et al.*, 2016).

Resistance mechanisms against AMPs that have been shown to develop include, cell surface charge alterations which prevent cationic AMPs binding to the cell surface or membrane remodelling in which decoy proteins bind to the membrane and block AMPs from binding to lipid rafts within the cell membrane (Epand and Vogel, 1999). Other adaptations to evade AMPs include using efflux pumps to expel them and mechanisms used by bacterial pathogens as modelled in AMP-resistant bacteria when interacting with the human immune system in Heimlich *et al.* (2014). These mechanisms include cytoplasmic degradation of AMPs targeting the transcriptional machinery, AMP degrading proteins and using outer membrane vesicles to restrict the movement of AMPs (Heimlich *et al.*, 2014). Whether fungal pathogens can adapt the same mechanisms to evade AFPs is not well elucidated.

2.4 Characteristics of antimicrobial lipopeptides

Many AFPs are also called lipopeptides (LPs), based on their chemical nature and hydrophobic interactions with water. LPs are amphipathic and can be cyclic or linear (α-helical or β-sheet), depending on the topology of the peptide chain. These molecules are composed of short (<50) chains of amino acids, with functional groups and a lipophilic fatty acid tail bound to the N-terminus of the peptide (Rautenbach *et al.*, 2016). They are

fast-acting antimicrobial compounds with natural biodegradability by proteases and natural stability to changing environments, particularly if cyclic with a strong terminal N- to C- bond (Rautenbach *et al*., 2015; Troskie *et al.,* 2014). Antifungal LPs also have a diversity of structures which result in multiple modes of action against the same pathogenic fungi.

An excellent example of the structural diversity regarding LP families with several different homologs can be found in LPs produced by *Pseudomona*s and *Bacillus* species. These include both linear and cyclic LPs grouped into main families based on peptide chain and lipid moiety length and composition, as well as the overall molecular configuration (e.g. different cyclisation patterns).

The four main groups of cyclic LPs produced by *Pseudomonas* species include syringomycin (9 amino acid in the peptide chain), viscosin (9 amino acids and a 3-hydroxydecanoic acid lipid tail), amphisin (11 amino acids and 3-hydroxydecanoic acid lipid tail) and tolaasin (19-25 amino acids and a 3-hydroxydecanoic acid or 3-hydroxyoctanoic acid lipid tail). Lesser cyclic LPs produced by *Pseudomonas* species include the putisolvins and arthrofactin, which are structurally different in terms of amino acid number and cyclisation patterns (Raaijmakers *et al*., 2010). Linear LPs produced by *Pseudomonas* species include syringofactins (Berti *et al.,* 2007) and peptin 31 (Fiore *et al*., 2008).

The main cyclic LP families produced by *Bacillus* species include surfactin, iturin and fengycin (Fig. 2.3). They differ in cyclisation patterns as well as peptide length and where specific amino acid residues attach to various points on the peptide chain. For instance, in terms of cyclisation, iturin is a macrolactame (large ring containing an amide bond), and both fengycin and surfactin are macrolactone rings (a large ring containing an ester bond) with their own cyclisation patterns (Raaijmakers *et al*., 2010). More recently described LPs produced by *Bacillus* species which fall outside of the three main families include kurstakin (Hathout *et al*., 2000), maltacines (Hagelin *et al*., 2007), polymyxins and bamylocin A (Lee *et al*., 2007). LPs within each family have different amino acid chain lengths, and each structural variant can form several homologues with different fatty acid chain isometry and variations in fatty acid chain length (Ongena and Jacques, 2008).

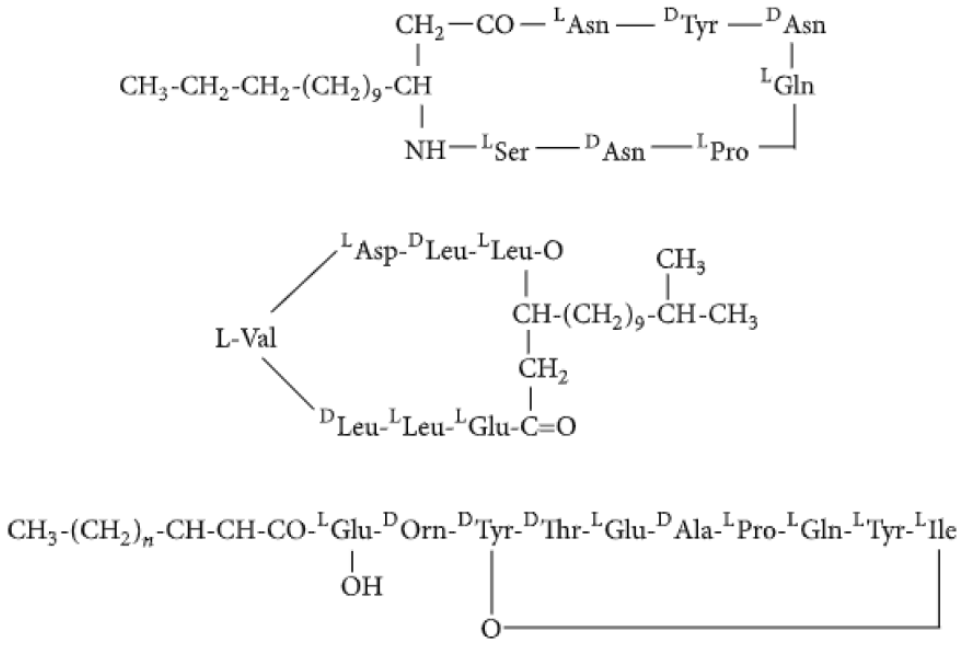

Figure 2.3. Cyclic structures of iturin (Top), surfactin (Middle) and fengycin A (Bottom), containing both hydrophobic and hydrophilic amino acids to indicate amphipathic nature (Meena and Kanwar, 2014).

The primary mode-of-action of LPs against bacteria is pore formation, by embedding into target cell membranes and disrupting cell integrity. Imbalances in transmembrane ion fluxes ensue that lead to cell death (Jenssen *et al.,* 2006). Several models which describe membrane-disruption by an AMP include the barrel-stave, carpet, toroidal pore and aggregate models (Jenssen *et al.,* 2006; Kumar *et al.,* 2018) (Fig. 2.4). These models describe membrane disruption in bacterial cell membranes by α-helical peptides. An exact model for the mode-of-action of cyclic LPs (β-sheet) on the fungal cell membrane has yet to be elucidated. However, the interaction has been localised to the lipid bilayers of the cell membrane (Kumar *et al.,* 2018; Lee *et al.,* 2003). A detergent-like model (Fig. 2.4 D) is said to be the most likely scenario for interactions involving α-helical and β-sheet AMPs, many of which are LPs (Kumar *et al.,* 2018). However, the electrostatic interaction between cationic LPs and anionic phospholipid head groups in the cell membrane remains vague. In this model, LPs increase above a specific threshold concentration in the cell membrane and form a micelle (aggregate of surfactant molecules surrounded by liquid). The micelle eventually breaks away from the cell membrane and leaves open pores through which nutrients and ions can leak out of the cell. This results in osmotic stress which arrests the cell (Ladokhin and White, 2001; Matsuzaki *et al*., 1996). Physiological changes to fungi treated with an antifungal LP can include growth inhibition,

hyphal swelling, hyperbranching, decreased hydrophobicity in treated hyphae, decreased intracellular pH, and decreased activity of mitochondria (Raaijmakers *et al*., 2010).

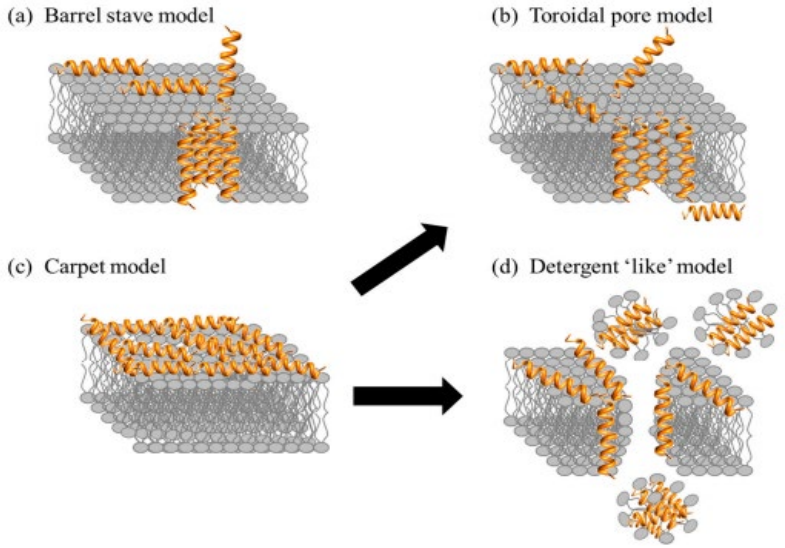

Figure 2.4. Proposed models for AMP mode-of-action including the barrel stave (a), toroidal pore (b), carpet (c) and detergent 'like' (d) models when interacting with a bacterial cell and causing membrane permeabilisation (Kumar *et al.*, 2018).

In addition to their membrane disrupting activities, antifungal LPs can interfere with cell wall synthesis, inhibit depolymerisation of the actin cytoskeleton (Koo *et al*., 2004), produce reactive oxygen species (ROS) which stimulate yeast cell apoptosis (Madeo *et al*., 2009) and disrupt other intracellular targets (De Luca and Walsh, 1999). A selection of antimicrobial LPs with different structures, antifungal activities and producer species are listed in Table 2.2.

Table 2.2 A Selection of antimicrobial LPs with corresponding structures, activities and producer species.

LP	Structure type	Activity	Producer	Reference
Mycosubtilin	Cyclic lipoheptapeptide	Antifungal	*Bacillus subtilis*	(Leclère *et al.,* 2005)
Syringomycin	Lipodepsipeptide	Antifungal, phytotoxic and haemolytic	*Pseudomonas syringae*	(Anselmi *et al.,* 2011)
Serrawettin	Cyclic lipopeptide	Surface active property	*Serratia marcescens W2*	(Chan *et al.,* 2013)
Polymyxin	Cyclic decapeptide	Antifungal, antibacterial and immune-modulating	*Paenibacillus polymyxa*	(Cardoso *et al.,* 2007, He *et al.,* 2007; Kim *et al.,* 2010)

Aureobasidin	Cyclic depsipeptide	Antifungal	*Aureobasidium pullulans*	(Balkovec, 1994; Lotrakul *et al.,* 2009)
Echinocandin	Cyclic hexapeptide	Inhibits β-glucan synthesis	*Aspergillus nidulans*	(Cappelletty and Eiselstein-McKitrick, 2007)
Fengycin	Cyclic lipopeptide	Antifungal (Inhibits β-glucan synthesis)	*Bacillus* and *Paenibacillus*	(Wang *et al.,* 2008; Wei *et al.,* 2010; Zhao *et al.,* 2014)
Iturin	Cyclic lipopeptide	Antifungal (Inhibits β-glucan synthesis)	*Bacillus subtilis*	(Maget-Dana and Peypoux, 1994; Zeriouh *et al.*, 2011)
Surfactin	Cyclic lipopeptide	Antimicrobial, antiviral, insecticidal and enhances hydrocarbon biodegradation	*Bacillus subtilis* *Bacillus amyloliquefaciens*	(Hwang *et al.,* 2007; Whang *et al.,* 2009)
Paenibacterin	Cyclic 13-residue lipopeptide	Antimicrobial (Disrupts phospholipid membrane)	*Paenibacillus thiaminolyticus*	(Huang and Yousef, 2014)

2.4.1 Biological functions of lipopeptides

Microorganisms produce LPs as a defence mechanism against antagonists and to overcome unfavourable environmental conditions. Natural antagonists include other competing microorganisms, attempting to colonise the same plant or animal surface, or microbial predators, like amoeboids (Li *et al.,* 2013b; Ilinskaya *et al.,* 2017). To survive unfavourable environmental conditions, even those caused by reaching a population limit, LPs have non-antagonistic functions which improve cell motility, biofilm formation and scavenging for micronutrients (Tran *et al*., 2007; Nielsen *et al*., 2005). Other functions of LPs are plant-related and improve plant health in exchange for nutrients or an attachment surface (Cawoy *et al*., 2014; Mhlongo *et al.,* 2018; Cordovez *et al.,* 2019).

2.4.1.1 Antagonistic functions of lipopeptides

The reason for increased LP production in the presence of a microbial predator or competing organisms have been well established in both bacteria and fungi (Vollenbroich *et al.,* 1997; Thrane *et al.,* 2000; Van de Mortel *et al.,* 2009; Raaijmakers *et al*., 2010; Chen *et al*., 2013). LPs are produced by these microbial species to deter competing microbes and predators from infringing on an established territory; thus, allowing the LP

producer to protect itself and its resources. However, the production of antimicrobial LPs can also improve the health of the plant or animal surfaces inhabited by these LP producing microbes (Li *et al.,* 2013a; Ilinskaya *et al.,* 2017). For example, in the human gut, both *Bacillus* and *Lactobacillus* species produce LPs which suppress the growth of pathogens, *Clostridium perfringens*, *Staphylococcus aureus*, and food contaminants, *Listeria monocytogenes*, *Salmonella enteritidis*, *Salmonella gallinarum, Escherichia coli*, *Bacillus cereus, Pasteurella haemolytica* and *Serratia marcescens* (Ilinskaya *et al.,* 2017). On the skin of mammals, commensal bacterial also protect the skin from infections caused by *S. aureus* (Li *et al.,* 2013). On plant surfaces, e.g. in the rhizosphere, LP producing microbes defend the plant surfaces from being colonised by phytopathogens (Cawoy *et al*., 2014; Mhlongo *et al.,* 2018). These cases demonstrate how the antagonistic functions of many LPs are important for both producer species and their associated hosts/symbionts. The antimicrobial activity of LPs includes antiviral, antibacterial, antifungal, anti-oomycete, antimycoplasma and antilarval activity (Meena and Kanwar, 2014; Vollenbroich *et al*., 1997; Thrane *et al*., 2000; Van de Mortel *et al*., 2009).

LPs with antibacterial activity include those which inhibit the growth of Gram-positive and Gram-negative bacteria. Gram-positive bacteria susceptible to *Bacillus* LPs include plant pathogens, *Xanthomonas campestris* and *Pseudomonas syringae*, and human pathogens, *Mycobacterium tuberculosis*, *Plasmodium* and *Staphylococcus* species (Makovitzki *et al.,* 2007; Nybroe and Sorensen, 2004). Gram-negative bacteria susceptible to polymyxin, an LP produced by *Paenibacillus polymyxa*, include food pathogens, *Salmonella, Klebsiella, Actinobacter, Fusobacterium, Pseudomonas and Escherichia* species (Meir *et al.,* 2017). It is theorised that the majority of Gram-negative bacteria have an innate tolerance to the majority of LPs which affect Gram-positive bacteria as the outer membrane serves as a permeability barrier for longer LPs which cannot traverse across it (Makovitzki *et al.,* 2007).

Antifungal activities of bacterially produced LPs include biological activity of fengycins against plant pathogens, including *Podosphaera fusca* (Romero *et al*., 2007), *Fusarium graminearum* (Wang *et al*., 2007) and *Botrytis cinerea* (Toure *et al*., 2004); the inhibition of growth in wood staining fungi, nematophagous fungi and environmental isolates of *Aspergillus flavus, Rhizoctonia solani*, *Penicillium roqueforti* and *Colletotrichum demiatum* by iturins (Raaijmakers *et al*., 2010); and some cases of antifungal activity

against *Botrytis cinerea*, *Sclerotinia sclerotiorum*, *Colletotrichum gloeosporioides* and *Phoma complanata* (Plaza *et al*., 2013) by surfactins. Combinations of all three bacterially produced LPs can also be used to improve their activity against specific phytopathogens.

Antimycoplasma and antilarval LPs have been applied to both mycoplasmas and several species of mosquito larvae (Meena and Kanwar, 2014). The susceptible mosquito species include *Anopheles stephensi*, *Culex quinquefasciatus* and *Aedes aegypti*, all of which are known vectors for spreading human diseases such as yellow fever, dengue fever and malaria (Meena and Kanwar, 2014). A surfactin producing *Bacillus* species was suggested as a promising biocontrol agent against these mosquito species, instead of using harmful chemical pesticides (Geetha *et al.,* 2010). Surfactin is also used to clear biotechnological products of mycoplasma contamination and treat human patients without cytotoxic effects. Mycoplasmas are major contaminants of mammalian tissue cultures and also serious contributors to acute urogenital infections, respiratory infections and contracting AIDS (Blanchard and Montagnier, 1994; Meena and Kanwar, 2014). Furthermore, some bacterial LPs produced by *Pseudomonas flourescens* (viscosin) and *Bacillus subtilis* (surfactin) have been shown to cause viral disintegration when applied to viral envelopes (Raaijmakers *et al*., 2010).

In addition to microbial competitors, predatory protozoa, amoebas and nematodes can also be deterred by LPs (Jousset *et al*., 2006; Andersen *et al.,* 2003; Mazzola *et al*., 2009). The nematode *Caenorhabditis elegans* is an excellent example of this as it displays lawn-avoidance patterns when serrawettin W2, produced by *Serratia marcescens,* is added to its immediate environment (Pradel *et al*., 2007). These lawn-avoidance patterns also differ when different LPs are used as a deterrent.

These cases of antimicrobial and antiparasitic activity, coupled with other antitumour, thrombolytic and antiadhesion properties of LPs (Meena and Kanwar, 2014), explain why there are numerous possible commercial applications for these bioactive compounds. Related to medicine, these applications could include biomedical and therapeutic treatments, while for agricultural applications, they could include use as a biocontrol or direct application as a biodegradable pesticide used in crop protection. Only now are LPs starting to be applied in these two industries. However, in the food, biotechnology and cosmetic industries, LPs are already used to preserve the texture, stability and volume of certain products (Meena and Kanwar, 2014). For example, surfactin is used in baking products to provide proper emulsification and prevent the aggregation of fat globules

(Mandal *et al.,* 2013). Other possible applications of LPs to industrial processes could involve eliminating bacterial biofilms from machinery by disrupting the biofilms or altering bacterial motility. Both biofilm formation and motility are non-antagonistic functions influenced by LP production.

2.4.1.2 Non-antagonistic functions of lipopeptides

The effects of LP production on motility is dependent mainly on the ability of LPs to act as a surfactant and change surface viscosity (Andersen *et al.,* 2003). *Pseudomonas fluorescens* demonstrates this on soft agar plates. Some bacteria, lacking genes essential to LP production, are unable to move around on solid agar media. Other studies show a recovery in swimming, swarming and twitching motilities after adding structurally related biosurfactants (Andersen *et al.,* 2003). Adding structurally unrelated synthetic biosurfactants like Triton X-100 and NP40, however, do not have any effect on several LP-deficient *Pseudomonas* and *Bacillus* mutants (Raaijmakers *et al*., 2010). Motility in these bacteria is thus dependent on more than just surface tension reduction but also the chemical attributes of the LPs involved.

Changes in surface viscosity caused by LPs can also influence cell differentiation and behaviours associated with biofilm formation. In this way, the addition of different LPs to different microbial communities can either promote or prevent biofilm formation (Raaijmakers *et al*., 2010). Within a biofilm, some LPs like rhamnolipids produced by *P. aeruginosa* may facilitate biofilm formation and the migration of different microbial subpopulations within the biofilm (Pamp and Tolker-Nielsen, 2007). Putisolvin (produced by *P. putida*), viscosin and massetolide (produced by *P. flourescens*) deficient mutants showed significantly less biofilm formation (Raaijmakers *et al*., 2010). Hofemeister *et al*. (2004) also suggested that surfactin, which facilitates biofilm formation in *B. subtilis* (Davey *et al*., 2003) may be important for oxygen and nutrient distribution as it maintains liquid channels throughout the biofilm. In contrast to these findings, a study conducted by Lopez *et al*. (2009) found surfactin-like molecules to induce a stress response in *B. subtilis* where it may have tried to protect itself from a similar, competing organism. This response included biofilm formation and the release of toxins.

Whether a LP facilitates or disrupts biofilm integrity may be dependent on physicochemical factors (e.g. pH or ionic charge) which determine whether a LP can facilitate or disrupt cell wall attachment to a surface. These factors can cause LPs to re-orient within the cell membrane, exposing either the hydrophobic or the hydrophilic end

of the molecule to the outer environment. If the hydrophobic fatty acid tail extends outward, attachment to a hydrophobic surface is facilitated. If the hydrophilic peptide chain is orientated to the outside, attachment to a hydrophilic surface is much more likely to occur (Mireles *et al*., 2001). These effects have been investigated in biofilms of *Listeria monocytogenes*, *Enterobacter sakazakii* (Mireles *et al*., 2001) and *Salmonella enterica* (Nitschke *et al*., 2009) treated with surfactin.

It has been suggested that bacterial LPs have a binding affinity for metal ions that provides these bacterial species with a competitive advantage in an otherwise toxic environment. As they chelate the metals, the metals become more bioavailable for use by the LP producer and less concentrated in the natural environment as a toxin. For example, surfactin has a natural binding affinity for Ca^{2+} ions, and with a simple substitution of its second amino acid, this affinity can be increased by 300% (Grangemard *et al*., 2001). Iturin has natural affinities for Na^{+}, K^{+} and Rb^{+} (Rautenbach *et al*., 2000). Furthermore, aromatic compounds can be removed from the soils using LPs and glycolipids (GLs) as they have a natural foaming ability and improve the bioavailability of these compounds using aromatic ring oxidation (Phale *et al*., 2007). This is useful for bioremediation efforts, although the biological relevance to the LP producer is simply an increase in the availability of carbon and sometimes nitrogen in the immediate environment.

It should be noted that although most of what is known about the natural production and biological function of LPs is based on bacterial producers, there are many fungal species which produce LPs with different biological functions. For example, LPs produced by *A. nidulans* are hypothesised to offer this filamentous fungus a competitive advantage against closely related organisms as many LP producing *Aspergillus* are also sensitive to foreign LPs (Chen *et al*., 2016). Non-antagonistic functions of LPs for fungal producers are covered in the next section and related to plant pathogenesis and induced systemic resistance.

2.4.1.3 Role in plant pathogenesis and induction of systemic resistance

Plant surfaces and interior parts are colonised by phylogenetically diverse microorganisms, from bacteria, fungi to microbes from other kingdoms. Plants provide sugars, amino acids and organic acids in root and soil exudates to maintain their

rhizosphere- and phyllosphere-associated microbiota. In return, these plant-microbe interactions have beneficial effects on plant health, i.e., improved nutrient acquisition (for example nitrogen fixation), (a)biotic stress tolerance, biocontrol and immune modulation (Stringlis *et al.,* 2018). Lipopeptides, among other compounds, produced by plant host-associated beneficial microbes defend the plant surface indirectly by triggering an immune reaction in the plant called induced systemic resistance (ISR) (Cawoy *et al*., 2014). This response increases the plant's ecological fitness through the secretion of the plant's own defensive peptides against invading phytopathogens (Mhlongo *et al.,* 2018). Some of these peptides eliminate detrimental symbionts, while others may facilitate further crosstalk between the plant and its symbiotic microbiota (Cawoy *et al*., 2014; Mhlongo *et al.,* 2018; Cordovez *et al.,* 2019). It is suggested that this crosstalk is facilitated by root exudates which supply plant-associated microbes with essential nutrients (sugars, amino acids and organic acids) and signalling molecules important for LP production. Lipopeptides can also be used by invading microbes that are detrimental to the plant's health to compete for plant-related microhabitats (Wolpert *et al.,* 1985).

2.4.2 Non-ribosomal and ribosomal biosynthesis of lipopeptides and other peptides

Lipopeptides are synthesised in response to environmental stimuli such as stress, plant exudates, or nutrient deficiency (Cacho *et al.,* 2012). They are synthesised by microorganisms usually as secondary metabolites using non-ribosomal peptide synthetases (NRPSs) or hybrid polyketide synthases and NRPSs (PKSs/NRPSs). In contrast to this, many other peptides are produced using ribosomal gene expression (Raaijmakers *et al*., 2010).

2.4.2.1 Non-ribosomal biosynthesis

Non-ribosomal biosynthetic pathways use multienzyme complexes organised in modules that possess iterative functions to convert substrates into more complex molecules in a sequential process (Fig. 2.5). The large multidomain NRPSs form part of even larger biosynthetic gene clusters (BGCs) incorporating various additional proteins related to transcriptional and posttranscriptional regulation as well as transport. Non-ribosomal biosynthesis can follow either a thiotemplate process, using multiple non-ribosomal synthetases (NRPSs), or a hybrid template process, using both NRPSs and polyketide synthase (PKS).

In the NRPS thiotemplate process (Stein *et al*., 1996), the modules can be divided into initiation and elongation modules. Initiation modules include adenylation domains (A), thiolation domains (T) and condensation domains (C). The A domain uses a single adenosine triphosphate (ATP) to convert a selected amino acid into aminoacyl adenylate. The T domain transports the aminoacyl adenylate to a conserved serine residue on the carrier protein domain. The C domain connects two adjacent modules by forming a bond between them and their respective aminoacyl substitutes (Geissler *et al.*, 2019). Elongation modules include the same A, T and C domains and elongate the peptide backbone until a termination module is added and the C domain catalyses a peptide bond between two amino acids. After that, the peptide is ready for macrocyclisation, cleavage and release. Cleavage uses a thioesterase (TE) if the LP is cyclic and is hydrolytic for linear LPs (Raaijmakers *et al*., 2010; Schneider and Marahiel, 1998).

Production of LPs with the hybrid NRPS and PKS template uses the NRPS system operating in conjunction with PKS and other fatty acid synthetases (Duitman *et al*., 1999; Tsuge *et al*., 2001; Hansen *et al*., 2007; Mizuno *et al*., 2013). As seen with the NRPS template, there are many modular enzymes involved, and elongation of the peptide backbone requires several rounds of condensation, adenylation and thiolation (CAT) before a termination module is added. The thioesterase domain (TE) then initiates macrocyclisation, cleavage and release of the mature peptide.

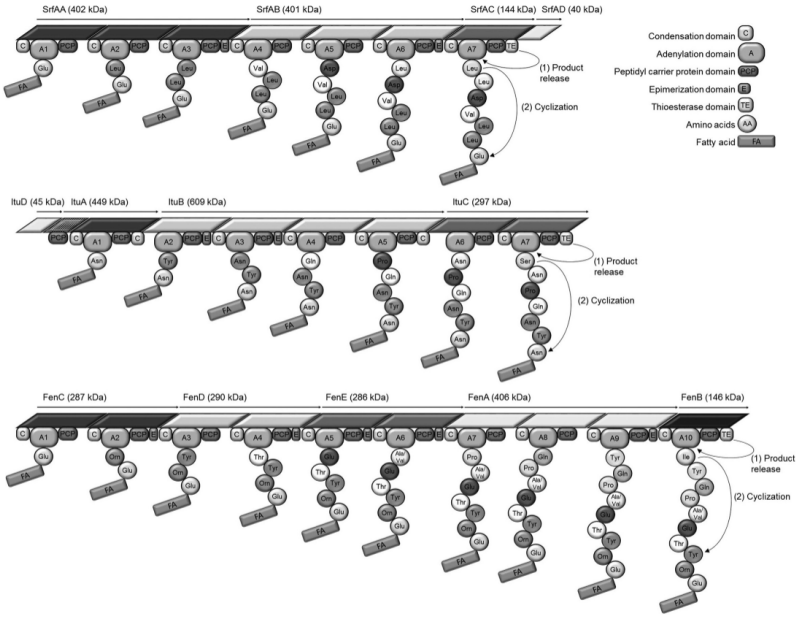

Figure 2.5. Schematic overview of NRPS thiotemplate process with respective modules, domains and amino acids involved in producing surfactin, iturin, and fengycin in *Bacillus* sp. This process was illustrated in Geissler *et al.* (2019).

2.4.2.2 Ribosomal biosynthesis

Ribosomal peptides are gene-encoded and thus restricted in diversity by the number of combinations made with 20 amino acids (Papagianni, 2003; McIntosh *et al.*, 2009). Structural genes are expressed in response to a stimulus and a large precursor molecule produced for post-transcriptional modification. This modification can include cyclisation, isomerisation and glycosylation before the core peptide is cleaved and released into the cytosol as a mature peptide (Arnison *et al.,* 2013; McIntosh *et al.*, 2009). Precursor molecules are guided through the cell and the post-transcriptional modification process by either a lead sequence on the N-terminus, a signal sequence on the N-terminus or a follower peptide on the C-terminus of the precursor molecule (Oman and van der Donk, 2010; Huo *et al*., 2012).

2.4.3 Culture optimisation for increased yields of specific lipopeptides

Several approaches are used to increase the production of LPs. The most effective techniques use media optimisation to provide essential nutrients for the production of these bioactive metabolites (Kumar *et al*., 2018; Rebotiloe *et al*., 2018) or they induce a stress response in the producer organism (Rautenbach *et al.*, 2016). The stress is suggested to emulate unfavourable environmental conditions in which the producer organism would have to compete for survival. In this situation, the producer organism would release LPs to provide a competitive advantage over other coexisting microorganisms.

Essential nutrients for the production of bioactive metabolites such as LPs include carbon and nitrogen. For this reason, adding yeast extract to the media (Costa *et al*., 2002; Narayana and Vijayalakshmi, 2008; Rebotiloe *et al*., 2018) or synthetic nitrogen often results in an increased yield of these compounds (Masurekar *et al*., 1992; Pretorius *et al*., 2015). Nitrogen-rich media such as Luria-Bertani (LB) and trypticase soy broth (TSB), which contain yeast extract, have also been used to increase the antimicrobial activity of *Bacillus* species as described by Kumar *et al*. (2018) and Malash *et al.* (2016), respectively. When excess nitrogen was added to *Glarea lozoyensis*, it increased the yield of the LP pneumocandin A_0 by 10-20-fold (Masurekar *et al*., 1992). However, in other efforts to increase antimicrobial activity, some nitrogen-rich media proved ineffective. For example, nutrient broth (NB) resulted in lower antimicrobial activities observed in *Bacillus* species in Costa *et al*. (2002), Kumar *et al*. (2018) and Rebotiloe *et al*. (2018). This may

be related to the nitrogen source and not the nitrogen concentration as NB contains beef extract while LB contains yeast extract as the organic nitrogen source. It is suggested that yeast extract is the preferred nitrogen source for *Bacillus* species (Rebotiloe *et al*., 2018).

Different carbon sources are also known to affect the antimicrobial activity and production of LPs. For example, in a study optimising LP production in *Bacillus amyloliquefaciens*, LP yields increased significantly when carbon sources were limited to only aromatic hydrocarbons (Masurekar *et al*., 1992). It was suggested that these specific LPs were involved in aromatic ring oxidation (Phale *et al*., 2007). Therefore, if sugar carbon sources are limited, production of these LPs must increase. The sugar alcohol, glycerol, has also been used to increase the yield of the LP pseudofactin in *Pseudomonas* with the addition of specific amino acids (Biniarz *et al.,* 2018). Carbon is used in the assimilation of lipids (Spier *et al.,* 2015) and therefore, it provides some of the necessary components for the production of pseudofactin (Biniarz *et al.,* 2018). In addition to this, water-miscible and water-immiscible carbon substrates have been used to increase production for different surfactin LPs in *Bacillus* and *Pseudomonas* species (Ndlovu *et al*., 2017). These findings all highlight the importance of understanding the cultured organism and its specific needs for producing certain bioactive compounds. The selected carbon source must provide essential nutrients for growth but can also be altered to induce LP production if the LP is involved in improving carbon bioavailability from aromatic carbons. In this way, the selected carbon source can also be used to induce stress in the producer organism.

As LPs are produced primarily as defensive compounds, environmental stress is often used to increase the production of these compounds. As mentioned, certain carbon sources can be used to limit carbon bioavailability. In addition to this nutrient deficiency, oxygen limitation, (Hayes *et al.,* 2019; Nihorimbere *et al*., 2011) and the presence of signalling molecules from root exudates (Ongena *et al*., 2007) or competing microorganisms (Blacutt *et al.,* 2016; Kulimushi *et al*., 2017) have proven effective. However, like specific nutrient availabilities, oxygen availability must not be so low as to eliminate any growth (Nihorimbere *et al*., 2012). Many aerobic organisms only produce high levels of LPs when provided with enough oxygen (Biniarze *et al.,* 2018; Pretorius *et al*., 2015). Temperature and pH must also allow for the production of sufficient biomass to yield biologically relevant amounts of the desired LP (Nihorimbere *et al*., 2012). Furthermore, growing microbial cultures beyond the stationary growth phase are often

used to increases the production of LPs (and all other secondary metabolites) without compromising on the number of cells available to produce these bioactive metabolites (Beltran-Gracia *et al.,* 2017). During stationary growth, both nutrients and oxygen will naturally become limiting as the population exceeds its environmental capacity and the cells will experience stress.

Signalling molecules which also play an important role in LP biosynthesis include quorum sensing (QS) molecules secreted by similar bacterial cells when the population reaches a certain cell density (Oslizlo *et al.,* 2014; Raaijmakers *et al*., 2010). This has been observed during the exponential and early stationary growth phases for *B. subtilis,* where at a certain cell density the ComX pheromone is produced at a high enough concentration to stimulate a two-component regulatory system involved in surfactin biosynthesis (Oslizlo *et al.,* 2014). The ComX can be provided exogenously and binds to *Bacillus* cell receptors which stimulate the regulatory system to expresses *srf* domains involved in LP production. Similar experiments have been conducted on *Pseudomonas* species and suggest that specific concentrations of N-3-hydroxyoctanoyl-homoserine lactone and ppul-rsaL-ppuR, both QS-sensing molecules, are respectively required for the production of cyclic LPs (pultisolvin I and II) in *P. putida* and uncharacterised biosurfactants in *P. fluorescence* (Cui *et al.,* 2005; Dubern *et al.,* 2006).

2.4.4 Feasible sources of antifungal lipopeptides

Lipopeptides are ubiquitous and can be detected in almost any environment using a combination of classical microbiology and analytical chemistry (Kulimushi *et al*., 2017). However, few habitats, even those associated with potent antimicrobial activity, have been investigated for antifungal LPs. It is suggested that this is because most pharmacological and agrochemical research focuses primarily on plant-based compounds and the older, more well-established, antifungal drug classes (Ibrahim *et al.,* 2016). Only recently, with the rapid decline in drug efficacy for existing antifungal drugs, are antifungal LPs receiving more attention.

One revisited source of antifungal compounds are medicinal plants. The microbiota associated with these medicinal plants has proven to be a rich source of bioactive compounds (Huang *et al.,* 2008; Kinsella *et al.,* 2009; Nath *et al.,* 2015; Mhlongo *et al.,* 2018; Ongena *et al.,* 2007; Rebotiloe *et al*., 2018). Similar to other plant-associated microbes, these microbial species are suggested to produce bioactive compounds and protect their host plant from invading organisms. In this manner, some of these bioactive

compounds may contribute to some of the medicinal plant's potent antimicrobial properties. This has been demonstrated in over 30 plants used in East Indian, Chinese and African traditional medicines (Huang *et al.,* 2008; Nath *et al*., 2015; Rebotiloe *et al*., 2018).

South African medicinal plants which remain mainly uncharacterised for any bioactive compounds produced by the plant-associated microbiota include buchu (*Agathosma betulina),* Cape aloe (*Aloe ferox*), cancer bush (*Sutherlandia frutescens*), African ginger (*Siphonochilus aethiopicus*), wild Malva (*Pelargonium cucullatum*), crossberry (*Grewia occidentalis*), shield ferns (*Polystichum pungens*), African wormwood (*Artemisia afra*), water berry trees (*Syzigium cordatum*) and South African geranium (*Pelargonium sidoides)* (Masondo and Makunga, 2019; Street and Prinsloo, 2013; van Vuuren, 2008). Of particular interest in the search for antimicrobial compounds, is the *P. sidoides* plant which is used in traditional African remedies to treat a wide range of microbial infections.

P. sidoides root tuber extract has antimicrobial activity against several bacteria (*Mycobacterium tuberculosis*, *Staphylococcus aureus*, *Streptococcus pneumonia*, *Klebsiella pneumonia*, *E. coli*, and *Pseudomonas aeruginosa*), fungi (*Aspergillus niger*, *Fusarium oxysporum* and *Rhizopus stolonifera*) and opportunistic yeast pathogens (*C. albicans*, *C. glabrata*, *C. krusei* and *C. neoformans*) (Mativandlela *et al*., 2006; Samie *et al*., 2019). *P. sidoides* tubers are used by Xhosa, Sotho, Khoisan and Zulu traditional healers to treat infected wounds, coughs, respiratory tract infections, internal haemorrhaging, stomach problems, diarrhoea, fever and kidney, liver or bladder complaints (Saraswathi *et al*., 2011). Other members of the same plant family have antioxidant and antitumor activity (*P. graveolens*), antiplasmodial activity (*P. panduriforme*, *P. falciparum*, *P. citronellum*, *P quercifolium* and *P. radens*), and insecticidal activity (*P. japonica*, and *P. hortorum*) (Mativandlela *et al*., 2006).

In Western medicine, *P. sidoides* root extract (EPs 7630) has proven to be effective in the treatment of acute bronchitis in a randomised, double-blind, placebo-controlled trial (Brown, 2012; Matthys *et al*., 2003) and approved for treating acute respiratory infections such as bronchitis. It is also added to many cold and flu medications because it has potent antioxidant and immune-boosting properties (Saraswathi *et al*., 2011). For example, in South Africa EPs 7630 is added to cold and flu medications such as Linctagon® and Flugon™. In Brazil, USA, Australia and many European countries, EPs 7630 is added to

cold and flu medications but branded differently UmckaCare or Kaloba, not EPs 7630 or *P. sidoides* extract (Saraswathi *et al*., 2011). Although each of its constituents may operate in concert with one another, the most active components of EPs 7630 are thought to be coumarins (e.g. umckalin) and flavonols (Street and Prinsloo, 2013). This has been determined using liquid chromatography and mass spectrometry (LC-MS) (Street and Prinsloo, 2013). LC-MS is usually the preferred method for the separation, detection and quantification of bioactive compounds in botanical extracts (Masondo and Makunga, 2019). However, even with LC-MS analysis, more than 20% of EPs 7630's constituents have yet to be elucidated (Street and Prinsloo, 2013).

Almost nothing is known about the microbial communities living in association with *P. sidoides* or any of the useful compounds they might produce. Only two studies have characterised endophytic fungi from *P. sidoides* roots or tubers (Aboobaker *et al.,* 2019; Mangany*i et al.,* 2019). In Aboobaker *et al.* (2019), 19 fungal isolates were characterised for antibacterial activity against Gram-positive (*Staphylococcus aureus* and *Enterococcus faecalis*) and Gram-negative bacteria (*Escherichia coli* and *Pseudomonas aeruginosa*) when combined with *P. sidoides* root extracts. One isolate, PS18, was identified as *Penicillium skrjabinii*, a species previously found in association with fynbos in Visagie *et al.* (2015). Crude extract prepared from this isolate had antibacterial activity against both the Gram-positive and Gram-negative bacteria tested. Since *P. sidoides* extracts have antibacterial activity against *S. aureus*, *E. coli* and *P. aeruginosa* (Kayser and Kolodziej, 1997; Moyo *et al.,* 2013), and when combined with some of the endophyte extracts they displayed even greater antibacterial activity (synergistic effect), it was suggested that the endophytic fungi isolated may contribute to some of the tuber extract's antibacterial activity (Aboobaker *et al.*, 2019). Furthermore, dibutyl phthalate was identified in PS18 extract using HPLC-MS and solid-phase trapping nuclear magnetic resonance (SPT-NMR). This compound is a phthalate known to be produced by plant species, *Streptomyces* sp. and one *Penicillium* species, *P. janthinellum*. In the quest for new, more effective antifungal drugs, it is important to investigate these microbes and their bioactive secondary metabolites. In future studies, they may provide humanity with another wave of antifungal drug solutions or crop protecting agricultural sprays.

2.5 Concluding Remarks

The effects of fungal diseases are a global phenomenon, with current antifungal solutions failing to match microorganisms they once so effectively eradicated. Millions of deaths and hundreds of tons of food waste continue to result from both prevailing and emerging fungal pathogens. Every year, cases of developed resistance against existing antifungal solutions rise as pathogens adapt to evade and neutralise antifungal drugs used extensively since the mid-late 1900s. Worse still, patient toxicity and toxic downstream effects on the natural environment are still being reported. For these reasons, the discovery of novel antifungal agents is imperative. These compounds need to be fast-acting and specific in their activity. They also need to be relatively stable and at least partially biodegradable for sustainable use in agricultural practice and crop protection.

Antimicrobial peptides, especially the antifungal LPs, are ideal candidates for new and improved antifungal drugs and agricultural applications. Their rapid activity, natural stability, biodegradability (in the natural environment) and antagonistic functions allow a broad range of possible applications. They are also easily cultured using microbial producers and media optimisation to maximise production. Unfortunately, many potential sources of antifungal LPs have yet to be investigated, and large-scale production of these peptides can still be further optimised. Potential sources of novel antifungal LPs include the marine environments, soils and plant-associated microbiotas. Micro-habitats associated with medicinal plants are particularly promising as they are already proven to produce a wealth of biologically active antimicrobial compounds. Microbes associated with South African medicinal plants are even more promising as they remain acutely neglected regarding their characterisation. Therefore, if characterised, they may be found to produce a very large number of novel LPs, some of which could be developed for future medical and agricultural applications.

2.6 References

Aboobaker Z, Viljoen A, Chen W, Crous PW, Maharaj VJ, van Vuuren S. 2019. Endophytic fungi isolated from *Pelargonium sidoides* DC: Antimicrobial interaction and isolation of a bioactive compound. South African Journal of Botany **122**: 535-542

Adnan M, Hamada M, Hahn M, Li G, Luo C. 2019. Fungicide resistance of *Botrytis cinerea* from strawberry to procymidone and zoxamide in Hubei, China. Phytopathology Research **1**: 1-12

Africa C, Abrantes P. 2017. *Candida* antifungal drug resistance in sub-Saharan African populations: A systematic review. F1000 Research **5**: 1-9

Al-Hatmi A, Meis J, de Hoog G. 2016. *Fusarium*: Molecular diversity and intrinsic drug resistance. PLOS Pathogen **12**: 1-8

Almeida F, Rodrigues ML, Coelho C. 2019. The still underestimated problem of fungal diseases worldwide. Frontiers in Microbiology **10**: 1-5

Andersen JB, Koch B, Nielsen TH. 2003. Surface motility in *Pseudomonas* sp. DSS73 is required for efficient biological containment of the root-pathogenic microfungi *Rhizoctonia solani* and *Pythium ultimum*. Microbiology **149**: 37-46

Anselmi M, Eliseo T, Zanetti-Polzi L, Fullone MR, Fogliano V, Di Nola A, Paci M, Grgurina I. 2011. Structure of the lipodepsipeptide syringomycin E in phospholipids and sodium dodecylsulphate micelle studied by circular dichroism, NMR spectroscopy and molecular dynamics. *Biochimica et Biophysica Acta* (BBA)-Biomembranes **1808**: 2102-2110

Arnison PG, Bibb MJ, Bierbaum G, Bowers AA, Bugni TS, Bulaj G, Camarero JA, Campopiano DJ, Challis GL, Clardy J, Cotter PD, Craik DJ, Dawson M, Dittmann E, Donadio S, Dorrestein PC, Entian K, Fischbach MA, Garavelli JS, Goransson U, Gruber CW, Haft DH, Hemscheidt TK, Hertweck C, Hill C, Horswill AR, Jaspars M, Kelly WL, Klinman JP, Kuipers OP, Link AJ, Liu W, Marahiel MA, Mitchell DA, Moll GN, Moore BS, Muller R, Nair SK, Nes IF, Norris GE, Olivera BM, Onaka H, Patchett ML, Piel J, Reaney MJT, Rebuffat S, Ross RP, Sahl H, Schmidt EW, Selsted ME, Severinov K, Shen B, Sivonen K, Smith L, Stein T, Sussmuth RD, Tagg JR, Tang G, Truman AW, Vederas JC, Walsh CT, Walton JD, Wenzel SC, Willey JM, van der Donk WA. 2013. Ribosomally synthesized and post-translationally modified peptide natural products: overview and recommendations for a universal nomenclature. Natural Products Report **30**: 108160

Azevedo M, Teixeira-Santos R, Silva A, Cruz L, Ricardo E, Pina-Vaz C, Rodrigues A. 2015. The effect of antibacterial and non-antibacterial compounds alone or associated with antifungals upon fungi. Frontiers in Microbiology **6**: 1-7

Azie N, Neofytos D, Pfaller M, Meier-Kriesche H-U, Quan S-P, Horn D. 2012. The PATH (Prospective Antifungal Therapy) Alliance® registry and invasive fungal infections: update 2012. Diagnostic Microbiology and Infectious Disease **73**: 293-300

Baindara P, Korpole S. 2016. Lipopeptides: status and strategies to control fungal infection. Recent trends in antifungal agents and antifungal therapy. Springer, New Delhi. **1**: 97-121

Balkovec JM. 1994. Section review: Anti-infectives: Lipopeptide antifungal agents, Expert Opinion on Investigational Drugs **3**: 65-82

Beltran-Gracia E, Macedo-Raygoza G, Villafaña-Rojas J, Martinez-Rodriguez A, Chavez-Castrillon Y, Espinosa-Escalante F, Di Mascio P, Ogura T, Beltran-Garcia, M. 2017. Production of lipopeptides by fermentation processes: Endophytic bacteria, fermentation strategies and easy methods for bacterial selection. Fermentation Processes **11**: 200-217

Berger S, El Chazli Y, Babu A, Coste A. 2017. Azole resistance in *Aspergillus fumigatus*: A consequence of antifungal use in agriculture? Frontiers in Microbiology **8**: 1024

Berti AD, Greve NJ, Christensen QH, Thomas MG. 2007. Identification of a biosynthetic gene cluster and the six associated lipopeptides involved in swarming motility of *Pseudomonas syringae* pv. Tomato DC3000. Bacteriology **189**: 6312-6323

Biniarz P, Coutte F, Gancel F, Łukaszewicz M. 2018. High-throughput optimization of medium components and culture conditions for the efficient production of a lipopeptide pseudofactin by *Pseudomonas fluorescens* BD5. Microbial Cell Factories **17**: 121

Blacutt A, Mitchell TR, Bacon CW, Gold SE. 2016. *Bacillus mojavensis* RRC101 lipopeptides provoke physiological and metabolic changes during antagonism against *Fusarium verticillioides*. Molecular Plant-Microbe Interactions **29**: 713-723

Blanchard A, Montagnier L. 1994. AIDS-associated mycoplasmas. Annual Review of Microbiology **48**: 687-712

Breeze E. 2019. 97 shades of gray: Genetic interactions of the gray mold, *Botrytis cinerea*, with wild and domesticated tomato. The Plant Cell **31**: 280-281

Brogden KA. 2005. Antimicrobial peptides: pore formers or metabolic inhibitors in bacteria? Nature Reviews Microbiology **3**: 238-250

Brown GD, Denning DW, Gow NAR, Levitz SM, Netea MG, White TC. 2012. Hidden killers: Human fungal infections. Science Translational Medicine **4**: 165

Cacho RA, Jiang W, Chooi YH, Walsh CT, Tang Y. 2012. Identification and characterization of the echinocandin B biosynthetic gene cluster from *Emericella rugulosa* NRRL 11440. Journal of the American Chemical Society **134**: 16781-16790

Campbell MA, Staats M, van Kan JAL, Rokas A, Slot JC. 2013. Repeated loss of an anciently horizontally transferred gene cluster in *Botrytis*, Mycologia. **105**: 1126-1134

Cappelletty D, Eiselstein-McKitrick K. 2007. The echinocandins. Pharmacotherapy **27**: 369-388

Cardoso LS, Araujo MI, Góes AM, Pacífico LG, Oliveira RR, Oliveira SC. 2007. Polymyxin B as inhibitor of LPS contamination of *Schistosoma mansoni* recombinant proteins in human cytokine analysis. Microbial Cell Factories **6**: 1

Casadevall A. 2017. Don't forget the fungi when considering global catastrophic biorisks. Health Security **15**: 341-342

Casadevall A. 2019. Global catastrophic threats from the fungal kingdom: Fungal catastrophic threats. Current Topics in Microbiology and Immunology **1**: 1-12

Cawoy H, Debois D, Franzil L, De Pauw E, Thonart P, Ongena M. 2014. Lipopeptides as main ingredients for inhibition of fungal phytopathogens by *Bacillus subtilis/amyloliquefaciens.* Microbial Biotechnology **8**: 281-295

Chan XY, Chang CY, Hong KW, Tee KK, Yin WF, Chan KG. 2013. Insights of biosurfactant producing *Serratia marcescens* strain W2.3 isolated from diseased tilapia fish: a draft genome analysis. Gut Pathogens **5**: 29

Chen AJ, Frisvad JC, Sun BD, Varga J, Kocsubé S, Dijksterhuis J, Kim D, Hong S, Houbraken J, Samson R. 2016. *Aspergillus* section *Nidulantes* (formerly *Emericella*): Polyphasic taxonomy, chemistry and biology. Studies in Mycology **84**: 1-118

Chen L, Yue Q, Zhang X, Xiang M, Wang C, Li S, Che Y, Ortiz-López F, Bills G, Liu, X, An Z. 2013. Genomics-driven discovery of the pneumocandin biosynthetic gene cluster in the fungus *Glarea lozoyensis*. BioMed Central Genomics **14**: 339

Cordovez V, Dini-Andreote F, Carrión VJ, Raaijmakers JM. 2019. Ecology and evolution of plant microbiomes. Annual Review of Microbiology **73**: 69-88

Costa E, Teixido N, Usall J, Atares E, Vinas I. 2002. The effect of nitrogen and carbon sources on growth of the biocontrol agent *Pantoea agglomerans* strain CPA-2. Letters in Applied Microbiology **35**: 117-120

Cui X, Harling R, Mutch P, Darling D. 2005. Identification of N −3-hydroxyoctanoyl-homoserine lactone production in *Pseudomonas fluorescens* 5064, pathogenic to broccoli, and controlling biosurfactant production by quorum sensing. European Journal of Plant Pathology **111**: 297–308

Damodaran T, Mishra VK, Jha SK, Gopal R, Rajan S, Ahmed I. 2019. First report of *Fusarium* Wilt in banana caused by *Fusarium oxysporum* sp. *cubense* tropical race 4 in India. Plant Disease **103**: 1022-1022

Datta A. 2009. Globalization: The African perspective. Jadavpur Journal of International Relations **13**: 131–140

Davey ME, Caiazza NC, O'Toole GA. 2003. Rhamnolipid surfactant production affects biofilm architecture in *Pseudomonas aeruginosa* PAO1. Journal of Bacteriology **185**: 1027-1036

De Crecy E, Jaronski S, Lyons B, Lyons TJ, Keyhani NO. 2009. Directed evolution of a filamentous fungus for thermotolerance. BioMed Central Biotechnology **9**: 74

De Luca AJ, Walsh TJ. 1999. Antifungal peptides: novel therapeutic compounds against emerging pathogens. Antimicrobial Agents and Chemotherapy **43**: 1-11

De Senna A, Lathrop A. 2017. Antifungal screening of bioprotective isolates against *Botrytis cinerea*, *Fusarium pallidoroseum* and *Fusarium moniliforme*. Fermentation **3**: 53

Dubern JF, Lugtenberg BJJ, Bloemberg GV. 2006. The ppuI-rsaL-ppuR quorum-sensing system regulates biofilm formation of *Pseudomonas putida* PCL1445 by controlling biosynthesis of the cyclic lipopeptides putisolvins I and II. Journal Bacteriology **188**: 2898-2906

Dubos RJ. 1939. Studies on a bactericidal agent extracted from a soil bacillus: i. preparation of the agent. its activity in vitro. Journal of Experimental Medicine **70**: 1-10

Duitman EH, Hamoen LW, Rembold M, Venema G, Seitz H, Saenger W, Bernhard F, Reinhardt R, Schmidt M, Ullrich C, Stein T, Leenders F, Vater J. 1999. The mycosubtilin synthetase of *Bacillus subtilis* ATCC6633: A multifunctional hybrid between a peptide synthetase, an amino acid transferase, and a fatty acid synthase. Proceedings of the National Academy of Sciences of the United States of America **96**: 13294-13299

El-Houssaini H, Elnabawy O, Nasser H, Elkhatib W. 2019. Correlation between antifungal resistance and virulence factors in *Candida albicans* recovered from vaginal specimens. Microbial Pathogenesis **128**: 13-19

Epand RM, Vogel HJ. 1999. Diversity of antimicrobial peptides and their mechanisms of action. *Biochimica et Biophysica Acta* (BBA) - Biomembranes **1462**:11-28

Fiore A, Mannina L, Sobolev AP. 2008. Bioactive lipopeptides of ice-nucleating snow bacterium *Pseudomonas syringae* strain 31R1. FEMS Letters **286**: 158–165

Fisher MC, Hawkins NJ, Sanglard D, Gurr SJ. 2018. Worldwide emergence of resistance to antifungal drugs challenges human health and food security. Science **360**: 739-742

Garcia-Solache MA, Casadevall A. 2010. Global warming will bring new fungal diseases for mammals. ASM Biology **1:** 1-3

Geetha I, Manonmani AM, Paily KP. 2010. Identification and characterization of a mosquito pupicidal metabolite of a *Bacillus subtilis* subsp. *subtilis* strain. Applied Microbiology and Biotechnology **86**: 1737-1744

Geissler M, Heravi KM, Henkel M, Hausmann R. 2019. Lipopeptide biosurfactants from B*acillus* species. *In* Biobased Surfactants. Elsevier **1**: 205-240

Godfray HC, Mason-D'Croz D, Robinson S. 2016. Food system consequences of a fungal disease epidemic in a major crop. Philosophical Transactions of the Royal Society B: Biological Sciences **371**: 20150467

Grangemard I, Wallach J, Maget-Dana R, Peypoux F. 2001. Lichenysin: a more efficient cation chelator than surfactin. Applied Biochemistry and Biotechnology **90**: 199-210

Gray KC, Palacios DS, Dailey I, Endo MM, Uno BE, Wilcock BC, Burke MD. 2012. Amphotericin primarily kills yeast by simply binding ergosterol. Proceedings of the National Academy of Sciences of the United States of America **109**: 2234-2239

Guinea J. 2014. Global trends in the distribution of *Candida* species causing candidemia. Clinical Microbiology and Infection **20**: 5-10

Hagelin G, Indrevoll B, Hoeg-Jensen T. 2007. Use of synthetic analogues in confirmation of structure of the peptide antibiotics maltacines. International Journal of Mass Spectrometry **268**: 254-264

Hahn M. 2014. The rising threat of fungicide resistance in plant pathogenic fungi: *Botrytis* as a case study. Journal of Chemical Biology **7**: 133-141

Hansen DB, Bumpus SB, Aron ZD, Kelleher NL, Walsh CT. 2007. The loading module of mycosubtilin: an adenylation domain with fatty acid selectivity. Journal of American Chemical Society **129**: 6366-6367

Hathout Y, Ho YP, Ryzhov V, Demirev P, Fenselau C. 2000. Kurstakins: A new class of lipopeptides isolated from *Bacillus thuringiensis*. Journal of Natural Products **63**: 1492-1496

Hayes DG, Solaiman DK, Ashby RD. 2019. Biobased surfactants: Synthesis, properties, and applications. 2nd ed. London: Academic Press 229

He Z, Kisla D, Zhang L, Yuan C, Green-Church KB, Yousef AE. 2007. Isolation and identification of a *Paenibacillus polymyxa* strain that coproduces a novel lantibiotic and polymyxin. Applied Environmental Microbiology **73**: 168-178

Heimlich DR, Harrison A, Mason KM. 2014. Host antimicrobial peptides in bacterial homeostasis and pathogenesis of disease. Antibiotics **3**: 645-676

Hofemeister J, Conrad B, Adler B. 2004. Genetic analysis of the biosynthesis of non-ribosomal peptide- and polyketide like antibiotics, iron uptake and biofilm formation by *Bacillus subtilis* A1/3. Molecular Genetics and Genomics **272**: 363-378

Howard SJ, Cerar D, Anderson MJ, Albarrag A, Fisher MC, Pasqualotto AC, Laverdiere M, Arendrup MC, Perlin DS, Denning DW. 2009. Frequency and evolution of azole resistance in *Aspergillus fumigatus* associated with treatment failure. Emerging Infection and Disease. **15**:1068-1076

Hua L, Yong C, Zhanquan Z, Boqiang L, Guozheng Q, Shiping T. 2018. Pathogenic mechanisms and control strategies of *Botrytis cinerea* causing post-harvest decay in fruits and vegetables. Food Quality and Safety **2**: 111-119

Huang W, Cai Y, Hyde K. Corke H, Sun M. 2008. Biodiversity of endophytic fungi associated with 29 traditional Chinese medicinal plants. Fungal Diversity **33**: 61-75

Huang E, Yousef AE. 2014. The lipopeptide antibiotic paenibacterin binds to the bacterial outer membrane and exerts bactericidal activity through cytoplasmic membrane damage. Applied and Environmental Microbiology **80**(9): 2700-2704

Huo L, Rachid S, Stadler M, Wenzel SC, Müller R. 2012 Synthetic biotechnology to study and engineer ribosomal bottromycin biosynthesis. Chemistry and Biology. **19**: 1278-1287

Hwang Y-H, Park B-K, Lim J-H, Kim M-S, Park S-C, Hwang M-H, Yun H-I. 2007. Lipopolysaccharide-binding and neutralizing activities of surfactin C in experimental models of septic shock. European Journal of Pharmacology **556**: 166-171

Ibrahim M. 2016. Phytochemical analysis and antibacterial activities of different callus extracts of *Pelargonium sidoides*. New Biotechnology **33**: 161

Ilinskaya ON, Ulyanova VV, Yarullina DR, Gataullin IG. 2017. Secretome of intestinal Bacilli: A natural guard against pathologies. Frontiers in Microbiology **8**: 1666

Jeffery-Smith A, Taori SK, Schelenz S, Jeffery K, Johnson EM, Borman A, Manuel R, Brown CS. 2018. *Candida auris*: A review of the literature. Clinical Microbiology Reviews. ASM **31**: 1-18

Jenssen H, Hamill P, Hancock REW. 2006. Peptide antimicrobial agents. Clinical Microbiology Reviews. ASM **19**: 491-511

Jousset A, Lara E, Wall LG, Valverde C. 2006. Secondary metabolites help biocontrol strain *Pseudomonas fluorescens* CHA0 to escape protozoan grazing. Applied and Environmental Microbiology. ASM **72**: 7083-7090

Kayser O, Kolodziej H. 1997. Antibacterial activity of extracts and constituents of *Pelargonium sidoides* and *Pelargonium reniforme*. Planta Medica **63**: 508-510

Keymanesh K, Soltani S, Sardari S. 2009. Application of antimicrobial peptides in agriculture and food industry. World Journal of Microbiology and Biotechnology **25**: 933-944

Khan N, Maymon M, Hirsch AM. 2017. Combating *Fusarium* infection using *Bacillus*-based antimicrobials. Microorganisms **5**: 75

Kim JF, Jeong H, Park S-Y, Kim S-B, Park YK, Choi S-K, Ryu C-M, Hur C-G, Ghim S-Y, Oh TK, Kim JJ, Park CS, Park S-H. 2010. Genome sequence of the polymyxin-producing plant-probiotic rhizobacterium *Paenibacillus polymyxa* E681. Journal of Bacteriology **192**: 6103-6104

Kinsella K, Schulthess CP, Morris TF, Stuart JD. 2009. Rapid quantification of *Bacillus subtilis* antibiotics in the rhizosphere. Soil Biology and Biochemistry **41**: 374-379

Köhler JR, Casadevall A, Perfect J. 2014. The spectrum of fungi that infects humans. Cold Spring Harbour Perspectives in Medicine **5**: 19273

Koo JC, Lee B, Young ME, Koo SC, Cooper JA, Baek D, Lim CO, Lee SY, Yun DJ, Cho MJ. 2004. Pn-AMP1, a plant defence protein, induces actin depolarization in yeasts. Plant and Cell Physiology. **45**: 1669-1680

Kullberg BJ, Arendrup MC. 2015. Invasive Candidiasis. The New England Journal of Medicine **373**: 1445-1456

Kulimushi P, Aries A, Franzil S, Onenga M. 2017. Stimulation of fengycin-type antifungal lipopeptides in *Bacillus amyloliquefaciens* in the presence of the maize fungal pathogen *Rhizomucor variabilis*. Frontiers in Microbiology **8**: 850

Kumar P, Kizhakkedathu JN, Straus SK. 2018. Antimicrobial peptides: Diversity, mechanism of action and strategies to improve the activity and biocompatibility *In Vivo*. Biomolecules **8**: 4

Kupferschmidt K. 2019. New drugs target growing threat of fatal fungi. Science **366**: 407

Ladokhin AS, White SH. 2001. 'Detergent-like' permeabilization of anionic lipid vesicles by melittin. *Biochimica et Biophysica Acta* (BBA)-Biomembranes **1514**: 253-260

Leclère V, Béchet M, Adam A, Guez JS, Wathelet B, Ongena M, Thonart P, Gancel F, Chollet-Imbert M, Jacques P. 2005. Mycosubtilin overproduction by *Bacillus subtilis* BBG100 enhances the organism's antagonistic and biocontrol activities. Applied and Environmental Microbiology **71**: 4577-84

Lee DG, Kim HK, Kim SA, Park Y, Park SC, Jang SH, Hahm KS. 2003. Fungicidal effect of indolicidin and its interaction with phospholipid membranes. Biochemical and Biophysical Research Communications **305**: 305-310

Lee SC, Kim SH, Park IH, Chung SY, Choi YL. 2007. Isolation and structural analysis of bamylocin A, novel lipopeptide from *Bacillus amyloliquefaciens* LP03 having antagonistic and crude oil-emulsifying activity. Archives of Microbiology **188**: 307-312

Lewis CM, Persoons A, Bebber DP, Kigathi RN, Maintz J, Findlay K, Bueno-Sancho V, Corredor-Moreno P, Harrington SA, Kangara N, Berlin A, García R, Germán SE, Hanzalová A, Hodson DP, Hovmøller MS, Huerta-Espino J, Imtiaz M, Mirza JI, Justesen AF, Niks RE, Omrani A, Patpour M, Pretorius ZA, Roohparvar R, Sela H, Singh RP, Steffenson B, Visser B, Fenwick PM, Thomas J, Wulff BBH, Saunders DGO. 2018. Potential for re-emergence of wheat stem rust in the United Kingdom. Communications Biology **1**: 1-9

Li Y, Han L, Zhang Y, Fu X, Chen X, Zhang L, Mei R, Wang Q. 2013a. Biological control of apple ring rot on fruit by *Bacillus amyloliquefaciens* 9001. The Plant Pathology Journal **29**: 168-172

Li D, Lei H, Li Z, Li H, Wang Y, Lai Y. 2013b. A novel lipopeptide from skin commensal activates TLR2/CD36-p38 MAPK signalling to increase antibacterial defence against bacterial infection. PLoS ONE **8**: 58288

Lopez D, Vlamakis H, Losick R, Kolter R. 2009. Cannibalism enhances biofilm development in *Bacillus subtilis*. Molecular Microbiology **74**: 609-618

Lotrakul P, Deenarn P, Prasongsuk S, Punnapayak H. 2009. Isolation of *Aureobasidium pullulans* from bathroom surfaces and their antifungal activity against some *Aspergilli*. African Journal of Microbiology Research **3**: 253-7

Lucas JA. 2017. Fungi, food crops, and biosecurity: Advances and challenges. Advances in Food Security and Sustainability **1**: 1-40

Madeo F, Carmona-Gutierrez D, Ring J, Büttner S, Eisenberg T, Kroemer G. 2009. Caspase-dependent and caspase-independent cell death pathways in yeast. Biochemical and Biophysical Research Communications **382**: 227-231

Maget-Dana R, Peypoux F. 1994. Iturins, a special class of pore-forming lipopeptides: biological and physicochemical properties. Toxicology **87**: 151-174

Makovitzki A, Viterbo A, Brotman Y, Chet I, Shai Y. 2007. Inhibition of fungal and bacterial plant pathogens *in vitro* and *in planta* with ultrashort cationic lipopeptides. Applied and Environmental Microbiology **73**: 6629-6636

Malash MA, El-Naggar MM, El Hassayeb HEA, Ibrahim MS. 2016. Production of antimicrobial pyrrol derivatives acting against some fish pathogens from marine *Bacillus pumilusm*. Global Veterinaria **17**: 495-505

Malayeri FA, Rezaei AA, Raiesi O. 2018. Antifungal agents: Polyene, azole, antimetabolite, other and future agents. Journal of Basic Research in Medical Sciences **5**: 48-55

Mandal SM, Barbosa AEAD, Franco OL. 2013. Lipopeptides in microbial infection control: scope and reality for industry. Biotechnology Advances **31**: 338-345

Manganyi MC, Tchatchouang C-DK, Regnier T, Bezuidenhout CC, Ateba CN. 2019. Bioactive compound produced by endophytic fungi isolated from *Pelargonium sidoides* against selected bacteria of clinical importance. Mycobiology **47**: 335-339

Masondo NA, Makunga NP. 2019. Advancement of analytical techniques in some South African commercialized medicinal plants: Current and future perspectives. South African Journal of Botany **126**: 40-57

Masurekar PS, Fountoulakis JM, Hallada TC, Sosa MS, Kaplan L. 1992. Pneumocandins from *Zalerion arboricola*. II. Modification of product spectrum by mutation and medium manipulation. The Journal of Antibiotics **45**: 1867-1874

Matejuk A, Leng Q, Begum M, Woodle M, Scaria P, Chou S, Mixson A. 2010. Peptide-based antifungal therapies against emerging infections. Drugs of the Future **35**: 197

Matsuzaki K, Nakamura A, Murase O, Sugishita K, Fujii N, Miyajima K. 1997. Modulation of magainin 2-lipid bilayer interactions by peptide charge. Biochemistry **36**: 2104-2111

Mativandlela SPN, Lall N, Meyer JJM. 2006. Antibacterial, antifungal and antitubercular activity of (the roots of) *Pelargonium reniforme* (CURT) and *Pelargonium sidoides* (DC) (*Geraniaceae*) root extracts. South African Journal of Botany **72**: 232-237

Mazzola M, de Bruijn I, Cohen MF, Raaijmakers JM. 2009. Protozoan-induced regulation of cyclic lipopeptide biosynthesis is an effective predation defence mechanism for *Pseudomonas fluorescens*. Applied and Environmental Microbiology **75**: 6804–6811

Mazu TK, Bricker BA, Flores-Rozas HY, Ablordeppey SY. 2016. The mechanistic targets of antifungal agents: An overview. Mini-Reviews in Medicinal Chemistry **16**: 555-578

Meena KR, Kanwar SS. 2014. Lipopeptides as the antifungal and antibacterial agents: applications in food safety and therapeutics. Biomed Research International **2015**: 473050

Meir O, Zaknoon F, Cogan U, Mor A. 2017. A broad-spectrum bactericidal lipopeptide with anti-biofilm properties. Scientific Reports **7**: 2198

Mercier A, Carpentier F, Duplaix C, Auger A, Pradier J-M, Viaud M, Gladieux P, Walker A-S. 2019. The polyphagous plant pathogenic fungus *Botrytis cinerea* encompasses host-specialized and generalist populations. Environmental Microbiology. **21**: 4808-4821

McIntosh JA, Donia MS, Schmidt EW. 2009. Ribosomal peptide natural products: bridging the ribosomal and nonribosomal worlds. Natural Product Reports **26**: 537559

Mhlongo MI, Piater LA, Madala NE, Labuschagne N, Dubery IA. 2018. The chemistry of plant-microbe interactions in the rhizosphere and the potential for metabolomics to reveal signalling related to defence priming and induced systemic resistance. Frontiers in Plant Science **9**: 112

Mireles JR, Toguchi A, Harshey RM. 2001. *Salmonella enterica* serovar *typhimurium* swarming mutants with altered biofilm forming abilities: surfactin inhibits biofilm formation. Journal of Bacteriology **183**: 5848-5854

Mizuno CM, Kimes NE, López-Pérez M, Ausó E, Rodriguez-Valera F, Ghai R. 2013. A hybrid NRPS-PKS gene cluster related to the bleomycin family of antitumor antibiotics in *Alteromonas macleodii* strains. PLoS ONE **8**: 76021

Moyo M, Aremu AO, Gruz J, Šubrtová M, Szüčová L, Doležal K, Van Staden J. 2013. Conservation strategy for *Pelargonium sidoides* DC: Phenolic profile and pharmacological activity of acclimatized plants derived from tissue culture. Journal of Ethnopharmacology **149**: 557–561

Mpoza E, Rhein J, Abassi M. 2018. Emerging fluconazole resistance: Implications for the management of cryptococcal meningitis. Medical Mycology Case Reports **19**: 30-32

Narayana KJP, Vijayalakshmi M. 2008. Optimization of antimicrobial metabolites production by *Streptomyces albidoflavus*. Research Journal of Pharmacology **2**: 4-7

Nath A, Chattopadhyay A, Joshi SR. 2015. Biological activity of endophytic fungi of *Rauwolfia serpentina Benth*: An ethnomedicinal plant used in folk medicines in Northeast India. Proceedings of the National Academy of Sciences, India Section B: Biological Sciences **85**: 233-240

Ndlovu T, Rautenbach M, Khan S and Khan W. 2017. Variants of lipopeptide and glycolipids produced by *Bacillus amyloliquefaciens* and *Pseudomonas aeruginosa* cultured in different carbon substrates. AMB Express **7**: 109

Nguyen LT, Haney EF, Vogel HJ. 2011. The expanding scope of antimicrobial peptide structures and their modes of action. Trends in Biotechnology. **29**: 46447210

Nicolas P. 2009. Multifunctional host defence peptides: intracellular-targeting antimicrobial peptides. FEBS Journal. **276**: 6483-6496

Nielsen TH, Nybroe O, Koch B, Hansen M, Sørensen J. 2005. Genes involved in cyclic lipopeptide production are important for seed and straw colonization by *Pseudomonas* sp. strain DSS73. Applied and Environmental Microbiology **71**: 4112-4116

Nihorimbere V, Cawoy H, Seyer A, Brunelle A, Thonart P, Ongena M. 2012. Impact of rhizosphere factors on cyclic lipopeptide signature from the plant beneficial strain *Bacillus amyloliquefaciens S499*. Microbiology Ecology. Federation of European Microbiological Societies **79**: 176-191

Nitschke M, Araujo LV, Costa S. 2009. Surfactin reduces the adhesion of food-borne pathogenic bacteria to solid surfaces. Letters in Applied Microbiology **49**: 241-247

Nybroe O, Sørensen J. 2004. Production of cyclic lipopeptides by fluorescent pseudomonads. *Pseudomonas*. Boston: Springer US **1**: 147-172

Oman TJ, van der Donk WA. 2010. Follow the leader: the use of leader peptides to guide natural product biosynthesis. Nature Chemical Biology **6**: 9-18

Ongena M, Jacques P. 2008. *Bacillus* lipopeptides: versatile weapons for plant disease biocontrol. Trends in Microbiology **16**: 115-125

Ongena M, Jourdan E, Adam A. 2007. Surfactin and fengycin lipopeptides of *Bacillus subtilis* as elicitors of induced systemic resistance in plants. Environmental Microbiology **9**: 1084-1090

Oslizlo A, Stefanic P, Dogsa I, Mandic-Mulec I. 2014. Private link between signal and response in Bacillus subtilis quorum sensing. Proceedings of the National Academy of Sciences of the United States of America **111**: 1586-1591

Pamp SJ, Tolker-Nielsen T. 2007. Multiple roles of biosurfactants in structural biofilm development by *Pseudomonas aeruginosa*. Journal of Bacteriology **189**: 2531-2539

Papagianni M. 2003. Ribosomally synthesized peptides with antimicrobial properties: biosynthesis, structure, function, and applications. Biotechnology Advances **21**: 465-499

Perea S, López-Ribot JL, Kirkpatrick WR, McAtee RK, Santillán RA, Martínez M, Calabrese D, Sanglard D, Patterson TF. 2001. Prevalence of molecular mechanisms of resistance to azole antifungal agents in *Candida albicans* strains displaying high-level fluconazole resistance isolated from human immunodeficiency virus-infected patients. Antimicrobial Agents and Chemotherapy **45**: 2676-2684

Perfect JR, Dismukes WE, Dromer F, Goldman DL, Graybill JR, Hamill RJ, Harrison TS, Larsen RA, Lortholary O, Nguyen MH, Pappas PG, Powderly WG, Singh N, Sobel JD, Sorrell TC. 2010. Clinical practice guidelines for the management of cryptococcal disease: 2010 update by the Infectious Disease Society of America. Clinical Infectious Diseases **50**: 291-322

Peterson E, Kaur P. 2018. Antibiotic resistance mechanisms in bacteria: Relationships between resistance determinants of antibiotic producers, environmental bacteria, and clinical pathogens. Frontiers in Microbiology **9**: 2928

Phale PS, Basu A, Majhi PD, Deveryshetty J, Vamsee-Krishna C, Shrivastava R. 2007. Metabolic diversity in bacterial degradation of aromatic compounds. Omics **11**: 252-279

Pianalto KM, Alspaugh JA. 2016. New horizons in antifungal therapy. Journal of Fungi **2**: 26

Płaza GA, Turek A, Król E. 2013. Antifungal and antibacterial properties of surfactin isolated from Bacillus subtilis growing on molasses. African Journal of Microbiology Research **7**: 3165-3170

Pradel E, Zhang Y, Pujol N, Matsuyama T, Bargmann CI, Ewbank JJ. 2007. Detection and avoidance of a natural product from the pathogenic bacterium *Serratia marcescens* by *Caenorhabditis elegans*. Proceedings of the National Academy of Sciences of the United States of America **104**: 2295-2300

Pretorius D, van Rooyen J, Clarke KG. 2015. Enhanced production of antifungal lipopeptides by *Bacillus amyloliquefaciens* for biocontrol of postharvest disease. New Biotechnology **32**: 243-252

Price CL, Parker JE, Warrilow AG, Kelly DE, Kelly SL. 2015. Azole fungicides - understanding resistance mechanisms in agricultural fungal pathogens. Pest Management Science **71**: 1054-1058

Price NS. 1995. The origin and development of banana and plantain cultivation. Bananas and Plantains **1**: 1-13

Raaijmakers JM, De Brujin I, Nybroe O and Ongena M. 2010. Natural functions of lipopeptides from *Bacillus* and *Pseudomonas*: more than surfactants and antibiotics. FEMS Microbiology Reviews **34**: 1037-1062

Rajasingham R, Smith RM, Park BJ, Jarvis JN, Govender NP, Chiller TM, Denning DW, Loyse A, Boulware DR. 2017. Global burden of disease of HIV-associated cryptococcal meningitis: An updated analysis. Lancet Infectious Disease **17**: 873-881

Rautenbach M, Swart P, van der Merwe MJ. 2000. The interaction of analogues of the antimicrobial lipopeptide, iturin A2, with alkali metal ions. Bioorganic and Medicinal Chemistry **8**: 2539-2548

Rautenbach M, Troskie A, Vosloo JA. 2016. Antifungal peptides: To be or not to be membrane active. Biochimie **130**: 132-145

Rautenbach M, Vosloo JA, Van Rensburg W, Engelbrecht Y. 2015. Natural antimicrobial peptides as green microbicides in agriculture: A proof of concept study on the tyrocidines from soil bacteria, Green Economy Research Report, Green Fund, Development Bank of Southern Africa, Midrand

Rebotiloe FM, Eunice UJ, Mahloro HSD. 2018. Isolation and identification of bacterial endophytes from *Crinum macowanii* Baker. African Journal of Biotechnology **17**: 1040-1047

Reid E, Orrel C, Stoloff K, Joska J. 2012. Psychotropic prescribing in HIV. Southern African Journal of HIV Medicine **13**: 188

Robbins N, Caplan T, Cowen LE. 2017. Molecular evolution of antifungal drug resistance. Annual Review of Microbiology **71**: 753-775

Robert VA, Casadevall A. 2009. Vertebrate endothermy restricts most fungi as potential pathogens. Journal of Infectious Disease **200**: 1623-1626

Robert V, Cardinali G, Casadevall A. 2015. Distribution and impact of yeast thermal tolerance permissive for mammalian infection. BioMed Central Biology **13**: 18

Romero D, de Vicente A, Rakotoaly RH. 2007. The iturin and fengycin families of lipopeptides are key factors in antagonism of *Bacillus subtilis* toward *Podosphaera fusca*. International Society for Molecular Plant-microbe Interactions **20**: 430-440

Samie S, Trollope KM, Joubert LM, Makunga NP, Volschenk H. 2019. The antifungal and *Cryptococcus neoformans* virulence attenuating activity of *Pelargonium sidoides* extracts. Journal of Ethnopharmacology **235**: 122-132

Sanguinetti M, Posteraro B, Fiori B, Ranno S, Torelli R, Fadda G. 2005. Mechanisms of azole resistance in clinical isolates of *Candida glabrata* collected during a hospital survey of antifungal resistance. Antimicrobial Agents and Chemotherapy **49**: 668-679

Saraswathi J, Venkatesh K, Nirmala B, Majid HH, Rani AR. 2011. Phytopharmacological importance of *Pelargonium* species. Journal of Medicinal Plants Research **5**: 2587-2598

Schneider A, Marahiel MA. 1998. Genetic evidence for a role of thioesterase domains, integrated in or associated with peptide synthetases, in non-ribosomal peptide biosynthesis in *Bacillus subtilis*. Archives of Microbiology. **169**: 404-410

Singh RP, Hodson D P, Huerta-Espino J, Jin Y, Bhavani S, Njau P, Herrera-Foessel S, Singh PK, Singh S, Govindan V. 2011. The emergence of Ug99 races of the stem rust fungus is a threat to world wheat production. Annual Review of Phytopathology **49**: 465–481

Sionov E, Chang YC, Garraffo HM, Kwon-Chung KJ. 2009. Heteroresistance to fluconazole in *Cryptococcus neoformans* is intrinsic and associated with virulence. Antimicrobial Agents and Chemotherapy **53**: 2804-2815

Spathelf BM, Rautenbach M. 2009. Anti-listerial activity and structure–activity relationships of the six major tyrocidines, cyclic decapeptides from *Bacillus aneurinolyticus*. Bioorganic and Medicinal Chemistry **17**: 5541-5548

Spier F, Buffon JG, Burkert CAV. 2015. Bioconversion of raw glycerol generated from the synthesis of biodiesel by different oleaginous yeasts: Lipid content and fatty acid profile of biomass. Indian Journal of Microbiology **55**: 415-422

Steenbergen JN, Shuman HA, Casadevall A. 2001. *Cryptococcus neoformans* interactions with amoebae suggest an explanation for its virulence and intracellular pathogenic strategy in macrophages. Proceedings of the National Academy of Sciences of the United States of America **98**: 15245-15250

Steenbergen JN, Nosanchuk JD, Malliaris SD, Casadevall A. 2004. Interaction of *Blastomyces dermatitidis*, *Sporothrix schenckii*, and *Histoplasma capsulatum* with *Acanthamoeba castellanii*. Infectious Immunology **72**: 3478-3488

Stein T, Vater J, Kruft V, Otto A, Wittmann-Liebold B, Franke P, Panico M, McDowell R, Morris HR. 1996. The multiple carrier model of non-ribosomal peptide biosynthesis at modular multi- enzymatic templates. Journal of Biological Chemistry **271**: 15428-15435

Street RA, Prinsloo G. 2013. Commercially important medicinal plants of South Africa: A review. Journal of Chemistry **2013**: 1-16

Stringlis IA, Zhang H, Pieterse CMJ, Bolton MD, de Jonge R. 2018. Microbial small molecules - weapons of plant subversion. Natural Product Reports **35**: 410-433

Thangavelu R, Mustaffa MM. 2012. Current advances in the *Fusarium* wilt disease management in banana with emphasis on biological control. Plant Pathology **11:** 273-298

Thrane C, Harder Nielsen T, Neiendam Nielsen M, Sørensen J, Olsson S. 2000. Viscosinamide-producing *Pseudomonas fluorescens* DR54 exerts a biocontrol effect on *Pythium ultimum* in sugar beet rhizosphere. FEMS Microbiology and Ecology **33**: 139-146

Toure Y, Ongena M, Jacques P, Guiro A, Thonart P. 2004. Role of lipopeptides produced by *Bacillus subtilis* GA1 in the reduction of grey mould disease caused by *Botrytis cinerea* on apple. Journal of Applied Microbiology **96**: 1151-1160

Tran H, Ficke A, Asiimwe T, Hofte M, Raaijmakers JM. 2007. Role of the cyclic lipopeptide massetolide A in biological control of *Phytophthora infestans* and in colonization of tomato plants by *Pseudomonas fluorescens*. New Phytologist **175**: 731-742

Troskie AM, de Beer A, Vosloo JA, Jacobs K, Rautenbach M. 2014. Inhibition of agronomically relevant fungal phytopathogens by tyrocidines, cyclic antimicrobial peptides isolated from *Bacillus aneurinolyticus*. Microbiology **160**: 2089-20101

Tsuge K, Akiyama T, Shoda M. 2001. Cloning, sequencing, and characterization of the iturin A operon. Journal of Bacteriology **183**: 6265-6273

Van Daele R, Spriet I, Wauters J, Maertens J, Mercier T, Van Hecke S, Brüggemann R. 2019. Antifungal drugs: What brings the future? Medical Mycology **57**: S328-S343

Van de Mortel JE, Tran H, Govers F, Raaijmakers JM. 2009. Cellular responses of the late blight pathogen *Phytophthora infestans* to cyclic lipopeptide surfactants and their dependence on G proteins. Applied and Environmental Microbiology **75**: 4950-4957

Van Vuuren SF. 2008. Antimicrobial activity of South African medicinal plants. Journal of Ethnopharmacology **119**: 462-472

Vermes A, Guchelaar HJ, Dankert J. 2000. Flucytosine: A review of its pharmacology, clinical indications, pharmacokinetics, toxicity and drug interactions. Journal of Antimicrobial Chemotherapy **46**: 171-179

Visagie CM, Houbraken J, Seifert KA, Samson RA, Jacobs K. 2015. Four new *Penicillium* species isolated from the fynbos biome in South Africa, including a multigene phylogeny of section Lanata-Divaricata. Mycological Progress **14**: 96

Vollenbroich D, Pauli G, Ozel M, Vater J. 1997. Antimycoplasma properties and application in cell culture of surfactin, a lipopeptide antibiotic from *Bacillus subtilis*. Applied and Environmental Microbiology **63**: 44-49

Walker LA, Gow NAR, Munro CA. 2010. Fungal echinocandin resistance. Fungal Genetics and Biology **47**: 117-126

Wang Q, Chen S, Zhang J, Sun M, Liu Z, Yu Z. 2008. Co-producing lipopeptides and poly-gamma-glutamic acid by solid-state fermentation of *Bacillus subtilis* using soybean and sweet potato residues and its biocontrol and fertilizer synergistic effects. Bioresource Technology **99**: 3318-3323

Wang J, Liu J, Chen H, Yao J. 2007. Characterization of *Fusarium graminearum* inhibitory lipopeptide from *Bacillus subtilis* IB. Applied Microbiology and Biotechnology **76**: 889-894

Watkinson SC, Boddy L, Money N. 2015. The fungi. 3 ed. [ebook] London: Academic Press. 1-102. Available at: https://books.google.co.za/books?hl=en&lr=&id=x8qcBAAAQBAJ&oi=fnd&pg=PP1&dq=Watkinson+SC,+Boddy+L,+Money+N.+2015.+The+fungi.+3+ed.+Academic+Press&ots=5-d35SbZP&sig=Z5e0uE4SqNzp31fZKWkT8nQHnE&redir_esc=y#v=onepage&q&f=false [Accessed 20 Feb. 2019]

Wei YH, Wang LC, Chen WC, Chen SY. 2010. Production and characterization of fengycin by indigenous *Bacillus subtilis* F29-3 originating from a potato farm. International Journal of Molecular Sciences **11**: 4526-4538

Whang L-M, Liu P-WG, Ma C-C, Cheng S-S. 2009. Application of rhamnolipid and surfactin for enhanced diesel biodegradation--effects of pH and ammonium addition. Journal of Hazardous Materials **164**: 1045-1050

Willey J, Sherwood L, Woolverton C. 2014. Prescott's microbiology. 10 ed. New York, NY: McGraw-Hill

Wolpert TJ, Macko V, Acklin W, Jaun B, Seibl J, Meili J, Arigoni D. 1985. Structure of victorin C, the major host-selective toxin from *Cochliobolus victoriae*. Experientia **41**: 1524-1529

Zeriouh H, Romero D, Garcia-Gutierrez L, Cazorla FM, de Vicente A, Perez-Garcia A. 2011. The iturin-like lipopeptides are essential components in the biological control arsenal of *Bacillus subtilis* against bacterial diseases of cucurbits. International Society for Molecular Plant-microbe Interactions **24**: 1540-1552

Zhao X, Han Y, Tan X, Wang J, Zhou Z. 2014. Optimization of antifungal lipopeptide production from *Bacillus* sp. BH072 by response surface methodology. Journal of Microbiology **52**: 324-332

CHAPTER 3

Isolation and Identification of *Pelargonium sidoides*-associated Microorganisms with Antifungal Activity

Chapter 3

Isolation and Identification of *Pelargonium sidoides*-associated Microorganisms with Antifungal Activity

3.1 Introduction

Medicinal plants are a rich source of bioactive compounds, many of which have potent antimicrobial properties against pathogenic fungi, bacteria and viruses (Albert, 2013; Rebotiloe *et al*., 2018). However, many microbial species associated with medicinal plants also produce antimicrobial compounds and remain largely under-investigated (Mhlongo *et al*., 2018; Huang *et al*., 2008; Nath *et al*., 2015). This is because most medicinal plant research focuses primarily on plant chemistry and not on the contribution of the associated microbiota to the plant's antimicrobial activity (Ibrahim *et al.,* 2016). It is, therefore, hypothesised that the microbiota associated with medicinal plants may represent an underutilised resource for discovering novel antifungal compounds (Huang *et al*., 2008; Nath *et al*., 201).

Plants and their associated microbiota share a complex symbiotic relationship where the plant supplies nutrients and an attachment surface for microbes (Kinsella *et al*., 2009; Koch *et al*., 2002; Ongena *et al*., 2007; Nihorimbere *et al*., 2009). In return, the beneficial microbes produce secondary metabolites that play a role in the improvement of the plant's overall health and growth (Cawoy *et al*., 2014), (a)biotic stress tolerance and pathogen resistance of their plant host (Huang *et al.,* 2008; Nath *et al.,* 2015). This is accomplished as secondary metabolites from plant microbiota trigger the plant's immune system (known as induced systemic resistance) or inhibit the growth of invading pathogens directly by producing bioactive compounds as a deterrent (Cawoy *et al*., 2014). Compounds produced by medicinal plant-associated microbes include phthalates, linoleic acid, LPs, bacteriocins and volatile organic compounds (Aboobaker *et al.,* 2019; Manganyi *et al.,* 2019; Mhlongo *et al*., 2018). Some of these compounds are already used, although not extensively, as commercial biocontrol agents in the agricultural sector; as stabilisers, antioxidants and emulsifiers in food-related and cosmetic industries; and as antimicrobials, antitumor or antithrombotic drugs in therapeutics and pharmaceuticals (Meena and Kanwar, 2014).

Historically, natural products are a good strategy when searching for new bioactive compounds as they provide a basis for both design and synthesis of derivatives aiming at optimising biological activity and minimising side effects. Endophytic fungi of medicinal plants are an alternative resource that might offer a high number of natural products with diverse chemical structures and novel pharmacological actions. However, the focus has mostly been on the antibacterial effects of endophytic fungal extracts, with antifungal studies severely lacking (de Carvalho et al., 2019). This is despite the global impact of drug resistant fungal species on food availability, as a result of agricultural crop losses and food spoilage, and on human health, as annual mortality rates caused by fungal infections are now comparable with that of HIV/AIDS, malaria and tuberculosis (Rajasingham *et al.,* 2017).

From a large number of medicinal plants indigenous to South Africa, *P. sidoides* DC has been reported to be the most studied in terms of its bioactive compounds and its commercialisation for primary health care. The antifungal activity of *P. sidoides* DC extracts has been reported in Mativandlela *et al*. (2006) and Samie *et al*. (2019). Recently, antibacterial properties of secondary metabolites produced by endophytic fungal isolates from *P. sidoides* leaf and tubers have also been reported in Manganyi *et al.* (2019) and Aboobaker *et al.* (2019). Furthermore, Aboobaker *et al.* (2019) have established a positive antimicrobial relationship between extracts from *P. sidoides* roots and endophytes by comparing different combinations for activity against Gram-positive and Gram-negative bacteria. In Western medicine, extracts of *P. sidoides* tubers are used to treat respiratory infections, colds and flu (Brown *et al*., 2012; Saraswathi *et al*., 2011).

In this study, microbiota associated with *P. sidoides* tubers were isolated, identified and screened for antifungal activity against a panel of fungal pathogens, including *Botrytis cinerea*, *Candida albicans*, *Cryptococcus neoformans* and *Fusarium oxysporum.* The panel was selected based on the significant impact of these fungi on human health and sustainable agriculture on a global scale (Al-Hatmi *et al.,* 2016; Fisher *et al*., 2018; Godfray *et al*., 2016; Mpoza *et al*., 2018; Pianalto and Alspaugh, 2016). Furthermore, some strains of the fungi in the panel have acquired resistance to all the current antifungal treatment options used to eradicate them.

3.2 Methods and Materials

3.2.1 Fungal strains

Duke University (Durham, North Carolina) kindly provided *C. neoformans* H99. *C. albicans* 1084, *F. oxysporum* f. sp. *cubensis* and *B. cinerea* were respectively sourced from local culture collections at the Department of Microbiology, Department of Plant Pathology and Institute for Wine Biotechnology at Stellenbosch University (Stellenbosch, South Africa).

3.2.2 Media components and consumables

Petri dishes (90 mm) were supplied by KIMIX (Cape Town, South Africa). Sterile red blood plates (2% agar, 5% sheep or horse blood) were supplied by National Health Laboratory Service, South Africa. Ethanol, media components for growth media (YPD, M9, MMN, ISP 6, DSMZ and LB) and agarose were supplied by Merck (Darmstadt, Germany). Growth media composition is included in Appendix A. Sodium hypochlorite was supplied by Prime Cleaning Suppliers (Montague Gardens, South Africa). PCR primers, Taq Readymix and KAPA Universal ladder were supplied by Iqaba Biotech (Pretoria, South Africa). High Pure PCR Gel Purification Kit was supplied by Roche (Basel, Switzerland). PCR Cloning Kit and 2 mL cryogenic storage tubes supplied by Thermo Fisher Scientific (Waltham, Massachusetts, USA).

3.3.1 Isolation of plant-associated microbes

Wild *P. sidoides* DC tubers were supplied by Parceval Pharmaceuticals (Wellington, South Africa) with adherence to the National Environmental Management Biodiversity Act (NEMBA), Act 10 of 2004, and the Bioprospecting, Access and Benefit Sharing (BABS) Regulations of 2008 (Reference: BABS/ ooo612N). Tubers were cut into rings using a heat sterilised scalpel and surface sterilised 3X by soaking in 70% ethanol (v/v in deionised water) for 30 sec., followed by 1% sodium hypochlorite (v/v in deionised water) for 30 sec. and washing with autoclaved deionised water for 30 sec. (Rebotiloe *et al.,* 2018). Surface sterilised tuber slices were macerated with pestle and mortar and the pulp re-suspended in 4 mL of physiological salt solution (0.9% [m/v] NaCl). Serially diluted (10^{-1}–10^{-3}) tuber pulp suspensions were spread onto yeast peptone dextrose (YPD), potato dextrose (PD) and Minimal Melin Norkrans (MMN) agar (Langer *et al.,* 2008) (supplemented with 10 µg/mL streptomycin and chloramphenicol) for fungal isolation. For

bacterial isolations, Luria-Bertani (LB), Minimal 9 (M9) (Hopwood, 2012), International *Streptomyces* Project (ISP 6) and Deutsche Sammlung von Mikroorganismen und Zellkulturen (DSMZ) (Everest *et al.,* 2014) agar were used supplemented with 10 µg/mL nalidixic acid and cycloheximide. All plates were incubated at 8°C, 26°C and 37°C. Pure cultures were maintained by re-streaking onto the same growth media (antibiotics omitted after one round) and incubating at the same growth temperatures as was used in the initial isolation of each single colony. Single colonies were distinguished from one another based on their different colony morphologies and different cell morphologies examined using a light microscope and 400X magnification.

3.3.2 Screening isolates with antifungal bioactivity

Pure cultures of *P. sidoides* tuber-associated isolates were screened against a panel of four fungal pathogens (*B. cinerea*, *C. albicans*, *C. neoformans* and *F. oxysporum)* for both broad-spectrum (effective against more than one of the panel members) and high relative antifungal activity using a modified double-layer agar overlay assay (Maricic and Dawid, 2014). For this, yeast cell cultures of *C. albicans* and *C. neoformans* were prepared from single colonies, grown for 48 h at 26°C on YPD agar, and incubated overnight in fresh test tubes containing 5 mL YPD media at 26°C and 200 rpm. Fungal spore suspensions of *B. cinerea* and *F. oxysporum* were prepared from YPD-grown mycelia grown (7 days at 26°C) and spores harvested with a glass microscope slide and suspended in sterile deionised water. Spore and cell preparations were enumerated with a haemocytometer for overlay assays. The *P. sidoides* tuber-associated isolates were cultured at 26°C in the middle of YPD agar plates with circular (1-2 cm radius) membrane inserts of sterile 0.45 µm polyvinylidene difluoride (PVDF) membrane (Biotrace, Cape Town, South Africa). After 24 h, a second layer of molten YPD agar, containing 1 x 10^4 yeast cells/mL or 1 x 10^3 fungal spores/mL, was poured around the PVDF-containing barrier. Following 48 h incubation at 26°C, antifungal activity was quantified by measuring the no growth/clear zones around the membrane perimeter. Freeze cultures were prepared for *P. sidoides* tuber-associated isolates with antifungal bioactivity using 5 mL liquid cultures incubated for 48 hours at 26 °C on a rotary wheel. Fungal isolates were grown in YPD and bacterial isolates in LB broth. Cryogenic storage tubes were filled with 400 µL of each liquid culture and 1.6 mL of 100% glycerol (final v/v 80%) before being stored at -80 °C. The haemolytic activity of *P. sidoides* tuber-associated isolates was evaluated on blood agar plates and incubated for 24 h at 26°C overnight (Samie *et al.*, 2019).

3.3.3 Identification of *P. sidoides*-associated isolates with antifungal activity

3.3.3.1 DNA extraction and primer selection

Bacterial cells were grown in LB broth at 26°C for 24 h before genomic DNA (gDNA) was extracted using a manual extraction method from Damm *et al.* (2008). Primers selected for PCR amplification of genes used in bacterial identification included those for 16S ribosomal ribonucleic acid (rRNA), *gyrA, recA* and *atpD* genes (Table 3.1). For polymerase chain reaction (PCR) amplification of 16S rRNA and *gyrA*, KAPA 2G Robust Hotstart Readymix (KAPA Biosystems, Massachusetts, USA) was used. For PCR amplification of *atpD* and *recA*, Q5 High-Fidelity DNA Polymerase (New England Biolabs, Ipswich, Massachusetts, USA) was used. Polymerase chain reaction (PCR) cycling conditions are included in Table 3.2.

Table 3.1. Selected bacterial primers and expected amplicon size for each targeted gene region.

Primer	Sequences (5'- 3')	Gene region	Expected size	Reference
27F	AGAGTTTGATCMTGGCTCAG	16S rRNA	~1460 bp	Looke *et al.*, 2011
1492R	GGTTACCTTGTTACGACTT			
P-gyrA-f	CAGTCAGGAAATGCGTACGTCCTT	*GyrA*	~690 bp	Rooney *et al*., 2009
P-gyrA-r	CAAGGTAATGCTCCAGGCATTGCT			
recA_63F	ATCGAGCGGTCGTTCGGCAAGGG	*RecA*	~530 bp	Lemaire *et al*., 2014
recA_504R	TTGCGCCTGGCTCAT			
atpD_237f	SCTGGGSCGYATCMTGAACGT	*AtpD*	~460 bp	Lemaire *et al*., 2014
atpD_771r	GCCGACACTTCCGAACCNGCCTG			

Fungal gDNA was extracted from mycelia using the Cetyl Trimethyl Ammonium Bromide (CTAB) method (Umesha *et al.,* 2016). Subsequently, the ITS, β-tubulin (*benA*), calmodulin (*caM*) and RNA Polymerase II subunit (*RPB2*) gene regions were PCR amplified using primers as indicated in Table 3.3. For ITS and *benA*, KAPA 2G Robust Hotstart Readymix (KAPA Biosystems, Massachusetts, USA) was used. For *caM* and *RPB2,* Q5 High-Fidelity DNA Polymerase (New England Biolabs, Ipswich, Massachusetts, USA) was used according to the manufacturers' recommendations. Cycling conditions are included in Table 3.4.

Table 3.2. PCR cycling conditions and reaction times for 30 cycles of amplification used before sequencing 16S rRNA, *gyrA*, *recA* and *atpD* gene regions for bacterial identification.

Gene region	Initial denaturation	Denaturation	Annealing	Extension	Final extension
16S rRNA	95°C, 3 min	94°C, 30s	52°C, 30s	72°C, 15s	72°C, 1 min
GyrA	94°C, 5 min	94°C, 30s	60°C, 30s	72°C, 30s	72°C, 1 min
RecA	98°C, 30s	98°C, 7s	53°C, 10s	72°C, 15s	72°C, 7.5 min
AtpD	98°C, 30s	98°C, 7s	55°C, 10s	72°C, 15s	72°C, 7.5 min

Table 3.3. Selected fungal primers and expected amplicon size for each targetted gene region.

Primer	Sequence (5'- 3')	Gene region	Expected size	Reference
ITS1	TCCGTAGGTGAACCTGCGG	ITS	~550 bp	Manter and Vivanco, 2007
ITS4	TCCTCCGCTTATTGATATGC			
Bt2a	GGTAACCAAATCGGTGCTGCTTTC	*BenA*	~400 bp	Guevara-Suarez *et al*., 2016
Bt2b	ACCCTCAGTGTAGTGACCCTTGGC			

5f2	GAY MGW GAT CAY TTY GG	*RPB2*	~500 bp	O'Donnell et al., 2010
7cr	CCC ATR GCT TGY TTR CCC AT			
CMD5	CCG AGT ACA AGG ARG CCT TC	*CaM*	~755 bp	Hong *et al*., 2006
CMD6	CCG ATR GAG GTC ATR ACG TGG			

Table 3.4. PCR cycling conditions used for the amplification of ITS, *benA, caM* and *RPB2* gene regions.

Gene region	Initial denaturation	Denaturation	Annealing	Extension	Final extension
ITS	95°C, 3 min	95°C, 15s	52°C, 30s	72°C, 30s	72°C, 1.5 min
***Ben*A**	95°C, 3 min	95°C, 15s	54°C, 45s	72°C, 1 min	72°C, 7 min
CaM	98°C, 30s	98°C, 7s	55°C, 10s	72°C, 15s	72°C, 7.5 min
RPB2	98°C, 30s	98°C, 7s	51°C, 10s	72°C, 15s	72°C, 7.5 min

*If required, 0.6 µl of 20 mg/mL BSA (bovine serum albumin) was added to improve PCR product yield and reduce non-specific binding of primers to GC-rich sequences.

All PCR products were visualised with 1.5% (w/v) agarose gel electrophoresis at 80 V for 60 minutes in 1x TAE buffer (20 mM sodium acetate, 40 mM Tris and 1.0 mM EDTA). Polymerase chain reaction product sizes were estimated with the KAPA Universal ladder after ethidium bromide (0.5 µg/mL) staining. In cases where multiple DNA products were observed, PCR amplicons of the correct size were excised and purified using the High Pure PCR Gel Purification Kit (Roche, Basel, Switzerland) and cloned using the CloneJet PCR Cloning Kit (Thermo Fisher Scientific, Waltham, Massachusetts, USA) according to the manufacturers' recommendations. Polymerase chain reaction products were Sanger sequenced at the Central Analytical Facility (CAF), Stellenbosch University, with the same primers included in Table 3.1 for bacteria and Table 3.3 for fungi.

3.3.3.2 NCBI BLAST analysis

Consensus sequences were assembled using forward and reverse complement sequences and manually curated by trimming low-quality sequence from non-overlapping ends using CLC Main Workbench version 7 (Qiagen, Hilden, Germany). For identification, consensus sequences (included in Appendix B) were subjected to the National Centre of Bioinformatic Information (NCBI) for a BLAST (Basic Local Alignment Search Tool) analysis (https://blast.ncbi.nlm.nih.gov/Blast.cgi). Basic Local Alignment Search Tool hits with a sequence similarity/identity of ≥98.65% (Kim *et al*., 2014) and 100% sequence coverage were accepted as members of the same genus. The same was true for a species-level identification if multiple genes from the same microbe had ≥98.65% sequence identity and 100% sequence coverage for a single species identity on the NCBI database.

3.3.3.3 Phylogenetic tree construction

For where a genus, but not a species-level identity could be found using NCBI BLAST analysis, phylogenetic trees were constructed to orientate the unidentified species within its identified genus. This comparison between the query sequence and genetic data from other closely related species required a multiple sequence alignment (MSA) with reference strains and ex-types downloaded from the NCBI.

For bacteria, MSAs for genus-level identifications were generated with 16S rRNA, BLAST results with ≥98.65% sequence identity and sequence 100% coverage and the appropriate reference strains and ex-types downloaded from the NCBI (Miranda *et al*., 2007; Sabir *et al.,* 2013; Celandroni et al., 2019). MSAs were constructed using CLC and MEGA 7 2.0 (Pennsylvania State University, Pennsylvania, USA) (for export as a ".nexus" file). For species-level identifications, MSAs were constructed using the same procedure as was used for genus-level identifications, but with BLAST results generated for g*yrA*, *recA* and *atpD* genes, respectively, and as one concatenated sequence. Reference strains and ex-types were downloaded from the NCBI and the NRRL/ARC (Agricultural Research Service Culture Collection; https://nrrl.ncaur.usda.gov/cgi-bin/usda/index.html) (Bhandari *et al*., 2013; Chun, 2000; Miranda *et al*., 2007). To construct MSAs for genus-level identifications of fungi, ITS gene region BLAST results (≥98.65% identity and 100% coverage) were aligned with type strains and ex-types downloaded from the NCBI as suggested by Visagie *et al*. (2014) and Visagie *et al*. (2016). For species-level

identifications, the same procedure was repeated with BLAST results for *benA*, *caM* and *RPB2* genes, and reference strains and ex-types downloaded from the NCBI as suggested by Visagie *et al*. (2016) for isolate A1 and by Visagie *et al*. (2016) and Prencipe *et al.* (2018) for isolate C5. A list of all reference strains, type strains and ex-types used for bacterial and fungal MSAs are included in Supplementary Table 1 and Supplementary Table 2, respectively.

Phylogenetic trees were constructed from MSAs using more than one tree drawing platform to eliminate any algorithm bias. The maximum parsimony (MP) algorithm (PAUP 4.0) (Duke University, North Carolina, USA) provided a heuristic search using a tree bisection and reconnection (TBR) and the maximum likelihood (ML) algorithm (PhyML 3.0) (Guindon *et al*., 2010; http://www.atgc-montpellier.fr) provided a HKY85 + G +I substitution model. A neighbour-joining (NJ) algorithm in PhyML 3.0 with a default substitution model (Katoh and Standley, 2013) was also used when PhyML proved ineffective for generating ML trees.

For the MP analysis, stepwise-addition options were set to random and TBR branch swapping options was set to save no more than 10 trees with a tree score below 5. Max trees were set to increase by 100 automatically and all trees were rooted with a defined outgroup and internal basal polytomy. All tree topographies were evaluated for reproducibility using 1000 pseudo-replicates (Miranda *et al*., 2007), a 50% bootstrap threshold and labelled using Adobe editor (Adobe Inc. California, USA). The saved MP trees were used to obtain favourable model parameters for the ML analysis. This was done using PhyML 3.0 (Guindon *et al.,* 2010; http://www.atgc-montpellier.fr) smart model selection tool. The same online platform was used to generate ML trees using a GTR + G substitution model. Bootstrap analysis was completed with 1000 replicates. FigTree v1.4.4 (http://tree.bio.ed.ac.uk/software/figtree/) and Adobe pdf editor (Adobe Inc. California, USA) was used to label trees with bootstrap values.

3.3.3.4 Phenotypic characterisation of bacterial isolates

Phenotypic information was collected using the Plate protocol B for Biolog GEN III microplate identification system (Biolog, Hayward, CA, USA) run by Onderstepoort Biological Products (Onderstepoort, South Africa). Plate protocol B was selected as it is suggested for strongly reducing and encapsulated bacteria, Gram-negative and Gram-positive bacteria. Nutrient BUG agar with 5% (v/v) sheep blood was used and incubated

at 33°C for 22 h (Biolog, 2016; Tamang *et al*., 2005). Comparing metabolic fingerprints with the Biolog species library species were classified based on an ID rank 1 with a SIM (similarity) value above 0.5 and a DIST (distance) value two distance points from the second choice (ID rank 2) (Biolog, 2016).

3.4 Results and Discussion

3.4.1 Bioactivity of *P. sidoides* tuber-associated microbiota

Sixty-eight morphologically different colonies were obtained from *P. sidoides* tubers. The majority of these isolates, 50, were morphologically distinct fungi, followed by ten yeast and eight bacterial isolates. Using colony morphology to discriminate between colonies, although time-efficient, may have under-represented bacterial and yeast isolates with similar colony morphologies.

Using the modified double-layer agar overlay and blood agar assay, ten isolates from *P. sidoides* tubers showed bioactivity (Table 3.5). Ten of the isolates showed antifungal activity against one or more of the fungal pathogens in the panel, with some also showing alpha and beta-haemolytic activity. Alpha-haemolytic activity resulted in partial red blood cell lysis and discolouration to the media. Beta-haemolysis resulted in full lysis of red blood cells and clear zone formation in the media (Buxton, 2005; Samie *et al*., 2019) (Table 3.5). Gamma-haemolytic organisms, such as C5, A1, A4 and A6, produced no discolouration or clear zones in the media.

In the overlay assay for antifungal activity, isolates A1 and C5, two filamentous fungi, were particularly active against the pathogenic yeasts, *C. neoformans* and *C. albicans,* and mildly active against *B. cinerea* and *F. oxysporum*. Isolate A1 had the highest relative activity against and produced the largest clear zones in lawns inoculated with *C. neoformans* cells (Table 3.6). Similarly, isolate C5 had the highest relative activity against and produced the largest clear zones, 3X the size of those produced by any of the other isolates, when grown antagonistically with *B. cinerea* and *F. oxysporum* spores (Table 3.6). Together with bacterial isolates YC2 and SC6, these fungal isolates showed activity against all four target species in the pathogen panel (Table 3.6). Therefore, isolates YC2, SC6, A1 and C5 were selected for identification and antifungal compound production and characterisation (full details described in Chapter 4).

Table 3.5. Antifungal and haemolytic activity in *P. sidoides* tuber-associated isolates.

Isolate	Overlay assay for antifungal activity				Haemolytic assay
	B. cinerea	*C. albicans*	*C. neoformans*	*F. oxysporum*	
SC5					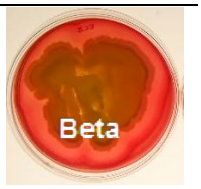
SC6					
SC7					
YC2					
PC1	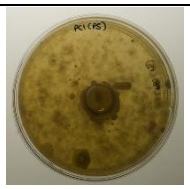	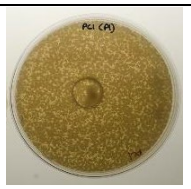			
C3					
C5	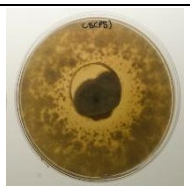	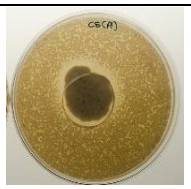			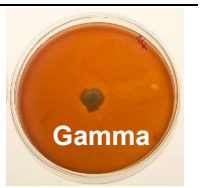
A1	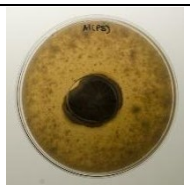	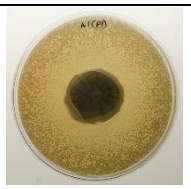		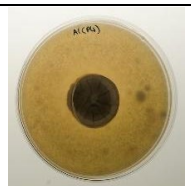	
A4					

A6					
(-)	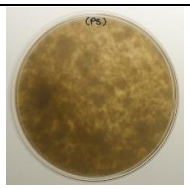	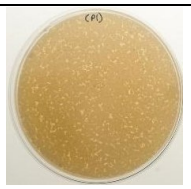		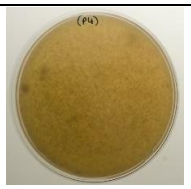	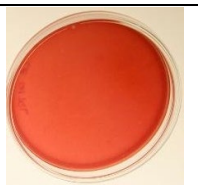

Table 3.6 Antifungal activity of *P. sidoides* tuber-associated isolates quantified with median clear zone diameter (mm).

Isolate	*C. neoformans*	*C. albicans*	*F. oxysporum*	*B. cinerea*
SC5	2.5	2.5	2.5	0
SC6	7.5	2.5	2.5	2.5
SC7	2.5	2.5	0	0
YC2	7.5	7.5	2.5	2.5
PC1	0	0	0	0
C3	2.5	0	2.5	0
C5	7.5	7.5	7.5	7.5
A1	12.5	7.5	2.5	2.5
A4	2.5	2.5	0	2.5
A6	2.5	0	0	2.5

3.4.4 Identification of bacterial isolates YC2 and SC6

Using a BLAST analysis of the NCBI for 16S rRNA, bacterial isolates YC2 and SC6 were placed in the *Bacillus* genus (Table 3.7). Isolate SC6 fell in the *B. cereus* clade while isolate YC2 was grouped with the *B. subtilis* clade. Findings were supported for both MP and ML algorithms by bootstrap values above 50%, with 1000 bootstrap replicates evaluating tree topography (Fig. 3.1).

Using an expanded set of genes, 16S rRNA, *gyrA* and *atpD,* to determine a species-level identification for bacterial isolate YC2, BLAST hits with ≥98.65% identity and 100% coverage, included *B. amyloliquefaciens, B. nakamurai* and *B. velezensis* (Table 3.7). *RecA* sequence data was omitted as all of the BLAST search results were well below

≥98.65% identity and multiple band sizes were observed after gel electrophoresis of the PCR amplicons. This suggests non-specific binding of the PCR primers to YC2 gDNA. To optimise, different concentrations of gDNA template (0.5x, 1x, 2X and 4X) and different annealing temperatures (52°C, 53°C, 57°C and 59°C) were employed. The most successful attempts, producing the fewest bands after gel electrophoresis, used 2x template gDNA and an annealing temperature of 53°C. Even with gel excision and purification using a High Pure PCR Gel Purification Kit (Roche, Basel, Switzerland) and amplicon cloning using CloneJet PCR Cloning Kit (Thermo Fisher Scientific, Waltham, Massachusetts, USA), sequencing results could not be improved to produce BLAST search results with ≥98.65% identity and multiple bands were produced after gel electrophoresis.

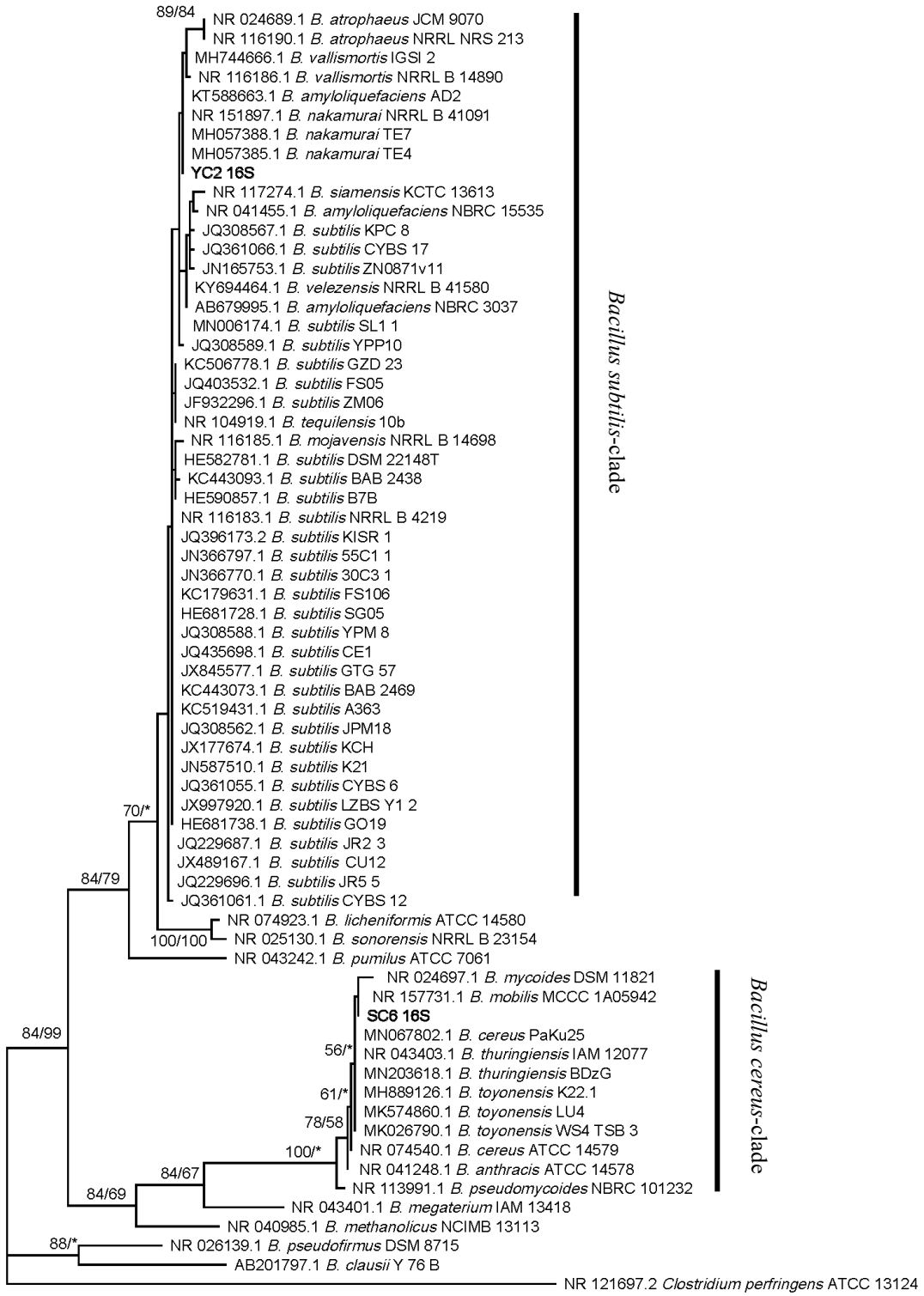

Figure 3.1. Phylogenetic tree constructed using 16S rRNA and *Bacillus* species downloaded from the NCBI. The selected outgroup was *Clostridium perfringens* ATCC 13124. Bootstrap values were presented on internal nodes with maximum parsimony and maximum likelihood, respectively. Bootstrap threshold was set to 50% with 1000 pseudo-replicates. *Values below 50% bootstrap threshold.

Table 3.7. Results of bacterial isolates' 16S rRNA, *gyr*A, *rec*A and *atp*D gene regions when compared to other nucleotide sequences on the NCBI database using a BLAST search.

Gene	Isolate	Query sequence size (bp)	BLAST results with ≥98.65% identity	Accession number	% identity
16S rRNA	YC2	1460	*B. amyloliquefaciens*	KT588663	99.59
			B. nakamuri	MH057388	99.52
	SC6	1419	*B. thuringiensis*	MN203618	98.73
			B. subtilis	MN186891	98.73
			B. cereus	MN067802	98.73
			B. toyonensis	MK026790	98.73
			B. wiedmannii	CP024684	98.73
			B. mobilis	CP031443	98.73
GyrA	YC2	416	*B. amyloliquefaciens*	MH464598	99.04
	SC6	415	NA		NA
RecA	YC2	678	NA		NA
	SC6		NA		NA
AtpD	YC2	1008	*B. velezensis*	KP064662	86.70
	SC6	NA	NA		NA

Using 16S rRNA in the BLAST analysis, bacterial isolate SC6 was found to be closely related to the following species: *B. thuringiensis, B. cereus, B. subtilis, B. toyonensis* and *B. mobilis* (Table 3.7). However, using the expanded set of genes, no species-level identification was made for this isolate. BLAST search results were inconclusive and sequence data omitted for SC6 *gyrA, atpD* and *recA* (Table 3.7). This was done because no PCR products were produced using *gyrA* primers and no usable sequence data generated for *atpD* and *recA.* The *gyrA* primers selected are used to identify species within the *B. subtilis* species complex (Rooney *et al*., 2009). Therefore, the lack of successful PCR amplification with the *gyrA* primers suggests that isolate SC6 does not fall within the *B. subtilis* species complex. No usable sequence data was produced by *atpD* and *recA* PCR reactions as, despite attempts to optimise PCR cyclisation, multiple amplicon sizes remained in PCR reactions and multiple bands were present after gel electrophoresis. The most successful attempts, producing the fewest bands after gel electrophoresis, used 2X template DNA and an annealing temperature of 51°C for *atpD*

and 57°C for *recA*. Even after gel purification using a High Pure PCR Gel Purification Kit (Roche, Basel, Switzerland) and amplicon cloning using CloneJet PCR Cloning Kit (Thermo Fisher Scientific, Waltham, Massachusetts, USA), multiple amplicon sizes remained and less than 98.65% identity was observed for the sequence data compared with other sequences deposited on the NCBI database.

Regarding the multiple PCR amplicons produced using YC2 and SC6 rRNA and the selected primers, further PCR optimisation may be required to increase the binding specificity to the targeted gene regions. This will ensure a single bright band after gel electrophoresis and enough of the correct PCR amplicon (i.e. amplicon of the correct size to represent a single gene region) to be sent in for sequencing.

Phylogenetic trees were generated with PAUP (MP with TBR and a heuristic search) and PhyML (ML with HKY85 +G +I) for a 16S rRNA tree (Fig. 3.1) and with PAUP and MAFFT (NJ and default settings) for *gyrA* and 16S rRNA+*gyrA* concatenated trees (Figs. 3.2 and 3.3, respectively). All tree topographies were evaluated with 1000 pseudo-replicates and a bootstrap threshold of 50%. For *gyrA* (Fig. 3.2), bacterial isolate YC2 was identified as a close relative of *B. velezensis* NRRL B 41580^{T}, with bootstrap values conferring a strong phylogenetic relationship. However, for the 16S rRNA+*gyrA* (Fig. 3.3) concatenated tree for bacterial isolate YC2, the isolate was identified as a very close relative of *B. amyloliquefaciens, B. methylotrophicus* and *B. velezensis* strains. This makes its species-level identification inconclusive using this genetic data set. Bacterial isolate SC6 lacked the additional/extended genes required to construct a concatenated tree, thus its species-level identification was also inconclusive using the genotypic approach for identification in this study.

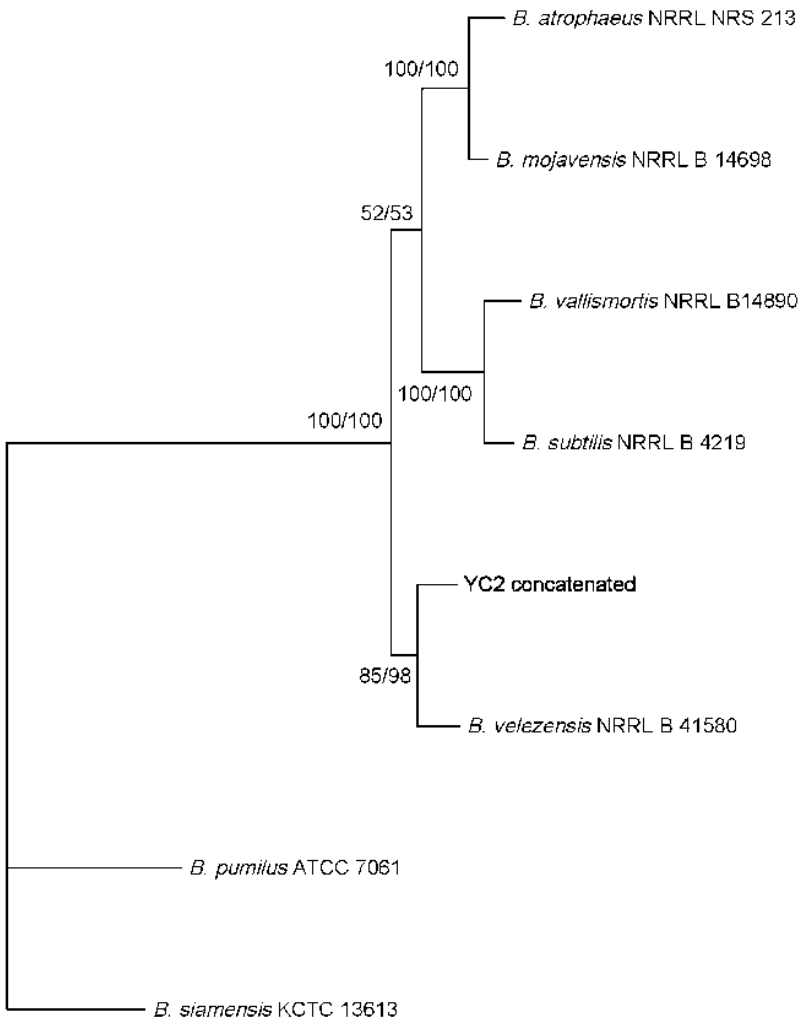

Figure 3.2. Phylogenetic tree generated using the *gyrA* gene of YC2 and of other *Bacillus* species downloaded from the NCBI database. The selected outgroup was *Bacillus siamensis* KCTC 13613. Bootstrap values were presented on internal nodes with maximum parsimony and neighbour joining, respectively. Bootstrap threshold was set to 50% with 1000 pseudo-replicates. *Values below 50% bootstrap threshold.

The Biolog assay confirmed that isolates YC2 and SC6 are closely related to *B. subtilis* and *B. cereus*, respectively (Appendix C). For isolate YC2, there was a similarity score of 0.653 for *B. subtilis/B. mojavensis* and a distance value of 5.010 between that value and more distantly related species (*B. vallismortis* and *B. atrophaeus*). Biolog results for isolate SC6 included a similarity score of 0.667 for *Bacillus cereus/pseudomycoides* and a distance value of 4.800 for more distantly related species (*B. thuringiensis, B. weihenstephanensis* and *B. mycoides*). These findings confirm the genus-level identifications suggested by BLAST analysis but do not provide any additional clarity regarding the species-level identifications of isolates YC2 and SC6. Thus, both of these species-level identifications remain inconclusive, even with the Biolog analysis.

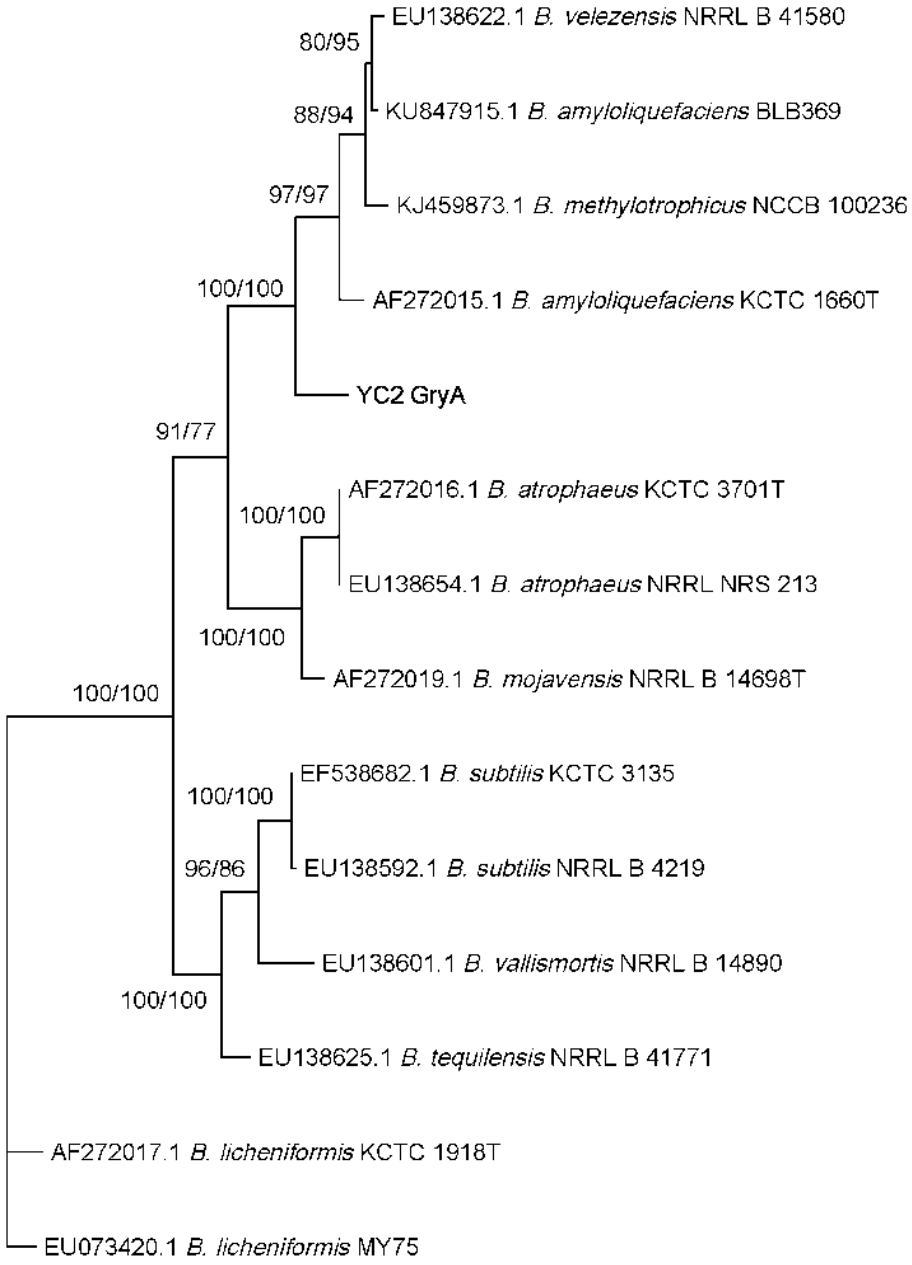

Figure 3.3. Phylogenetic tree generated using a concatenated gene sequence (16S rRNA and *gyrA* gene) of YC2 and of other *Bacillus* species downloaded from the NCBI database. The selected outgroup was *Bacillus licheniformis* MY75. Bootstrap values were presented on internal nodes with maximum parsimony and neighbour joining, respectively. Bootstrap threshold was set to 50% with 1000 pseudo-replicates. *Values below 50% bootstrap threshold.

3.4.5 Identification of fungal isolates A1 and C5

Several possible identities were suggested for fungal isolates A1 and C5. Using the ITS gene region, possible *Penicillium* identities included *P. crustosum, P. christenseniae, P. expansum, P. cyclopium, P. commune, P. griseofulvum* and *P. solitum* for isolate A1 (100% sequence coverage and 100% sequence similarity) and *P. consobrinum,*

P. corylophilum, P. aotearoae, P. terrenum, P. melinii, P. maclennaniae and P. *rubefaciens* for isolate C5 (100% sequence coverage and 99% sequence similarity) (Table 3.8). Using the β-tubulin (*benA*), calmodulin (*caM*) and RPB2 (*RPB2*) gene regions, some of these possible identities were further substantiated (Table 3.8).

Table 3.8. Results of fungal sequence comparison with the NCBI database using a BLAST search for ITS, *benA*, c*aM* and *RPB2.*

Gene region	Isolate	Query sequence size (bp)	BLAST results with ≥98.65% identity	Accession number	% identity
ITS	**A1**	494	*P. commune*	MK179259	100
			P. crustosum	MH427070	100
			P. expansum	MH879835	100
			P. cyclopium	MH865559	100
			P. solitum	KT279817	100
			P. griseofulvum	KX234323	100
	C5	581	*P. consobrinum*	MG490874	99.83
BenA	**A1**	416	*P. crustosum*	MN031402	99.04
			P. janczewskii	MG832200	99.04
			P. digiatum	LC057674	99.04
			P. solitum	GQ221183	99.04
	C5	415	*P. rubefaciens*	JX141072	99.31
CaM	**A1**	548	*P. corylophilum*	AY678548	96.83
	C5	442	*P. allii*	AY678584	99.09
RPB2	**A1**	694	*P. rubefaciens*	KP064662	100
	C5	802	*P. cellarum*	MG714855	97.63
			P. polonicum	KF021558	97.63
			P. freii	AY641058	97.63

Phylogenetic trees for A1 and C5 were generated with both ML and MP algorithms (Figs. 3.4-3.6). In the ITS gene region phylogeny, isolate A1 was shown to clade with the *P. corylophilum*-clade (100% bootstrap) and isolate C5 with the *P. viridicatum*-clade (79% bootstrap) (Fig. 3.4). Trees for *benA*, *caM* and *RPB2* phylogeny are included in Supplementary Figs. 1-6 (Appendix D).

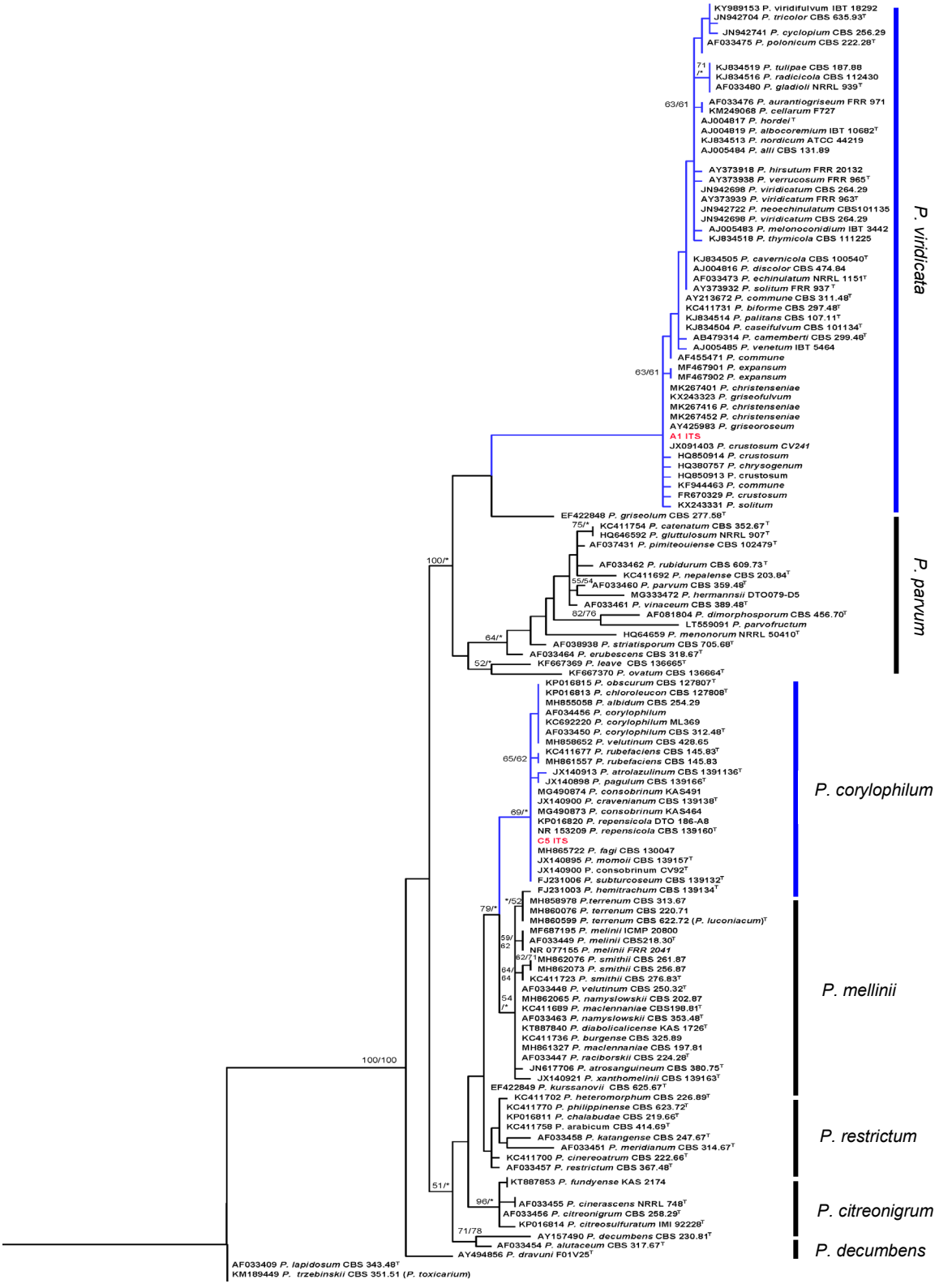

Figure 3.4 Phylogenetic tree generated using the ITS gene region of A1 and C5 and of other *Penicillium* species downloaded from the NCBI database I. The selected outgroup was *Penicillium toxicarium* CBS 351.51. Bootstrap values were presented on internal nodes with maximum parsimony and maximum likelihood, respectively. Bootstrap threshold was set to 50% with 1000 pseudo-replicates. *Values below 50% bootstrap threshold.

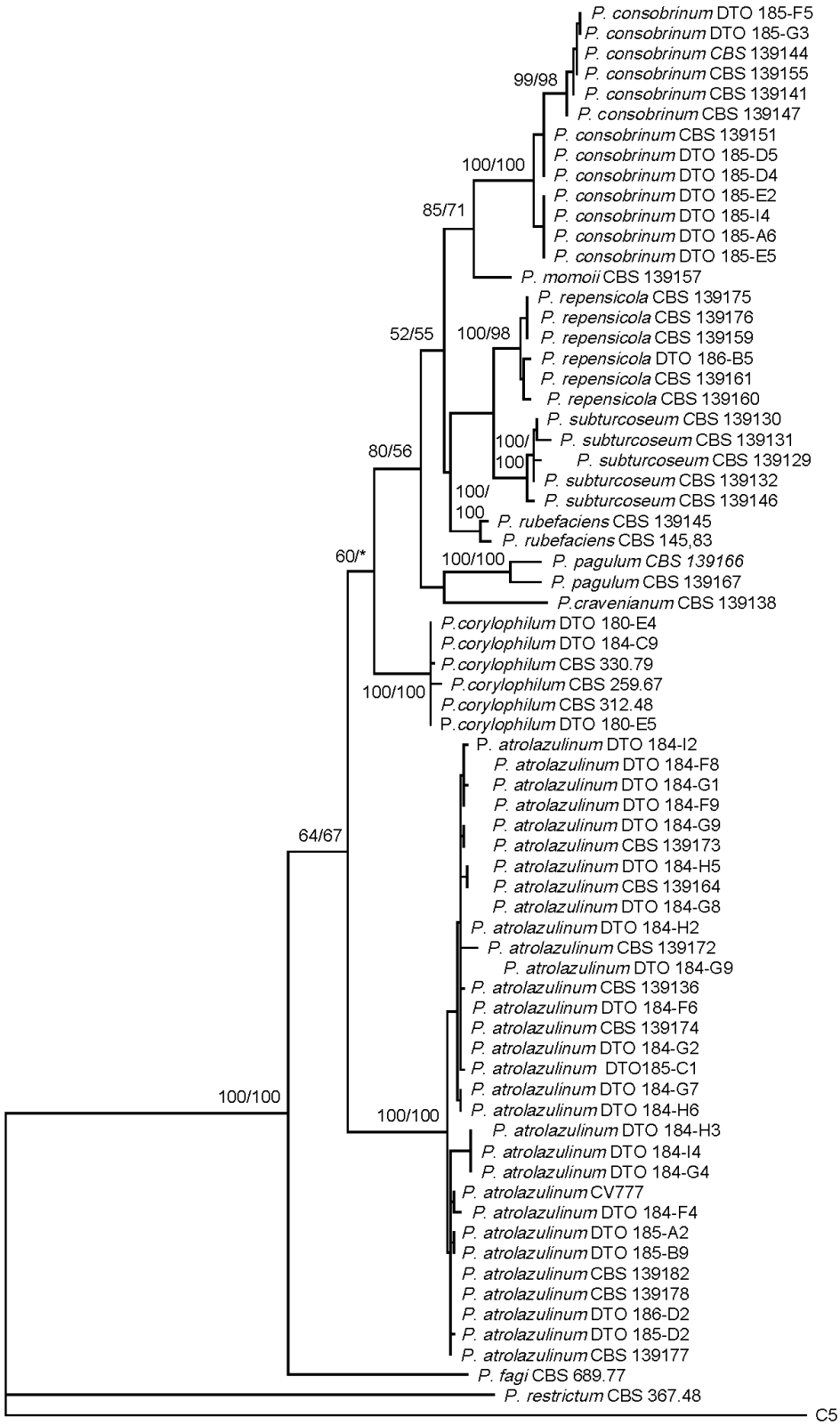

Figure 3.5. Phylogenetic tree generated using concatenated gene sequences (*benA*, *caM* and *RPB2*) from isolate C5 and from other *P. corylophilum* species downloaded from the NCBI database. The selected outgroup was *Penicillium restrictum* CBS 367.48. Bootstrap values were presented on internal nodes with maximum parsimony and maximum likelihood, respectively. Bootstrap threshold was set to 50% with 1000 pseudo-replicates. *Values below 50% bootstrap threshold.

Using an expanded set of genes, phylogenetic trees were constructed using *caM* and *RPB2* (Figs. 3.5 and 3.6). Interestingly, fungal isolate C5 separated from all other members of its proposed species clade from the ITS gene region phylogeny (Fig. 3.5). This suggests that the isolate may be a novel species or a member of a *Penicillium* clade not represented by the ex-types or type strains used comparing concatenated *benA*, *caM* and *RPB2* sequences (Visagie *et al*., 2016). The selected outgroup may also be too closely related to ex-types used to characterise the *P. corylophilum* clade. Therefore, it is suggested that a more distantly related outgroup is used in future studies. It is also suggested that isolate C5 be compared with other phylogenetic data sets using additional gene regions for multi-locus analysis in future studies. Furthermore, morphology and exudate data should be used in a polyphasic approach to complement genetic data and resolve the species-level identification of this particular fungal isolate.

Using an expanded set of genes, ITS, *caM* and *benA* gene regions, to characterise the A1 isolate, it clustered with the ex-type strain *P. crustosum* NRRL 968 (Fig. 3.6). This correlated well with the initial BLAST results and phylogenetic analysis for individual gene regions of ITS (Table 3.8) and *benA*, *caM* and *RPB2* in Supplementary Figs. 3-6 (Appendix D). However, the bootstrap value/confidence interval, supporting the relatedness of these two taxa was too low for them to be considered members of the same species (Mariadassou *et al.,* 2019). In future studies, more gene regions or additional ex-types and type strains will be required to improve resolution between these *P. viridicatum* taxa. Exudate data and morphology data sets could also be used to complement genetic data and help resolve the species-level identity of this particular fungal isolate.

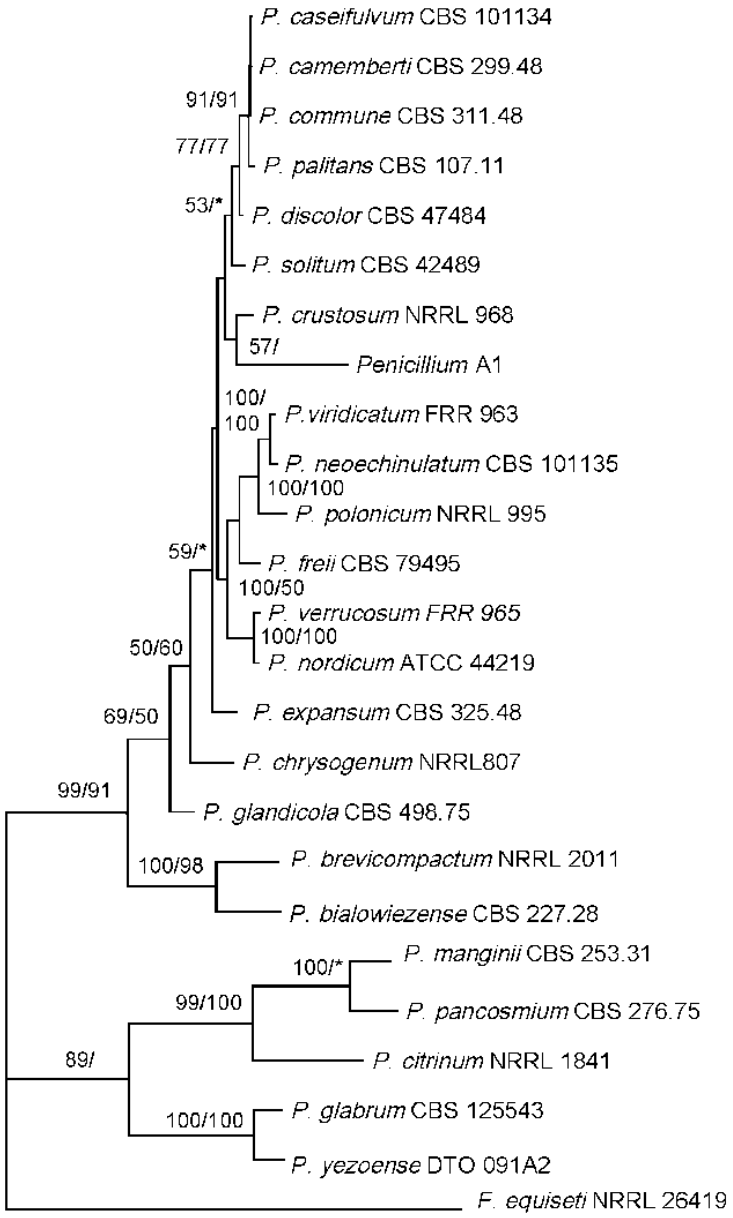

Figure 3.6. Phylogenetic tree generated using concatenated gene sequences (ITS, *benA* and *caM* gene regions) of isolate A1 and of other *P. viridicata* species downloaded from the NCBI database. The selected outgroup was *Fusarium equiseti* NRRL 26419. Bootstrap values were presented on internal nodes with maximum parsimony and maximum likelihood, respectively. Bootstrap threshold was set to 50% with 1000 pseudo-replicates. *Values below 50% bootstrap threshold.

3.5 Conclusions

In this study, the *P. sidoides* plant has been shown to host ten microbes with antifungal activity against at least one of the following pathogenic fungi: *C. neoformans, C. albicans, B. cinerea* and *F. oxysporum*. The fact that these isolates inhibit the growth of the pathogenic fungi and many studies on medicinal plants have characterised bioactive

compounds in the associated microbiota, suggests that these isolates may also produce bioactive compounds with unrecognised antifungal potential.

The antifungal microbes identified after screening for both broad-spectrum and relative antifungal activity were members of the genera *Bacillus* and *Penicillium.* Many species from these genera are known to produce well-characterised antifungal peptides (AFPs), although only a few *Penicillium* have been identified in association with *P. sidoides*, and only one identified to a species-level, *P. skrjabinii* (Aboobaker *et al.,* 2019; Mangany*i et al.,* 2019). Therefore, the identification of all the bacterial and possibly some of the fungal isolates (if confirmed as any *Penicillium* sp. other than *P. skrjabinii*) are new findings for microbes associated with *P. sidoides*.

In future studies, to improve on the species-level identifications of both bacteria and fungi isolated in this study, the genetic data used could be extended to include additional gene regions, ex-types and type strains. Alternatively, other taxonomic techniques could be used. However, for bacteria, using phenotypic data in a Biolog test did not improve on the genotypic data used, and still, no species-level identification was elucidated. Therefore, for these isolates, additional genotypic data or further optimisation of the PCR reactions for *gyrA, recA* and *atpD,* may be the best course of action to confer a species-level identity. The value of these species-level identities will be narrowing the search for which bioactive compounds are being produced as many online databases, like NORINE database (Caboche *et al*., 2007), ChemSpider (https://www.chemspider.com/) and Pub Chem https://pubchem.ncbi.nlm.nih.gov/), contain lists of bioactive compounds with their corresponding producer species.

The identification and characterisation of microbial species living in association with *P. sidoides* also add to the indigenous knowledge concerning this South African medicinal plant and some of its adaptive strategies. If a positive relationship is found between the presence of these microbial species and the plant's antimicrobial activity, in future studies, it would further strengthen the case made by Aboobaker *et al.* (2019) for members of the *P. sidoides* microbiota contributing to some of the plant's antimicrobial properties. The assumption would then be, as it is for other medicinal plant-associated microbes, that these microbes are beneficial to *P. sidoides*.

The inhibition of pathogenic fungi like *C. neoformans, C. albicans, B. cinerea* and *F. oxysporum,* is important when these pathogens cause life-threatening diseases in Sub-

Saharan Africa, and large-scale crop losses, globally. Microbes which inhibit these fungi may have the potential for use as biocontrol agents or to produce bioactive compounds which can be developed for use as antifungal drugs in the future. An added benefit is that microbes grow far quicker than, and produce bioactive compounds far more efficiently, than most plants do. To harvest compounds from microbial cultures, as opposed to plant parts, can also be cheaper and less labour intensive, while saving the natural plant stocks from over-harvesting.

3.6 References

Aboobaker Z, Viljoen A, Chen W, Crous PW, Maharaj VJ, van Vuuren S. 2019. Endophytic fungi isolated from *Pelargonium sidoides* DC: Antimicrobial interaction and isolation of a bioactive compound. South African Journal of Botany **122**: 535-542

Albert M. 2013. Peptides as triggers of plant defence. Journal of Experimental Botany **64**: 5269-5279

Al-Hatmi A, Meis J, de Hoog G. 2016. *Fusarium*: Molecular diversity and intrinsic drug resistance. PLOS Pathogen **12**: 1-8

Bhandari V, Ahmod N, Shah H, Gupta R. 2013. Molecular signatures for *Bacillus* species: demarcation of the *Bacillus subtilis* and *Bacillus cereus* clades in molecular terms and proposal to limit the placement of new species into the genus *Bacillus*. International Journal of Systemic and Evolutionary Microbiology **63**: 2712-2726

Biolog. 2016. Gen III Microplate Instructions for Use. Biolog, Hayward, CA, USA

Brown GD, Denning DW, Gow NAR, Levitz SM, Netea MG, White TC. 2012. Hidden killers: Human fungal infections. Science Translational Medicine **4**: 165

Buxton R. 2005. Blood agar plates and hemolysis protocols. ASM: Washington, D. C.

Caboche, S, Pupin M, Leclere, V, Fontaine A, Jacques P, Kucherov, G. 2007. NORINE: a database of nonribosomal peptides. Nucleic Acids Research **36**: 326-331

Cawoy H, Debois D, Franzil L, De Pauw E, Thonart P, Ongena M. 2014. Lipopeptides as main ingredients for inhibition of fungal phytopathogens by *Bacillus subtilis/amyloliquefaciens.* Microbial Biotechnology **8**: 281-295

Celandroni F, Vecchione A, Cara A, Mazzantini D, Lupetti A, Ghelardi E. 2019. Identification of *Bacillus* species: Implication on the quality of probiotic formulations. PLOS ONE **14**: 1-13

Chun J. 2000. Phylogenetic analysis of *Bacillus subtilis* and related taxa based on partial *gyrA* gene sequences. Antonie van Leeuwenhoek **78**: 123-127

Damm U, Mostert L, Crous P, Fourie P. 2008. Novel *Phaeoacremonium* species associated with necrotic wood of *Prunus* trees. Persoonia – Molecular Phylogeny and Evolution of Fungi **20**: 87-102

Das S, Dash H, Mangwani N, Chakraborty J, Kumari S. 2014. Understanding molecular identification and polyphasic taxonomic approaches for genetic relatedness and phylogenetic relationships of microorganisms. Journal of Microbiological Methods **103**: 80-100

de Carvalho CR, Ferreira MC, Amorim SS, da Silva Florindo RH, de Assis JCS, Zani CL, Rosa LH. 2019. Bioactive compounds of endophytic fungi associated with medicinal plants Recent Advancement in White Biotechnology through Fungi. Fungal Biology. Springer 303-361

Everest GJ, le Roes-Hill M, Rohland J, Enslin S, Meyers PR. 2014. *Amycolatopsis roodepoortensis* sp. nov. and *Amycolatopsis speibonae* sp. nov.: antibiotic-producing actinobacteria isolated from South African soils. Journal of Antibiotics **67**: 813–818

Fisher M, Hawkins N, Sanglard D, Gurr S. 2018. Worldwide emergence of resistance to antifungal drugs challenges human health and food security. Science **360**: 739-742

Godfray H, Mason-D'Croz D, Robinson S. 2016. Food system consequences of a fungal disease epidemic in a major crop. Philosophical Transactions of the Royal Society B: Biological Sciences **371**: 20150467

Guevara-Suarez M, Sutton D, Cano-Lira J, García D, Martin-Vicente A, Wiederhold N, Guarro J, Gené J. 2016. Identification and antifungal susceptibility of *Penicillium*-like fungi from clinical samples in the United States. Journal of Clinical Microbiology **54**: 2155-2161

Guindon S, Dufayard JF, Lefort V, Anisimova M, Hordijk W, Gascuel O. 2010.

New algorithms and methods to estimate maximum-likelihood phylogenies: assessing the performance of PhyML 3.0. Systematic Biology **59**: 307-21

Hong SB, Cho H-S, Shin HD. 2006. Novel *Neosartorya* species isolated from soil in Korea. International Journal of Systematic and Evolutionary Microbiology **56**: 477-486

Hopwood DA. 2012. Natural product biosynthesis by microorganisms and plants, Part A. Preface. Methods in Enzymology **515**: 24-25

Huang W, Cai Y, Hyde K. Corke H, Sun M. 2008. Biodiversity of endophytic fungi associated with 29 traditional Chinese medicinal plants. Fungal Diversity **33**: 61-75

Huang E, Yousef AE. 2014. The lipopeptide antibiotic paenibacterin binds to the bacterial outer membrane and exerts bactericidal activity through cytoplasmic membrane damage. Applied and Environmental Microbiology **80**: 2700-2704

Ibrahim M. 2016. Phytochemical analysis and antibacterial activities of different callus extracts of *Pelargonium sidoides*. New Biotechnology **33**: 161

Katoh K, Standley D. 2013. MAFFT multiple sequence alignment software version 7: Improvements in performance and usability. Molecular Biology and Evolution **30**: 772-780

Kim M, Oh H, Park S, Chun J. 2014. Towards a taxonomic coherence between average nucleotide identity and 16S rDNA gene sequence similarity for species demarcation of prokaryotes. International Journal of Systematic and Evolutionary Microbiology **64**: 346-351

Kinsella K, Schulthess CP, Morris TF, Stuart JD. 2009. Rapid quantification of *Bacillus subtilis* antibiotics in the rhizosphere. Soil Biology and Biochemistry **41**: 374-379

Koch B, Nielsen TH, Sorensen D. 2002. Lipopeptide production in *Pseudomonas* sp. strain DSS73 is regulated by components of sugar beet seed exudate via the *Gac* two component regulatory system. Applied and Environmental Microbiology **68**: 4509-4516

Langer I, Krpata D, Peintner U, Wenzel WW, Schweiger P. 2008. Media formulation influences i*n vitro* ectomycorrhizal synthesis on the European aspen *Populus tremula* L. Mycorrhiza **18**: 297-307

Lemaire B, Dlodlo O, Chimphango S, Stirton C, Schrire B, Boatwright J, Honnay O, Smets E, Sprent J, James E, Muasya A. 2014. Symbiotic diversity, specificity and distribution of rhizobia in native legumes of the Core Cape Subregion (South Africa). Federation of European Microbiological Societies Microbiology Ecology **91**: 1-17

Looke M, Kristjuhan K, Kristjuhan A. 2011. Extraction of genomic DNA from yeasts for PCR-based applications. Biotechniques **50**: 325-328

Manganyi MC, Tchatchouang C-DK, Regnier T, Bezuidenhout CC, Ateba CN. 2019. Bioactive compound produced by endophytic fungi isolated from *Pelargonium sidoides* against selected bacteria of clinical importance. Mycobiology **47**: 335-339

Manter D, Vivanco J. 2007. Use of the ITS primers, ITS1 and ITS4, to characterize fungal abundance and diversity in mixed-template samples by qPCR and length heterogeneity analysis. Journal of Microbiological Methods **71**:7-14

Mariadassou M, Bar-Hen A, Kishino H. 2019. Tree evaluation and robustness testing. Reference module in life sciences. Encyclopaedia of Bioinformatics and Computational Biology **2**: 736-745

Maricic N, Dawid S. 2014. Using the overlay assay to qualitatively measure bacterial production of and sensitivity to pneumococcal bacteriocins. Journal of Visualized Experiments **1**: 1-4

Mativandlela S, Lall N, Meyer J. 2006. Antibacterial, antifungal and antitubercular activity of (the roots of) *Pelargonium reniforme* (CURT) and *Pelargonium sidoides* (DC) (Geraniaceae) root extracts. South African Journal of Botany **72**: 232-237

Meena KR, Kanwar SS. 2014. Lipopeptides as the antifungal and antibacterial agents: applications in food safety and therapeutics. Biomed Research International **2015**: 473050

Mhlongo MI, Piater LA, Madala NE, Labuschagne N, Dubery IA. 2018. The chemistry of plant-microbe interactions in the rhizosphere and the potential for metabolomics to reveal signalling related to defence priming and induced systemic resistance. Frontiers in Plant Science **9**: 112

Miranda C, Martins O, Clementino M. 2007. Species-level identification of *Bacillus* strains isolates from marine sediments by conventional biochemical, 16S rDNA gene sequencing and inter-tRNA gene sequence lengths analysis. Antonie van Leeuwenhoek **93**: 297-304

Mpoza E, Rhein J, Abassi M. 2018. Emerging fluconazole resistance: Implications for the management of cryptococcal meningitis. Medical Mycology Case Reports **19**: 30-32

Nath A, Chattopadhyay A, Joshi S. 2015. Biological activity of endophytic fungi *of Rauwolfia serpentina* Benth: An ethnomedicinal plant used in folk medicines in Northeast India. Proceedings of the National Academy of Sciences, India Section B: Biological Sciences **85**: 233-240

Nihorimbere V, Fickers P, Thonart P, Ongena M. 2009. Ecological fitness of *Bacillus subtilis* BGS3 regarding production of the surfactin lipopeptide in the rhizosphere. Environmental Microbiology Reports **1**: 124-130

O'Donnell K, Sutton, DA, Rinaldi MG, Sarver BAJ, Balajee SA, Schroers HJ. 2010. An Internet-accessible DNA sequence database for identifying fusaria from human and animal infections. Journal of Clinical Microbiology **48**: 3708-3718

Ongena M, Jourdan E, Adam A. 2007. Surfactin and fengycin lipopeptides of *Bacillus subtilis* as elicitors of induced systemic resistance in plants. Environmental Microbiology **9**: 1084–1090

Pianalto K, Alspaugh J. 2016. New horizons in antifungal therapy. Journal of Fungi **2**: 26

Prencipe S, Siciliano I, Gatti C, Garibaldi A, Gullino ML, Botta R, Spadaro D. 2018. Several species of *Penicillium* isolated from chestnut flour processing are pathogenic on fresh chestnuts and produce mycotoxins. Food Microbiology **76**: 396-404

Rajasingham R, Smith RM, Park BJ, Jarvis JN, Govender NP, Chiller TM, Denning DW, Loyse A, Boulware DR. 2017. Global burden of disease of HIV-associated cryptococcal meningitis: An updated analysis. Lancet Infectious Disease **17**: 873-881

Rebotiloe F, Eunice U, Mahloro H. 2018. Isolation and identification of bacterial endophytes from *Crinum macowanii* Baker. African Journal of Biotechnology **17**: 1040-1047

Rooney A, Price N, Ehrhardt C, Swezey J, Bannan J. 2009. Phylogeny and molecular taxonomy of the *Bacillus subtilis* species complex and description of *Bacillus subtilis* subsp. *Inaquosorum* subsp. Nov. International Journal of Systematic and Evolutionary Microbiology **59** : 2429-2436

Sabir JSM, Abo-Aba SEM, Sabry A, Hussein RM, Bahieldin A, Baeshen NA. 2013. Isolation, identification and comparative analysis of 16S rDNA of *Bacillus subtilis* grown around *Rhazya stricta* roots. Life Science Journal **12**: 980-986

Samie S, Trollope KM, Joubert LM, Makunga NP, Volschenk H. 2019. The antifungal and *Cryptococcus neoformans* virulence attenuating activity of *Pelargonium sidoides* extracts. Journal of Ethnopharmacology **235**: 122-132

Saraswathi J, Venkatesh K, Baburao N. 2011. Phytopharmacological importance of *Pelargonium* species. Journal of Medicinal Plant Research **5**: 2587-2598

Umesha S, Manukumar HM, Raghava S. 2016. A rapid method for isolation of genomic DNA from food-borne fungal pathogens. Biotech **6**: 123

Visagie, C, Houbraken J, Frisvad J, Hong S, Klaassen C, Perrone G, Seifert, K, Varga, J, Yaguchi T, Samson R. 2014. Identification and nomenclature of the genus *Penicillium*. Studies in Mycology **78**: 343-371

Visagie C, Seifert K, Houbraken J, Samson R, Jacobs K. 2016. A phylogenetic revision of *Penicillium* sect. *Exilicaulis*, including nine new species from fynbos in South Africa. IMA Fungus **7**: 75-117

CHAPTER 4

Production and Characterisation of Antifungal Compounds from *Pelargonium sidoides*-associated Microorganisms

Chapter 4

Production and Characterisation of Antifungal Compounds from *Pelargonium sidoides*-associated Microorganisms

4.1 Introduction

Microbiota associated with the tubers of the South African medicinal plant *P. sidoides* DC were isolated, putatively identified and screened for antifungal activity against *B. cinerea*, *C. albicans*, *C. neoformans* and *F. oxysporum* (information provided in Chapter 3). These same isolates (SC6, YC2, C5 and A1) were found to have broad-spectrum and high relative antifungal activities before being evaluated for LP production. Culturing conditions for LP production were optimised and the extracted compounds characterised in terms of their structure and potential antifungal and haemolytic bioactivities. Lipopeptides were selected as the compounds of interest because they have low levels of resistance developed against them and possess characteristics which make them ideal candidates for future clinical and agricultural applications. These characteristics include rapid-action, antimicrobial potency, structural diversity and biodegradability into harmless amino acids (Raaijmakers *et al*., 2006; Rautenbach *et al*., 2016; Troskie *et al*., 2014).

Culturing techniques for producing high levels of LPs typically use media optimisation approaches to provide microbial producers with necessary nutrients and to induce a stress response to stimulate increased LP production. For example, pneumocandin A_0 is produced by *Zalerion arboricola* when carbon availability is kept low to induce stress while nitrogen is added in excess to provide essential nutrients for the assimilation of amino acids which make up the backbone of every antifungal peptide (AFP) (Biniarz *et al.,* 2018; Masurekar *et al*., 1992; Ndlovu *et al*., 2017). Growing cultures, of *Bacillus subtilis* and *Bacillus amyloliquefaciens,* to the stationary growth phase also stimulates antifungal LP production as the media becomes oxygen and nutrient limiting and this emulates a starvation event (Jin *et al.*, 2015; Pretorius *et al*., 2015).

For antifungal screening, the same target species panel were used as described in Chapter 3, as these fungal pathogens are prone to develop drug resistance which increases human mortality and reduce food availability on a global scale (Al-Hatmi *et al.,* 2016; Fisher *et al*., 2018; Godfray *et al*., 2016; Mpoza *et al*., 2018; Pianalto and Alspaugh,

2016). Therefore, secondary metabolites which inhibit their growth could be further developed to treat important clinical and agricultural diseases in future studies. Antifungal activity was evaluated against different fungal morphologies as the morphogenic plasticity of many pathogenic fungi affects survival in a changing environment, pathogenicity and drug susceptibility (Wurster *et al.,* 2019).

The structural characterisation of peptides, including LPs, is made possible with analytical methods such as high-performance liquid chromatography (HPLC), thin-layer chromatography, chiral gas chromatography (GC), mass spectrophotometry (MS), nuclear magnetic resonance (NMR), crystallography and Fourier transform IR infrared (IR) spectroscopy (Raaijmakers *et al*., 2010). Other detection methods include immunological and PCR-based methods (Giacomodonato *et al*., 2001; Hsieh *et al*., 2004; Joshi and McSpadden Gardener, 2006; Mohammadipour *et al*., 2009). Using high or ultra-performance liquid chromatography (HPLC or UPLC), unknown peptides are separated according to their physical attributes (e.g. hydrophobicity-polarity balance or amphipathic balance). Reverse-phase chromatography is employed to reduce the complexity of the sample mixture and allow for easier MS analysis. During UPLC-MS, compounds are separated based on their physical attributes and mass-to-charge (*m/z*) ratios. Characteristic spectra with mass-to-charge (*m/z*) data are used to determine a compound's molecular mass. The accuracy or difference of molecular mass values is compared using parts per million (ppm) mass error to that of other compounds deposited on online or in-house databases. The ppm mass error cut off is usually set to smaller than 20 for *Mr* or *m/z* values (Rautenbach *et al*., 2017). Accessible online databases include the antimicrobial peptide (ADP) database (Wang *et al.,* 2015), the SatPdb database for ribosomal therapeutic peptides (Singh *et al*., 2016) and the non-ribosomal peptide (NORINE) database (Caboche *et al*., 2007).

To accurately determine the structure of unknown peptides which do not match any of the molecular mass profiles deposited on online or in-house databases, tandem mass spectrometry (MS/MS) can be used (Fig. 4.1). In MS/MS, precursor ions are separated for each compound using collision-dissociation (CID) methods like electrospray ionisation (ESI) or matrix-assisted laser desorption/ ionisation (MALDI). These techniques ionise individual peptide molecules into precursor molecules. ESI is used more regularly than MALDI for peptide fragmentation as it produces ions with multiple charges, and this increases the mass range of the analyser used. The precursor ions and resulting

fragments can be used to determine the elemental composition of a compound or to formulate a putative fragmentation scheme for a peptide.

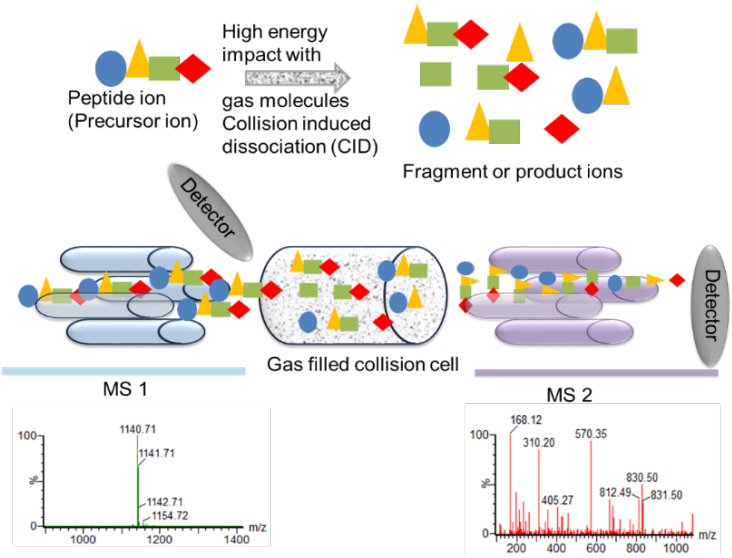

Figure 4.1. Peptide ionisation using tandem MS to produce two separate ion spectra. One ion spectrum with precursor ion/ions (MS1) and one ion spectrum with fragmented peptide ions, fragmented into individual product ion molecules, (MS2) (scheme courtesy M Rautenbach).

4.2 Material and Methods

4.2.1 Fungal strains

Two opportunistic yeast pathogens, with relevance to human health and disease (*Cryptococcus neoformans* and *Candida albicans*), and two filamentous fungi, which act as agricultural phytopathogens (*Botrytis cinerea* and *Fusarium oxysporum*), were selected to evaluate the antifungal activity of *P. sidoides* tuber isolates. The sample source of each target organism is provided in Table 4.1.

Table 4.1. Fungal species used in antifungal assays as target organisms.

Fungal species and strain	Source
Cryptococcus neoformans H99	Duke University (Durham, North Carolina)
Candida albicans CAB 1084	Department of Microbiology, *Stellenbosch University
Fusarium oxysporum f. sp. *cubensis*	Department of Plant Pathology, *Stellenbosch University
Botrytis cinerea	Institute for Wine Biotechnology, *Stellenbosch University

*Stellenbosch University (Stellenbosch, South Africa).

4.2.2 Media components and consumables

Petri dishes (90 mm) were supplied by KIMIX (Cape Town, South Africa). Centrifuge tubes, syringes and low-binding pipette tips were supplied by Lasec (Cape Town, South Africa). Cellulose acetate syringe filters (0.22 µm) were supplied by Pall Life Sciences (New York, USA). HPLC vials were supplied by Thermo Fisher Scientific (Massachusetts, USA). Sterile red blood plates (2% agar, 5% sheep or horse blood) were supplied by (National Health Laboratory Service, South Africa). The breathable film, calcium chloride and Coomasie blue R-250 were supplied by Sigma-Aldrich (Missouri, USA). Acetonitrile, hydrochloric acid, acetic acid, agarose and media components for YPD, MMN, LB and M9 media were supplied by Merck (Darmstadt, Germany). Growth media compositions are included in Appendix A.

4.3 Methods

4.3.1 Culturing for antifungal lipopeptide production

Four *P. sidoides*-associated microbes were selected for having broad-spectrum and high relative antifungal activity against *B. cinerea*, *C. albicans*, *C. neoformans* and *F. oxysporum* (Table 3.6) (Chapter 3). These isolates (Fig. 4.2) were then cultured for LP production using liquid and solid media and stressed and un-stressed conditions. Stressed conditions used minimal growth media and stationary liquid cultures (oxygen limiting) while un-stressed conditions used rich growth media and agitated liquid cultures. Compounds were extracted from culture supernatant and cell biomass using 70% acetonitrile (v/v with deionised water), acidified and lyophilised to preserve activity.

Figure 4.2. Microbes isolated from wild *P. sidoides* tubers and grown on solid yeast peptone dextrose media. Each with antifungal activity against *B. cinerea*, *C. albicans*, *C. neoformans* and *F. oxysporum.*

Liquid cultures were grown in 96-well plates with a single bashing bead (425-600 µ) placed in each well (Ndlovu *et al*., 2017). Wells were filled with 900 µl of rich or minimal media and inoculated with 100 µl of either 1 x 10^4 cells/mL for bacterial isolates (YC2 and SC6), or 1 x 10^3 spores for fungal isolates (A1 and C5). Rich media included yeast

peptone dextrose (YPD) and Luria-Bertani (LB), while minimal media included MMN and M9 media. All media compositions are included in Appendix A. Each isolate was allocated two columns and one column of un-inoculated medium served as growth control. A breathable film was used to seal each plate and prevent contamination. Plates were incubated at 26°C for seven days for bacterial isolates or ten days for fungal isolates. Shaken cultures were incubated on a floor shaker at 140 rpm during this time. After incubation, all cultures were put into a centrifuge and spun down at 3000 rpm for ten minutes at 4°C to separate the liquid supernatant from cell biomass. The liquid supernatant from each well was removed and each column pooled into a 50 mL centrifuge tube. To each well of remaining biomass, 600 µl of 70% (v/v) acetonitrile (ACN) was added and the 96-well plates re-sealed with breathable film. From this point, only low-binding pipette tips (Lasec, Cape Town, South Africa) and glassware were used. The preparation of glassware for this purpose is specified in Appendix E. The biomass was agitated at 140 rpm for 4 h at 4°C and then aliquoted into McCartney bottles before storage with the falcon tubes at – 80°C overnight. This was done in preparation for drying in a VirTis BenchTop™ K series freeze dryer/lyophiliser supplied by United Scientific (Cape Town, South Africa). After 24 h of drying, the biomass samples were stored at – 80°C and the supernatant samples agitated with 4.8 mL of 70% ACN. Supernatant samples were stored at – 80°C and both sets of samples freeze-dried one more time. For the culturing of microbial producers on solid media, the same techniques were repeated without bashing beads and with cell and spore inoculums added to 800 µl of molten rich or minimal agar media.

To further increase the yield of LPs extracted from liquid cultures, larger cultures were grown in 100 mL flasks filled with 50 mL of growth media. Flasks were prepared according to Appendix E. These cultures contained only rich media and were incubated at 26°C for ten days for bacterial isolates and 14 days for fungal isolates. As before, cell inoculum was 1 x 10^4 cells/mL or 1 x 10^3 spores/mL for bacterial and fungal isolates, respectively. After incubation, 30 mL of culture volume was removed, acidified, freeze-dried and resuspended in 70% (v/v) CAN. Acidification used 32% HCl (v/v) to adjust culture supernatants to a pH of 2.5. This was done so peptide molecules would precipitate and form a pellet after storage in a 4°C fridge overnight and centrifugation at 11 300 x g for 30 minutes. This concentrated pellet was washed and suspended in10 mL of deionised water, before re-adjusting the pH to 7.5 with 2.5M NaOH. Samples were frozen overnight at -80°C and freeze-dried. Samples were re-suspended in 5 mL 70% ACN (v/v) and

agitated at 140 rpm on a shaker. After agitation, they were sonicated for ten minutes in a sonification water bath to improve extract homogeneity. These homogenous samples were frozen overnight at -80°C and freeze-dried again before storage.

The success of each culturing technique was evaluated using an agar diffusion assay for broad-spectrum and relative antifungal activity against *C. neoformans*, *C. albicans*, *B. cinerea* and *F. oxysporum*.

4.2.3 Bioactivity of antifungal extracts

4.2.3.1 Antifungal activity against single cells and pathogenic spores

A medium-throughput agar diffusion assay was generated by placing half a sterile 96 well PCR plate in 20 mL molten YPD agar in a standard petri dish and allowed to solidify, generating multiple wells per plate. This technique was modelled after a protease assay used by Du Preez van Staden *et al*. (2016). The YPD agar was seeded with 1 x 10^4 yeast cells or 1 x 10^3 fungal spores and the antifungal agent was added to the wells. The experiment contained duplicates, and each well was filled with 25 µl antifungal extract dissolved in 50% (v/v) ACN (final concentration 50 mg/mL). A negative control well was filled with 50% (v/v) ACN and a positive control well filled with 50 mg/mL Amphotericin B (m/v in deionised water). All plates were incubated for 48 h at 26 ºC, and clear zone formation was used to indicate a positive result for antifungal activity. A zone size greater than 10 mm in diameter was taken as a strong positive result, greater than 5 mm a medium strength result, smaller than 5 mm diameter was a weak positive result, and no clear zones were taken as a negative result. Results were graded 3, 2, 1 or 0, respectively.

4.2.3.2 Antifungal activity against fungal mycelia

To test *F. oxysporum* and *B. cinerea* for antifungal sensitivity in their hyphal growth forms, a 24-well assay was performed (Troskie *et al*. 2012). This assay used solid YPD media in a sterile 24-well plate and fungal plugs or fungal spores (1 x 10^4 spores) from each fungal pathogen as an inoculum. Each well in the plate was filled with 1 mL YPD molten agar and allowed to cool before placing a 2 mm x 2 mm gel slices of mycelia (7 days old after incubation at 26℃) or 100 µl spore suspension in the centre of the well. Wells were treated with 20 µl of extract produced by *P. sidoides*-associate microbes at concentrations of 50 mg/mL, 25 mg/mL, 12, 5 mg/mL and 6, 25 mg/mL, respectively. After 24, 48, 72 and

96 h, colony diameters were measured and compared to the negative control (untreated fungal mycelia). Mycelia were stained with 100 µl of blue dye (0.063% [w/v] Coomasie blue R-250, 50% [v/v] Methanol and 10% [v/v] acetic acid) and de-stained 24 h later with 100 µl de-stain (12.5% isopropanol and 10% acetic acid; v/v). This process was repeated after 48 and 72 h to ensure all residual stain was completely removed. Stained hyphae were mounted on a glass slide and images captured at 1000 x magnification using a Nikon Ellipse E400 light microscope connected to a Nikon dsfi2 camera and a Nikon digital sight ds-u3 camera controller.

4.2.3.3 Haemolytic assays

Sterile red blood plates were used in the haemolytic toxicity assays, and 20 µl of each antifungal extract spotted onto a single plate. Plates were incubated at 37°C for 48 h and characterised as alpha (full cell lysis produces a clear zone around treatment), beta (cell toxicity produces a colour change around treatment) or gamma haemolytic (does not change the appearance of the blood agar) (Buxton, 2005).

4.2.4. Analysis of antifungal extracts using mass spectrometry

4.2.4.1 Glassware and sample preparation for MS

Glass 2 mL vials were used to contain samples of antifungal extract after antimicrobial peptide extraction and sample lyophilisation (freeze-drying). Glass vials were prepared according to Appendix E. The freeze-dried extracts were dissolved in 50% ACN (v/v) to a final concentration of 5 mg/mL. To dilute and purify the mixture, 100 µL was placed in a wide neck septum, in an Eppendorf tube, and centrifuged at 1000 rpm for 10 min. Next, 20 µL was added from the top of the first wide-necked septum to 180 µL of 50% ACN (v/v) in a second wide-necked septum. The final concentration used in LC-MS analysis was 500 µg/mL of each antifungal extract.

4.2.4.2 Compound characterisation with UPLC-MS

Compounds in crude extracts were separated using UPLC™ linked to ESMS. For UPLC, a C_{18} reverse-phase analytical column (Acquity UPLC® HSS T3, 1.8 µm particle size, 2.1 × 150 mm, Waters Corporation, Dublin, Ireland) with a flow rate of 0.300 mL/min using a 0.1% formic acid (A) to acetonitrile (B) gradient (100% A from 0 to 0.5 min for loading, gradient was from 0.06 to 60.06% B from 0.5 to 10 min and then 80.06 to 0.06% B from 15 to 20 min) was attached to a Waters Quadrupole Time-of-Flight

Synapt G2 (Waters Corporation, Milford, USA) mass spectrometer. Cone voltage was set to 15V, the capillary voltage was 2.5 kV, source temperature was 120°C, desolvation temperature was 275°C, and the flow rate was 650 L/hr (N_2 gas). The ions in each UPLC-MS peak were decomposed with a collision energy (CE) gradient of 30-80 eV in the trap collision cell with CV at 15 V. The CE in transfer collision cell was set at 0 eV, and the collision gas was delivered at 0.5×10^{-3} bar Ar. Centroid mode data were collected in MS^2 from 150–2000 *m/z*. The rest of the instrument settings were as described above for the MS mode.

Data acquisition was performed in positive mode by scanning a MS range of 150–2000 *m/z*. Results were analysed using MassLynx software 4.01 (Waters Corporation, Milford, USA). Unknown compound identities were confirmed using a *de novo* search method where the *m/z* values in major peaks on the UPLC-MS spectrum were filtered using an in-house database of known contaminants and peptides and then to non-ribosomal peptides in the NORINE database (Caboche *et al*., 2007). The in-house database was supplied by Prof. Marina Rautenbach at the Department of Biochemistry, Stellenbosch University, who also assisted with the identification of the unknown peptides found in this study. A part per million (ppm) mass error of greater than 20 or less than -20 was used as a cut-off for MS peaks from different compounds (Rautenbach *et al*., 2017). From the MS^2 (MS/MS) fragmentation spectrum, the mass distances between neighbouring peaks of fragmented precursor ions were compared with known ion fragmentation patterns/ion fingerprints found in published literature. These fragmented ions were also compared using ppm mass error as with the MS peaks (Rautenbach *et al*., 2017). The ion fingerprints also revealed possible amino acid sequences for each unknown analyte with specific column retention times.

4.3 Results and Discussion

4.3.1 Screening culture conditions to produce antifungal compounds

P. sidoides tuber-associated microbial isolates (SC6, YC2, C5 and A1) were cultured using various culture conditions to increase the likelihood of antifungal metabolite production. Culturing conditions included liquid and solid media and stressed and un-stressed conditions. Stressed conditions used minimal growth media (M9 and MMN) and stationary liquid cultures, while un-stressed conditions used rich growth media (LB and YPD) and liquid cultures with shaking. Extraction techniques were tailored to extract

peptides from either culture supernatant or cell biomass. Both the culture conditions and extraction techniques were evaluated with an agar diffusion assay. The results for the most effective culturing conditions and extraction techniques are included in Table 4.2.

The most effective culturing conditions used stationary 50 mL liquid cultures with rich media and compounds extracted from the culture supernatant after stationary growth. These results confirm the credibility of using low levels of dissolved oxygen and certain nutrient availabilities, as suggested by Jin *et al*. (2015) and Pretorius *et al.* (2015) for bacterial strains, and by Sena *et al.* (2018), for *Penicillium* species, to stimulate the production of antimicrobial metabolites. Using a liquid media may have provided a greater culture volume and nutrient diffusion than solid media.

Table 4.2. Clear zone diameters (mm) of isolate SC6, YC2, C5 and A1 extracts spotted onto solid YPD media laced with either pathogenic yeast cells (*C. albicans* or *C. neoformans*) or spores (*F. oxysporum* or *B. cinerea*). All extracts were produced by *P. sidoides*-associated microbes and grown in liquid rich-media under oxygen-limited conditions.

	C. neoformans		***C. albicans***		***F. oxysporum***		***B. cinerea***	
Culture	****Lawn 1**	**Lawn 2**	**Lawn 1**	**Lawn 2**	**Lawn 1**	**Lawn 2**	**Lawn 1**	**Lawn 2**
YC2-A	12	15	12	12	13	12	13	12
YC2-B	16	17	12	12	11	11	11	13
YC2-C	15	16	12	12	9	11	11	13
SC6-A	6	5	5	5	*~3	*~3	*~3	*~3
SC6-B	4	4	4	4	*~3	*~3	*~3	*~3
SC6-C	5	5	4	4	*~3	*~3	*~3	*~3
*****A1-A**	5	5	6	6	*~2	*~2	*~2	*~2
*****A1-B**	6	6	7	7	*~2	*~2	*~2	*~2
C5-A	0	0	0	0	0	0	0	0
C5-B	0	0	0	0	0	0	0	0
C5-C	0	0	0	0	0	0	0	0

*Clear zones were observed after 32 h but overwhelmed by fungal mycelia at 48 h incubation when final measurements were taken to quantify clear zone diameter and antifungal activity for the microbial extracts tested.

**Lawn 1 and Lawn 2 are technical repeats/replicates of the same experiment.

*** One culture of the triplicate A1 cultures, A1-C, did not grow and produced no data for this experiment. Therefore, this culture was omitted from Table 4.2.

Extraction, storage and purification techniques from Ndlovu *et al.* (2017) proved effective and preserved antifungal activity for all but the C5 culture extracts. No antifungal activity was observed for compounds extracted from C5 cultures using 70% ACN (v/v) (Table 4.2) and using other organic solvents (80% Isopropanol, 80% methanol and 100% methanol; v/v) did not improve on this result. Antifungal extracts of YC2, SC6 and A1 culture supernatant and cell biomass, respectively, had near-identical antifungal activities in the agar diffusion assay. This suggests that antifungal metabolites were excreted extracellularly and retained inside the cell or on the cell surface. As freeze-dried culture supernatants dissolved more easily in 70% ACN (v/v) than the freeze-dried cell biomass, only the supernatants were sent for UPLC-MS analysis. This was important as the C_{18} reverse-phase analytical column (Acquity UPLC® HSS T3, Waters Corporation, Dublin, Ireland) used in the UPLC-MS analysis had a 1.8 µm particle size and analysing samples with large undissolved particles could have prevented sample constituents from moving through the column.

When optimising the agar diffusion assay, 70% ACN (v/v) was found to have no antifungal activity. This attributes any observed antifungal activity to compounds dissolved in the organic solvent and not the solvent. Amphotericin B provided an effective positive control for antifungal activity. Extracts produced by isolates YC2, SC6 and A1 (Table 4.2) were all found to have antifungal activity against target pathogens *C. albicans* and *C. neoformans*. Extracts produced by YC2 were also antifungal against *F. oxysporum* and *B. cinerea*, but results for extracts produced by isolates SC6 and A1 were inconclusive. For these extracts, clear zones 2-3 mm in diameter would appear around wells inoculated with antifungal extract and be overwhelmed by fungal mycelia just before the 48h incubation period. Therefore, the clear zones for SC6 and A1 extracts should have been measured after a shorter incubation period (e.g. 32 h) when screening for antifungal activity against *F. oxysporum* and *B. cinerea* spores.

4.3.2 Antifungal activity against different fungal morphologies

Antifungal activity was evaluated against different fungal morphologies as pathogenic fungi can spread and grow in multiple growth forms, which affect their pathogenicity and drug susceptibility (Wurster *et al.,* 2019). This morphogenetic plasticity allows them to survive in different environments as they invade plant or animal tissues, as hyphae, or spread in the natural environment as unicellular yeasts or spores, which aid in rapid dispersal (Perez-Nadales *et al.,* 2014). The most difficult to treat growth morphologies,

apart from particularly resilient spore types (e.g. chlamydospores), include fungal hyphae embedded in host tissue. For example, the hyphal morphology of *C. albicans* has elevated chitin levels which protect β (1, 3)–glucan synthetases in the cell membrane from being inhibited by echinocandins such as caspofungin (Braun and Calderon, 1978; Lenardon *et al*., 2010). Similarly, hyphal growth morphologies of *B. cinerea* and *F. oxysporum* use elevated chitin levels and improved metabolism of certain amino acids to decrease their drug sensitivity to echinocandins (Makovitzki *et al*., 2007). Hyphae embedded in plant tissue are also protected from antifungal compounds which cannot penetrate to bind to cell targets essential for growth inhibition (Parente-Rocha *et al*., 2017; Dyakov and Zinovyeva, 2007).

In Table 4.3, the results of all the antifungal assays are shown. Extracts of YC2, SC6 and A1, were tested against *C. albicans* and *C. neoformans* unicellular yeast cells and *B. cinerea* and *F. oxysporum* spores and fungal mycelia. All three extracts had fungistatic activity against *C. albicans* and *C. neoformans* unicellular yeast cells, and *B. cinerea* and *F. oxysporum* spores, in the agar diffusion assay (Table 4.3). Although, as mentioned in 4.4.1, SC6 and A1 extracts only had antifungal activity against *B. cinerea* and *F. oxysporum* spores after 32 h incubation at 26 ºC. YC2 extracts still had antifungal activity against *B. cinerea* and *F. oxysporum* spores after 48 h incubation at 26°C. Therefore, in this assay, YC2 extract had the strongest antifungal activity.

Table 4.3. Antifungal activity against different forms of pathogenic fungi for extracts harvested from microbial producers YC2, SC6 and A1.

***Antifungal activity against pathogenic spores/cells**

	C. neoformans	*C. albicans*	*F. oxysporum*	*B. cinerea*
YC2	15.2	12	11.2	12.2
SC6	4.8	4.3	****~3	****~3
A1	5.5	6.5	****~2	****~2

****Antifungal activity against fungal mycelia/hyphal growth phase**

		F. oxysporum	*B. cinerea*
YC2		2	2
SC6		***NA	***NA
A1		***NA	***NA

*Values represent the average clear zone diameter (mm) measured for wells treated with YC2, SC6 or A1 extract in the agar diffusion assay. This assay was composed of small wells in solid YPD media laced with pathogenic spores (*B. cinerea* and *F. oxysporum*) or yeast cells (*C. albicans* or *C. neoformans*). Clear zone diameters were indicative of a positive result.

**Values represent strong fungistatic (3), weak fungistatic (2) or negative result (0).

***Not applicable (NA) as these extracts were not tested in this antifungal assay.

****Refer to Table 4.2.

The hyphal sensitivity of *B. cinerea* and *F. oxysporum* colonies to several different concentrations of YC2 extract can be seen in Figs. 4.3 and 4.4. After 24 h, 48 h, 72 h and 96 h incubation, colony diameters of the treated fungal plugs and spores were dramatically reduced (Figs. 4.3A-D). This was in comparison to untreated fungal plugs and spores used as a positive control. The treatment was fungistatic for colonies inoculated with fungal plugs as these colonies continued to expand at a reduced rate after 24-96 h incubation (Fig. 4.3A). The treatment was fungicidal for colonies inoculated with spore suspension as these colonies did not expand in diameter after 24 h incubation. Quantitative data is supplied for the inhibition of *B. cinerea* and *F. oxysporum* hyphal growths in Fig. 4.4.

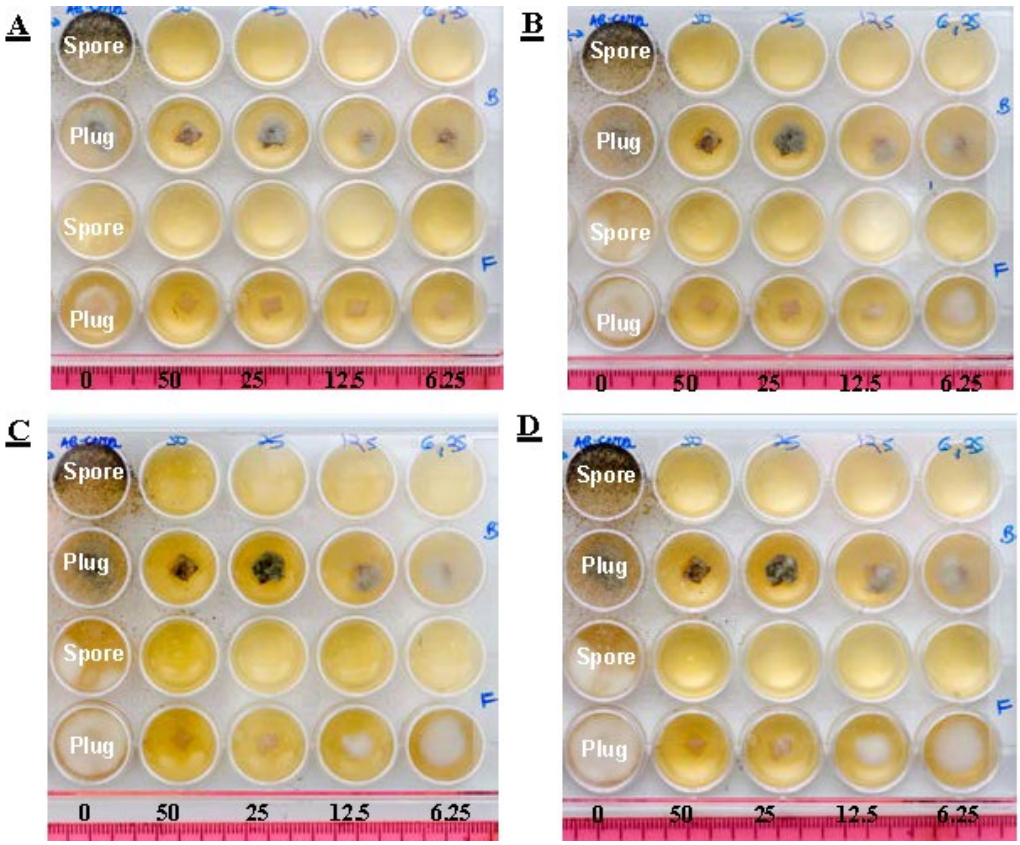

Figure 4.3. Hyphal sensitivity assays were reviewed after A) 24 h, B) 48 h, C) 72 h and D) 96 h incubation with five different concentrations (0.00-50.00 mg/mL) of YC2 extract from culture YC2 A. Each well was inoculated with pathogenic spores and fungal plugs, respectively. Colonies of *B. cinerea* were black-green in colouration and *F. oxysporum* colonies were white. A concentration of 0 mg/mL YC2 extract was used as a negative control.

Concerning the fungistatic effects of YC2 extract on *B. cinerea* and *F. oxysporum* fungal plugs, all concentrations of YC2 extract were effective in inhibiting the growth of fungal mycelia and reducing the rate at which the treated colonies were able to expand. These results are substantiated with error bars for standard error in Figs. 4.4A and B. After 96 h incubation at 26°C, the most effective treatment of both *B. cinerea* and *F. oxysporum* were respectively, 50 mg/mL, 25 mg/mL, 12.5 mg/mL, and 6.25 mg/mL YC2 extract (Figs. 4.3A-B). However, for *B. cinerea,* some lower concentrations of YC2 extract were more effective than higher concentrations if applied to fungal plugs and incubated for 24 h, 48 h and 72 h (Fig. 4.3B). For example, 12.5 mg/mL of YC2 extract proved more effective than 25 mg/mL of YC2 extract in reducing colony diameters of *B. cinerea* when incubating fungal plugs for 24 h, 48 h and 72 h. Similarly, 6.25 mg/mL of YC2 extract proved more effective than 12.5 mg/mL of YC2 extract in reducing colony diameters of *B. cinerea* after 24 h incubation. These findings allude to some heterogeneity within the crude extracts prepared from isolate YC2.

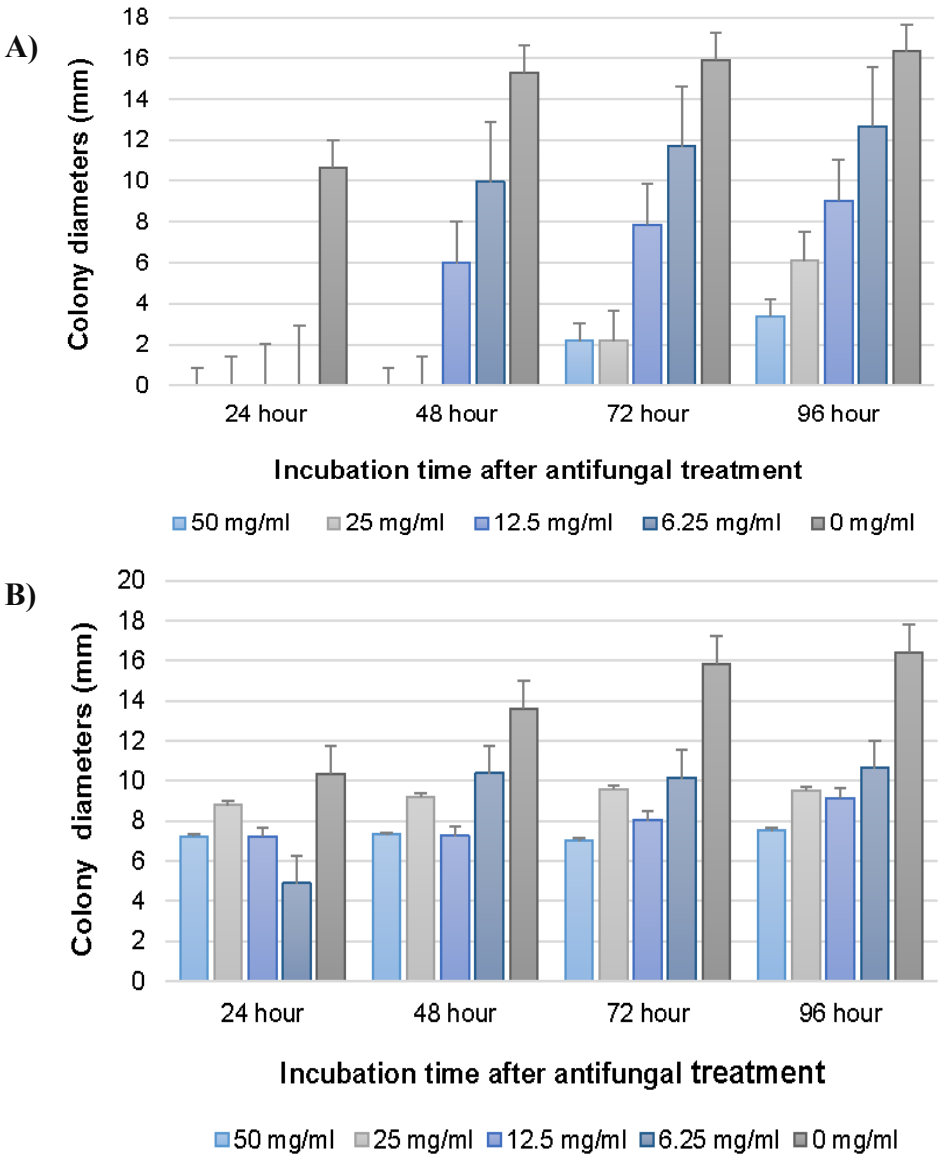

Figure 4.4. Comparison of colony diameters formed around A) *F. oxysporum* and B) *B. cinerea* fungal plugs treated with five different concentrations of YC2 extract. A concentration of 0 mg/mL antifungal agent served as a negative control. Each bar represents one fungal plug treated with a specific concentration of antifungal extract and error bars depict standard error.

A visual inspection was performed with light microscopy to identify signs of hyphal stress in treated and untreated *B. cinerea* and *F. oxysporum* hyphae (Figs. 4.5A-F). The untreated hyphae (Figs. 4.5A - B) were compared with those treated with 50 mg/mL YC2 extract (Figs. 4.5C-D). Signs of stress-induced in the hyphae of filamentous fungi include irregular branching patterns (e.g. hyper branching, aborted lateral branching or dichotomous hyphal tip branching), hyphal swelling, a reduction in spore formation, the disappearance of hyphal nuclei and irregularities in the cytoplasm (Troskie *et al*., 2014; Munoz *et al.,* 2006; Mania *et al*., 2010). Irregularities in the cytoplasmic structure include

a loss of electric potential, cell leakage and cell lysis. In treated *B. cinerea* and *F. oxysporum* hyphae, irregular branching patterns (Figs. 4.7E-F), a reduction in spore formation (Figs. 4.5C-F) and irregularities/leakages in the cytoplasm were observed (Figs. 4.5C-D). These findings confirm that treated hyphae were negatively affected by YC2 extract on a microscopic/cellular level.

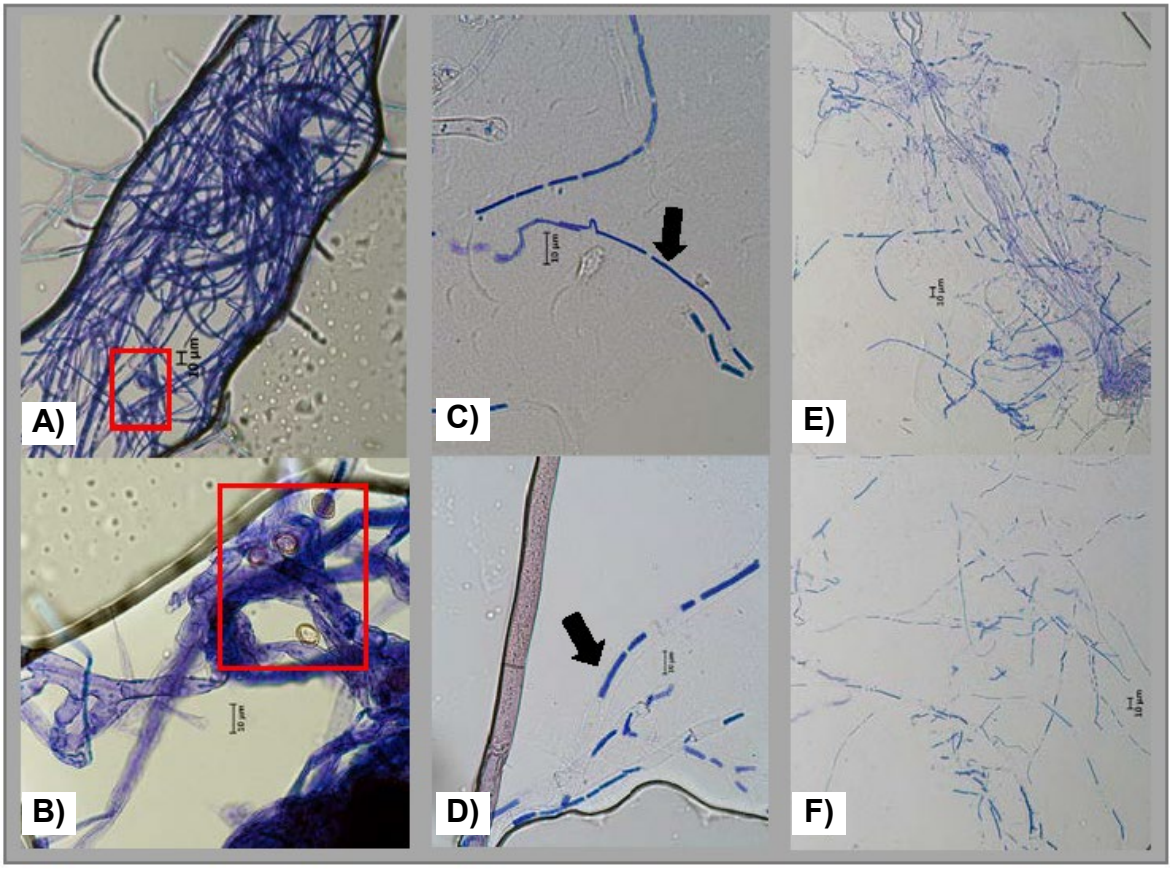

Figure 4.5. Visual results for stained *B. cinerea* and *F. oxysporum* hyphal cells viewed at 1000x magnification with a light microscope and a digital camera. Antifungal treatment was 50 mg/mL YC2 extract. A) Untreated *F. oxysporum*, B) untreated *B. cinerea*, C) treated *F. oxysporum* with constricted cytoplasm, D) treated *B. cinerea* with constricted cytoplasm, E) treated *F. oxysporum* with hyper-branching and F) treated *B. cinerea* displaying hyper-branching. Red squares indicate fungal spores and black arrows indicate some areas of cytoplasm within compromised hyphae.

4.3.3 Haemolytic activity of antifungal extracts

Antifungal extracts were tested for haemolytic activity and two found to cause full erythrocyte lysis and cell toxicity, respectively. *Bacillus* YC2 extract was beta-haemolytic (full erythrocyte lysis) and *Bacillus* SC6 extract was alpha-haemolytic (erythrocyte toxicity), while extracts obtained from *Penicillium* A1 and *Penicillium* C5 were both gamma haemolytic (non-toxic to erythrocytes tested) (Fig. 4.6).

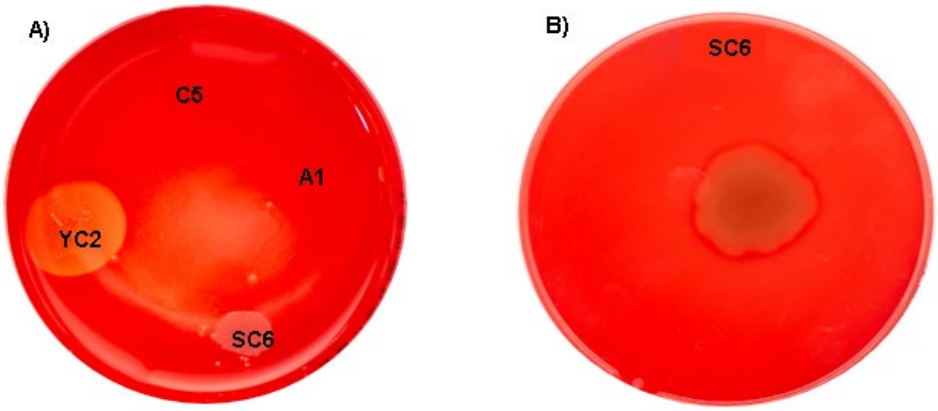

Figure 4.6. Haemolytic assay A) for YC2, SC6, A1 and C5 extracts after 48 h incubation at 37°C and B) for SC6 extract incubated at 37°C for an extra 24 h to enhance the discolouration observed around the treatment zone (Area treated with SC6 extract). This discolouration was indicative of erythrocyte toxicity and alpha-haemolytic activity.

4.3.4 Identification and characterisation of putative lipopeptides produced by *Bacillus* sp. YC2

In the ESMS analysis of crude extracts harvested from bacterial isolate YC2 (putatively identified as a *Bacillus* species), two compound complexes were detected in positive mode using the prescribed scanning range of 150-2000 *m/z* (Fig. 4.7A). These compounds had mass-to-charge ratios comparable to those of previously identified bacterial LPs (Table 4.4) and appeared as multiple, closely associated, peaks with both single and double charges, on the same ion spectrum. Singly charged ions within each compound complex also differed in molecular mass and produced a range of closely related mass peaks on the MS1 spectrum (Fig. 4.7B). MaxEnt 3 deconvolution of the multiprotonated spectra confirmed complex 1 to have a M_r range of 1015-1080 and complex 2 to have a M_r range of 1462-1530. MaxEnt (Maximum Entropy) 3 algorithm of MassLynx 4.01 processes the multi-protonated *m/z* data to find the accurate M_r of the analytes. It also improves the signal to noise ratio of biopolymer data or data containing compounds with multiple charges by extracting the useful zero-charge spectra from noisy multiply charged *m/z* data (Ferrige *et al*., 1992).

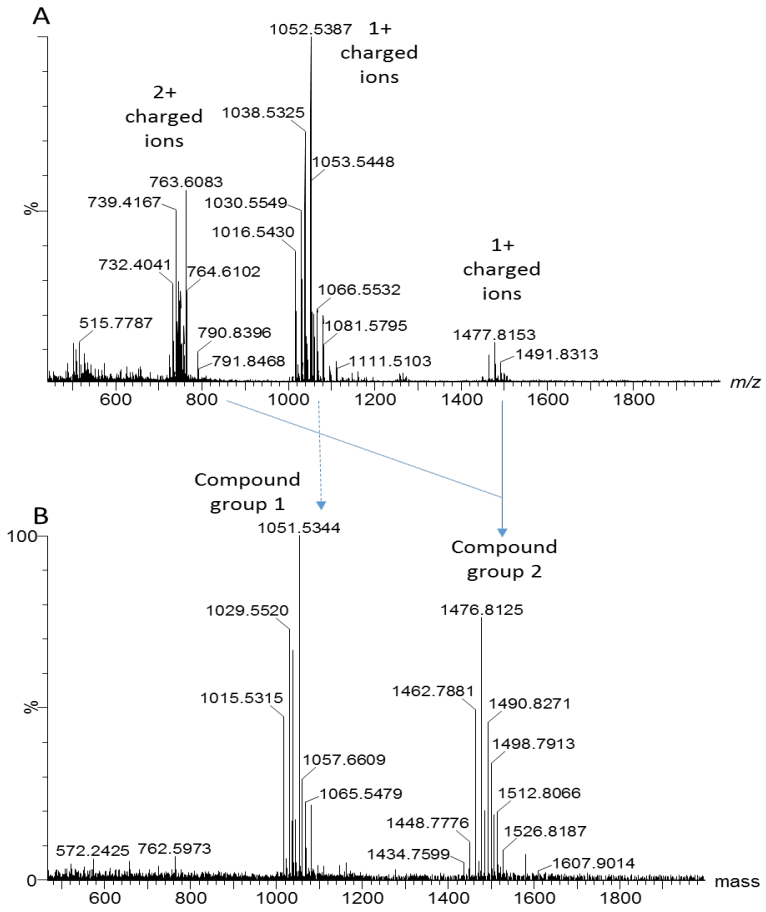

Figure 4.7. ESMS analysis of crude antifungal extract harvested from YC2 flask culture. **A.** Representative mass spectrum when scanning a range of 150-2000 *m/z* in positive mode. The singly (1+) and doubly charged ions (2+) are indicated. **B.** The MaxEnt 3 generated mass spectrum is showing two main compound complexes (1 and 2).

Both multiple charges and slight variations in *m/z* of subsequent peaks on the ion spectra are commonly observed for LPs. This is because conservative differences in amino acid composition (Leu/Ile/Val, Asp/Asn; Gln/Glu, Lys/Orn), amidation (15 Da), hydroxylation (16 Da) and differences in fatty acid acyl chain (CH_2 groups (~14 Da)) or salt ion adducts (Cl, Na of K adducts), can result in many variations in M_r detection of the same compound. These variants often have similar activities and perform similar biological functions to those first identified for the reference producer organism. They can be distinguished from one another after the elimination of certain adducts and CH_2 groups and the elucidation of the amino acid sequence.

Since multiple LPs and lipopeptide variants are produced under different culturing conditions, media optimisation is essential when producing LPs in a stable, reproducible, manner. For this reason, culturing should be done in triplicate (three biological repeats),

and all culturing conditions kept the same as much as possible. Extraction techniques should also be standardised to extract the same amount of the same LPs from each microbial culture. Technical repeats can be used to extract more than one sample from the same microbial culture and further ensure the reproducibility of stable producers.

In Table 4.4, the reproducibility of culturing and extraction techniques was evaluated for three cultures of bacterial producer YC2. For each main peak (representative of a single compound or several closely related compound variants), the *m/z* value and percentage peak area were recorded. Signal peaks with low signal intensities (less than 10% of the total ion count) were omitted from this comparison. The main peaks labelled peak 1- peak 6B, were detected within a set range of retention times and consistently produced in samples from all three YC2 cultures, as seen in Fig. 4.8 (UPLC-MS for C1-C3). Interestingly, complex 1 compounds (doubly charged ions 508-529 *m/z* using UPLC-MS) were eluted between 6.93 and 9.73 min and complex 2 compounds (doubly charged ions 732-753 *m/z* using UPLC-MS) only eluted after 9.73 min. This elution pattern depended on the amphipathic balance of the peptide in the complex with the more hydrophobic complex 2 eluting later from the C18 matrix.

Table 4.4. Compound retention time (Rt), *m/z* value and percentage peak area for main compounds detected in three cultures of YC2.

Main peak	Retention time (min)	Culture 1		Culture 2		Culture 3	
		Main *m/z*	%Peak Area	Main *m/z*	%Peak Area	Main *m/z*	%Peak Area
1	6.94-6.96	508.7814	22.0	508.7815	36.6	1016.5437	40.1
2A	7.63-7.68	515.7886	9.4	515.7878	12.7	1030.5583	8.6
2B	7.76-7.78	515.7886	6.4	515.7886	7.5	1030.5605	11.6
3A	8.78-8.82	522.7938	2.3	522.7938	1.5	522.7896	3.8
3B	8.98-8.99	522.7938	6.9	522.7938	7.7	522.7915	3.0
4A	9.71-9.73	529.7960	1.7	529.7960	5.1	529.7983	4.0
4B	9.83-9.85	732.4042	34	732.4042	15.1	732.4063	6.6
5A	10.21-10.23	739.4167	3.5	739.4049	4.3	739.4150	7.1
5B	10.32-10.34	739.4167	8.8	739.4167	3.7	739.4152	10.1
6A	10.69-10.73	746.9281	2.1	746.4150	0.7	746.4209	2.7
6B	10.89-10.93	753.4222	3.1	753.4342	5.2	753.4265	2.5

As seen in Fig. 4.8 and Table 4.4, the retention times (Rt) of measured peaks (eluted compounds) was reasonably reproducible between all three cultures of YC2 (longest Rt

range was 0.04 min for compound 6A or 6B). Certain main peaks fraction eluted closely as they probably are variants with slightly different amino acid sequences or lipid moieties. This was confirmed by ESMS, where the M_r was calculated for each ion signal produced in all three cultures (Figs. 4.8 B1-B3).

The percentage peak areas, however, differed greatly between the three culture extracts produced by YC2 (largest disparity was ~11% difference between percentage peak area measured for a single compound in one culture sample and the average percentage peak area for that same compound in all three extracts analysed) (Table 4.4). This is indicative of different amounts of the same compound being produced at different levels between the three cultures and particularly between cultures 1 and 2 versus culture 3. A reason for different levels of production could include slight differences in nutrient availability or cell inoculum.

To improve reproducibility, it is suggested to upscale the production and use more sensitive weighing equipment for media preparation and culture inoculation as media components were weighed out with a gram scale (accuracy limited to two decimal points) and differences in cell inoculum could have been caused by human error when counting cells with a haemocytometer and pipetting cells into flask cultures. All these things considered, natural genetic variation between different bacterial cells will likely cause some variation between final and percentage yield to persist.

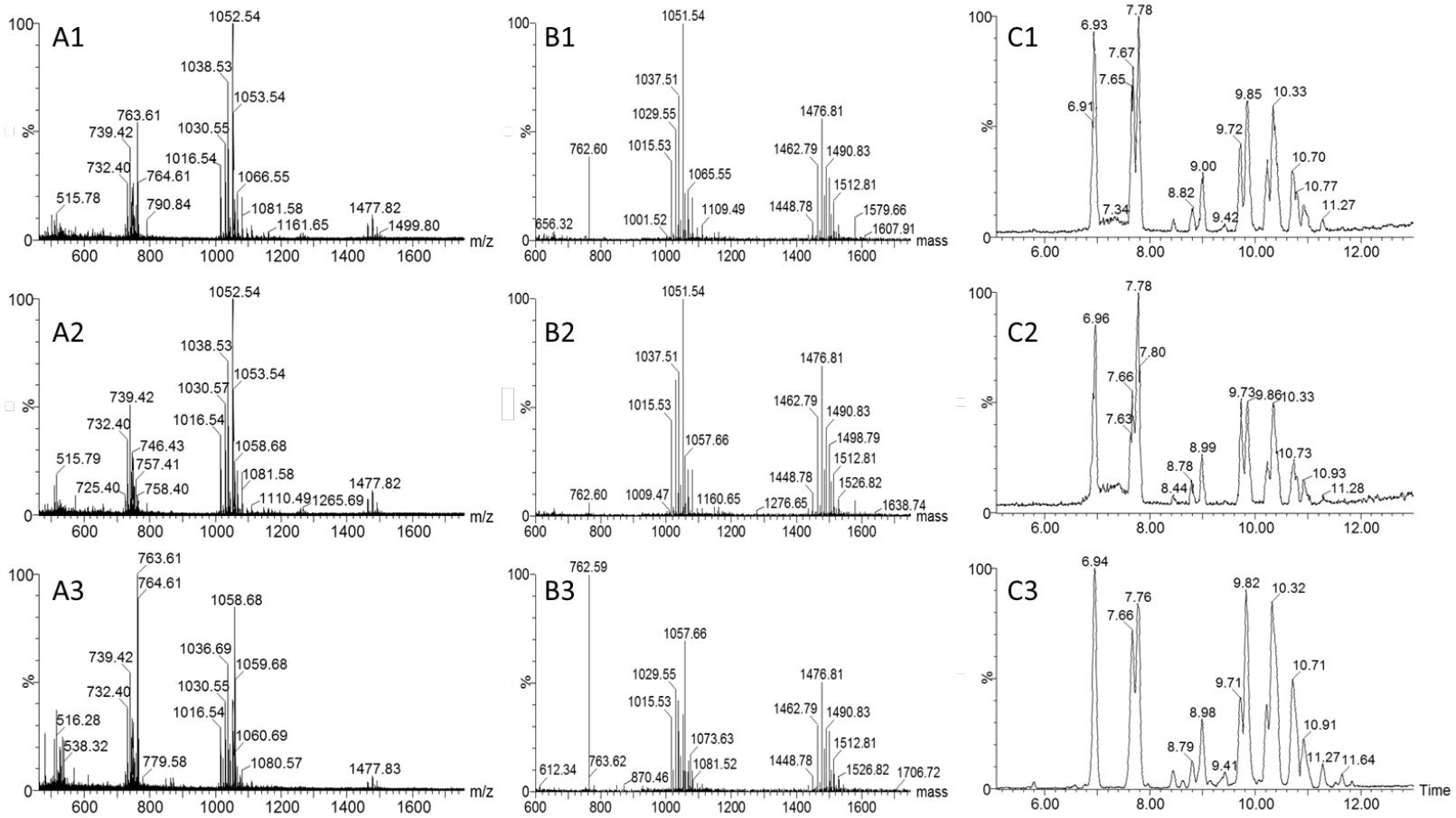

Figure 4.8. Ion spectra (A1-A3), corresponding mass spectra generated with MaxEnt 3 (ESMS) (B1-B3) and UPLC-MS chromatograms (C1-C3) with % base peak ions signal produced for YC2 cultures 1-3. Main peaks with ion intensities greater than 10% contribution have been as with 1-6B (Table 4.4) compared regarding *m/z* value and between peaks common to all three YC2 cultures (refer to Table 4.4).

4.3.4.1 Elucidation of the identity of components in complex 1

The addition of ion adducts often alters a compound's detected molecular mass. To accurately identify a compound using its molecular mass, these adducts must be removed. This was done for compounds contained in complex 1 of the YC2 extracts analysed with MaxEnt 3 (ESMS). In Fig. 4.9, sodium adducts (M_r plus 21.9820 Da) were considered together with putative CH_2 groups (14.0157) differences to classify the four different compound variants (compounds A-D).

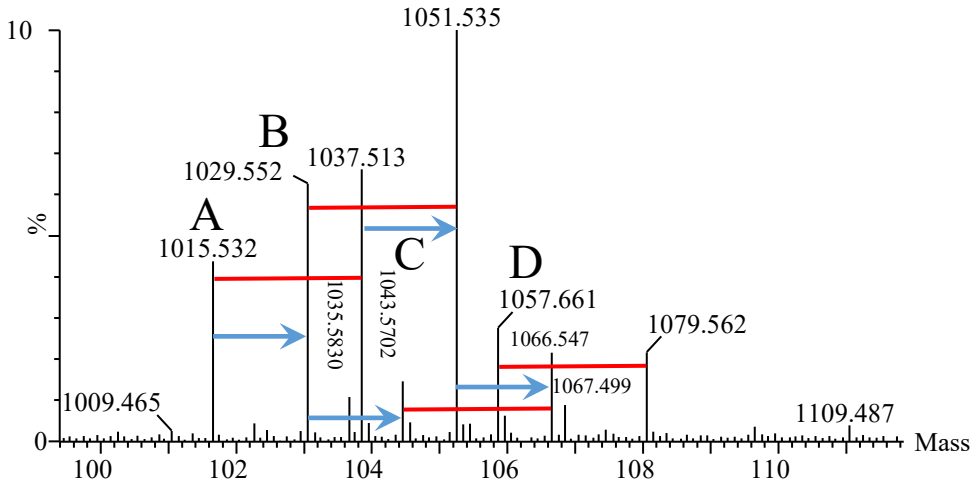

Figure 4.9. Representative mass spectrum generated with MaxEnt 3 of complex 1 from YC2 culture A. The blue arrows indicate the related compounds differing with a putative CH_2 group. The red lines show the relationship of sodium adducts of compounds A–D.

As stated before, the fact that the multiple additions of 14 Da was found is indicative of lipopeptides with different lengths of the fatty acid tail and possible differences in amino acid sequence. The small differences in a single peptide can alter peptide-column retention/elution time. In addition to this, peptide variants with longer fatty acid tails often elute later than identical peptides with shorter fatty acid tails. Different Leu/Ile groups often elute closer in retention time than peptide variants with a Val amino acid group in the amino acid sequence (Ndlovu *et al*., 2017). In the analysis of complex 1, this phenomenon can be seen most clearly for compounds 1B and 1B' and 1C and 1C' (Fig. 4.10). They exhibit two separate peaks for the same spectra; with perhaps one change in an amino acid group altering their peptide structure. The results from Fig. 4.10 concerning the *m/z* and Rt values for peaks detected on the UPLC-MS and ESMS for YC2 culture 1 could be compared with results from the analysis of surfactin, a LP of similar size (Rautenbach *et al*., 2017). Similar antifungal LPs, iturins and fengycin, are also included in Table 4.5 as they may also be possible matches.

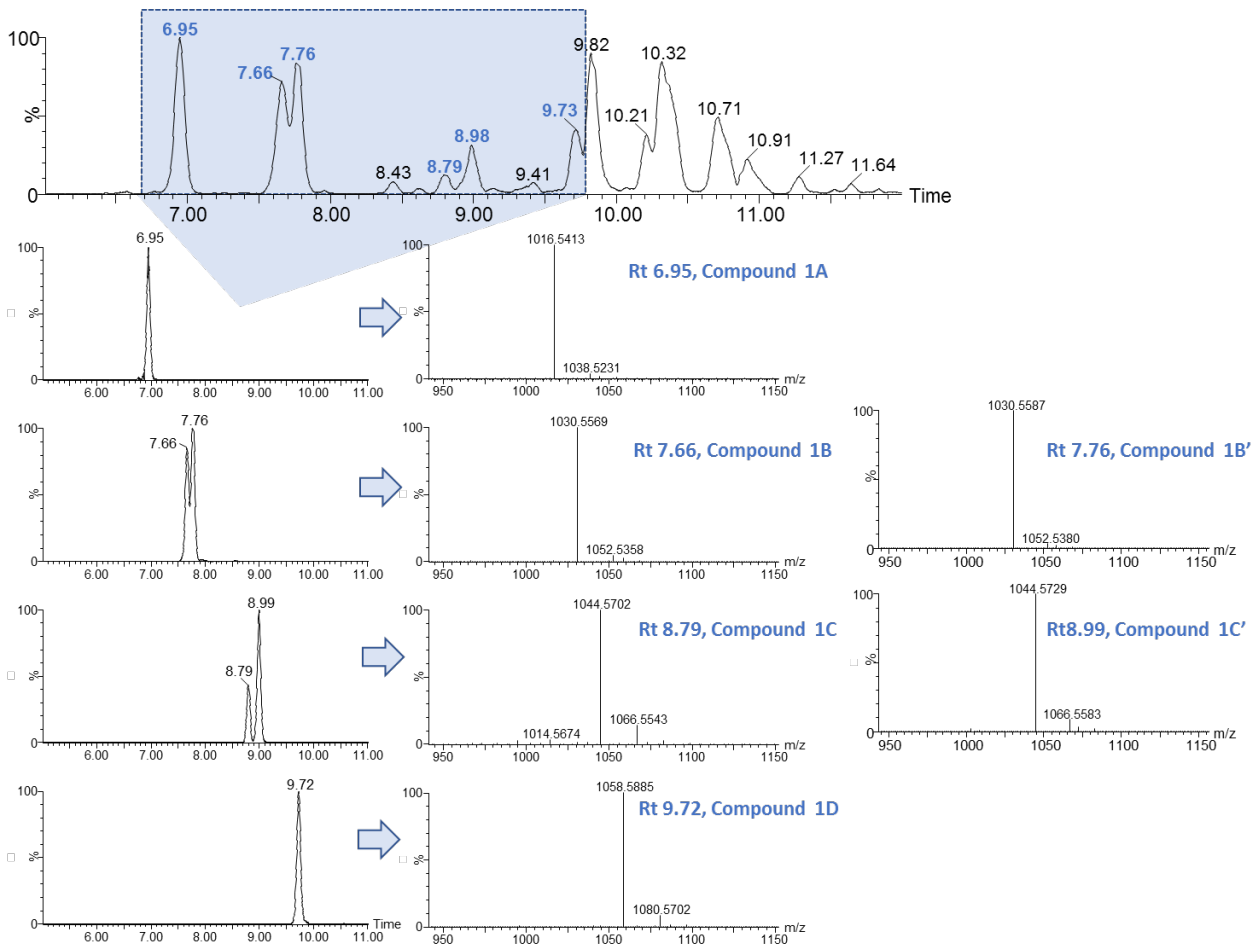

Figure 4.10. Mass extracted UPLC-MS profiles (left) of the full chromatogram (top) of the YC2 extract sampled from culture 1. The main peaks with retention times (Rt in min) and main singly charged molecular ion in each of the peaks correlating to complex 1 are indicated. The ion spectra were generated with the TOF-transform function of MassLynx 4.01.

The results of a search in the NORINE database for non-ribosomally produced peptides matching *m/z* values from complex 1 are included in Table 4.5. The search was conducted using a specific molecular mass search range (for complex 1 main peaks) and filters for cyclic LP structure types and compounds produced by bacteria. The results included seven peptide families and nine types: bacillomycin, iturin, surfactin, anabaenopeptilide, microcystin, barangamide, didemnin, nordidemnin and tamandarin. Only the first three peptide families were produced by terrestrial bacteria and likely identities for the compounds extracted from bacterial cultures of YC2. As many *Bacillus* species are known antibiotic surfactant producers and possible identities for bacterial producer YC2 (refer to Chapter 3), it is expected that many of its peptide sequences stored on NORINE would match the molecular masses of some of the main compounds detected in sample A of YC2 extract.

Table 4.5. YC2 complex 1 result for possible peptide identities and producer organisms as stored on the NORINE database and found using molecular weight to define search range.

Search range (M_r)	NORINE result	Compound *Mr*	Function	Known producer organism
1015-1030	Bacillomycin L-1	1020.5128	Antibiotic	*Bacillus subtilis*
	Microcystin-M(O)R	1028.5001	Toxin	*Microcystis*
	[ADMadda5] Microcystin-Lr; Microcystin-LHar	1022.5437	Toxin	*Oscillatoria agardhii*
	Microcystin-LW	1024.5270	Toxin	*Microcystis aeruginosa*
	[D-Asp3] Microcystin-RR	1023.5502	Toxin	*Microcystis aeruginosa*
	Microcystin-FR	1028.5331	Toxin	*Microcystis*
	[L-Ser7] Microcystin-E(OMe)E(OMe)	1015.4750	Toxin	*Nostocaceae (Anabaena)*
1030-1044	Iturin A-2	1042.5448	Antibiotic	*Bacillus subtilis*
	Bacillomycin L-3; Bacillomycin L-2	1034.5284	Antibiotic, Surfactant	*Bacillus subtilis*
	Bacillomycin D-1	1030.5335	Antibiotic, Surfactant	*Bacillus subtilis*
	Surfactin aC15	1035.6831	Antibiotic	*Bacillus subtilis*
	Microcystin-HphR	1029.5409	Toxin	*Nostocaceae (Anabaena)*
	[D-Ser1] Microcystin-LR	1038.5386	Toxin	*Nostocaceae*
	Microcystin-YM(O)	1035.4623	Toxin	*Microcystis aeruginosa*
	Microcystin-RR	1037.5658	Toxin	*Microcystis aeruginosa*
	Microcystin-LR	1040.5543	Toxin	*Nostocaceae*
	[D-Asp.Dha7] Microcystin-HtyR	1031.5202	Toxin	*Nostocaceae (Anabaena)*
	Microcystin-LHar	1036.5593	Toxin	*Nostocaceae*
1044-1052	Anabaenopeptilide 202A	1049.5070	Unknown	*Anabaena (Cyanobacteria)*
	Bacillomycin D-2; Bacillomycin D-3	1044.5492	Antibiotic, Surfactant	*Bacillus subtilis*
	Bacillomycin L-5; Bacillomycin L-4	1048.5440	Antibiotic, Surfactant	*Bacillus subtilis*
	Iturin C-1	1043.5288	Surfactant	*Bacillus subtilis*
	Microcystin YR	1044.5280	Toxin	*Microcystis aeruginosa*
	[D-Asp3] Microcystin-HtyR	1044.5280	Toxin	*Aphanizomenon*

	[Dha7] Microcystin-HtyR	1045.5358	Toxin	*Nostocaceae (Anabaena)*
1052-1058	Iturin A-3, A-4 and A-5	1056.5604	Antibiotic, Surfactant	*Bacillus subtilis*
	Microcystin-LR	1052.5910	Toxin	*Nostocaceae*
	Microcystin-RR	1051.5451	Toxin	*Nostocaceae*
1058-1080	Anabaenopeptilide 202B	1069.4523	Unknown	*Anabaena (Cyanobacteria)*
	Barangamide B, C and D	1077.7162	Unknown	*Theonella swinhoei*
	Didemnin B	1069.5947	Antibiotic, Antitumor	*Tridemnum cyanophorum*
	Nordidemnin N	1069.5947	Antibiotic, Antitumor	*Tridemnum solidum*
	Tamandarin A	1057.6311	Antibiotic, Antitumor	*Didemnidae*
	Iturin A-6 and A-7; Bacillomycin F-1 and F-2	1070.5761	Antibiotic, Surfactant	*Bacillus subtilis*
	Bacillomycin D-4 and D-5	1058.5648	Antibiotic, Surfactant	*Bacillus subtilis*
	Iturin C-3	1071.5600	Antibiotic, Surfactant	*Bacillus subtilis*
	Iturin C-2	1057.5444	Antibiotic, Surfactant	*Bacillus subtilis*
	Microcystin-HtyR	1063.5464	Toxin	*Nostocaceae*
	[L-Ser7] Microcystin-HtyR	1058.5437	Toxin	*Nostocaceae (Anabaena)*
	[DAsp3.ADMAdda5. Dhb7] Microcystin-HtyR	1072.5230	Toxin	*Nostocaceae*
	Microcystin-WR	1067.5440	Toxin	*Microcystis*

In Table 4.5, however, the exact identification of a specific LP within its peptide family can be difficult since as the identification is dependent on the accuracy of the monoisotopic mass of the compound being separated with UPLC-MS. Literature can be used to compare several variations of the separated compounds to other similar compounds, but an exact match is not always found. For this reason, a mass error ppm value of less than 20 must be used to identify possible matches for the observed compound or compound variant. In both Table 4.5 and Table 4.6, several different LP sequences are compared to the nearest hit (*Mr* or *m/z* value) in complex 1.

In Table 4.6, all the mass differences of the nearest hits within one mass unit (1 Dalton) and a number of the suggested LPs is summarised. The hits nearest to complex 1 (A-D) matched most closely to iturin A, mycosubtillin and bacillomycin F with iturin C and bacillomycin D having a similar pattern but with 1 dalton mass difference (Table 4.5). None of the surfactins or other LPs showed exact or near hits and therefore were not included. This warranted further analysis of the iturin and analogues as these LPs tend to bind to sodium and other salts. The exact *m/z* values of different molecular ions and adducts were calculated and compared with the detected values in complex 1 (Table 4.7). From data in Table 4.7, it is clear that the identity of the complex could not be determined purely from the accurate molecular mass and that complex 1 could be either iturin A, bacillomycin F, mycosubtilin or a related LP.

Table 4.6. Detailed summary of the structures and *Mr* values of the nearest complex 1 hits.

Peptide	Lipopeptide structure	M_r
Iturin A	C_{12}, C_{13}, C_{14}, C_{15} [L-Asn-D-Tyr-D-Asn-L-Gln-L-Pro-D-Asn-L-Ser]	1014.5134, 1028.5291, 1042.5447, 1056.5604
Iturin C	C_{12}, C_{13}, C_{14}, C_{15} [L-Asp-D-Tyr-D-Asn-L-Gln-L-Pro-D-Asn-L-Ser]	1015.4975, 1029.5131, 1043.5288, 1057.5444
Mycosubtilin	C_{12}, C_{13}, C_{14}, C_{15} [L-Asn-D-Tyr-D-Asn-L-Gln-L-Pro-D-Ser-L-Asn]	1014.5134, 1028.5291, 1042.5447, 1056.5604
Bacillomycin F	C_{11}, C_{12}, C_{13}, C_{14} [L-Asn-D-Tyr-D-Asn-L-Gln-L-Pro-D-Asn-L-Thr]	1014.5134, 1028.5291, 1042.5447, 1056.5604
Bacillomycin D	C_{13}, C_{14}, C_{15}, C_{16} [L-Asn-D-Tyr-D-Asn-L-Pro-L-Gln-D-Ser-L-Thr]	1016.5212, 1030.5368, 1044.5525, 1058.5681

To elucidate the structure of compound group 1 and specifically 1A (*m/z* 1015. 53) in crude extract from culture YC2-A further, collision-induced dissociation (CID) was used to generate a fragment ion profile. This molecular ion was chosen because it is separated well from the rest and the CID fragmentation pattern was not compromised by contaminants.

In Fig. 4.11, precursor ions from a complex 1 variant (variant 1A with *m/z* of 1015. 53) were analysed using CID in MSe mode during UPLC-MS at Rt 6.95. The variant had several fragments comparable to the sequences of the iturins and analogues (Table 4.6). However, it did not fully correlate with any of the known iturin group. From the fragments, it was likely that variant A1 is likely an iturin/mycosubtilin with a cyclic structure, $C_{11}H_{21}NO$ beta-amino fatty acid residue, and a peptide sequence containing proline, serine, tyrosine, asparagine and glutamine.

The complex fragmentation pattern was further analysed in detail by Prof. Rautenbach (Stellenbosch University). It was suggested that the structure is that of an iturin with a C11 beta-amino fatty acid and a D-Asn to D-Gln mutation in the peptide yielding the following putative cyclic sequence: beta-amino C_{11}-L-Asn-D-Tyr-D-Asn-L-Gln-L-Pro-D-Gln-L-Ser (Fig. 4.11). It was denoted as C11 Iturin A_Q, as a variant of iturin A. From the correlation between our data and that of literature, complex 1 could be identified with confidence as members of the iturin family with varying lipid tail lengths. However, the putative peptide sequence that was identified is novel and must be further investigated to classify this complex as a new member of the iturin group.

Table 4.7. Comparison between the nearest complex 1 hit and cyclic peptides focusing on the iturin group of peptides and using accurate mass to charge ratios and ppm mass error to distinguish a match (indicated with bold font). Only hits with mass differences of less than 20 or more than -20 ppm are included as significant.

Proposed identity	Fatty acid chain	Theoretical *Mr*	*m/z* $[M+H]^+$	*m/z* $[M+Na]^+$	Complex 1 hit	Ppm (mass error)
Iturin A	**C16**	1056.5604	1057.5682	**1079.5502**	1079.5623	**-11**
	C14	1042.5447	**1043.5525**	1065.5345	1043.5702	**-17**
	C13	1028.5291	**1029.5369**	**1051.5189**	1029.5520,1051.5350	**-15, -15**
	C12	1014.5134	**1015.5212**	**1037.5032**	1015.5320,1037.5234	**-11, -19**
Bacillomycin F	**C14**	1056.5604	1057.5682	**1079.5502**	1079.5623	**-11**
	C13	1042.5447	**1043.5526**	1065.5345	1043.5702	**-17**
	C12	1028.5291	**1029.5369**	**1051.5189**	1029.5520, 1051.5350	**-15, -15**
	C11	1014.5134	**1015.5213**	**1037.5032**	1015.5320, 1037.5234	**-11, -19**
Mycosubtilin	**C16**	1056.5604	1057.5682	**1079.5502**	1079.5623	**-11**
	C14	1042.5447	**1043.5526**	1065.5345	1043.5702	**-17**
	C13	1028.5291	**1029.5369**	**1051.5189**	1029.5520, 1051.5350	**-15, -15**
	C12	1014.5134	**1015.5213**	**1037.5032**	1015.532, 1037.5234	**-11, -19**

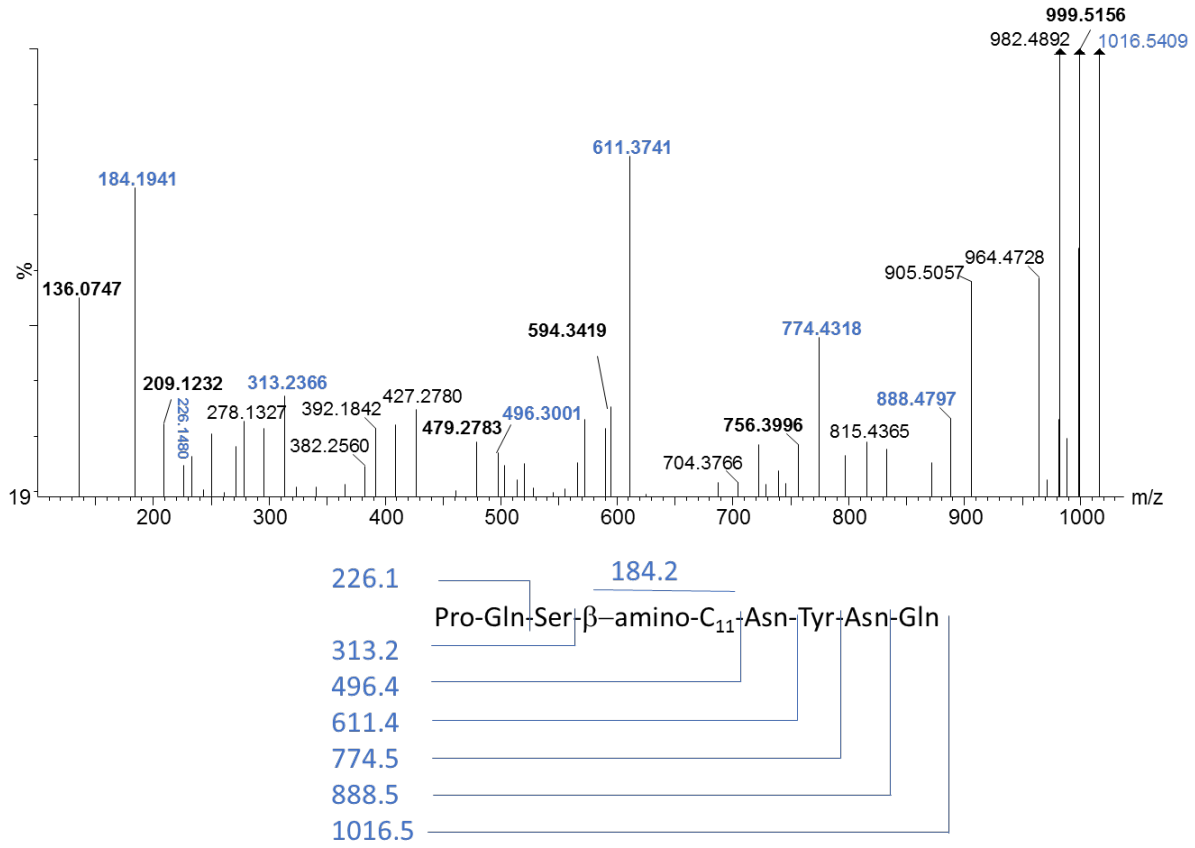

Figure 4.11. CID spectra generated in the MSe mode during the UPLC-MS of precursor ions for compound 1A variant (Rt 6.95, *Mr* was 1015. 53) detected in complex 1 of YC2 extract A. A putative sequence of a cyclic iturin-like LP with ring-opening at proline was derived from the spectrum. The fragmentation scheme is given below with theoretical *m/z* values for each fragment (data courtesy M Rautenbach). Correlating b-type fragments on the spectrum is highlighted in blue with expected *m/z* values and fragment indicated on the structure below. The fragments in bold on the spectrum all correlated to the putative sequence of C11 iturin A_Q.

4.3.4.2 Elucidation of identities of compounds in complex 2

As stated above, the addition of ion adducts will alter a compound's detected isotopic mass and must be removed in order to determine its molecular mass; used in unknown peptide identification. In Fig. 4.12, a mass spectrum was generated by MaxEnt 3 of complex 2 of YC2 culture A and showing the difference between compounds with sodium adducts and those with only CH_2 groups. Six compound variants were identified, denoted A-F in Fig. 4.12.

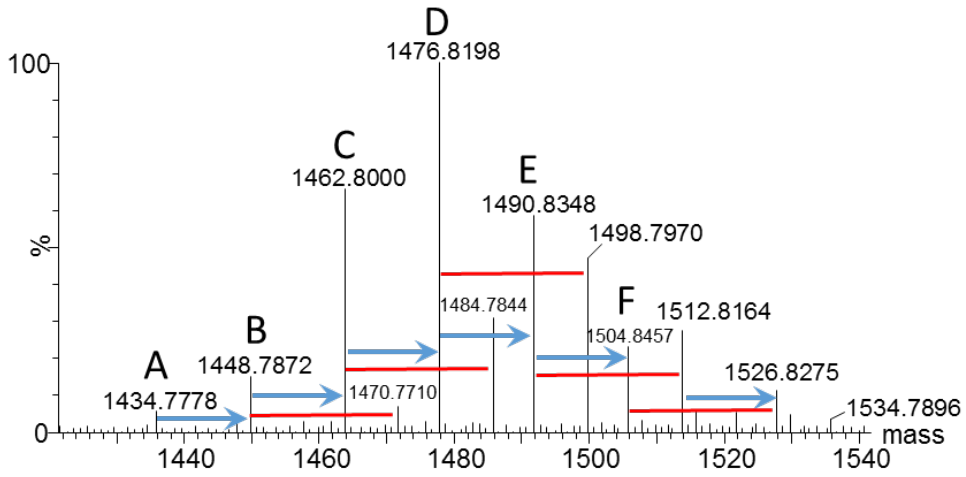

Figure 4.12. Representative mass spectrum generated with MaxEnt 3 of complex 2 from YC2 culture A. The blue arrows indicate the related compounds differing with a putative CH_2 group. The red lines show the relationship of sodium adducts of compounds A–F.

Retention times for the six compounds detected in complex 2 of YC2 extract (Fig. 4.12) were compared to findings presented by de Souza *et al*. (2018) and two compounds found to have Rt values similar to fengycin A variants. The complete results of retention times for main peaks detected for complex 2 compounds using UPLC-MS included 8.43, 8.93, 9.82, 10.32, 10.71, 10.92 min are in Fig. 4.13. Additional peaks, appearing near the main peaks, included 9.42, 10.21, 10.72 and 11.64 min. These peaks are likely variants with slightly different amino acid sequences or different lengths of fatty acid tail.

In Table 4.8, two complex 2 compounds, compounds 2C and 2D, had Rt values and molecular masses comparable to fengycins documented in de Souza *et al*. (2018). The retention times and *Mr* values for surfactins and iturins recorded in the same paper (de Souza *et al*., 2018) and two additional papers (Ndlovu *et al*., 2017; Rautenbach *et al*., 2017) were not however comparable with compounds 2C and 2D (ppm exceeding 20 or below -20).

Table 4.8. Comparison between fengycin variants identified by de Souza *et al*. (2018) and two compounds separated from complex 2 of YC2-A using UPLC-MS.

Peptide	Suggested peptide structure	M_r	Complex 2 nearest hit	ppm error	UPLC R_t (min)
Fengycin A	cyclo[($C_{72}H_{110}N_{12}O_{20}$)-L-Glu-D-Orn-D-Tyr-D-Thr-L-Glu-D-Ala-L-Pro-L-Gln-L-Tyr-L-Ile]	1462.8185	1462.8185	17	10.66
Fengycin AiC17	cyclo($C_{73}H_{112}N_{12}O_{20}$)-L-Glu-D-Orn-D-Tyr-D-Thr-L-Glu-D-Ala-L-Pro-L-Gln-L-Tyr-L-Ile]	1476.8330	1476.8330	14	10.44

In Table 4.9, the results of a NORINE search for complex 2 compounds are presented using the same search parameters as for complex 1 compounds. The molecular weight range was selected to cover all significant peaks detected in complex 2 (1434-1527 *m/z*) using MaxEnt 3 (Table 4.9). Findings included several families of peptaibols, glycolipids, peptides and LPs. Producer organisms ranged from several species of sea sponge to bacteria and one fungus. As samples from YC2-A were all extracted from a bacterial culture (as confirmed with 16S rRNA), the most relevant results were those produced by *Bacillus* species and actinobacteria. Of these, the fengycins (produced by *Bacillus subtilis*) had the nearest *Mr* value to compounds 2C and 2D and were also produced by the same bacterial sub-group identified for isolate YC2 using a BALST search of the NCBI, phylogenetic tree construction and a biolog assay (Information presented in Chapter 3). Therefore, these two compound variants were investigated further using MSe mode, during UPLC-MS, to generate characteristic ion fragmentation patterns.

Table 4.9. YC2 complex 2 results for possible peptide identities and producer organisms as stored on the NORINE database and found using molecular weight to define search range.

Search range (M_r)	NORINE result	Result *Mr*	Activity	Known producer organism
1462-1477	Fengycin A iC17	1476.8116	Antibiotic	*Bacillus subtilis*
	Fengycin A	1462.7959	Antibiotic	*Bacillus subtilis*
1477-1490	Kahalalide F (peptide)	1462.9320	Antibiotic	*Elysia grandifolia* (sea slug)
1490-1499	Kahalalide G (peptide)	1494.9425	Unknown	*Elysia grandifolia* (sea slug)
	Balhimycin (glycopeptide)	1488.4204	Antibiotic	*Amycolatopsis* (Actinomycetales)
	CDa4a	1495.5290	Antibiotic	*Streptomyces roseosporus*
1499-1513	Bergofungin (peptaibol)	1510.8759	Antibiotic	*Emericellopsis donezkii* (fungi)
	Callipeltin K	1508.8562	Antibiotic, toxin	*Latrunculia* sp. (fire sponge)
	Callipeltin A	1504.8613	Antibiotic, toxin	*Callipelta* sp. (sea sponge)
1513-1527	MM49721 (glycopeptide)	1525.5661	Antibiotic	*Nocardia orientalis* (Actinomycetales)
	Dechloro-balhimycin V (glycopeptide)	1518.5715	Antibiotic	*Amycolatopsis* (Actinomycetales)
	Bergofungin A (pepibiol)	1524.8916	Antibiotic	*Emericellopsis donezkii* (fungi)
	Orienticin C	1522.6028	Antibiotic	*Nocardia orientalis* (Actinomycetales)

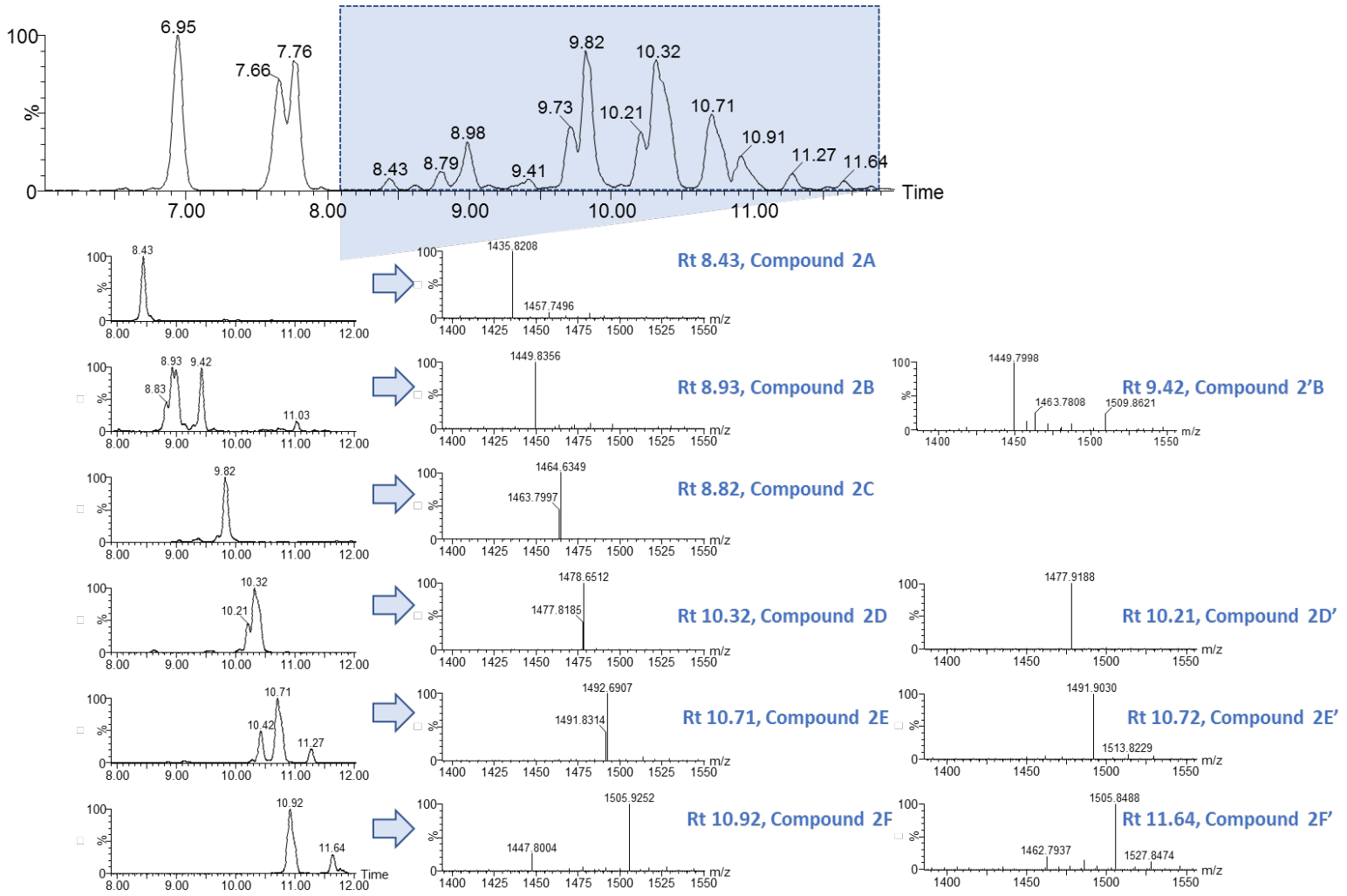

Figure 4.13. Mass extracted UPLC-MS profiles (left) of the full chromatogram (top) of the YC2-A extract. The main peaks with Rt in minutes and the main ion in each of the peaks correlating to complex 2 are indicated. The peak at 10.42 min could not be analysed due overlap. Ion spectra were generated with the TOF-transform function of MassLynx 4.01.

4.3.4.3 Confirmation that complex 2 compounds are from the fengycin group

Compounds contained in complex 2 (2C and 2D), with *Mr* values comparable to those of compounds stored on the NORINE database, were further investigated using ion dissociation fragmentation patterns. These patterns were generated with CID and MSe mode (Fig. 4.14) during UPLC-MS at 9.82 and 10.32 and 10.21 min.

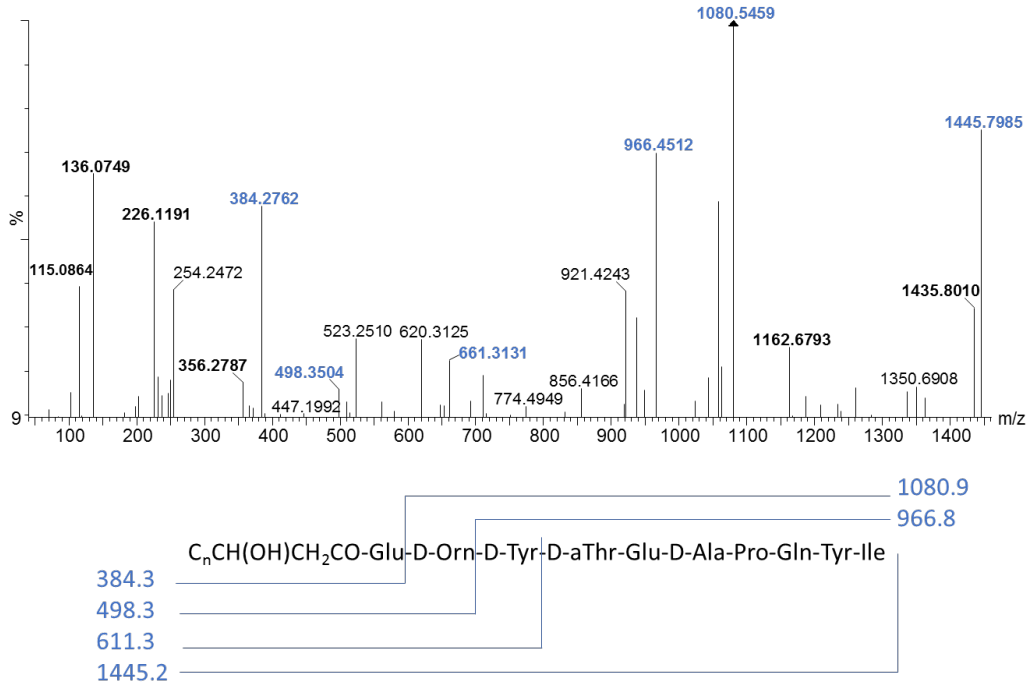

Figure 4.14. CID spectra generated in the MSe mode during the UPLC-MS of precursor ions for a compound variant (Rt 9.82, *Mr* was 1463) detected in complex 2 of YC2 extract A at Rt 9.82 with M_r was 1463 Da. This pattern was compared to a fragmentation scheme included in Gong *et al*. (2015) and theoretical *m/z* values for each fragment of complex 2 variant added below the CID spectra (data courtesy M Rautenbach). Correlating b and y fragments are highlighted in blue with the expected *m/z* values and fragments indicated on the structure below. Ring opening was predicted at the lactone bond. The fragments in blue font on the spectrum all correlated to the sequence of fengycin A.

Several precursor ions were compared to findings in Gong *et al*. (2015) and had common *m/z* values to precursor ions eluted from fengycin A (also known as fengycin IX or plipastatin A) eluted at similar retention time (Table 4.9). These fingerprint ions included 115, 226, 356, 661, 966, 1080 and 1162 *m/z* and could be used to suggest the final structure of compound 2C (Fig. 4.14). Two of these values are characteristic of main breakage points in fragmentation schemes for fengycin A in Gong *et al*. (2015), Bie *et al*. (2009), Pecci *et al*. (2010) and Wang *et al*. (2004). These two fragments include the y-fragments with *m/z* of

966 and 1080 (see Fig. 4.14). From the correlation between our data and that of literature, complex 2 could be identified with confidence as members of the fengycin A family with varying lipid tail lengths.

This means that two of the compound groups contained in extracts prepared from bacteria YC2 are likely to be, according to UPLC-MS and MS/MS analysis, a fengycin A complex and a peptide complex with LPs similar to iturin A. The significance of this is that these compounds are well-known antifungal LP and the techniques used in this chapter were effective in selecting them from other compounds produced by the cultured microorganisms. Therefore, these same techniques could be used to select for other, even some previously uncharacterised antifungal LPs, if they are present in YC2 extract.

In addition to this, cultured bacteria YC2 could be used to produce both fengycins and iturins for future studies to develop these compounds for future application to clinical infections of *C. albicans* and *C. neoformans* or the phytopathogens *B. cinerea* and *F. oxysporum*. Both fengycins and iturins are known to have strong antifungal activities.

Fengycins A and B are known to have antifungal activity against some filamentous fungi and oomycetes, but not many yeast pathogens or bacterial species (Meena and Kanwar, 2014). Therefore, studies which confirm antifungal activity against *B. cinerea* and *F. oxysporum* (Nam *et al*., 2015; Toral *et al*., 2018; Toure *et al*., 2004) are more numerous than those describing its antifungal activity against *C. albicans* and *C. neoformans* (Pathak and Keharia, 2014). Iturin A is an antifungal LP known to have antifungal activity against *C. albicans* (Devi *et al*., 2019; Pathak and Keharia, 2014) and quite recently against *C. neoformans* (Devi *et al*., 2019). Previously, it was known to have antifungal activity against *B. cinerea* (Dang *et al.,* 2019) and *F. oxysporum* (Ambrico and Trupo, 2017) and when used in combination with fengycin to A, to have enhanced antifungal activity against *Fusarium graminearum* (Gong *et al*., 2015). Other studies which find LP mixtures of iturins and fengycins to have a strong antifungal activity to a range of fungal pathogens include those conducted by Li *et al*. (2016), Olfa *et al*. (2015) and Toure *et al*. (2004).

4.3.5 Identification and characterisation of compounds produced by *Bacillus* SC6

UPLC-MS and ESMS analysis of crude extracts harvested from *Bacillus* SC6 revealed a complex profile of compounds with variable reproducibility between biological repeats (triplicate cultures and extracts). Different levels of different compounds were also detected.

For this reason, only a preliminary analysis was conducted of compounds produced. Furthermore, more significant optimisation of culturing and extraction techniques may be required for this organism.

The compounds produced by *Bacillus* SC6 were profiled by UPLC-MS in positive mode using a scanning range of 150-2000 *m/z.* The UPLC-MS profiles were different for the three culture extracts, but a number of lipophilic compounds (late eluting) correlated between the extracts and include three main compound groups with *m/z* 680.49, 850.24 and 924.26 (Fig. 4.15).

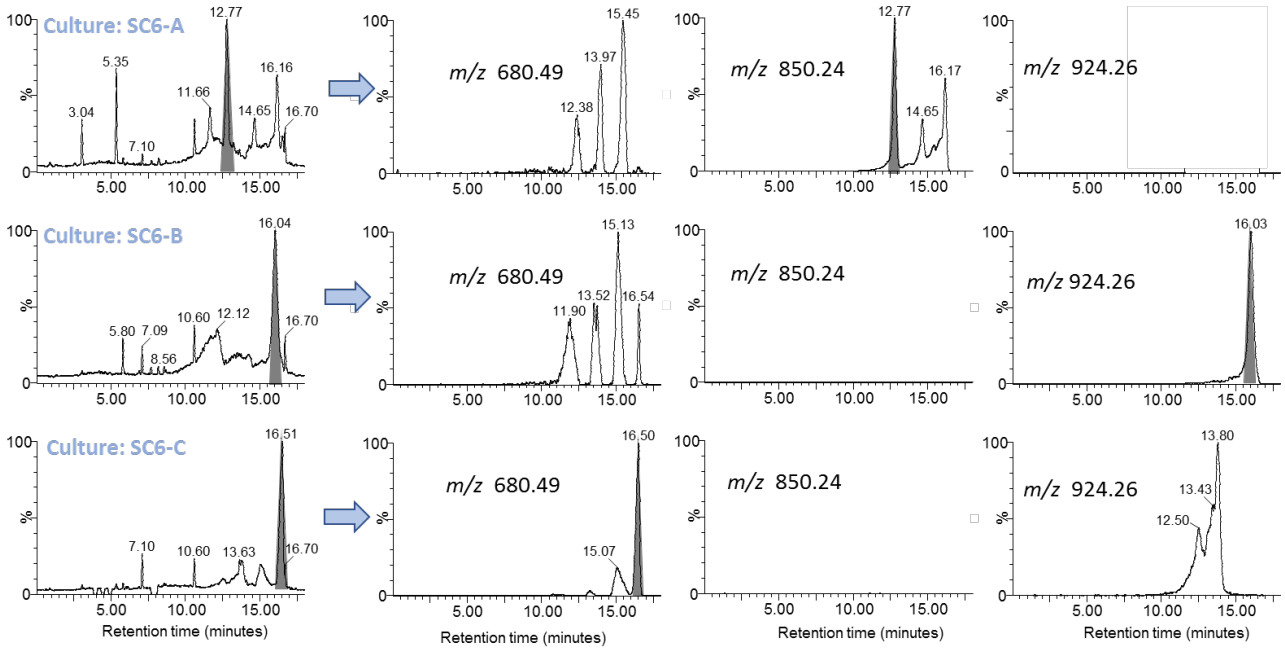

Figure 4.15. UPLC-MS profile (left panel) and extraction of the molecular ion peaks (*m/z* 680.49, 850.24 and 924.26) of the main compounds detected in each of the antifungal extracts produced by SC6-A, SC6-B and SC6-C. The grey shaded peak in each UPLC-MS profile corresponds with the major compound detected in the extract.

Similar compounds such as the group correlating to *m/z* 680.49 were produced in SC6-A and SC6-B cultures, but at about 10-fold levels than SC6-C (Fig. 4.15). The compound group at *m/z* 850.24 were only found in SC6-A, while the compound group at *m/z* 924.26 was detected in SC6-B with lower amounts in SC6-C (Fig. 4.15). The fact that more than one peak with the same main compounds were found could either indicate structural analogues or aggregation/interaction with itself other compounds leading to changing the chromatographic behaviour. Whether these compounds are known antifungal lipopeptides, can only be determined with more in-depth structural analysis. When the peaks corresponding to compound group 3A with *m/z* 680.49 (M_r=679.4719) were further analysed

it revealed a second smaller compound at *Mr* 662.4465, which is 17 Da smaller, indicating the loss of an OH group (Fig. 4.16). All four the peaks detected displayed similar major compounds, except the peak at 11.9 minutes that contain a smaller compound at *m/z* = 550.63. At 16.5 minutes, a spectra peak at 1341.9192 was observed and it is interesting of which the M_r is the sum of the two major compounds (Fig 4.16). This could indicate that the compounds associate or aggregate with each other and possibly other compounds, which could explain our observation of four peaks (Fig 4.15).

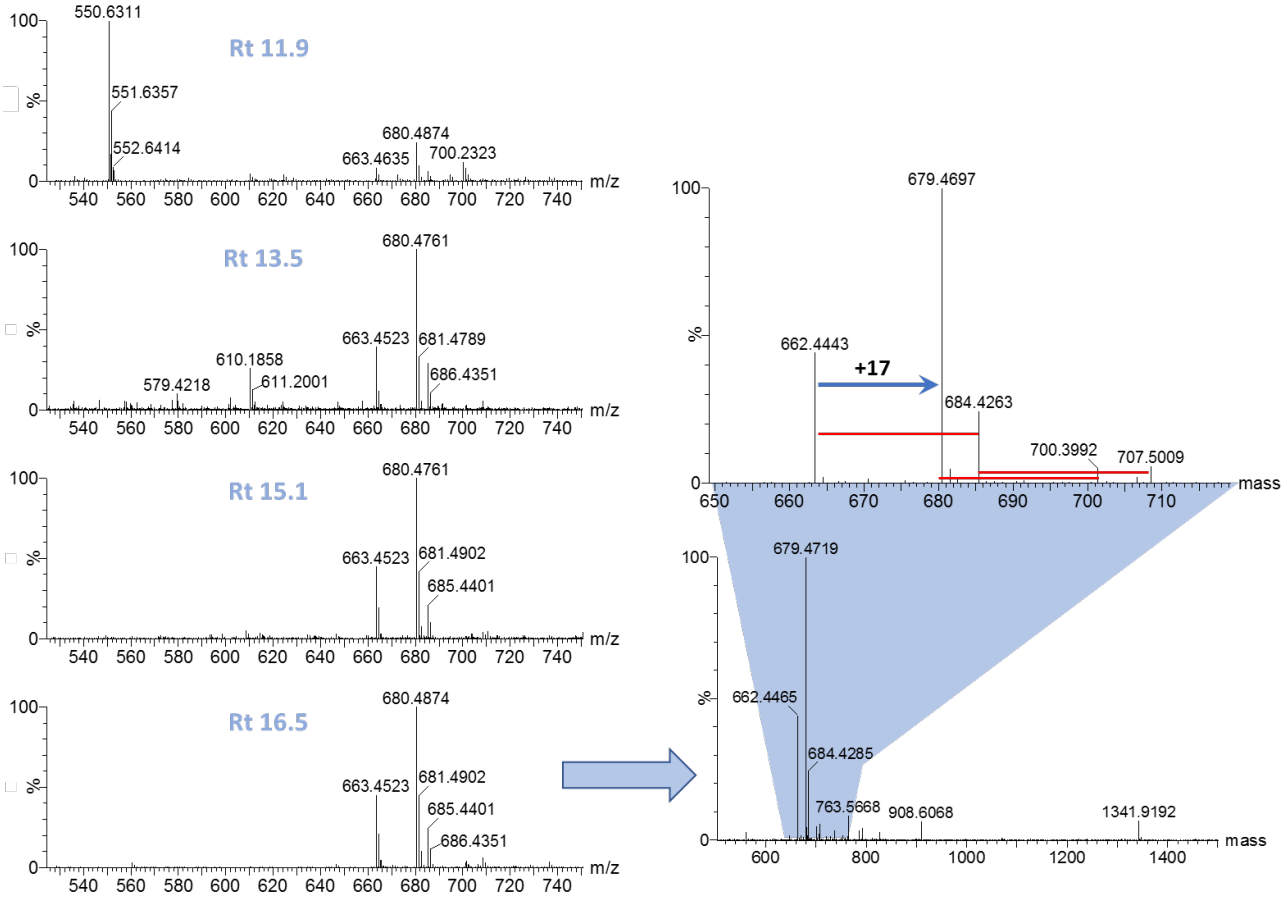

Figure 4.16. ESMS analysis of compound 3A and the four different peak fractions. The spectra on the left are combined positive ion spectra representing each of the four peak that were identified to contain a compound with *m/z*=680.48. The mass spectra on the right are that from the peak at Rt 16.5 minutes and were generated using the MaxEnt 3 algorithm of MassLynx 4.01 from multiple charged positive ion spectrum.

Mass spectra of compounds 3B and 3C in SC6-A and SC6-C culture extracts further analysed and deconvoluted using the MaxEnt 3 algorithm of MassLynx 4.01 (Fig 4.17). For compound 3B we found monoisotopic M_r values of 849.2386 and 851.2357. For compound 3C we found monoisotopic M_r values of 923.2614, 925.2607 and 927.2604. In both analyses, there are a 2.00 mass unit difference in the detected compound M_r values. This

could indicate that there are differences in saturation (double bonds) in aliphatic chains that may be part of a lipid moiety related to the lipophilic nature and late elution from C_{18} column.

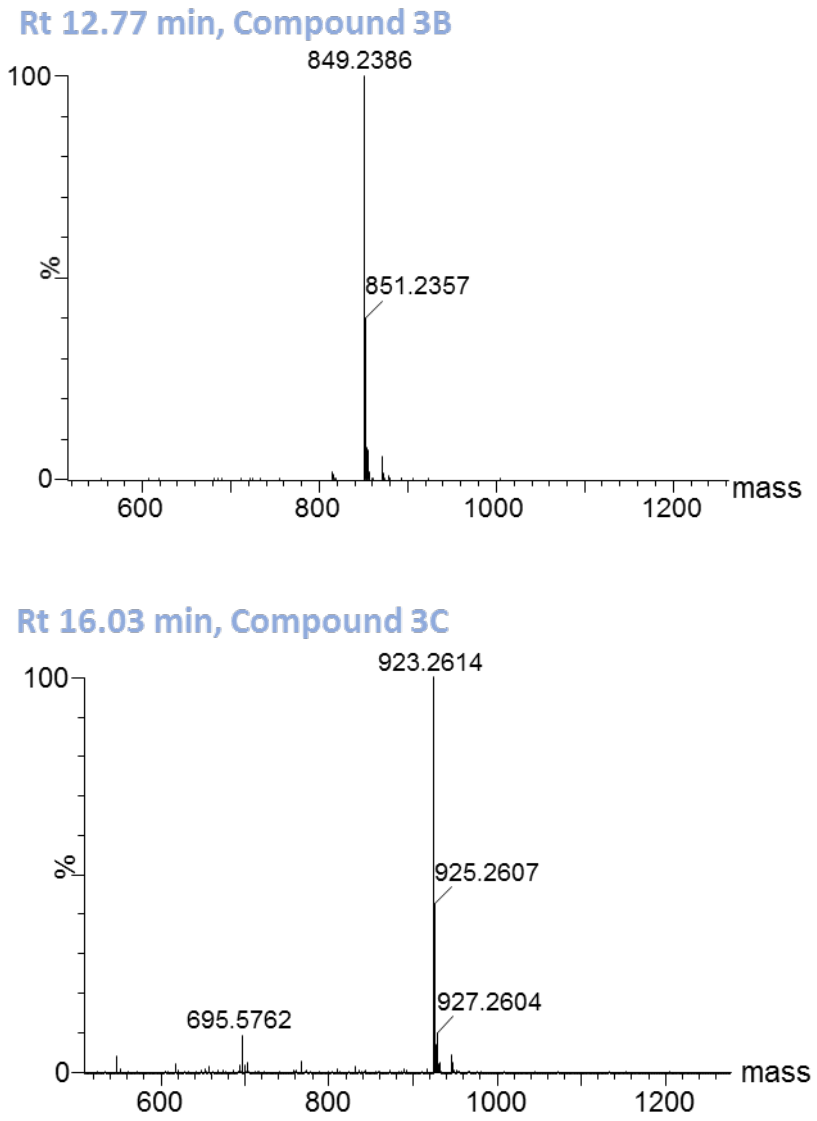

Figure 4.17. Deconvoluted mass spectra of the two main compounds in SC6-A (compound 3B) and SC6-B (compound 3C). The mass spectra were generated with the MaxEnt 3 algorithm of MassLynx 4.01 from multiply charged positive ion spectra.

In Table 4.10, the molecular weight range of each compound (3A, 3B and 3C) was used and compared with bacterial peptides and LPs on the NORINE database. The results for compound 3A included enterobactin, capreomycin and miraziridine. The nearest database hits found using a molecular weight range for compound 3C included two keramamides and one microcystin. Both sets of results were evaluated for significance using ppm mass error as before with YC2.

NORINE results for compounds 3A-3C were also cross-referenced with literature to evaluate whether they had any known antifungal activity. Capreomycin IA was found to be a protein synthesis inhibitor with powerful anti-tuberculosis activity (Lin *et al*., 2014). Just as other tuberactinomycins, it has macrocyclic polypeptide ring structures but is not known for its antifungal activity (Cai *et al.,* 2012). Enterobactin has no suggested antibiotic capability but promotes the growth of certain bacterial species as it acts as a metal siderophore which chelates iron (Bairwa *et al.,* 2017). Miraziridine is a protease inhibitor (Tabares *et al.,* 2012), which together with keramamides L and J, is produced by *Theonella* species, a genus of marine sponges. Keramamides are cyclic peptides with several structural variants and potent cytotoxic activity against several human cell lines, including epidermoid carcinoma and murine leukaemia cell lines (Gogineni and Hamann, 2018). This makes them the focus of pharmacological research which mines the marine environment for peptides and other bioactive compounds with potential as a novel anti-cancer treatment (Gogineni and Hamann, 2018). As none of these compounds are known to be antifungal, it is suggested that the most abundant compounds detected in compound groups 3A and 3C may not be responsible for any antifungal activity observed.

After the evaluation of each NORINE result for significance using ppm mass error as an indication of a similar peptide compound being found, all suggested identities were found to be well outside the prescribed ppm mass error (Table 4.10). This could allude to the antifungal compounds being analysed being novel peptide structures to the antifungal LPs contained in the databases used for comparison. It could also allude to a limitation in using the NORINE database as the only point of reference when identifying rare or unknown antimicrobial peptides. Alternatively, although these compounds are highly lipophilic, they could be from another class of compounds, such as the glycolipids, which include rhamnolipids or polyenes. However, none of the molecular masses that we detected correlated with known rhamnolipids or polyenes (results not shown). We also ruled out the common background ions such as detergents, common contaminants such those related to the use of plastics (minimally is in this study) in ESMS analyses (fisher scientific, n.d.). A ChemSpider (https://www.chemspider.com/) and PubChem (https://pubchem.ncbi.nlm.nih.gov/) also did not reveal any likely candidates, therefore it is still possible that these compounds are either not the active entities or novel.

Table 4.10. SC6 complex compounds 3A, 3B and 3C analysis for possible peptide identities and producer organisms stored on the NORINE database.

Search range	NORINE result	Activity	Producer	Result *Mr*	Complex 3 nearest hit	ppm error
662-680 (Compound 3A)	Capreomycin IA	Antibiotic	*Streptomyces*	668.3467	none	
	Enterobactin	Siderophore	*Escherichia coli*	669.1442	none	
	Miraziridine	Protease inhibitor	*Theonella*	668.3857	none	
849-851 (Compound 3B)	No search results					
923-928 (Compound 3C)	Keramamide L	Toxin	*Theonella*	926.4457	925.2607 927.2604	1279 -879
	Keramamide J	Toxin	*Theonella*	922.4007	923.2614	-933
	Microcystin	Toxin	*Microcystis aeruginosa*	923.5004	923.2614	259

4.3.6 Identification and characterisation of compounds produced by *Penicillium* A1

In the production of the same compounds, at similar levels/amounts, the flask cultures of *Penicillium* A1 were as variable as those found with *Bacillus* SC6. Both A1-B and A1-C produced the same main compound with a *m/z* of 998.2902 (Fig. 4.18, Fig 4.19). As second compound with m/z 628.38 was also found in both culture extract. However, the culture A1-B yielded a much higher amount of both the compounds (Fig 4.18). The results from culture A1-A could not be further analysed because of cross-contamination with the compounds from *Bacillus* SC6, specifically *m/z* 680.4874, and were not analysed further.

The closest results for compound 4A included several ribosomally synthesised peptides (geodiamolide D, globomycin SF-1902 A2, guineamide B) and 4B only showed one hit Apramide D. The ppm error between the closest NORINE hits and complex 4 did not fall within the limits and was above 20 or below -20 ppm (Table 4.11). This means that they are unlikely the same compound and compounds 4A and 4B are still unknown. A ChemSpider (https://www.chemspider.com/), PubChem (https://pubchem.ncbi.nlm.nih.gov/) and general

literature search also did not reveal any likely candidates, therefore it is possible that these compounds are either not the active entities or novel.

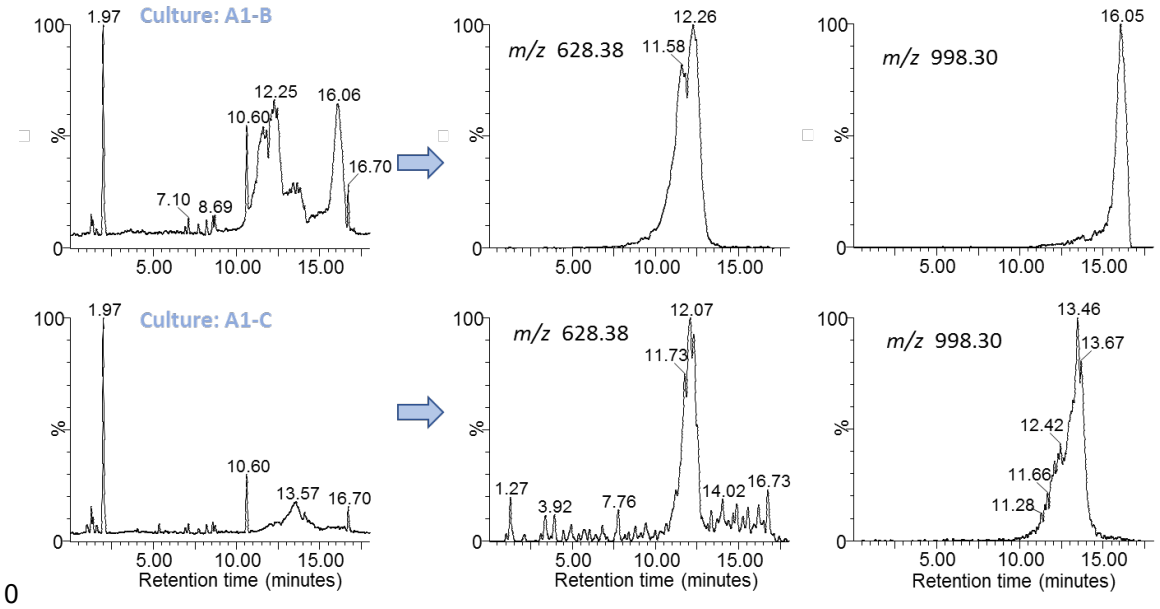

0

Figure 4.18. UPLC-MS profile (left panel) and extraction of the molecular ion peaks (*m/z* 628.38 and 998.30) of the main compounds detected in each of the antifungal extracts produced by A1-B and A1-C.

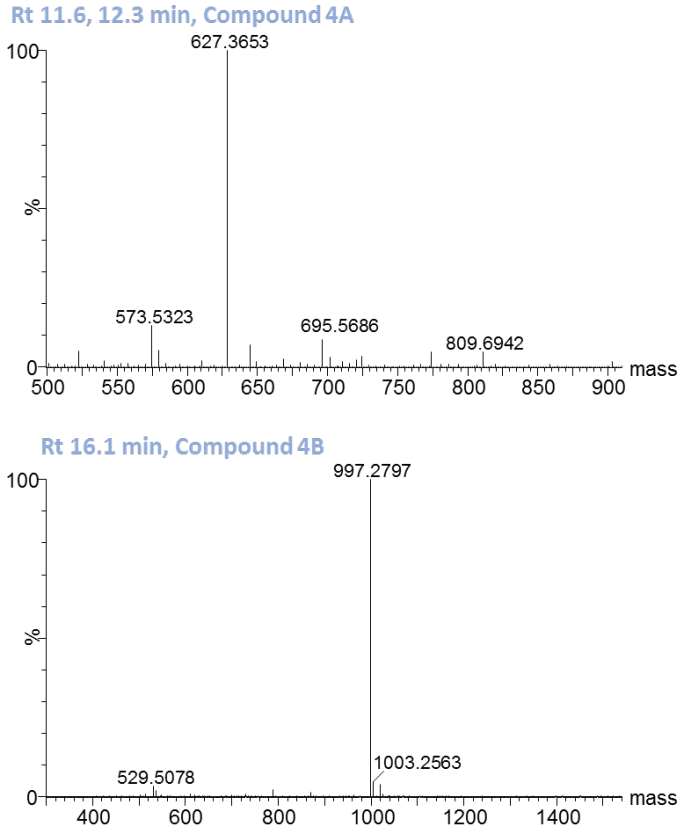

Figure 4.19. Deconvoluted mass spectra of compound 4A (top, *m/z* 628.38 in Fig 4.18) and compound 4B (bottom, *m/z* 998.30 in Fig. 4.18) from A1 extracts. The mass spectra were generated with the TOF-transform algorithm of MassLynx 4.01 from multiply charged positive ion spectra.

Table 4.11. Results for *Penicillium* A1 produced compounds, 4A and 4B, respectively when compared with stored peptides on the NORINE database using M_r in the structure search.

Search range	NORINE result	Activity	Producer	Result M_r	Complex 4 nearest hit	ppm error
627-628 (Compound group 4A)	Geodiamolide D	Toxin	*Axinellidae*	627.1805	627.3653	-295
	Guineamide B	Toxin	*Lyngbya majuscula*	627.3091	627.3653	-90
	Globomycin SF-1902 A2	Antibiotic	*Streptomyces halstedii*	627.3843	627.3653	30
997-1004 (Compound group 4B)	Apramide D	Antibiotic	*Lyngbya confervoides*	1003.6055	1003.3653	239

4.4 Conclusions

The successful characterisation of lipophilic antifungal compounds extracted from stationary liquid cultures of *P. sidoides*-associated microbes confirmed that stress-inducing culturing conditions and nitrogen-rich media (Biniarz *et al.,* 2018; Pretorius *et al*., 2015), can be used to produce quantifiable levels of antifungal compounds in the microbes isolated from *P. sidoides* tubers. Additionally, using a liquid medium may provide a greater culture volume and nutrient diffusion, as opposed to culturing on solid media. The extraction and purification techniques designed according to Ndlovu *et al*. (2017) also proved effective in preserving the antifungal activity of the presumed peptides.

The antifungal LPs identified using UPLC-MS and MSe analysis of characterised YC2 extract included two LPs/variants (iturins and fengycins) with well-known antifungal activity against the selected panel of target organisms (*B. cinerea*, *C. albicans*, *C. neoformans* and *F. oxysporum*), especially if used synergistically. Therefore, techniques for the effective production, extraction and characterisation of these compounds should be maintained for future studies to evaluate them for clinical (if gamma haemolytic) and agricultural applications. Other resolved compounds detected in YC2 extract, remain uncharacterised due to time constraints and the complexity of even relatively pure peptide extracts. In this way, the UPLC-MS and MSe analysis were not exhaustive and more antifungal LPs may be contained in extracts produced by the *Bacillus* sp. YC2. In microbial extracts produced by bacterium SC6 and fungus A1, there were a number of resolved compounds which were not identified using UPLC-MS analysis and database searches. As extraction and purification

techniques were selected to capture LPs, this suggests that the databases used to identify antifungal peptides in this study were incomplete.

The putative peptide extracts produced by *P. sidoides*-associated microbes, YC2, SC6, A1 and C5, were all found to have some broad-spectrum activity against spore and cell morphologies of the selected target organisms. However, only YC2 extract was tested against the hyphal growth morphology. In future studies, for development as a clinical application, this extract should be tested against different fungal morphologies associated with pathogenicity (e.g. yeasts with hyphae) and under conditions which emulate clinical infection. However, some chemical alteration may be required to negate toxic side effects as YC2 extract was found to be beta-haemolytic. In future studies, for development as an agricultural application, this extract should be tested against different fungal morphologies associated with phytopathogenicity (e.g. mycelia) and under conditions which emulate a plant infection.

4.5 References

Al-Hatmi A, Meis J, de Hoog G. 2016. *Fusarium*: Molecular diversity and intrinsic drug resistance. PLOS Pathogen **12**: 1-8

Ambrico A, Trupo M. 2017. Efficacy of cell free supernatant from *Bacillus subtilis* ET-1, an iturin A producer strain, on biocontrol of green and gray mold. Postharvest Biology and Technology **134**: 5-10

Bairwa G, Hee Jung W, Kronstad J. 2017. Iron acquisition in fungal pathogens of humans. Metallomics **9**: 215-227

Bie X, Lu Z, Lu F. 2009. Identification of fengycin homologues *from Bacillus subtilis* with ESI-MS/ CID. Journal of Microbiological Methods **79**: 272-278

Biniarz P, Coutte F, Gancel F, Łukaszewicz M. 2018. High-throughput optimization of medium components and culture conditions for the efficient production of a lipopeptide pseudofactin by *Pseudomonas fluorescens* BD5. Microbial Cell Factories **17**: 121

Braun PC, Calderone, RA. 1978. Chitin synthesis in *Candida albicans*: Comparison of yeast and hyphal forms. ASM **135**: 1472-1477

Buxton R. 2005. Blood agar plates and hemolysis protocols. ASM, Washington, D. C

Caboche, S, Pupin M, Leclere, V, Fontaine A, Jacques P, Kucherov, G. 2007. NORINE: a database of nonribosomal peptides. Nucleic Acids Research **36**: 326-331

Cai H, Sun Z, Huang Z, Shi L, Zhao Y, Kunz H, Li Y. 2012. Fully synthetic self-adjuvanting thioether-conjugated glycopeptide lipopeptide antitumor vaccines for the induction of complement-dependent cytotoxicity against tumor cells. Chemistry - A European Journal **19**: 1962-1970

Dang Y, Zhao F, Liu X, Fan X, Huang R, Gao W, Wang S, Yang C. 2019. Enhanced production of antifungal lipopeptide iturin A by *Bacillus amyloliquefaciens* LL3 through metabolic engineering and culture conditions optimization. Microbial Cell Factories **18**: 68

de Souza C, Martins F, Zocolo G, Figueiredo J, Canuto K, de Brito E. 2018. Simultaneous quantification of lipopeptide isoforms by UPLC-MS in the fermentation broth from *Bacillus subtilis* CNPMS22. Analytical and Bioanalytical Chemistry **410**: 6827-6836

Devi S, Kiesewalter H, Kovács R, Frisvad J, Weber T, Larsen T, Kovács Á, Ding L. 2019. Depiction of secondary metabolites and antifungal activity of *Bacillus velezensis* DTU001. Synthetic and Systems Biotechnology **4**: 142-149

Du Preez van Staden A, Dicks L, Deane S. 2016. Ph. D. thesis. University of Stellenbosch. Stellenbosch, South Africa. *In vitro* and *In vivo* Characterisation of Amyloliquecidin. A Novel Two-Component Lantibiotic Produced by *Bacillus amyloliquefaciens*

Dyakov Y, Zinovyeva S. 2007. Plant parasite microorganisms. Comprehensive and Molecular Phytopathology **1**: 19-47.

Ferrige A, Seddon M, Green B, Jarvis S, Skilling J, Staunton J. 1992. Disentangling electrospray spectra with maximum entropy. Rapid Communications in Mass Spectrometry **6**: 707-711

Fisher M, Hawkins N, Sanglard D, Gurr S. 2018. Worldwide emergence of resistance to antifungal drugs challenges human health and food security. Science **360**: 739-742

Fisher scientific (n.d.). Common background contamination ions in mass spectrometry. [Image] Available at: https://beta- static.fishersci.ca/content/dam/fishersci/en_US/documents/programs/scientific/brochures-and-catalogs/posters/fisher-chemical-poster.pdf [Accessed 9 Dec. 2019]

Giacomodonato MN, Pettinari MJ, Souto GI, Mendez, BS, Lopez NI. 2001. A PCR-based method for the screening of bacterial strains with antifungal activity in suppressive soybean rhizosphere. World Journal of Microbiology and Biotechnology **17**: 51-55

Godfray H, Mason-D'Croz D, Robinson S. 2016. Food system consequences of a fungal disease epidemic in a major crop. Philosophical Transactions of the Royal Society B: Biological Sciences **371**: 20150467

Gogineni V, Hamann MT. 2018. Marine natural product peptides with therapeutic potential: Chemistry, biosynthesis, and pharmacology. *Biochimica et Biophysica Acta* (BBA)-General Subjects **1862**: 81-196

Gong A, Li H, Yuan Q, Song X, Yao W, He W, Zhang J, Liao Y. 2015. Antagonistic mechanism of iturin A and plipastatin A from *Bacillus amyloliquefaciens* S76-3 from wheat spikes against *Fusarium graminearum*. PLOS ONE **10**: 0116871

Hsieh FC, Li MC, Lin TC, Kao SS. 2004. Rapid detection and characterization of surfactin-producing *Bacillus subtilis* and closely related species based on PCR. Current Microbiology **49**: 186-191

Jin H, Li K, Niu Y, Guo M, Hu C, Chen S, Huang F. 2015. Continuous enhancement of iturin A production by *Bacillus subtilis* with a stepwise two-stage glucose feeding strategy. BioMed Central Biotechnology **15**: 53

Joshi R, McSpadden Gardener BB. 2006. Identification and characterization of novel genetic markers associated with biological control activities in *Bacillus subtilis*. Phytopathology **96**: 145-154

Lenardon M, Munro C, Gow N. 2010. Chitin synthesis and fungal pathogenesis. Current Opinion in Microbiology **13**: 416-423

Lin Y, Li Y, Zhu N, Han Y, Jiang W, Wang Y, Si S, Jiang J. 2014. The antituberculosis antibiotic capreomycin inhibits protein synthesis by disrupting interaction between ribosomal proteins L12 and L10. Antimicrobial Agents and Chemotherapy **58**: 2038-2044

Li X, Zhang Y, Wei Z, Guan Z, Cai Y, Liao X. 2016. Antifungal activity of isolated *Bacillus amyloliquefaciens* SYBC H47 for the biocontrol of peach gummosis. PLOS ONE **11**: 1-22

Makovitzki A, Viterbo A, Brotman Y, Chet I, Shai Y. 2007. Inhibition of fungal and bacterial plant pathogens *in vitro* and i*n planta* with ultrashort cationic lipopeptides. Applied and Environmental Microbiology **73**: 6629-6636

Mania, D, Hilpert K, Ruden S, Fischer R, Takeshita N. 2010. Screening for antifungal peptides and their modes of action in *Aspergillus nidulans*. Applied and Environmental Microbiology **76**: 7102-7108

Masurekar P, Fountoulakis J, Hallada T, Sosa M, Kaplan L. 1992. Pneumocandins from *Zalerion arboricola*. II. Modification of product spectrum by mutation and medium manipulation. The Journal of Antibiotics **45**:1867-1874

Meena KR, Kanwar SS. 2014. Lipopeptides as the antifungal and antibacterial agents: applications in food safety and therapeutics. Biomed Research International **2015**: 473050

Mohammadipour M, Mousivand M, Jouzani GS, Abbasalizadeh S. 2009. Molecular and biochemical characterization of Iranian surfactin-producing *Bacillus subtilis* isolates and evaluation of their biocontrol potential against *Aspergillus flavus* and *Colletotrichum gloeosporioides*. Canadian Journal of Microbiology **55**: 395-404

Mpoza E, Rhein J, Abassi M. 2018. Emerging fluconazole resistance: Implications for the management of cryptococcal meningitis. Medical Mycology Case Reports **19**: 30-32

Munoz A, Lopez-Garcia B, Marcos JF. 2006. Studies on the mode of action of the antifungal hexapeptide PAF26. Antimicrobial Agents and Chemotherapy **50**: 3847-3855

Nam J, Jung M, Kim P, Lee H, Kim S, Lee C. 2015. Structural characterization and temperature-dependent production of C17-fengycin B derived from *Bacillus amyloliquefaciens* subsp. *plantarum* BC32-1. Biotechnology and Bioprocess Engineering **20**: 708-713

Ndlovu T, Rautenbach M, Khan S and Khan W. 2017. Variants of lipopeptide and glycolipids produced by *Bacillus amyloliquefaciens* and *Pseudomonas aeruginosa* cultured in different carbon substrates. AMB Express **7**: 109

Olfa T, Antonio D, Sana A, Imen B, Salem E, Mohamed Najib A, Bruno C, Vincenzo L, Ferid L, Maria Luisa M. 2015. Synergistic fungicidal activity of the lipopeptide bacillomycin D with amphotericin B against pathogenic *Candida* species. Federation of European Microbiological Societies Yeast Research **15**: 1-22

Parente-Rocha J, Bailão A, Amaral A, Taborda C, Paccez J, Borges C, Pereira M. 2017. Antifungal resistance, metabolic routes as drug targets, and new antifungal agents: An overview about endemic dimorphic fungi. Mediators of Inflammation **1**: 1-16

Pathak K, Keharia H. 2014. Identification of surfactins and iturins produced by potent fungal antagonist, *Bacillus subtilis* K1 isolated from aerial roots of banyan (*Ficus benghalensis*) tree using mass spectrometry. Biotechnology **4**: 283-295

Pecci Y, Rivardo F, Martinotti M, Allegrone G. 2010. LC/ESI-MS/MS characterisation of lipopeptide biosurfactants produced by the *Bacillus licheniformis* V9T14 strain. Journal of Mass Spectrometry **45**: 772-778

Perez-Nadales E, Nogueira MFA, Baldin C, Castanheira S, El Ghalid M, Grund E, Lengeler K, Marchegiani E, Mehrotra PV, Moretti M, Naik V, Oses-Ruiz M, Oskarsson T, Schäfer K, Wasserstrom L, Brakhage AA, Gow NAR, Kahmann R, Lebrun M-H, Perez-Martin J, Di Pietro A, Talbot NJ, Toquin V, Walther A, Wendland J. 2014. Fungal model systems and the elucidation of pathogenicity determinants. Fungal Genetics and Biology **70**: 42–67

Pianalto K, Alspaugh J. 2016. New horizons in antifungal therapy. Journal of Fungi **2**: 26

Pretorius D, van Rooyen J, Clarke K. 2015. Enhanced production of antifungal lipopeptides by *Bacillus amyloliquefaciens* for biocontrol of postharvest disease. New Biotechnology **32**: 243-252

Raaijmakers JM, de Bruijn I, de Kock MJ. 2006. Cyclic lipopeptide production by plant-associated *Pseudomonas* spp.: diversity, activity, biosynthesis, and regulation. Molecular Plant-Microbe Interactions **19**: 699-710

Raaijmakers JM, De Brujin I, Nybroe O and Ongena M. 2010. Natural functions of lipopeptides from *Bacillus* and *Pseudomonas*: more than surfactants and antibiotics. FEMS Microbiology Reviews **34**: 1037-1062

Rautenbach M, Troskie A, Vosloo J. 2016. Antifungal peptides: To be or not to be membrane active. Biochimie **130**: 132-145

Rautenbach M, Vlok N, Eyéghé-Bickong H, van der Merwe M, Stander M. 2017. An electrospray ionization mass spectrometry study on the "*In Vacuo*" hetero-oligomers formed by the antimicrobial peptides, surfactin and gramicidin S. Journal of the American Society for Mass Spectrometry **28**: 1623-1637

Sena HH, Sanches MA, Rocha DFS, Segundo WOPF, de Souza ÉS, de Souza JVB. 2018. Production of biosurfactants by soil fungi isolated from the amazon forest. International Journal of Microbiology **2018**: 1-8

Singh S, Chaudhary K, Dhanda S, Bhalla S, Usmani S, Gautam A, Tuknait A, Agrawal P, Mathur D, Raghava G. 2016. SATPdb: a database of structurally annotated therapeutic peptides. Nucleic Acids Research **44**: 1119-1126

Tabares P, Degel B, Schaschke N, Hentschel U, Schirmeister T. 2012. Identification of the protease inhibitor miraziridine A in the Red sea sponge *Theonella swinhoei*. Pharmacognosy Research **4**: 63-66

Toral L, Rodríguez M, Béjar V, Sampedro I. 2018. Antifungal activity of lipopeptides from *Bacillus* XT1 CECT 8661 against *Botrytis cinerea*. Frontiers in Microbiology **9**: 1315

Toure Y, Ongena M, Jacques P, Guiro A, Thonart P. 2004. Role of lipopeptides produced by *Bacillus subtilis* GA1 in the reduction of grey mould disease caused by *Botrytis cinerea* on apple. Journal of Applied Microbiology **96**: 1151-1160

Troskie AM, de Beer A, Vosloo JA, Jacobs K, Rautenbach M. 2014. Inhibition of agronomically relevant fungal phytopathogens by tyrocidines, cyclic antimicrobial peptides isolated from *Bacillus aneurinolyticus*. Microbiology SGM **160**: 2089-20101

Troskie AM, Vlok NM, Rautenbach M. 2012. A novel 96-well gel-based assay for determining antifungal activity against filamentous fungi. Journal of Microbiological Methods **91**: 551-558

Wang J, Liu J, Chen H, Yao J. 2007. Characterization of *Fusarium graminearum* inhibitory lipopeptide from *Bacillus subtilis* IB. Applied Microbiology and Biotechnology **76**: 889-894

Wang G, Li X, Wang, Z. 2015. APD3: The antimicrobial peptide database as a tool for research and education. Nucleic Acids Research **44**: 1087-1093

Wang J, Liu J, Wang X, Yao J, Yu Z. 2004. Application of electrospray ionization mass spectrometry in rapid typing of fengycin homologues produced by *Bacillus subtilis*. Letters in Applied Microbiology **39**: 98-102

Wurster S, Kumaresan PR, Albert ND, Hauser PJ, Lewis RE, Kontoyiannis DP. 2019. Live monitoring and analysis of fungal growth, viability, and mycelial morphology using the incucyte neurotrack processing module. ASM **10**: 1-18

CHAPTER 5

Final Discussion and Conclusions

Chapter 5

5.1 Potential of *P. sidoides* tuber-associated microbiota as a resource for antifungal compounds.

In this study, a collection of fungi, yeasts as well as bacteria, were isolated from *Pelargonium sidoides* tubers and screened for antifungal compound production. Two *Penicillium* species (isolates A1 and C5) and two *Bacillus* species (isolates YC2 and SC6) were found to have broad-spectrum antifungal activity against a medically and agriculturally relevant panel of pathogenic fungi. Isolate A1 also had the highest relative antifungal activity against *Cryptococcus neoformans* and isolate C5 the highest relative antifungal activity against *Botrytis cinerea* and *Fusarium oxysporum*. Most studies to date have focused on the antimicrobial properties and underlying chemistry of *P. sidoides* plant extracts, except for two recent studies describing the antibacterial activity of tuber endophytic fungi (Aboobaker *et al.,* 2019; Manganyi *et al.,* 2019). The latter studies also focused on bioactive compounds such as linoleic acid and dibutyl phthalate produced by *P. sidoides* fungal endophytes. This study is the first to address the gap in knowledge concerning the potential of *P. sidoides* tuber-associated microbiota to produce antifungal compounds and lipopeptides (LPs) specifically.

The focus on antifungal compounds and LPs was prioritised due to the critical need for new antifungal treatment options to augment existing antifungal drugs. Current options are deemed increasingly ineffective to defend humans, animals and plants from the increasing number of drug resistant and emerging pathogenic fungal threats (Casadevall, 2019). Secondly, this study was motivated by the lack of data on antifungal compounds produced by the *P. sidoides* tuber-associated microbiota and the potential of this unexplored resource to provide novel antifungal compounds, including LPs that could drive future antifungal drug discovery efforts. Future studies bioprospecting for novel antifungal compounds could expand the search to other bioactive compounds in the same *P. sidoides* microbiota or characterise antifungal LPs produced by microbes associated with other medicinal plants with antifungal activity.

In this study, the most promising microbial antifungal compound producer was a bacterial LP producer, denominated isolate YC2. This strain of *Bacillus*, putatively identified as a close relative of *Bacillus velezensis*, was able to consistently produce similar amounts of the same potent secondary metabolites in every culture within every triplicate analysed with LC-MS.

This excellent reproducibility in LP production may be exceedingly valuable when scaling up LP production as many bacterial and fungal strains produce different amounts of the same secondary metabolites in a culture-independent manner (Sonjak *et al.,* 2005; Walker *et al.,* 2011; Wang *et al.,* 2019). This was demonstrated by Sonjak *et al.* (2005) with bacterial species, including some *Bacillus* sp., and by Wang *et al.,* (2019) with *Penicillium* species, including several strains of *Penicillium crustosum* and *Penicillium commune*. These isolates were all found to produce different levels of the same, or different secondary metabolites, even when isolated from the same environment and provided with the same growth media.

The pathogenic fungi, namely *C. neoformans, C. albicans, B. cinerea* and *F. oxysporum,* selected in this study are known to acquire drug resistance which compromises human health, especially in Sub-Saharan Africa, and agricultural yields, around the world. This is due in part to the long-term exposure of these fungi to the same non-biodegradable antifungal drug compounds (Adnan *et al.,* 2019; Berger *et al.,* 2017; Chen *et al*., 2016; Gray *et al*., 2012). Therefore, it is imperative that more studies bioprospect for novel, more biodegradable, antifungal compounds with activity against them. Biodegradable antifungal compounds will reduce the likelihood of resistance developing in the future as they do not accumulate in the natural environment at the same rate as other synthetic chemicals (Fisher *et al*., 2018). This gives both environmental and pathogenic fungi less time to develop resistance against these compounds.

Other challenges to producing LPs, besides the selection of a reliable hyperproducing strain, such as YC2, include high production costs and technical problems which decrease final yields. These technical problems include proper optimisation of the appropriate identification and purification techniques to extract all the LPs produced in the culturing process (Beltran-Gracia *et al.,* 2017; Biniarz *et al.,* 2018). Current detection and purification techniques include using polymerase chain reaction (PCR) based techniques, chiral gas chromatography mass spectrometry (GC-MS), high- or ultra-performance liquid chromatography-mass spectrometry (HPLC or UPLC-MS) or matrix-assisted laser desorption ionisation- time of flight- mass spectrometry (MALDI-TOF-MS) (Beltran-Gracia *et al.,* 2017). Although nuclear magnetic resonance (NMR) crystallography and Fourier transform IR infrared (IR) spectroscopy can also be used (Raaijmakers *et al*., 2010).

High costs associated with production include the cost of raw materials used in the feedstock and the optimisation of the culture conditions, which sometimes include aeration. Cheap raw materials used as a feedstock can include bran, potato peels, molasses, soybean and rice

(Beltran-Gracia *et al.,* 2017; Sena *et al.,* 2018). These materials contain enough carbon and nitrogen for LP production. Additional nutrient sources which can increase production yields by several-fold include supplementation with additional nitrogen sources such as tryptone or nitrate, amino acids like leucine or valine, divalent cations such as Mn^{2+} and Fe^{2+} (Beltran-Gracia *et al.,* 2017; Biniarz *et al.,* 2018; Costa *et al*., 2002; Masurekar *et al*., 1992; Narayana and Vijayalakshmi, 2008; Pretorius *et al*., 2015; Rebotiloe *et al*., 2018). Sulphates and chlorides, $ZnSO_4$, $FeCl_3$ and $MnSO_4$, can also be added to increase the production of iturins, surfactins and fengycins, specifically (Beltran-Gracia *et al.,* 2017). To date, only surfactins are produced commercially from bacterial cultures as years of research finally optimised the process to make it affordable (300-500 €/kg) for large-scale production (Biniarz *et al.,* 2018). Other biosurfactants, like mycosubtilin, fengycin, iturin and lichenysin are still being optimised but remain too expensive for use in the pharmaceutical, agricultural or food industry (Biniarz *et al.,* 2018). In future studies, isolate YC2 will still have to be cultured at larger volumes to upscale the production and extraction of iturin and fengycin. The success of these attempts will determine whether the production and extraction processes are commercially viable or require further research and optimisation.

The significance of YC2 extracts having antifungal activity against pathogenic spores (*B. cinerea* and *F. oxysporum*) and yeasts (*C. neoformans* and *C. albicans*), both of which initiate and spread infection, is that in future studies these extracts could be tested as preventative agents on crops (Shin *et al.,* 2017; Tymon and Johnson, 2014). Preventative fungicides are often favourable as they are applied in the early disease stages, before much crop damage or losses are incurred, and are often the most effective treatments to reducing disease (Mueller *et al.,* 2004). Most antifungal agents have either preventative functions or curative functions, although some compounds can be active against more than one growth morphology (Tymon and Johnson, 2014). Curative fungicides are able to inhibit the growth of fungal infections composed of mycelia, which due to the high chitin content in the cell wall, may be more difficult to treat than fungal spores, e.g. conidiospores, or pathogenic yeasts (Braun and Calderon, 1978; Lenardon *et al*., 2010). As YC2 extracts had antifungal activity against both *B. cinerea* and *F. oxysporum* spores and mycelia, the extracts may have potential for application as both a curative and a preventative agent to plant infections caused by *B. cinerea* and *F. oxysporum*. As iturin and fengycin were detected at high levels in all the YC2 extracts, these antifungal LPs are likely to have curative and preventative properties against *B. cinerea* and *F. oxysporum*. Although, this would need to be determined by purifying these individual compounds and testing for antifungal activity against both *B.*

cinerea and *F. oxysporum* spores and mycelia. The same iturin and fengycin fractions could be evaluated for antifungal activity against *C. neoformans* and *C. albicans* yeast cells, to determine the individual contributions made by these compounds to the preventative functions of the YC2 extracts.

The antifungal LPs identified in YC2 extract, iturin A_Q (a novel iturin A analogue) and fengycin A, confirm the efficacy of the culturing and extraction techniques used to culture microbes for increased LP production. They also highlight the sensitivity of the analytical techniques used to identify peptide structures using UPLC-MS and tandem MS. The only limitations to using these techniques are related to the number of peptides and peptide fragmentation patterns stored on online databases and described in scientific literature. Without a number of spectral data sets and retention times generated by previously characterised peptides or standards, few potential matches can be found for any given compound, even if the previously characterised compounds are present in newer data sets (Biniarz *et al.,* 2018; Lubec and Afiehi-Sadat*,* 2007; Karpievitch *et al.,* 2010). This highlights a need for the broader scientific community to keep adding high-quality spectral data to online databases (Lubec and Afiehi-Sadat*,* 2007). To ensure the submission of only high quality, parts per million (ppm) error should always be used and a selection criterion, followed by fragmentation (Rautenbach *et al*., 2017).

Highlighting the importance of a genetic component to unravelling the identity of compounds produced in an uncharacterised microbial extract, was the identification of isolate YC2 as a member of the genus *Bacillus*. The main cyclic LPs produced by *Bacillus* are surfactin, iturin and fengycin (Raaijmakers *et al.,* 2010). For this reason, UPLC-MS data (Retention time, *Mr* and *m/z*) for these cyclic compounds found in literature and on the NORINE database were compared with that of the YC2 extracts at an early stage in the analysis. Bacterial isolate SC6 may be a member of the *Bacillus* genus, but of a species not known to produce any antifungal LPs, as neither surfactin, fengycin, iturin, or any of the less commonly produced *Bacillus* LPs (e.g. kustakins, maltacines, polymoxins and bamylocins) was detected in SC6 extracts after UPLC-MS analysis. Isolate A1 was identified as a *Penicillium* species. Of the many *Penicillium* sp. characterised, few are known to produce any antifungal peptides (AFPs) or biosurfactants (Garrigues *et al.,* 2017; Sena *et al.,* 2018). Those that are known to produce AFPs, produce mainly short cysteine-containing peptides, and those known to produce biosurfactants, produce mainly glycolipids and other unidentified

biosurfactants (Camargo-de-Morais *et al.,* 2003; Garrigues *et al.,* 2017; Sena *et al.,* 2018; Luna-Velasco *et al.,* 2007).

To improve on the identification of YC2, SC6, A1, C5, and other microbes isolated from *P. sidoides* in this study, it is recommended that whole genome shotgun sequencing be implemented in future studies. This technology is becoming increasingly affordable and will provide a more accurate species-level identification than multi-locus analyses.

5.2 Suggestions for Future Studies

To complement UPLC-MS analysis and evaluate whether certain biosynthetic gene clusters (BGCs) associated with LP production, are included in the genomes of the microbes identified in this study (Information included in Chapter 3), specific PCR amplicons (for BGCs associated with antimicrobial LP synthesis), or whole genomes should be compared with online BGC databases like antiSMASH (Blin *et al.,* 2017). This database contains various BGCs and their corresponding producer species (Blin *et al.,* 2017). Findings made after a database comparison could then be compared with the bioactive compounds identified using UPLC-MS analysis (Information presented in Chapter 4) of fengycin A and iturin A_Q to determine whether this combined approach is effective in narrowing the search for known bioactive compounds contained in microbial extracts. Previous studies which have used this combined approach to mine microbes which produce LPs in environmental samples include those by Chen *et al.* (2019), Müller *et al.* (2007) and Zhoa *et al.* (2019). The combined approach can also be used as a high-throughput genome-based approach to mining medicinal plants for microbes which are likely to produce these compounds, before actually culturing these organisms, screening for bioactivity or extracting the bioactive compounds for characterisation using UPLC-MS analysis. This may save time and money in future studies.

In summary, the contribution of microbiota to the antimicrobial properties of South African medicinal plants remains vastly unexplored and future studies should be extended beyond the scope of *P. sidoides*. A deeper exploration of these medicinal plant-microbiota associations may lead to potentially new antifungal treatment options.

5.3 References

Aboobaker Z, Viljoen A, Chen W, Crous PW, Maharaj VJ, van Vuuren S. 2019. Endophytic fungi isolated from *Pelargonium sidoides* DC: Antimicrobial interaction and isolation of a bioactive compound. South African Journal of Botany **122**: 535–542

Adnan M, Hamada M, Hahn M, Li G, Luo C. 2019. Fungicide resistance of *Botrytis cinerea* from strawberry to procymidone and zoxamide in Hubei, China. Phytopathology Research **1**: 1-12

Beltran-Gracia E, Macedo-Raygoza G, Villafaña-Rojas J, Martinez-Rodriguez A, Chavez-Castrillon Y, Espinosa-Escalante F, Di Mascio P, Ogura T, Beltran-Gracia, M. 2017. Production of lipopeptides by fermentation processes: Endophytic bacteria, fermentation strategies and easy methods for bacterial selection. Fermentation Processes **11**: 200-217

Berger S, El Chazli Y, Babu A, Coste A. 2017. Azole resistance in *Aspergillus fumigatus*: A consequence of antifungal use in agriculture? Frontiers in Microbiology **8**: 1024

Biniarz P, Coutte F, Gancel F, Łukaszewicz M. 2018. High-throughput optimization of medium components and culture conditions for the efficient production of a lipopeptide pseudofactin by *Pseudomonas fluorescens* BD5. Microbial Cell Factories **17**: 121

Blin K, Wolf T, Chevrette MG, Lu X, Schwalen CJ, Kautsar SA, Suarez Duran HG, de Los Santos, EL, Kim HU, Nave M, Dickschat JS. 2017. antiSMASH 4.0—improvements in chemistry prediction and gene cluster boundary identification. Nucleic acids research **45**: 36-41

Braun PC, Calderone RA. 1978. Chitin synthesis in *Candida albicans*: Comparison of yeast and hyphal forms. Journal of Bacteriology **133**: 1472-1477

Camargo-de-Morais MM, Ramos SAF, Pimentel MCB, de Morais MA, Lima Filho JL. 2003. Production of an extracellular polysaccharide with emulsifier properties by *Penicillium citrinum*. World Journal of Microbiology and Biotechnology **19**: 191-194

Casadevall A. 2019. Global catastrophic threats from the fungal kingdom: Fungal catastrophic threats. Current Topics in Microbiology and Immunology **1**: 1-12

Chen AJ, Frisvad JC, Sun BD, Varga J, Kocsubé S, Dijksterhuis J, Kim D, Hong S, Houbraken J, Samson R. 2016. *Aspergillus* section *Nidulantes* (formerly *Emericella*): Polyphasic taxonomy, chemistry and biology. Studies in Mycology **84**: 1-118

Chen R, Wong HL, Burns BP. 2019. New approaches to detect biosynthetic gene clusters in the environment. Medicines **6**: 32

Costa E, Teixido N, Usall J, Atares E, Vinas I. 2002. The effect of nitrogen and carbon sources on growth of the biocontrol agent *Pantoea agglomerans* strain CPA-2. Letters in Applied Microbiology **35**: 117-120

Fisher M, Hawkins N, Sanglard D, Gurr S. 2018. Worldwide emergence of resistance to antifungal drugs challenges human health and food security. Science **360**: 739-742

Garrigues S, Gandía M, Popa C, Borics A, Marx F, Coca M, Marcos JF, Manzanares P. 2017. Efficient production and characterization of the novel and highly active antifungal protein AfpB from *Penicillium digitatum*. Scientific Reports **7**: 14663

Gray KC, Palacios DS, Dailey I, Endo MM, Uno BE, Wilcock BC, Burke MD. 2012. Amphotericin primarily kills yeast by simply binding ergosterol. Proceedings of the National Academy of Sciences of the United States of America **109**: 2234-2239

Karpievitch YV, Polpitiya AD, Anderson GA, Smith RD, Dabney AR. 2010. Liquid chromatography mass spectrometry-based proteomics: Biological and technological aspects. The Annuals of Applied Statistics **4**: 1797-1823

Lenardon MD, Munro CA, Gow NAR. 2010. Chitin synthesis and fungal pathogenesis. Current Opinion in Microbiology **13**: 416-423

Lubec G, Afjehi-Sadat L. 2007. Limitations and pitfalls in protein identification by mass spectrometry. Chemical Reviews 1**07**: 3568-3584

Luna-Velasco MA, Esparza-García F, Cañízares-Villanueva RO, Rodríguez-Vázquez R. 2007. Production and properties of a bioemulsifier synthesized by phenanthrene-degrading *Penicillium* sp. Process Biochemistry **42**: 310-314

Manganyi MC, Tchatchouang C-DK, Regnier T, Bezuidenhout CC, Ateba CN. 2019. Bioactive compound produced by endophytic fungi isolated from *Pelargonium sidoides* against selected bacteria of clinical importance. Mycobiology **47**: 335-339

Masurekar PS, Fountoulakis JM, Hallada TC, Sosa MS, Kaplan L. 1992. Pneumocandins from *Zalerion arboricola*. II. Modification of product spectrum by mutation and medium manipulation. The Journal of Antibiotics **45**: 1867-1874

Mueller DS, Jeffers SN, Buck JW. 2004. Effect of timing of fungicide applications on development of rusts on daylily, geranium, and sunflower. Plant Disease **88**: 657-661

Narayana KJP, Vijayalakshmi M. 2008. Optimization of antimicrobial metabolites production by *Streptomyces albidoflavus*. Research Journal of Pharmacology **2**: 4-7

Pretorius D, van Rooyen J, Clarke KG. 2015. Enhanced production of antifungal lipopeptides by *Bacillus amyloliquefaciens* for biocontrol of postharvest disease. New Biotechnology **32**: 243-252

Raaijmakers JM, De Brujin I, Nybroe O and Ongena M. 2010. Natural functions of lipopeptides from *Bacillus* and *Pseudomonas*: more than surfactants and antibiotics. Federation of European Microbiological Societies Microbiology Reviews **34**: 1037-1062

Rautenbach M, Vlok N, Eyéghé-Bickong H, van der Merwe M, Stander M. 2017. An electrospray ionization mass spectrometry study on the "*In Vacuo*" hetero-oligomers formed by the antimicrobial peptides, surfactin and gramicidin S. Journal of the American Society for Mass Spectrometry **28**: 1623-1637

Rebotiloe FM, Eunice UJ, Mahloro HSD. 2018. Isolation and identification of bacterial endophytes from *Crinum macowanii* Baker. African Journal of Biotechnology **17**: 1040-1047

Müller C, Nolden S, Gebhardt P, Heinzelmann E, Lange C, Puk O, Welzel K, Wohlleben W, Schwartz D. 2007. Sequencing and analysis of the biosynthetic gene cluster of the lipopeptide antibiotic friulimicin in *Actinoplanes friuliensis*. Antimicrobial agents and chemotherapy. **51**: 1028-1037

Sena HH, Sanches MA, Rocha DFS, Segundo WOPF, de Souza ÉS, de Souza JVB. 2018. Production of biosurfactants by soil fungi isolated from the amazon forest. International Journal of Microbiology **2018**: 1-8

Shin J-H, Fu T, Park KH, Kim KS. 2017. The effect of fungicides on mycelial growth and conidial germination of the ginseng root rot fungus, *Cylindrocarpon destructans*. Mycobiology **45**: 220–225

Sonjak S, Frisvad JC, Gunde-Cimerman N. 2005. Comparison of secondary metabolite production by *Penicillium crustosum* strains, isolated from Arctic and other various ecological niches. Federation of European Microbiological Societies. Microbiology and Ecology **53**: 51-60

Tymon L, Johnson DA. 2014. Fungicide resistance of two species of *Alternaria* from potato in the Columbia Basin of Washington. Plant Disease **98**: 1648-1653

Walker V, Bertrand C, Bellvert F, Moënne-Loccoz Y, Bally R, Comte G. 2011. Host plant secondary metabolite profiling shows a complex, strain-dependent response of maize to plant growth-promoting rhizobacteria of the genus *Azospirillum*. New Phytologist **189**: 494-506

Wang S-S, Liu J-M, Sun J, Sun Y-F, Liu J-N, Jia N, Fan B, Dai X-F. 2019. Diversity of culture-independent bacteria and antimicrobial activity of culturable endophytic bacteria isolated from different *Dendrobium* stems. Scientific Reports **9**: 10389

Zhao H, Liu YP, Zhang LQ. 2019. *In silico* and genetic analyses of cyclic lipopeptide synthetic gene clusters in *Pseudomonas* sp. 11K1. Frontiers in Microbiology **10**: 544

APPENDIX A: Growth Media

YPD agar (pH. 6.5; g/L):

24 g Agarose (Sigma Aldridge)

20 g Peptone powder (Merck Biolabs)

10 g Yeast extract powder (Merck Biolabs)

6.4 g D+ Glucose anhydrous (Merck)

10 µg/mL Streptomycin (Sigma Aldridge)

10 µg/mL Chloramphenicol (Sigma Aldridge)

PDA agar (pH. 5.6; g/L):

PDA powdered agar (Merck Biolabs)

10 µg/mL Streptomycin (Sigma Aldridge)

10 µg/mL Chloramphenicol (Sigma Aldridge)

MMN (pH. 5.6; mg/L):

500.0 mg Monopotassium phosphate (Sigma Aldridge)

250.0 mg Ammonium phosphate dibasic (Sigma Aldridge)

150.0 mg Magnesium sulfate heptahydrate (Sigma Aldridge)

50.0mg Calcium chloride dehydrate (Merck)

25.0 mg Sodium chloride (Merck)

12.0 mg Iron (II) chloride hexahydrate (Merck)

1.0 mg Thiamine HCL (Sigma Aldridge)

2500 mg D+ Glucose anhydrous (Merck)

9000 mg Agarose (Sigma Aldridge)

10 µg/mL Streptomycin (Sigma Aldridge)

10 µg/mL Chloramphenicol (Sigma Aldridge)

ISP 6 (pH. 7; g/L):

15.0 g Peptone powder (Merck Biolabs)

5.0 g Protease peptone (Merck Biolabs)

0.5 g ferric ammonium citrate (Sigma Aldridge)

1.0 g K_2HPO_4 (Sigma Aldridge)

0.08 g $Na_2S_2O_2$ (BHD)

1.0 g Yeast extract (Merck Biolabs)

15.0 g Bacteriological agar (Merck Biolabs)

10 µg/mL Nalidixic acid (Sigma Aldridge)

10 µg/mL Cycloheximide (Sigma Aldridge)

DSMZ (pH. 7.2; g/L):

10.0 g D+ Glucose anhydrous (Merck)

5.0 g Peptone powder (Merck Biolabs)

5.0 g Yeast extract powder (Merck Biolabs)

5.0 g Beef extract powder (BD)

0.74 g $CaCO_3$ (Sigma Aldridge)

15.0 g bacteriological agar (Merck Biolabs)

10 µg/mL Nalidixic acid (Sigma Aldridge)

10 µg/mL Cycloheximide (Sigma Aldridge)

LB agar (**pH. 7.5; g/L):**

LB agar powder (Merck biolabs)

10 µg/mL Nalidixic acid (Sigma Aldridge)

10 µg/mL Cyclohexamide (Sigma Aldridge)

M9 (pH. 7.0; g/L):

10.0 g Sodium phosphate dibasic (Sigma Aldridge)

3.0 g Dipotassium phosphate (Sigma Aldridge)

0.6 g Sodium chloride (Merck)

20.0 g Ammonium chloride (Merck)

5.0 g D+ Glucose anhydrous (Merck)

20.0 g Agarose (Sigma Aldridge)

10 µg/mL Nalidixic acid (Sigma Aldridge)

10 µg/mL Cycloheximide (Sigma Aldridge)

APPENDIX B: Curated Gene Sequences

YC2 (16S rRNA):

GAACGCTGGCGGCGTGCCTAATACATGCAAGTCGAGCGGACAGATGGGAGCTTGCTCCCTG
ATGTTAGCGGCGGACGGGTGAGTAACACGTGGGTAACCTGCCTGTAAGACTGGGATAACTCC
GGGAAACCGGGGCTAATACCGGATGCTTGTTTGAACCGCATGGTTCAAACATAAAAGGTGGC
TTCGGCTACCACTTACAGATGGACCCGCGGCGCATTAGCTAGTTGGTGAGGTAACGGCTCAC
CAAGGCAACGATGCGTAGCCGACCTGAGAGGGTGATCGGCCACACTGGGACTGAGAACACG
GCCCAGACTCCTACGGGAGGCAGCAGTAGGGAATCTTCCGCAATGGACGAAAGTCTGACGG
AGCAACGCCGCGTNGAGTGATGAAGGTTTTCGGATCGTAAAGCTCTTGGTTGTTAGGGAAGA
ACAAGTGCCGTTCGAATAGGGCGGCACCTTGACGGTACCTAACCAGAAAGCCACGGCTAACT
ACGTGCCAGCAGCCGCGGTAATACGTAGGTGGCAAGCGTTGTCCGGAATTATTGGGCGTAAA
GGGCTCGCAGGCGGTTTCTTNAAGTCTGATGTGAAAGCCCCCGGCTCAACCGGGGAGGGTC
ATTGGAAACTGGGGAACTTGAGTGCAGAAGAGGAGAGTGGAATTCCACGTGTAGCGGTGAAA
TGCGTAGAGATGTGGAGGAACACCAGTGGCGAAGGCGACTCTCTGGTCTGTAACTGACGCTG
AGGAGCGAAAGCGTGGGGAGCGAACAGGATTAGATACCCTGGTAGTCCACGCCGTAAACGA
TGAGTGCTAAGTGTTAGGGGGTTTCCGCCCCTTAGTGCTGCAGCTAACGCATTAAGCACTCC
GCCTGGGGAGTACGGTCGCAAGACTGAAACTCAAAGGAATTGACGGGGGCCCGCACAAGCG
GTGGAGCATGTGGTTTAATTCGAAGCAACGCGAAGAACCTTACCAGGTCTTGACATCCTCTGA
CAATCCTAGAGATAGGACGTCCCCTTCGGGGGCAGAGTGACAGGTGGTGCATGGTTGTCGTC
AGCTCGTGTCGTGAGATGTTGGGTTAAGTCCCGCAACGAGCGCAACCCTTGATCTTAGTTGC
CAGCATTCAGTTGGGCACTCTAAGGTGACTGCCGGTGACAAACCGGAGGAAGGTGGGGATG
ACGTCAAATCATCATGCCCCTTATGACCTGGGCTACACACGTGCTACAATGGACAGAACAAAG
GGCAGCGAAACCGCGAGGTTAAGCCAATCCCACAAATCTGTTCTCAGTTCGGATCGCAGTCT
GCAACTCGACTGCGTGAAGCTGGAATCGCTAGTAATCGCGGATCAGCATGCCGCGGTGAATA
CGTTCCCGGGCCTTGTACACACCGCCCGTCACACCACGAGAGTTTGTAACACCCGAAGTCGG
TGAGGTAACCTTTATGGAGCCAGCCGCCGAAGGTGGACA

YC2 (*gyrA*):

ATGAGCGTTATCGTCTCCCGGGCGCTTCCGGATGTGCGTGACGGCCTGAAGCCGGTCCACA
GACGGATTTTATACGCGATGAATGATTTAGGCATGACCAGTGACAAGCCGTATAAAAATCCG
CCCGTATCGTCGGTGAAGTTATCGGTAAATATCACCCGCACGGCGACTCAGCGGTTTACGAG
TCAATGGTCAGAATGGCGCAGGATTTTAACTATCGCTACATGCTTGTCGACGGACACGGCAAC
TTCGGTTCGGTAGACGGCGATTCAGCGGCTGCGATGCGTTATACAGAAGCGAGAATGTCAAA
AATCGCAATGGAAATCCTCCGGGACATTACGAAAGACACGATTGATTATCAAGATAACTATGA
CGGCGCAGAAAGAGAGCCTGTCGTCATGCCTTCGAGATTTCCGAATCTGCTCGTAAACGGGG
CTGCCGGCATCGCGGTCGGAATGGCGACAAACATTCCGCCTCACCAGCTGGGCGAAGTCAT
TGACGGAGTGCTTGCCGTAAGCGAAAACCCTGATATTACAAACCAGGAGCTGATGGAATTCAT
CCCTGGGCCTGATTTCCCGACAGCCGGCCAGATCTTGGGCCGGAGCGGAATCCGCAAGGCA
TATGAATCGGGACGGGGATCTATCACCATCCGGGCAAAGGCTGAAATTGAACAGACCTCTTC
TGGC

YC2 (*atpD*):

TCGCGAATGCATCTAGATTCTGGGNCGTATCATGAACGTCCATCAGGAGCATCCGAGCAATT
GTGCTTCCTTTGATGACATTCGGACGAATATCGCCTACATGTGCGACAAATACAATAACATTCA
CTCACTTGGGGTGCACCTCGCATTTAACGGCCCGTTTGATGCGGACTTAACCAACAGCATCG

TGGCAGACATTGAAGAGCTGCTTGAATATGAGAAATATGAAAGCCTTCTGCATTTGTTTCTTGA
GCTGCTGCATGTGGTCAAAGACCGCAACCTTGACCCTGACTGGCGAACGAAGGCCCCGCGT
GTCACGAAAAAAAGCTTCGACTTGCAGCAGGCGCAAAAGCTTCTTTTGAAAGCGGAAAAGAAA
TTGGGCGTTACGCACTTTGGAAGGGCGCTTAAAGCGCTGATTGCTGATTTACTGCATGTGGAT
CTTAATTAAATTGGATGTGGTATGGTGAGTAAATATCATTTTTCAACTATTGTTTCGAGGACACA
TATCTTTAAATTGATGCCGATGATCCATTCTCTCCATGAGCATTGCCGCGATTTTCATCTGTAT
GTGCTGTGTGTCGATCAGAAAGCGTATGAGCTGCTTCAGCAGGTGCCGTGGGAGCATGTGAC
ATTTGTGCAGCTCCATGAAATGGAGGACCCGGAGCTGCTTGAGGCAAAAAGCAGCCGAACGT
TTCACGAATATTGCTGGACGCTCAAACCGGCGTTTTTGTTCCATGTCATGTCCGAGTATGACG
AAGCTGAATATTTTGCCCATCTGGATACCGATCTCTTTTTCTTTTCTGACTTGGAAAGCTTGTTT
ATGGAAAAGCCGGATGCGTCGCTGTTTCTGACAGACCACCGCAATTCTGAACGGTTTATGCCT
TATTACAAGCGGACGGGTCAGTACAACACCGGTTTTGTCGGCGCGCGGAATACAGAGGAAGC
GTACAGGCCGGTTCGGAAGTGTCGGCAATCGGATCCCGGGCCCGTCGACTGCAGAGGCCTG
CA

SC6 (16S rRNA):

ATGCAAGTCGAGCGAATGGATTGAGAGCTTGCTCTCANGAAGTTAGCGGCGGACGGGTGAGT
AACACGTGGGTAACCTGCCCATAAGACTGGGATAACTCCGGGAAACCGGGGCTAATACCGGA
TAANATTTTGAACTGCATGGTTCGAAATTGAAAGGCGGCTTCGGCTGTCACTTATGGATGGAC
CCGCGTCGCATTAGCTAGTTGGTGAGGTAACGGCTCACCAAGGCAACGATGCGTAGCCGAC
CTGAGAGGGTGATCGGCCACACTGGGACTGAGACACGGCCCAGACTCCTACGGGAGGCAGC
AGTAGGGAATCTTCCGCAATGGACGAAAGTCTGACGGAGCAACGCCGCGTGAGTGATGAAG
GCTTTCGGGTCGTAAAACTCTGTTGTTAGGGAAGAACAAGTGCTAGTTGAATAAGCTGGCACC
TTGACGGTACCTAACCAGAAAGCCACGGCTAACTACGTGCCAGCAGCCGCGGTAATACGTAG
GTGGCAAGCGTTATCCGGAATTATTGGGCGTAAAGCGCGCGCAGGTGGTTTCTTAAGTCTGA
TGTGAAAGCCCACGGCTCAACCGTGGAGGGTCATTGGAAACTGGGAGACTTGAGTGCAGAA
GAGGAAAGTGGAATTCCATGTGTAGCGGTGAAATGCGTAGAGATATGGAGGAACACCAGTGG
CGAAGGCGACTTTCTGGTCTGTAACTGACACTGAGGCGCGAAAGCGTGGGGAGCAAACAGG
ATTAGATACCCTGGTAGTCCACGCCGTAAACGATGAGTGCTAAGTGTTAGAGGGTTTCCGCC
CTTTTAGTGCTGAAGTTAACGCATTAAGCACTCCGCCTGGGGGAGTACGGCCGCAAGGCTGA
AACTCAAAGGAATTGACGGGGGGCCCGCACCAAGCGGTGGAGCATGTGGTTTAATNTCGAAG
CAACGCGAAGNAACCTTACCCAGGTCTTGACATCCTCTGAAAACCCTAGAGATAGGGCTTCTC
CTTCGGGAGCAGNAGTGANCAGGTGGTGCATGGTTTGTCGTCNGCTCGTGTGNNCGTGAGA
TGTTGGGTTAAGTCCCGCAACGAGCGCAACCCTTGATCTTAGTGTGCCATCATTAAGTTGGGC
ACTCTAAGGNTGACTGCCGGTGACAAACCGGAGGAAGGTGGGGATGACGTCAAATCATCATG
CCCCTTATGACCTGGGCTACACACGTGCTACAATGGACGGTACAAAGAGCTGCAAGACCGCG
AGGTGGAGCTAATCTCATAAAACCGTTCTCAGTTCGGATTGTAGGCTGCAACTCGCCTACATG
AAGCTGGAATCGCTAGTAATCGCGGATCAGCATGCCGCGGTGAATACGTTCCCGGGCCTTGT
ACACACCGCCCGTCACACCACGAGAGTTTGTAACACCCGAAGTCGGTGGGGTAACC

A1 (ITS):

CTCTGGGTCCAACCTCCCACCCGTGTTTATTTTACCTTGTTGCTTCGGCGGGCCCGCCTTAAC
TGGCCGCCGGGGGGCTTACGCCCCCGGGCCCGCGCCCGCCGAAGACACCCTCGAACTCTG
TCTGAAGATTGAAGTCTGAGTGAAAATATAAATTATTTAAAACTTTCAACAACGGATCTCTTGGT
TCCGGCATCGATGAAGAACGCAGCGAAATGCGATACGTAATGTGAATTGCAAATTCAGTGAAT
CATCGAGTCTTTGAACGCACATTGCGCCCCCTGGTATTCCGGGGGGCATGCCTGTCCGAGCG

TCATTGCTGCCCTCAAGCCCGGCTTGTGTGTTGGGCCCCGTCCCCCGATCTCCGGGGGACG
GGCCCGAAAGGCAGCGGCGGCACCGCGTCCGGTCCTCGAGCGTATGGGGCTTTGTCACCC
GCTCTGTAGGCCCGGCCGGCGCTTGCCGATCAACCCAAATTTTTATCCAGGTTGACCTCG

A1 (*benA*):

TGGGAAGAGCCCGACTTTTTTTTTTCGCGTTGGGTATCAATTGACAGGTTCCTAACTGGATTA
CAGGCAAACCATCTCTGGCGAGCACGGTCTCGATGGCGATGGACAGTAAGTTTTAACAGTGA
TAGGGGTTTCCGGTGGATTACACATCTGATATCTTCCTAGGTACAATGGTACCTCCGACCTCC
AGCTCGAGCGTATGAACGTCTACTTCAACCATGTGAGTCCAACGACAGGAAACCGAATAATAG
TGCATCATCTGATCGGATGTTTTCCTTGATAATCTAGGCCAGCGGTGACAAGTACGTTCCCCG
TGCCGTTCTCGTCGATTTGGAGCCTGGTACCATGGACGCTGTCCGCTCCGGTCCCTTCGGCA
AGCTTTTCCGCCCCGACAACTTCGTCTTCGGTCAGTCCGG

A1 (*caM*):

CAGGACAAGGATGGCGATGGTGAGTGCGATCGATCCTGACAGCTCGTCCCGGGKGCTACTG
GCGATCRACGATACACAATTCACAGAAAGAGATATACTGAGACGTATGATCAATAGGCCAGAT
TACCACCAAGGAGCTGGGCACTGTCATGCGCTCTCTGGGCCARAACCCCTCTGAGTCTGAGC
TGCAGGACATGATCAACGAGGTTGATGCCGACAACAACGGCACCATTGACTTCCCCGGTATG
AAATCCTCCWTAGTTTTGCCGATCGGGGCCCACAGGACTGATCTCCGCCCGCAGAGTTCCTC
ACCATGATGGCCCGTAAGATGAAGGACACCGATTCCGAGGAGGARATTCGCGAGGCCTTCAA
GGTTTTCSACCGCGACAACAACGGCTTCATCTCCGCTGCTGAGCTGCGCCACGTCATGACCT
CCATCGGA

A1 (*RPB2*):

GCGACAGCTTCACAACACCCACTGGGGTCTTGTGTGCCCTGCCGAAACTCCTGAAGGCCAGG
CTTGTGGTCTCGTCAAGAACTTGGCTCTTATGTGCTACATTACTGTGGGTACGCCCAGCGAGC
CCATCATCGACTTCATGATTCAGCGTAACATGGAGGTTCTGGAAGAATTCGAGCCTCAAGTTA
CACCCAACGCTACAAAGGTCTTTGTCAACGGTGTTTGGGTCGGTATCCATCGCGACCCGTCT
CATCTCGTCACTACCATGATGTCTCTGCGTCGACGAAACATGATCTCGCACGAGGTCAGCTTG
GTTCGTGATATTCGTGACCGCGAGTTCAAGATCTTCACGGATACTGGTCGTGTCTGCCGACC
CTTGTTCACCATTGATAACGACCCGAAGAGTGAGAACGCCGGATCGTTGGTTCTCAATAAAGA
GCACATTCGGAAGCTCGAGATGGACAAGGAATTGCCAGCAGATATGGATGCCGAAGACCGCA
GAGAGCGTTATTTCGGATGGGAGGGCTTGGTACGATCCGGTGCCGTGGAGTTGGTGGATGC
CGAGGAAGAGGAAACCATTATGATTGTCATGACGCCTGAAGACTTGGAAATTTCCAAGCAACT
TCAGGCCGGCTACGCGTTGCCAGAGACCGACTCGGATGACCCCAATAAGCGAGTCCGTTCC
ATTCTCAGT

C5 (ITS):

CCTCCGCTTATTGATATGCTTAAGTTCAGCGGGTATCCCTACCTGATCCGAGGTCAACCTGAA
AAAAGATTGATTGTTGTCGGCAAGCGCCGGCCGGGCCTACAAGAGCGGGTGACAAAGCCCC
ATACGCTCGAGGACCGGACGCGGTGCCGCCGCTGCCTTTCGGGCCCGTCCCCCGGGAAGG
AGGACGGGGCCCAACACACAAGCCGTGCTTGAGGGCAGCAATGACGCTCGGACAGGCATGC
CCCCCGGAATACCAAGGGGCGCAATGTGCGTTCAAAGACTCGATGATTCACTGAATTCTGCA
ATTCACATTACGTATCGCATTTCGCTGCGTTCTTCATCGATGCCGGAACCAAGAGATCCGTTG

TTGAAAGTTTTAACTTATTTAGCTAATTGCTCAGACTGCAATCTTCAGACAGTGTTCAATGGTG
TCTTCGGCGGGCGCGGGCCAGAGGGCAGAAGCCCCCCGGCGGCCGTGAGGCGGGCCCGC
CGAAGCAACAAGGTACAATAAACATGGGTGGGAGGTTGGACCCAGAGGGCCCTCACTCGGT
AATGATCCTTCCGCAAGGTTCACCTAC

C5 (*benA*):

GCTGTCNGGTACGTGCAGAACTAGACATATTCATCAATTGAGACTATAAGAAACGATTTACTG
ACTTGATTCCAGGCAAACCATTGCTGGCGAGCACGGNCTTGACGGCGATGGCCAGTAAGTCG
CCCAAAATTCGACCCGACACGAAATAGCGGTCTGATGTTTTGATATAGGTACGCTGGTGTTTC
CGATCTCCAGCGCGAGCGCATGAACGTCTACTTCAACGAGGTATGTGTCACACTAATGTCTC
GACCGATCTAATCTAATCTCAATTTGTTTTCCTTCAGGCTAGCAACGACAAGTACGTTCCCCGT
GCCGTTCTGGTCGACTTGGAGCCCGGTACCATGGACGCTGTCCGTGCCGGNCCCNTCGGCA
AGCTCTTCCGTCCCGACAACTTCTTCTTCGGCCAGTCTGG

C5 (*caM*):

TCCGAGTACAAGGAGGCCTTCTCCCTGTTTGTGAGTGATTCCACCTATAAATCGAAGACGTGA
AGGTCGAAAATGCTGACCGGAAGTTTGTTTTGTTGCGGAATAGGACAAGGATGGCGATGGTA
CGTGATGGTCGCCCCCCCGACAGCTCAGTCGAGCCCACGACAGTGTCCTCTGCGATCGAATT
TCAAGAGAAACGTATTCTAACATACAATTCTCCCAATAGGACAAATCACCACCAAGGAGCTTG
GCACCGTCATGCGCTCGCTGGGCCAGAACCCCTCCGAGTCTGAGTTGCAGGATATGATCAAC
GAGGTTGACGCCGACAACAACGGCACCATTGACTTCCCTGGTACTTAACCATAACCCACTGAT
ATAAACGAGAGACGGCTATTGACGTGCGATAGAATTCCTCACCATGATGGCTCGTAAGATGAA
GGACACCGATTCCGAGGAGGAGATCCGCGAGGCATTCAAGGTTTTCGATCGCGATAACAACG
GTTTCATTTGCCGCCGCCCAGCTGCGCCACGTCATGACCTCCATCGGA

C5 (*RPB2*):

CACACCCATTGGCAGAGATGGAAAGATTGCCAAACCTCGCCAACTCCATAATACTCATTGGGG
CCTGGTCTGCCCGGCCGAGACACCCGAAGGTCAAGCTTGTGGTTTGGTCAAGAACCTGGCA
CTGATGTGTTACATCACAGTTGGTACACCTGCCGAGCCCATCGTGGACTTCATGATTCAACGT
AACATGGAAGTCCTCGAGGAGTTTGAACCGCAAGTGACACCCAACGCGACAAAGGTGTTTGT
CAATGGTGTCTGGGTGGGTATTCACCGGGACCCTTCGCACCTTGTTACTACGATGCAGAATCT
GCGTCGACGAAACATGATCTCCCACGAAGTCAGTTTGATTCGTGACATTCGTGAACGGGAGTT
CAAAATCTTCACTGATACTGGACGTGTATGTCGGCCACTGTTCGTTATCGATAACGACCCCAA
GAGTGAGAACTCGGGTGGATTGGTCCTTAACAAGGACCACATTCGGAAGCTTGAGTCCGACA
AAGACTTGCCAACAGACTTGGGCCCAGAAGAACGCCGGGAACAATACTTTGGATGGGATGGC
CTGGTACGTTCTGGAGCAGTTGAGTATGTCGACGCCGAAGAAGAGGAAACCATCATGATTGT
CATGACCCCCGAGGACCTTGAGATATCTCGCCAGCTTCAGGCCGGCTACGCTCTGCCAGAAG
ACGAAACCAGCGACCCCAACAAGCGTGTTCGGTCGATTCTCAGCCAGCGTGCCCACACCTGG
ACGCACTGCGAAATTCACCCTAGTATGATCTTGGGTGTTTGCGCCAGTATTATT

APPENDIX C: Results from Biolog GEN III Identification System

Isolate SC6 Results:

Program	OmniLog 2.3		
User	Matshepo		
Data File	SU1_428_180620_A.D5E		
Data Location	C:\Program Files\Biolog\OL_DC_23\SU1\Data_2018\06\		
Instrument	OmniLog	Project	SU1
Instrument S/N	428	Start Time	Jun 20 2018 3:43 PM
Data Mode	ID	Lapse Time	Jun 21 2018 1:47 PM
Read Mode	Normal ID	ID Called At	22.00Hrs
Plate Position	2-A	Target Incubation	22 Hrs
Plate Type	GEN III		
Plate Protocol	B		
Customer	Dr H Volschenk - Stellenbosch University		
Sample	SC6		
Sample Area			
Date Sampled			
Temperature	33*C		
Date of Assay	20/06/2018		
Analyst	Matshepo		
Biolog Database	Biolog GEN III 2_6_1_08.I5G		
Status	Final ID		
Result	Species ID: Bacillus cereus/pseudomycoides		
Comment			
Notice			

Rank	SIM	DIST	PROB	Organism Type	Species
1	0.667	4.800	0.667	GP-Rod-SB	Bacillus cereus/pseudomycoides
2	0.137	5.263	0.215	GP-Rod-SB	Bacillus cereus/thuringiensis
3	0.132	5.282	0.209	GP-Rod-SB	Bacillus cereus/weihenstephanensis
4	0.082	5.575	0.132	GP-Rod-SB	Bacillus cereus/mycoides

Key: <x: positive, x: negative, <x-: mismatched positive, x+: mismatched negative, {x: borderline, -x: less than A1 well

Well Color Values

Plate	1	2	3	4	5	6	7	8	9	10	11	12
A	97	< 173	< 199	< 194	{ 136	109	109 +	103	95	< 239	< 240	47
B	102	83	89	{ 131	{ 125 +	< 215	95	85	90	< 230	85 +	47
C	< 193	89	{ 127	79	107	82	101	85	< 184	< 240	55	< 220
D	107	94	79	90	{ 129	< 215	< 161	57	93	40	55	65
E	< 195	111	111	{ 112	{ 129	{ 119	{ 135	87	< 180	56	< 227	63
F	{ 114 +	103	92	< 167	103	{ 117	103	89	97	55	{ 107	< 243 -
G	94	< 202	104	{ 158	106	{ 121	103	< 180	{ 123	{ 151	85 +	< 242
H	{ 135	{ 113	{ 120	{ 119	107	< 187	{ 122	{ 148	{ 155	< 253	< 211	{ 171

Report Date: June 21 2018 1:47 PM (report version: 2.3)

Isolate YC2 Results:

Program	OmniLog 2.3		
User	Matshepo		
Data File	SU1_428_180620_A.D5E		
Data Location	C:\Program Files\Biolog\OL_DC_23\SU1\Data_2018\06\		
Instrument	OmniLog	Project	SU1
Instrument S/N	428	Start Time	Jun 20 2018 3:43 PM
Data Mode	ID	Lapse Time	Jun 21 2018 1:46 PM
Read Mode	Normal ID	ID Called At	22.00Hrs
Plate Position	1-A	Target Incubation	22 Hrs
Plate Type	GEN III		
Plate Protocol	B		
Customer	Dr H Volschenk - Stellenbosch University		
Sample	YC2		
Sample Area			
Date Sampled			
Temperature	33°C		
Date of Assay	20/06/2018		
Analyst	Matshepo		
Biolog Database	Biolog GEN III 2_6_1_08.I5G		
Status	Final ID		

Result	Species ID: Bacillus subtilis/mojavensis
Comment	
Notice	

Rank	SIM	DIST	PROB	Organism Type	Species
1	0.653	5.010	0.668	GP-Rod-SB	Bacillus subtilis/mojavensis
2	0.107	5.852	0.180	GP-Rod-SB	Bacillus vallismortis
3	0.069	6.122	0.118	GP-Rod-SB	Bacillus subtilis/atrophaeus
4	0.019	6.906	0.035	GP-Rod-SB	Bacillus subtilis ss subtilis

Key: <x: positive, x: negative, <x-: mismatched positive, x+: mismatched negative, {x: borderline, -x: less than A1 well

Well Color Values

Plate	1	2	3	4	5	6	7	8	9	10	11	12
A	69	< 157	{ 125	{ 123	< 171	{ 110	{ 123	82	69	< 253	< 251	< 207
B	{ 85	82	61	< 150	{ 118	< 156 -	48	46	48	< 243	< 242	{ 159
C	< 169	{ 126	< 155	44	48	42	39	40	68	< 246	48	55
D	< 159	< 154	48	{ 120	< 161	44	55	60	43	31	{ 102	58
E	{ 83	64	{ 101 +	< 166 -	{ 110	{ 132	{ 92	62	52	48	{ 104	63
F	70 +	{ 84	70	{ 83	58	66	51 +	49	54 +	49	{ 99	< 223 -
G	{ 57	{ 98	56	{ 127	{ 122	66	54	< 194	28	60	< 215	< 266
H	79	{ 69	50	67	48	{ 101	61	72	{ 87	83	{ 134	{ 128

Report Date: June 21 2018 1:46 PM (report version: 2.3)

APPENDIX D: Supplementary Figures and Tables

Supplementary Table 1. Ex-type, type and reference strains used in phylogenetic tree construction for *Bacillus* species (Miranda *et al*., 2008; Sabir *et al.,* 2013; Celandroni *et al.,* 2019; Bhandari *et al.,* 2013).

Species	**16S rRNA**	***GyrA***	***AtpD***
B. subtilis	NRRL B 4219 (NR_116183)	NRRL B 4219 (EU138592), KCTC 3135T (EF_538682)	168 (NC_000964.3)
B. methylotrophicus	x	NCCB 100236 (KJ459873)	
B. amyloliquefaciens	NBRC 15535 (NR_041455)	BLB 369 (KU847915), KCTC 1660T (AF272015)	
B. siamensis	KCTC 13613 (NR_117274)	KCTC 13613 (KC608573)	
B. tequilensis	10b (NR_1049190)	NRRL B-41771 (EU138625)	
B. vallismortis	NRRL B 14890 (NR_116186)	NRRL B-14890T (EU138601)	
B. mojavensis	NRRL B 14698 (NR_116185)	NRRL B 14698T (AF272019)	
B. atrophaeus	NRRL NRS 213 (NR_116190)	NRRL NRS 213 (EU138654), KCTC 3701T (AF272016)	
B. pumilus	ATCC 7061 (NR_043242)	ATCC 7061 (KF194263)	
B. aerophilus	KACC 16563 (NR_042339)		
B. altitudinis	41KF2b (NR_042337)	DSM 21631 (JX513938)	
B. licheniformis	ATCC 14580 (NR_074923)	MY75 (EU073420), KCTC 1918T (AF272017)	ATCC 14580 (NC_006270.3)

B. sonerensis	NRRL B 23154 (NR_025130)		
B. idriensis	SMC 4352-2 (NR_043268)		
B. nakamuri	NRRL B 41091 (NR_151897)		
B. velezensis	NRRL B 41580 (KY694464)	NRRL B 41580 (EU138622)	
B. anthracis	ATCC 14578 (NR_041248)		
B. mobilis	MCCC 1A05942 (NR_157731)		
B. mycoides	DSM 11821 (NR_024697)		
B. cereus	ATCC 14579 (NR_074540)		
B. thuringiensis	IAM 12077 (NR_043403)		
B. pseudomycoides	NBRC 101232 (NR_113991)		
B. megaterium	IAM 13418 (NR_043401)		
B. methanolicus	NCIMB 13113 (NR_040985)		
B. pseudofirmus	DSM 8715 (NR_026139)		
B. clausii	Y 76 B (AB201797)		
C. perfringens	ATTC 13124 (NR_1216097)		

Supplementary Table 2. Ex- type and type strains used in phylogenetic tree construction for *Penicillium* species using ITS and *benA* gene regions.

Species:	**ITS**		***benA***	
	A1	**C5**	**A1**	**C5**
P. albicoremium	AJ004819		AY674326	
P. allii	AJ005484		AY674331	
P. alutaceum		AF033454		KJ834430
P. aotearoae		KT887874		KT887835
P. arabicum		KC411758		KP016750
P. atrolazulinum		JX140913		JX141077
P. atrosanguineum		JN617706		KJ834435
P. aurantiogriseum	AF033476		AY674296	
P. bioforme	KC411731		FJ930944	
P. burgense		KC411736		KJ834437
P. camemberti	AB479314		FJ930956	
P. canis		KJ511291		KF900167
P. carlsbadiense	KV989138		KY989013	
P. caseifulvum	KJ834504		AY674372	
P. catenatum		KC411754		KJ834438
P. cavernicola	KJ834505		KJ834439	
P. cellarum	KM249068		KMK249108	
P. chalabudae		KP016811		KP016748
P. christenseniea	KY989134		KY989009	
P. cinerascens		AF033455		JX141041
P. cinereoatrum		KC411700		KJ834442
P. citreonigrum		AF033456		EF198621
P. citreosulfuvatum		KP016814		KP016753
P. commune	AY213672		AY674366	
P. consobrinum		JX140900		JX141135
P. corylophilum		AF033450		JX141042
P. cravenianum		JX140888		JX141076
P. crustosum	JX091403		AY674353	
P. cyclopium	JN942742		AY674310	
P. decumbers		AY157490		KJ834446
P. diabolicalcense		KT887840		KT887801

P. dimorphosporum		AF081804		KJ834448
P. discolour	AJ004816		AY674350	
P. dravuni		AY494856		
P. echinulatum	AF033473		AY674342	
P. erubescens		AF033464		HQ646566
P. fagi		AF481124		KJ834471
P. freii	JN942698		AY674290	
P. fundyense		KT887853		KT887814
P. gladiola	AF033480		AY674287	
P. griseolum		EF422848		EF506213
P. guttulosum		HQ646592		HQ646576
P. hemitrachum		FJ231003		JX141048
P. hermansii		MG333472		MG386214
P. hesseltinei	KY989128		KY989000	
P. heteromorphum		KC411702		KJ834455
P. hirusutum	AY373918		AF003243	
P. hordei	AJ004817		AY674347	
P. katangense		AF033458		KP016757
P. krussanovii		EF422849		KP016758
P. laeve		KF667369		KF667365
P. lapidosum		AF033409		KJ834465
P. maclennaniae		KC411689		KJ834468
P. melinii		AF033449		KJ834471
P. melonoconidium	AJ005483		AY674304	
P. menonorum		HQ646591		HQ646573
P. meridianum		AF033451		KJ834472
P. momoii		JX140895		JX141073
P. namyslowskii		AF033463		JX141067
P. neoechinulatum	JN942722		AF003237	
P. nepalense		KC411692		KJ834474
P. nordicum	KJ834513		KJ834476	
P. ovatum		KF667370		KF667366
P. pagulum		JX140898		JX141070
P. palitans	KJ834514		KJ834480	
P. parvum		AF033460		HQ646568
P. pervofructum		LT559091		LT627645

P. philippinense		KC411770		KJ834482
P. pimiteouiense		AF037431		HQ646576
P. polonicum	AF033475		AY674305	
P. punicae				KX839673
P. raciborskii		AF033447		JX141069
P. radicola	KJ834516		AY674357	
P. repensicola				JX141149
P. restrictum		AF033455		KJ834486
P. rubefaciens		KC411677		KJ834487
P. rubidurum		AF033462		HQ646574
P. smithii		KC411723		KJ834492
P. solitum	AY373932		AY674356	
P. striatisporum		AF038938		JX141156
P. subturcoseum		FJ231006		JX141161
P. terrenum		AM992111		KJ834496
P. thymicola	KJK834518		AY674321	
P. tricolor	JN942704		AY674313	
P. tulipae	KJ834519		AY674344	
P. velutinum		AF033448		JX141170
P. venetum	AJ005485		AY674335	
P. verrucosum	AY373938		AY674323	
P. vinaceum		AF033461		HQ646575
P. viridicatum	AY373939		AY674295	
P. viridifulvum	KY989153		KY989028	
P. xanthomelinii		JX140921		JX141120

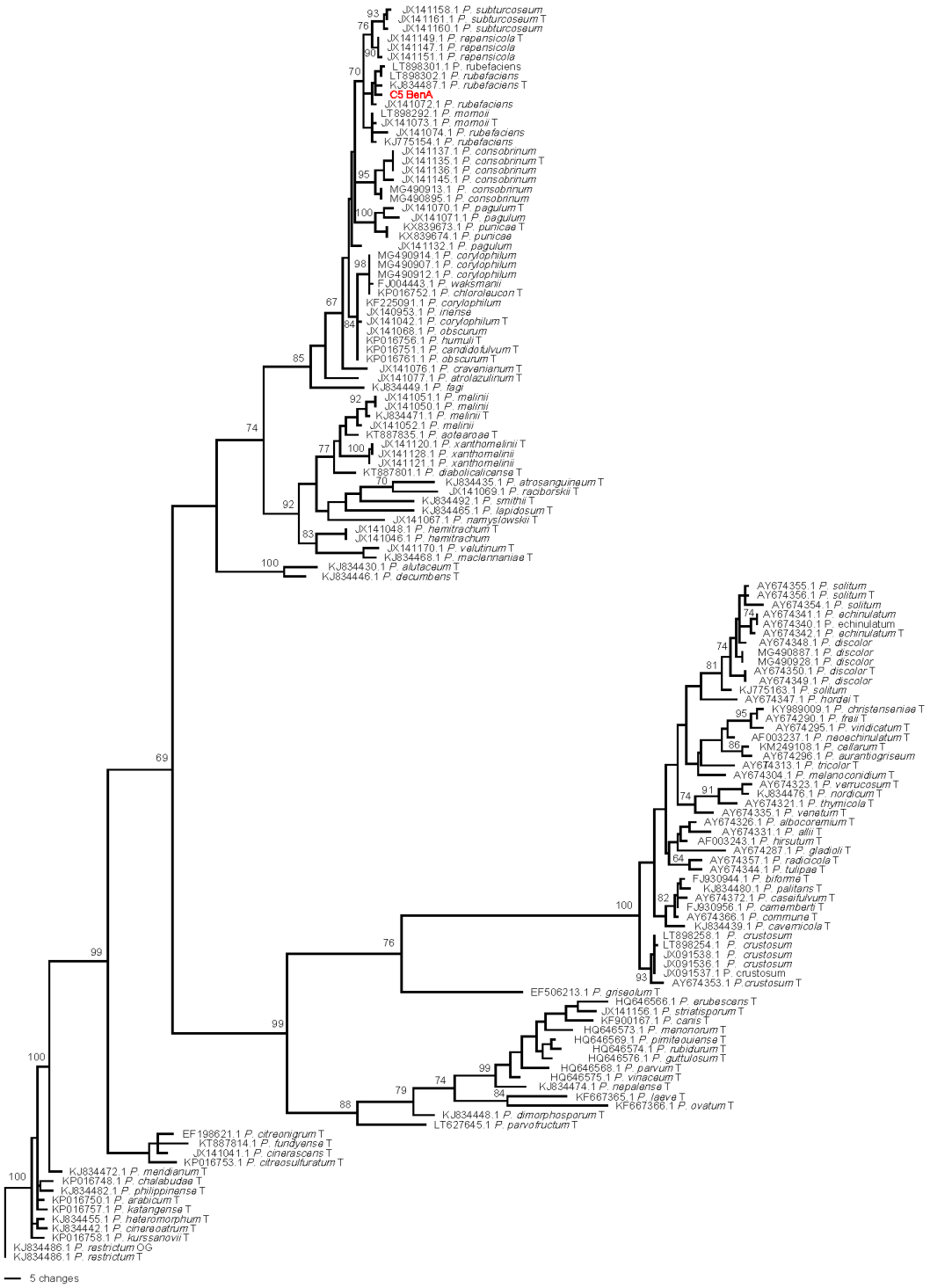

Supplementary Figure 1. Phylogenetic tree constructed using *benA* and *Penicillium* species downloaded from the NCBI. The selected outgroup was *P. restrictum* CBS 367.48. Bootstrap values were presented on internal nodes with maximum parsimony. Bootstrap threshold was set to 50% with 1000 pseudo-replicates. *Values below 50% bootstrap threshold.

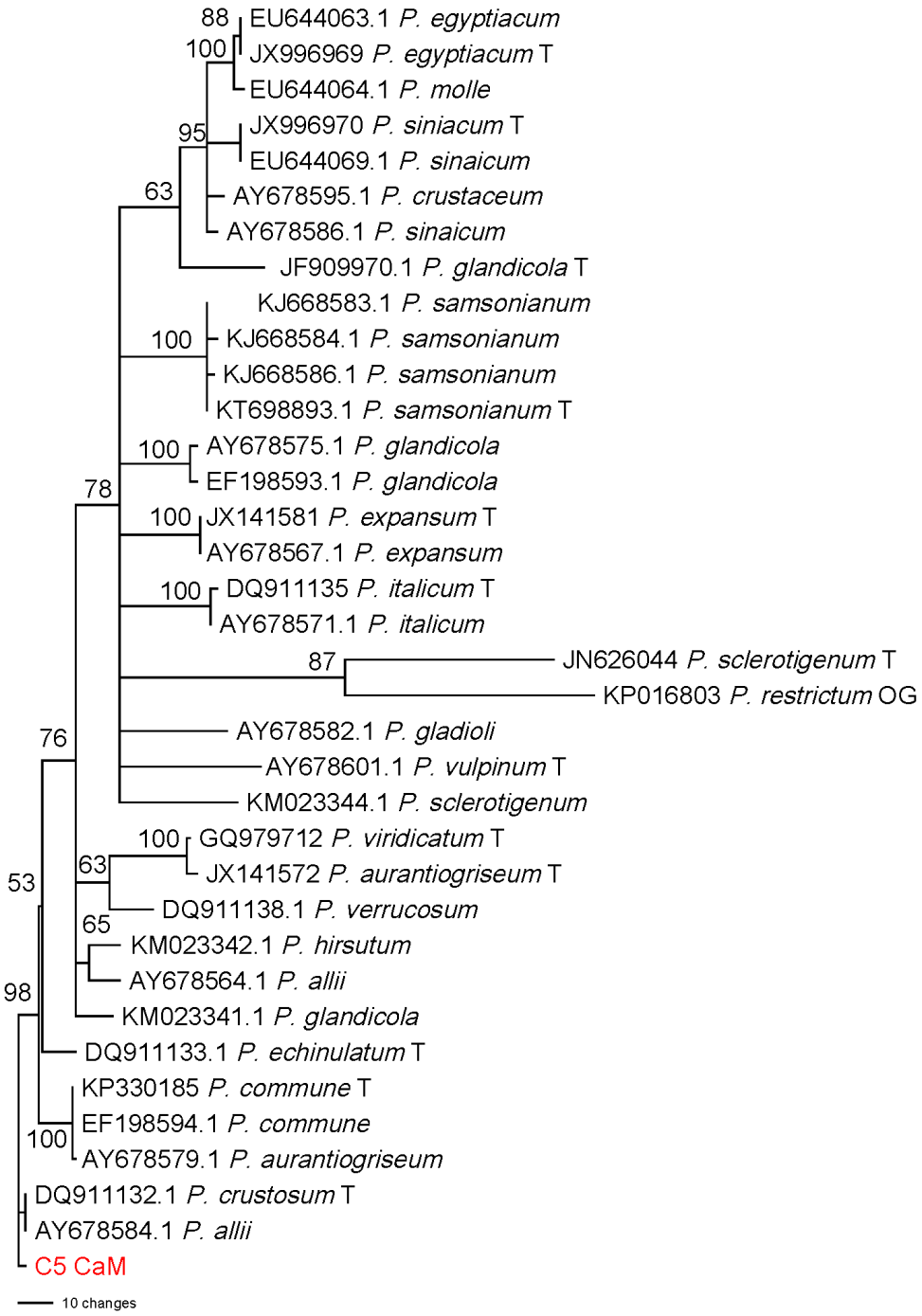

Supplementary Figure 2. Phylogenetic tree constructed using *caM* and *Penicillium* species downloaded from the NCBI. The selected outgroup was *P. restrictum* CBS 367.48. Bootstrap values were presented on internal nodes with maximum parsimony. Bootstrap threshold was set to 50% with 1000 pseudo-replicates. *Values below 50% bootstrap threshold.

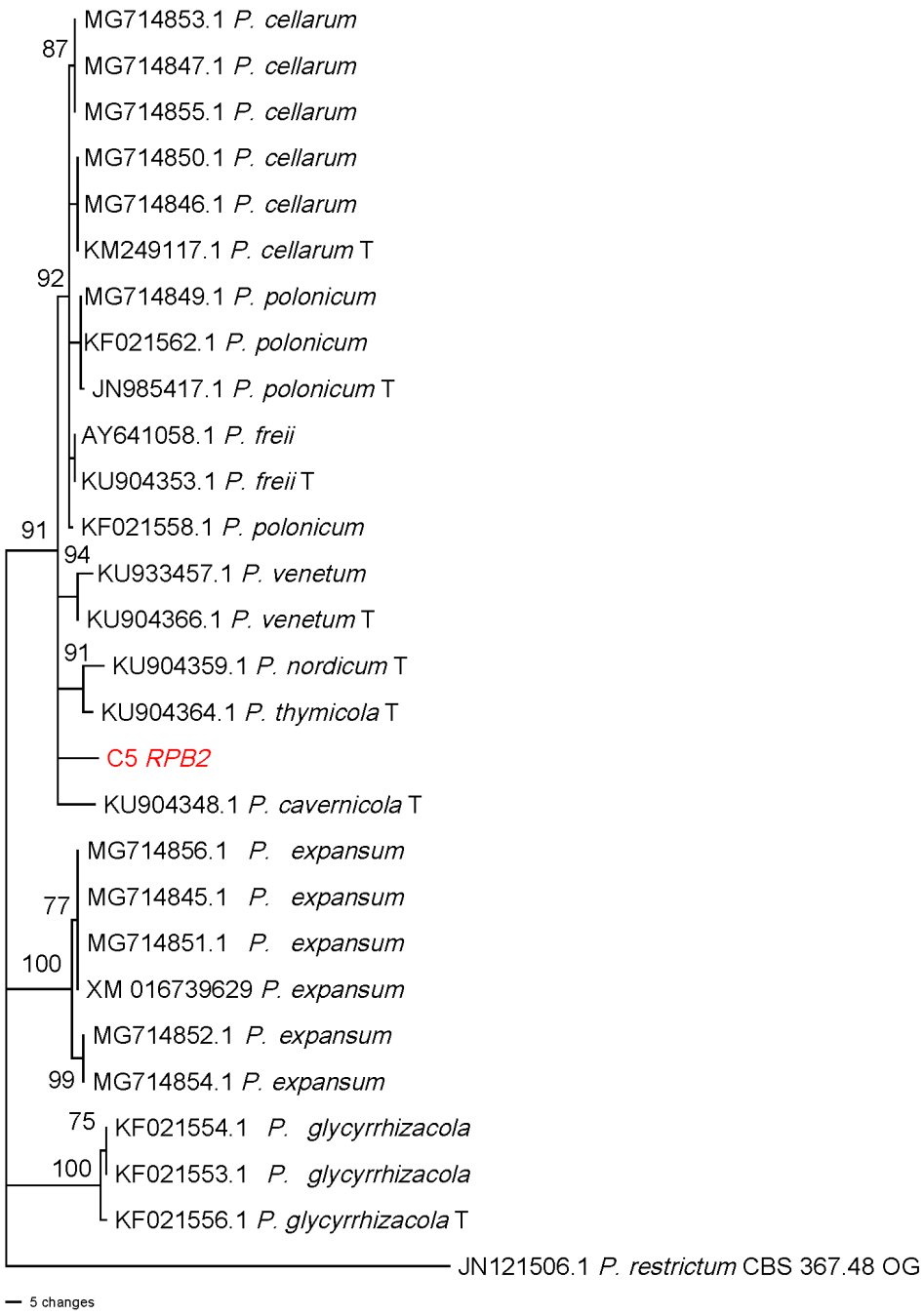

Supplementary Figure 3. Phylogenetic tree constructed using *RPB2* and *Penicillium* species downloaded from the NCBI. The selected outgroup was *P. restrictum* CBS 367.48. Bootstrap values were presented on internal nodes with maximum parsimony. Bootstrap threshold was set to 50% with 1000 pseudo-replicates. *Values below 50% bootstrap threshold.

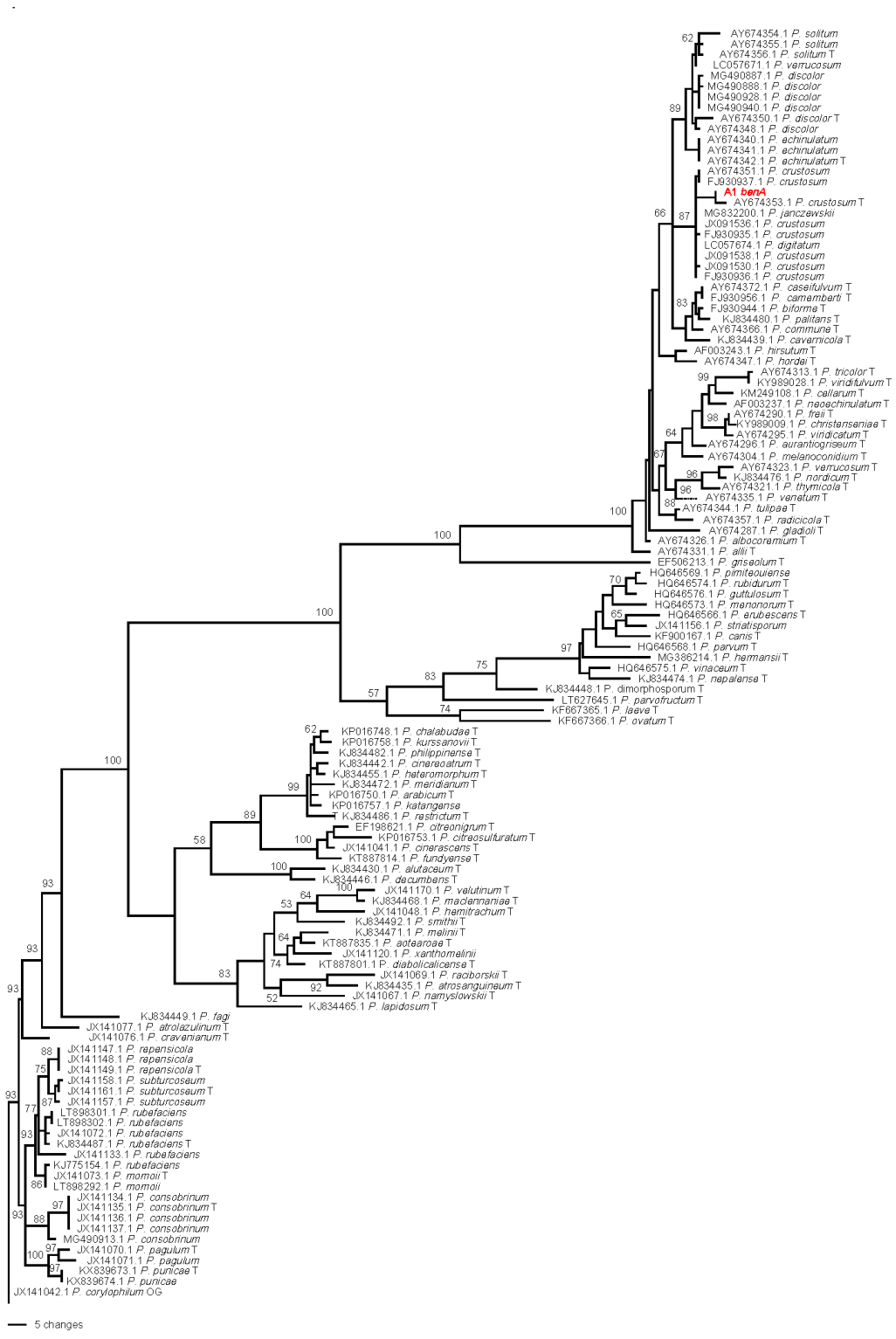

Supplementary Figure 4. Phylogenetic tree constructed using *benA* and *Penicillium* species downloaded from the NCBI. The selected outgroup was *P. corylophilum* CBS 312.48. Bootstrap values were presented on internal nodes with maximum parsimony. Bootstrap threshold was set to 50% with 1000 pseudo-replicates. *Values below 50% bootstrap threshold.

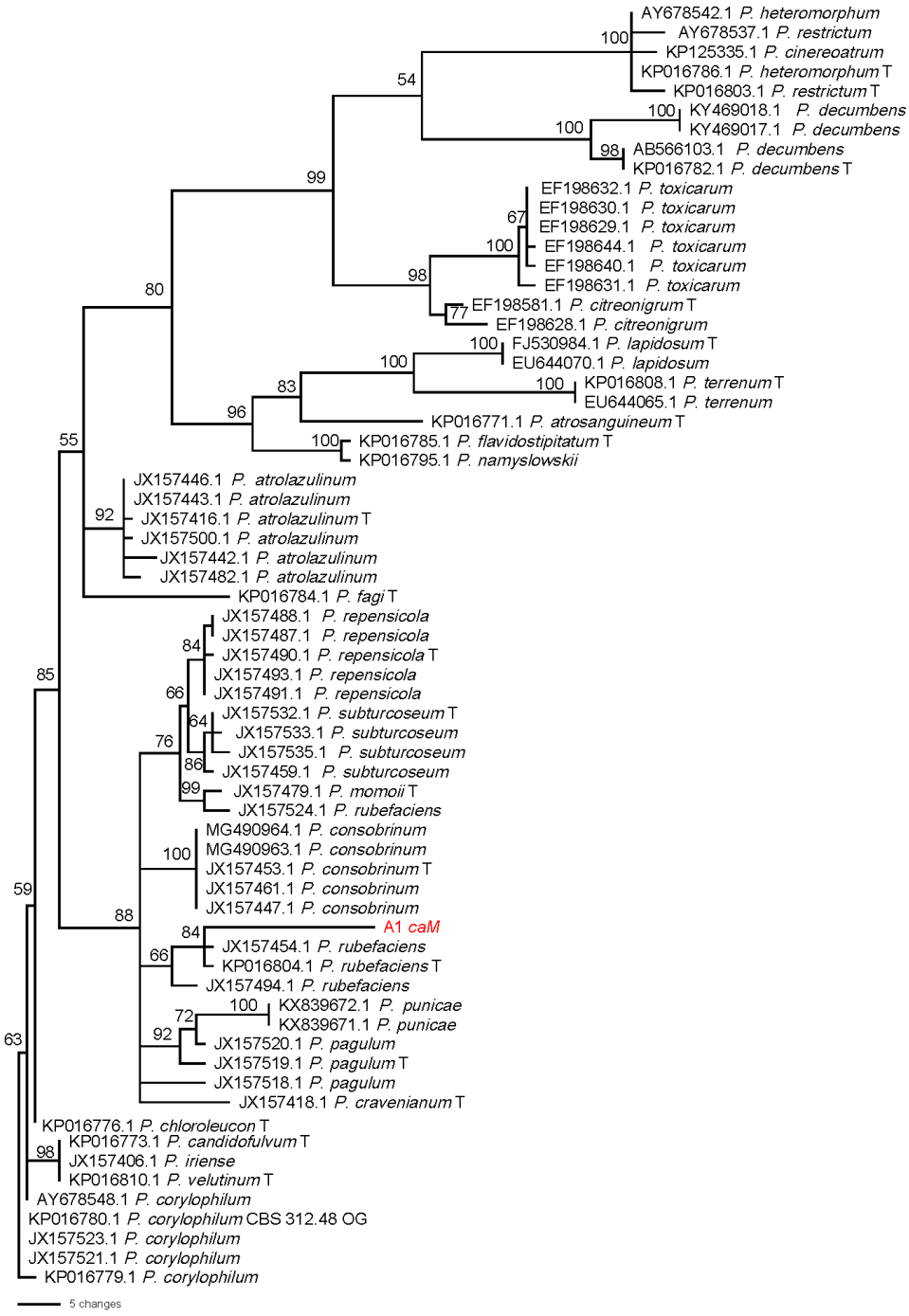

Supplementary Figure 5. Phylogenetic tree constructed using *caM* and *Penicillium* species downloaded from the NCBI. The selected outgroup was *P. corylophilum* CBS 312.48. Bootstrap values were presented on internal nodes with maximum parsimony. Bootstrap threshold was set to 50% with 1000 pseudo-replicates. *Values below 50% bootstrap threshold.

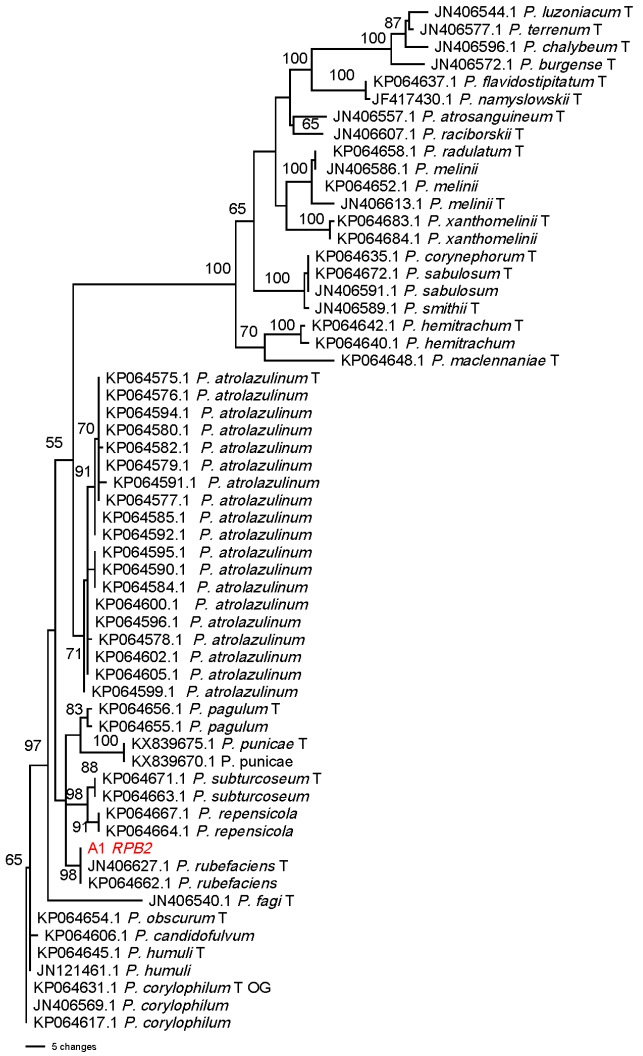

Supplementary Figure 6. Phylogenetic tree constructed using *RPB2* and *Penicillium* species downloaded from the NCBI. The selected outgroup was *P. corylophilum* CBS 312.48. Bootstrap values were presented on internal nodes with maximum parsimony. Bootstrap threshold was set to 50% with 1000 pseudo-replicates. *Values below 50% bootstrap threshold.

References

Bhandari V, Ahmod N, Shah H, Gupta R. 2013. Molecular signatures for *Bacillus* species: demarcation of the *Bacillus subtilis* and *Bacillus cereus* clades in molecular terms and proposal to limit the placement of new species into the genus *Bacillus*. International Journal of Systemic and Evolutionary Microbiology **63**: 2712-2726

Celandroni F, Vecchione A, Cara A, Mazzantini D, Lupetti A, Ghelardi E. 2019. Identification of *Bacillus* species: Implication on the quality of probiotic formulations. PLOS ONE **14**: 1-13

Miranda C, Martins O, Clementino M. 2007. Species-level identification of *Bacillus* strains isolates from marine sediments by conventional biochemical, 16S rDNA gene sequencing and inter-tRNA gene sequence lengths analysis. Antonie van Leeuwenhoek **93**: 297-304

Sabir JSM, Abo-Aba SEM, Sabry A, Hussein RM, Bahieldin A, Baeshen NA. 2013. Isolation, identification and comparative analysis of 16S rDNA of *Bacillus subtilis* grown around *Rhazya stricta* roots. Life Science Journal **12**: 980-986

APPENDIX E: Glassware Preparation

All glassware was prepared according to Ndlovu *et al.,* (2017) to remove contaminants like plastic or oil residues from these surfaces. In addition to this, the use of glassware and low-binding plastic pipette tips limited any loss in peptide activity caused as peptides bind to hydrophobic plastic materials. These materials may emulate the hydrophobicity nature of the outer cell membrane, a target for many bioactive antimicrobial peptides, including some cyclic LPs (Rautenbach *et al*., 2016).

Glassware and Sample Preparation for culturing

1. Wash glassware with soap and deionised water.
2. Wash with 1% sodium hypochlorite (v/v in deionised water) and rinse with deionised water.
3. Spray with 90% ethanol (v/v in deionised water) and rinse with deionised water.
4. Dry in an oven set to 50 ˚C.

Glassware and Sample Preparation for LC-MS

1. Label 4 mL glass vials with a glass engraver.
2. Wash vials with soap, deionised water, 90% ethanol (v/v) and water again.
3. Dry vials at 80˚C overnight.
4. Pyrolize in a 500˚C oven overnight.
5. Return vials to 80˚C oven to cool for approximately 4 h.
6. Prepare analytical mass scale (Mettler Toledo, Ohio, USA) by placing anhydrous calcium chloride inside the chamber to absorb excess moisture.
7. After 1 h, weigh empty vials analytically three times.
8. Calculate the average mass for each empty vial.
9. Weigh vials with sample added to them three times.
10. Calculate the average mass for each filled vial.
11. Subtract the average mass of the filled vials from the average mass of the empty vials to calculate the mass of each lyophilised sample.

References

Ndlovu T, Rautenbach M, Khan S and Khan W. 2017. Variants of lipopeptide and glycolipids produced by *Bacillus amyloliquefaciens* and *Pseudomonas aeruginosa* cultured in different carbon substrates. AMB Express **7**: 109

Rautenbach M, Troskie A, Vosloo JA. 2016. Antifungal peptides: To be or not to be membrane active. Biochimie **130**:132-145